Analysis and Design for Thermally Autonomous Housing in Resource-Constrained Communities: A Case Study in Bhuj, India

by

Madeline S. Gradillas

Bachelor of Architecture
College of Architecture, Planning, and Landscape Architecture, The University of Arizona, 2003

Submitted to the Department of Architecture
in Partial Fulfillment of the Requirements for the Degree of

Master of Science in Architecture Studies

at the

Massachusetts Institute of Technology

June, 2015

Signature of Author:

Department of Architecture
May 21st, 2013

Certified by:

Leon R. Glicksman
Professor of Building Technology and Mechanical Engineering
Thesis Supervisor

Accepted by:

Takehiko Nagakura
Associate Professor of Design and Computation
Chair of the Department Committee on Graduate Students

Thesis Supervisor
Leon R. Glicksman, PhD
Professor of Building Technology and Mechanical Engineering

Thesis Readers
Miho Mazereeuw
Assistant Professor and Director of the Urban Risk Lab at MIT

Tejas Kotak
Director of Research at the Hunnarshala Foundation for Building Technology and Innovations

Analysis and Design for Thermally Autonomous Housing in Resource-Constrained Communities: A Case Study in Bhuj, India

by

Madeline S. Gradillas

Submitted to the Department of Architecture
on May 21, 2015 in partial fulfillment of the requirements for the
Degree of Master of Science in Architecture Studies

Abstract

In the 2010 International Workshop on Housing, Health and Climate Change Meeting Report, the World Health Organization identifies housing as a primary cause of poor health in developing countries. The report cites inadequate protection from extreme heat as one of six major concerns for healthy housing environments. As India's population rapidly increases, informal settlements face particular heat risk because of harsh climate conditions, sub-standard building construction and lack of access to electricity for mechanical cooling. There is a need for housing to provide thermal comfort and health by passive means at low cost.

Climate specific passive cooling techniques are well known, but are rarely implemented in informal settlements because of density, lack of resources, design integration, and materials availability. This thesis is situated in the practical connection of two normally disparate parts: applied research in passive cooling techniques, and design for development. The work presented results from the establishment of an international co-design partnership between MIT and The Hunnarshala Foundation for Building Technology and Innovations, an NGO based in the hot and arid region of Bhuj, India. It presents data analysis and co-design work that drove the development, field prototyping, and evaluation of appropriate, implementable building solutions to improve thermal conditions in affordable housing in hot and arid climates. New low-cost, multi-layered roof assembly designs are presented and evaluated. Experimental results show that even in severe arid climates the interior conditions can approach ASHRAE and EN 15251 Adaptive Thermal Comfort standards through most of the operating hours. The results of this research will be an important contribution to the designs of the initial phase of the large-scale Rajiv Awas Yojana Slum Free Bhuj re-development housing construction over the next five years in Western India.

Thesis Supervisor: Leon R. Glicksman
Title: Professor of Building Technology and Mechanical Engineering

Acknowledgments

This research was funded by the MIT Tata Center for Technology and Design. I am grateful to the Tata Center not only for its financial support, but also for establishing a community of Tata Fellows and program that gives us the unique opportunity to develop our academic research while addressing some of the practical challenges the world faces.

I am thankful for this tremendous learning experience, and for having worked under the patient and expert guidance of Dr. Leon Glicksman. I also would like to thank Miho Mazereeuw and Aditya Barve for their support and for facilitating the connection to the Hunnarshala Foundation, and also to Mr. Sandeep Virmani for encouraging the formation of a partnership between the Tata Center and Hunnarshala.

To all the members of the Hunnarshala Foundation, words cannot justify the utmost appreciation I have for your collective engagement and enthusiasm, and for the sheer amount of time and work so many of you have put into this project. From persistent and jovial daily Gujarati language lessons to the labor intensive construction of the thermal field lab at Paraspar, I am overcome with gratitude for your enduring commitment to the international transfer of ideas and collaborative research process. I am especially grateful to Mr. Tejas Kotak, the Director of Research at Hunnarshala, for welcoming me and this extensive project into his lab and for all his support with the design and implementation of the project. And to Pradip Rangani, the Bhuj Project Manager for this research, abhar. Without your thorough attention to the many dynamic project details, this research would not exist.

Thank you to the entire MIT Building Technology Faculty and Staff for developing a program that cultivates the rigorous and open exchange of ideas among its community members. And to my colleagues in the Building Technology Lab: your academic, technical, and practical advice has been invaluable. A special thank you goes to David, Jeff, and Alonso for your generosity, accessibility, expertise and good humor for these past two years.

To my immediate and extended family and friends, my gratitude and love for you of course precedes and extends far beyond this project or any distinct period of time. To my Mom and Dad, Ernie and his family, Anna and hers and to Miguel and his, I love you all very much.

Table of Contents

List of Figures

List of Tables

Chapter 1

Introduction

In the 2010 International Workshop on Housing, Health and Climate Change Meeting Report, the World Health Organization (WHO) identifies housing as a primary cause of poor health in developing countries. The report also cites inadequate protection from extreme heat as one of six major concerns for healthy housing environments (WHO, 2010). As the population of India rapidly increases, informal settlements face particular heat risk because of harsh climate conditions, substandard building construction and lack of access to electricity for mechanical cooling. There is a need for to improve thermal comfort and health in housing by passive means at low cost.

Much of content and scope of this research stems from a close collaboration with the Hunnarshala Foundation, an NGO based in Bhuj, India. Bhuj, in the hot and arid Kutch region of Gujarat, is rebuilding itself after being near the epicenter of a devastating earthquake in 2001. With rebuilding efforts come innovation in building techniques, housing design, planning, and policy. Hunnarshala is a primary facilitator in this effort. Through engagement with local communities, as well as state and national government agencies, and with a commitment to craft and craftsman empowerment, Hunnarshala pioneers shifts in housing policies as well as building guidelines and techniques to holistically improve the built environment. Improving indoor thermal conditions in housing is a current priority for Hunnarshala.

Similar to the rest of nation, 33% of the Bhuj population lives in slums (Hunnarshala Foundation, 2013). Hunnarshala has been appointed as the Project Management Agency for the *Slum Free Bhuj* project as part of the Indian Ministry of Housing and Urban Poverty Alleviation's (MHUPA) Rajiv Awas Yojana (RAY) *Slum Free India* initiative. The goal of *Slum Free Bhuj* is to provide improved housing for more than 11,000 families currently living in slums, in the next five years. The larger RAY *Slum Free India* plan seeks to provide appropriate housing for those living in slums nationwide, in excess of 1 million houses, by 2022 (MHUPA, 2013). In addition to being the Project Management Agency, which oversees planning, design and building of slum re-developments, the Hunnarshala Foundation also plans to draft a set of building guidelines, which includes improved thermal performance criteria for RAY to use nationally.

Thermal Autonomy is defined as "the percent of occupied time over a year where a thermal zone meets or exceeds a given set of thermal criteria through passive means only" (Levitt et al., 2013). Passive cooling techniques such as building shading and natural ventilation as well as thermal performance of materials are well established and researched, but are rarely seen implemented effectively in informal settlements

because of density, and lack of resources, design integration, and materials availability. Existing slum and slum re-development housing perform poorly in Bhuj's extreme climate. Construction types of informal housing vary, but generally house roofs are uninsulated and made out of sheet materials that provide very little resistance to heat from intense solar radiation. Night Flush Ventilation, or naturally ventilating buildings only during night hours, can passively cool buildings and occupants in a hot an arid environments, but the success of this technique depends on the amount of thermal mass in the house, as well as the position, size and operation of windows or openings. These aspects must be integrated into the design phase so that housing benefits from the latent passive cooling benefit its climate provides.

This thesis presents data analysis and co-design work that drove the development, field prototyping, and evaluation of appropriate, implementable building solutions to improve thermal conditions in affordable housing in hot and arid climates. The novelty of the project lies in the practical connection of two normally disparate parts: applied research in passive cooling techniques, and design for development. Sections 1.1 and 1.2 of this chapter are devoted to the description of significant theories, research and issues relevant to both these parts. Section 1.3 then positions this work by describing the scope and objectives of the project as well as overall structure of the thesis.

1.1 Design with Climate and Passive Cooling

In the 1963 text *Design With Climate*, Victor Olgyay states, "[t]he aim in designing a structure thermally is to establish a an indoor environment which most nearly approaches comfort conditions in a given climatic setting. In architectural terms this means that . . . a building should utilize the natural possibilities to improve conditions without the aid of mechanical apparatus". In response to the rapid increase in mechanical systems and energy use in the 1950's and 60's that lead to the energy crises of the 1970's, architectural scholars such as Victor and Aladar Olgyay and Reyner Banham examined the natural forces behind, and the potential of, bioclimatic, or climate responsive, building design. Scholars such as Amos Rapoport and Bernard Rudofsky (Figure 1.1) used geographic, cultural and formal comparisons to qualitatively look to vernacular and historic precedents for clues to link building form, envelope and operation to climate (Rapoport, 1969; Rudofsky, 1964). In the *Manual of Tropical Housing and Building*, where tropical climates are defined as those where "heat is the dominant problem", O.H. Koenigsberger characterized climate into the general regions of hot-dry, warm-humid, composite and tropical upland climates. Each region was then systematically characterized with lists of physiological objectives for occupants, form and planning objectives, and space and envelope design recommendations (Koenigsberger, 1974). Again, vernacular examples were included to illustrate design with climate strategies, (Figure 1.2) but the quantitative impact of those strategies were not evaluated. It is from these texts of the 60's and 70's that architects who are interested in bioclimatic building design now follow a set of well defined rules of thumb. For hot and arid climates such as Bhuj, those rules of thumb based on traditional construction are summarized as follows:

Figure 1.1 – Traditional courtyard houses typical to hot-dry Marrakesh. (Rudofsky, 1964, p. 54)

Heat Avoidance

Shade or protect openings, walls, and roofs from direct solar radiation.
Use light colors to reflect solar radiation.
Minimize opening area and make openings operable.

Night Flush Ventilation with Thermal Mass

Most effective in climates with high diurnal temperature swings.
Keep windows closed during day and open at night to flush out hot air and to discharge heat stored in thermal mass.

Evaporative Cooling

Removal of sensible heat from the air due to the gain in latent heat from evaporation.

Around the time these texts, which remain esteemed sustainable design references for architects, were published, experimental research specific to building design with climate was underway. Amid growing interest in the effects of climate on architecture and occupants in tropical and hot climates, a series of experiments were conducted at the Israel Institute of Technology in Haifa (Givoni, 1976). Figures 1.3 and 1.4 as well as Table 1.1 show comparative results of a number of Baruch Givoni's experiments to

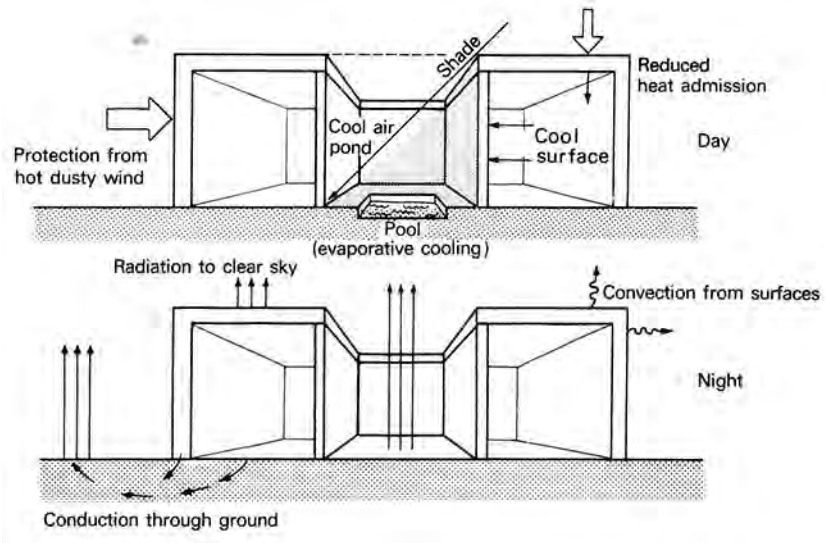

Figure 1.2 – O.H. Koenigsberger Courtyard House Diagram. (Koenigsberger, 1974, p. 205) Rule of thumb Design with Climate strategies for hot and arid climates are illustrated such as protection from solar radiation, evaporative and radiative cooling, and use of thermally massive elements as heat sinks.

quantify and compare the thermal effects of building orientation, material, envelope and operation on indoor environments that are also relevant to this project. The results uphold the well-known design with climate tenants of the Olgyay and Koenigsberger texts. It should be noted that Givoni asserts that a modification to the the high thermal mass/small opening areas model of traditional architecture could result in a cooler interior. In the *Principles of Building Design and Construction in Desert Regions* section of the book he states, "[t]he use of modern insulating materials in conjunction with those of high heat capacity allows the openings to be larger while maintaining or even improving on the thermal conditions obtained in traditional buildings." and that "Suitable for this purpose are high heat capacity concrete walls externally insulated . . . [t]he roofing should be of a similar composite construction" (Givoni, 1976, p. 345,347). Givoni's experiments definitively show that internal conditions are in no small part linked to the combinations of thermal resistances and heat capacities of the materials that surround them.

In an effort to summarize the prolific but diffuse research by Givoni and many others, Jeffrey Cook compiled *Passive Cooling*. *Passive Cooling* was published in 1989 as one volume in a twelve volume series documenting research, significant results and developments in technology sponsored by the US federal government's National Solar Energy Program, spanning from 1975 to 1986 (Cook, 1989). The term "Passive Cooling" was defined to describe indoor environmental control systems that use natural phenomena and heat sinks to cool building interiors, and do not rely on mechanical systems. In the introductory chapter Cook states; "Passive cooling resources are the natural heat sinks of the planet — those thermal transfer opportunities that generally balance the continuous energy inputs from our sun . . . [t]he three heat sinks of nature are the sky, the atmosphere, and the earth" (Cook, 1989, p. 4). The text is divided into four main parts: *Ventilative Cooling*, *Evaporative Cooling*, *Radiative Cooling*, and *Earth Coupling*, each part containing a description of concepts and examples of applied designs. Of particular interest embedded in this text are the separate discussions of double layer and radiant cooling

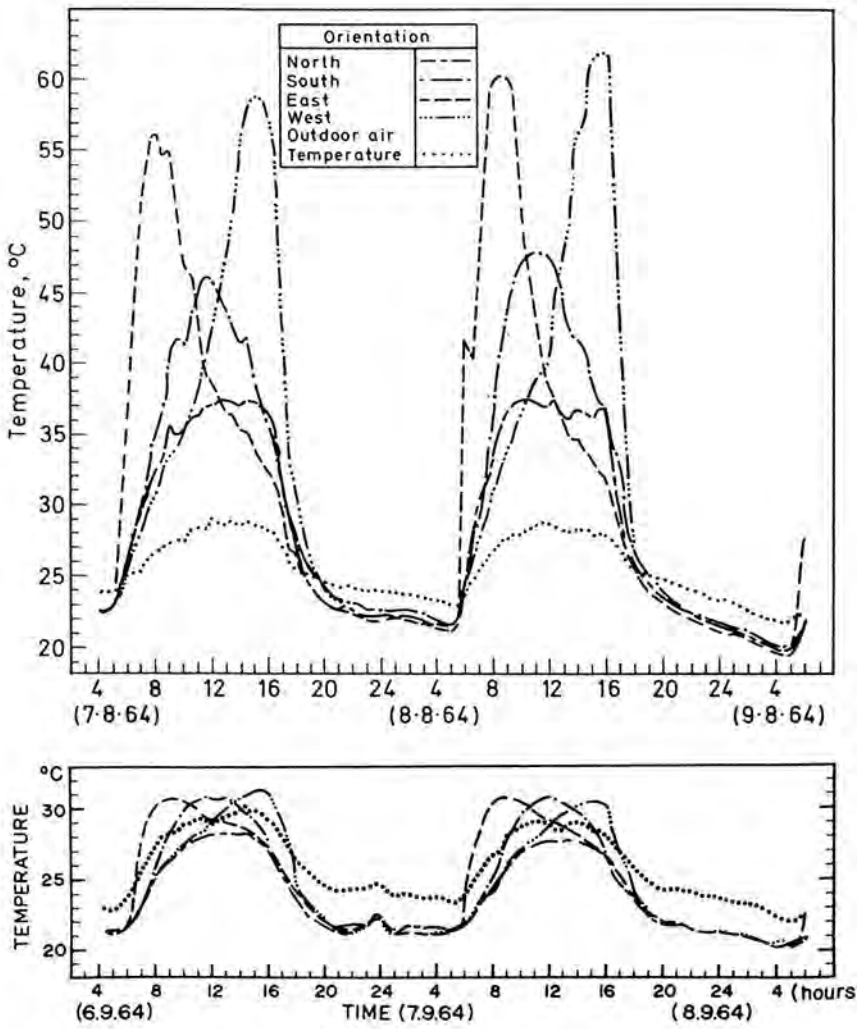

Figure 1.3 – Results from one of Baruch Givoni's *Man, Climate and Architecture* field experiments in Haifa, Israel (Dry-summer Mediterranean climate). Upper: Measured external surface temperatures of grey (absorptivity, α 0.6) lightweight concrete (Ytong) walls with different orientations. Lower: Measured external surface temperatures of white colored Ytong walls (absorptivity, α 0.11) with different orientations. Results show that (Givoni, 1976, p. 218)

roofs. Cook and contributors mention on several occasions the "Skytherm" (patented in 1971 by Harold Hay) and various other roof pond systems: roof assembly designs in which roof water ponds are cooled at night through radiation to the sky and then are able to maintain cool temperatures during the day due to an exterior movable insulated shading system. In the text the Skytherm system was touted as the "only system that . . . provides both cooling and heating with virtually no expenditure of electrical power" (Cook, 1989, p. 95). Indeed, despite some problems with water leakage and lack of structural integrity of some of the test roofs, an insulated roof pond system tested in Bangalore, India decreased indoor temperatures by an average of 3° to 4°C (Prasad et al., 1979). However, as potentially effective as these systems are, questions arise about the applicability of these systems to the slum and slum re-development

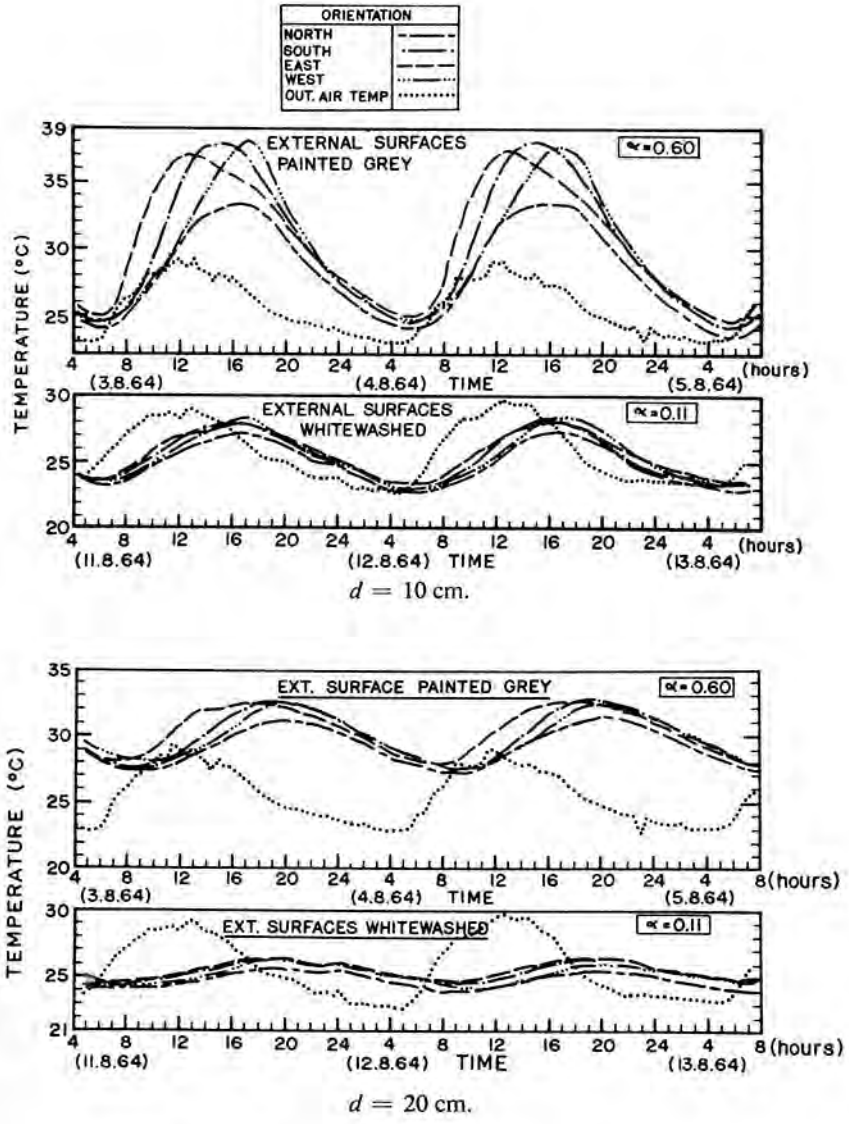

Figure 1.4 – Results from one of Baruch Givoni's *Man, Climate and Architecture* field experiments in Haifa, Israel (Dry-summer Mediterranean climate). Measured internal surface temperatures of walls of different orientation, thickness and external color (absorptivities, α of 0.6 and 0.11). (Givoni, 1976, p. 223)

house context. The most prohibitive aspect of such roofs lies in the need for perhaps arduous daily operation for effective thermal performance. In the *Ventilative Cooling* section of Jeffrey Cook's Book, Dr. Subrato Chandra identified the predominant source of heat in roof attic spaces as radiation during the day from solar gain, the transfer of which can be greatly reduced with the use of radiant barriers. The text briefly mentions the use of double layered naturally ventilated roofs as systems that are "sometimes used to reduce the heat gain" but does not give any quantitative evidence of how much of a reduction occurs. It only then states that "compared to the double-roof design, a radiant barrier . . . is much more cost effective", without further explanation of the benefits or drawbacks of double-layer roof assemblies

Effect of ventilation on the temperatures of the indoor air and western surface (deviations from maximum outdoor air temperature, deg C) [13.6]

External colour	Point	Ventilation conditions	Material and thickness: Concrete 12 cm	Concrete 22 cm	Hollow concrete blocks 20 cm	Ytong 12 cm	Ytong 22 cm	Ordinary curtain walls 7 cm	Insulated curtain walls 16 cm
Grey	Indoor air	Without ventilation	8·0	3·3	3·5	4·6	2·2	5·8	5·1
		Night ventilation	7·2	1·9	1·7	3·4	0·2	4·8	3·7
		Permanent ventilation	1·0	−0·4	−0·3	0·5	−0·2	0·3	0·4
		Effect of night vent.	−0·8	−1·4	−1·8	−1·2	−2·0	−1·8	−1·4
		Effect of permanent vent.	−7·0	−3·7	−3·8	−4·1	−2·4	−5·5	−4·7
	Western surface	Without ventilation	13·2	6·3	6·8	7·8	2·7	9·3	6·6
		Night ventilation	12·9	4·6	5·2	6·9	0·7	8·4	4·3
		Permanent ventilation	10·1	3·5	2·8	4·5	0·1	3·7	1·7
		Effect of night vent.	−0·3	−1·7	−1·6	−0·9	−2·0	−0·9	−2·3
		Effect of permanent vent.	−3·1	−2·8	−5·0	−3·3	−2·6	−5·6	−4·9
White	Indoor air	Without ventilation	−1·0	−1·8	−2·3	−1·8	−3·2	−1·1	−1·9
		Night ventilation	−2·7	−2·5	−2·8	−2·7	−4·8	−0·5	−3·1
		Permanent ventilation	−1·1	−1·4	−1·4	−0·8	−2·0	0·0	−1·0
		Effect of night vent.	−1·7	−0·7	−0·5	−0·9	−1·6	0·6	−1·2
		Effect of permanent ventilation	−0·1	0·4	0·9	1·0	1·2	1·1	0·9
	Western surface	Without ventilation	−1·1	−1·6	−2·2	−1·7	−3·1	−1·2	−1·8
		Night ventilation	−2·1	−2·8	−2·8	−2·2	−4·5	−0·3	−2·7
		Permanent ventilation	−1·9	−3·1	−2·5	−0·8	−3·6	−0·4	−0·9
		Effect of night vent.	−1·0	−1·2	−0·6	−0·5	−1·4	0·9	−0·9
		Effect of permanent ventilation	−0·8	−1·5	−0·3	0·9	−0·5	0·8	0·9

Table 1.1 – Results from one of Baruch Givoni's *Man, Climate and Architecture* field experiments in Haifa, Israel (Dry-summer Mediterranean climate). Impact of wall construction and ventilation control on indoor temperatures. Measured deviations from maximum outdoor air of western wall surface and air temperatures. Results show that Night Flush ventilation reduces indoor air temperatures anywhere from 0.3 °C to 2.3 °C depending on wall absorptivity, α, and construction type (Givoni, 1976, p. 271)

(Cook, 1989, p. 74).

More recent research continued to evaluate the theories and findings from the 60's, 70's and 80's. A wealth of experimental studies were conducted in various hot climates to test the cooling effects of lightweight buildings versus heavyweight construction (Pearlmutter and Meir, 1995), amount of thermal mass present (La Roche and Givoni, 2002) indirect evaporative cooling ceiling ponds and porous material systems (Krüger et al., 2010; Bravo and González, 2013; Wanphen and Nagano, 2009; Meng and Hu, 2005), position of radiant barrier in double layer roofs (Chang et al., 2008), operable double layer insulated roof systems (La Roche and Givoni, 2002) and night flush ventilation in thermally massive buildings (Givoni, 2011). In his presentation of experimental data from many of the aforementioned various test cell studies, Givoni summarized his own night flush ventilation research at UCLA by noting that "interior mass coupled with the indoor space is a pre-requisite for effective use of night ventilation to lower indoor maximum temperatures" (Givoni, 2011, 1700).

Though ample experimental evidence exists to quantify and support passive cooling theories, few of these experiments directly address the challenges of the construction, operation and implementation of such systems in resource-constrained settings or settings outside lab/field testing environments. In

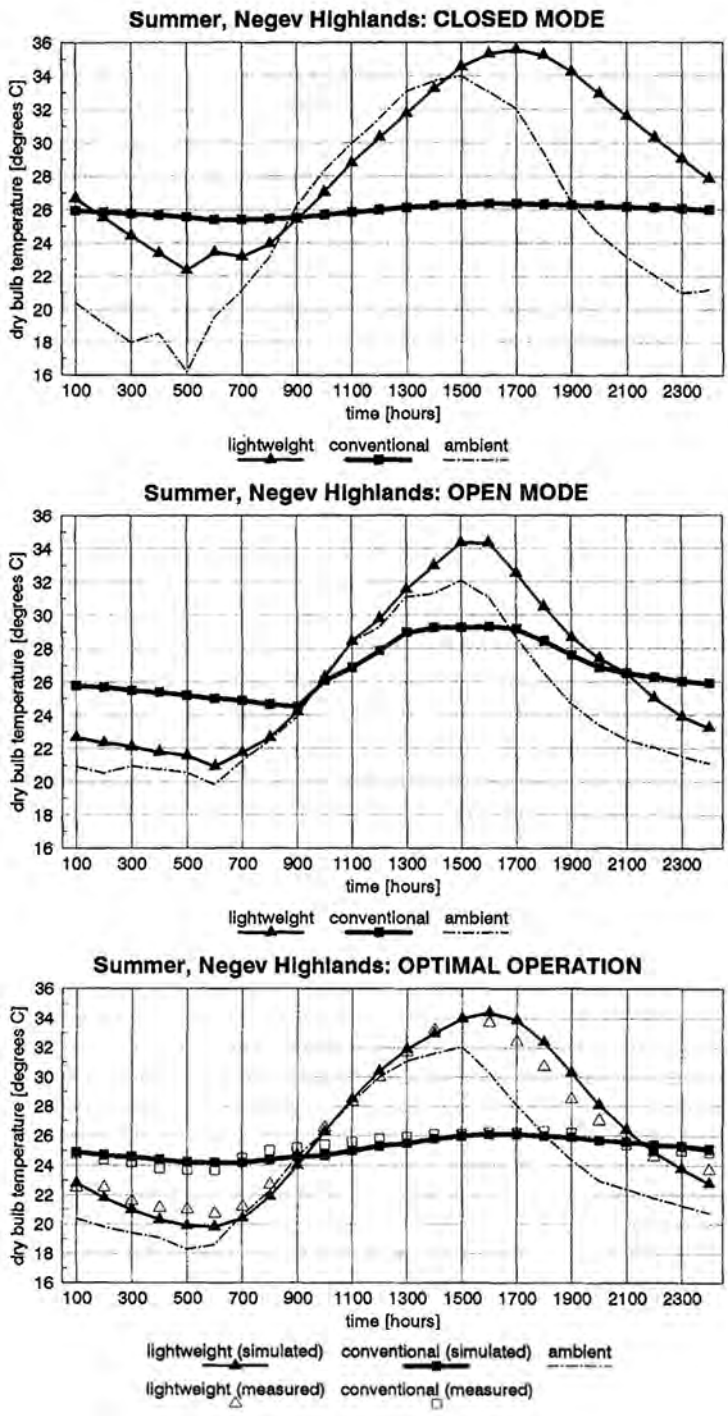

Figure 1.5 – Effect of ventilation schedule on indoor temperature of insulated thermal mass vs lightweight construction types. Upper: With windows constantly closed. Middle: With windows constantly open. Lower: With windows open for night flush ventilation. (Pearlmutter and Meir, 1995, p. 447-448)

Assessing the Climatic Implications of Lightweight Housing in a Peripheral Region, David Pearlmutter and Isaac Meir, researchers at the University of Negev, Israel, compare seasonal thermal performance of a "conventional" insulated thermal mass building to that of a "geographically indiscriminate" factory built lightweight aid house similar to those provided to thousands of recent immigrants to the region (Pearlmutter and Meir, 1995). Similar to the previously mentioned studies, the houses were monitored with the windows constantly closed, constantly open, as well as on a night flush schedule (Figure 1.5) The results clearly demonstrate the "conventional" buildings' superior performance, however the study ends there, without mention of possible mass housing design alternatives. In the introduction of *The Effect of Heat Gain on Performance of a Radiant Cooling System*, Pablo La Roche explains that the metal sheet roofs commonly found in developing countries are effective at cooling indoor air temperatures at night via radiation but ineffective during the day because of their low resistance to solar irradiation (La Roche and Givoni, 2002). He proposes one of Givoni's designs as a solution: a double-layered roof with hinged interior insulative panels, that can be mechanically opened and closed to resist heat transfer during the day but allow for radiant cooling at night. Experimental data showed that these roofs had a significant cooling effect, with maximum indoor air temperatures averaging 7.9 °C lower than outdoor air temperatures (Figure 1.6). It is worthy to note that also in this experiment, roof performance was dependent on the level of conductive heat transfer through the walls as well as presence of thermal mass in the room. Though the study begins with mention of one roof material common in developing countries, it does not propose alternatives for insulation materials or operation mechanisms for proper deployment to resource-constrained communities.

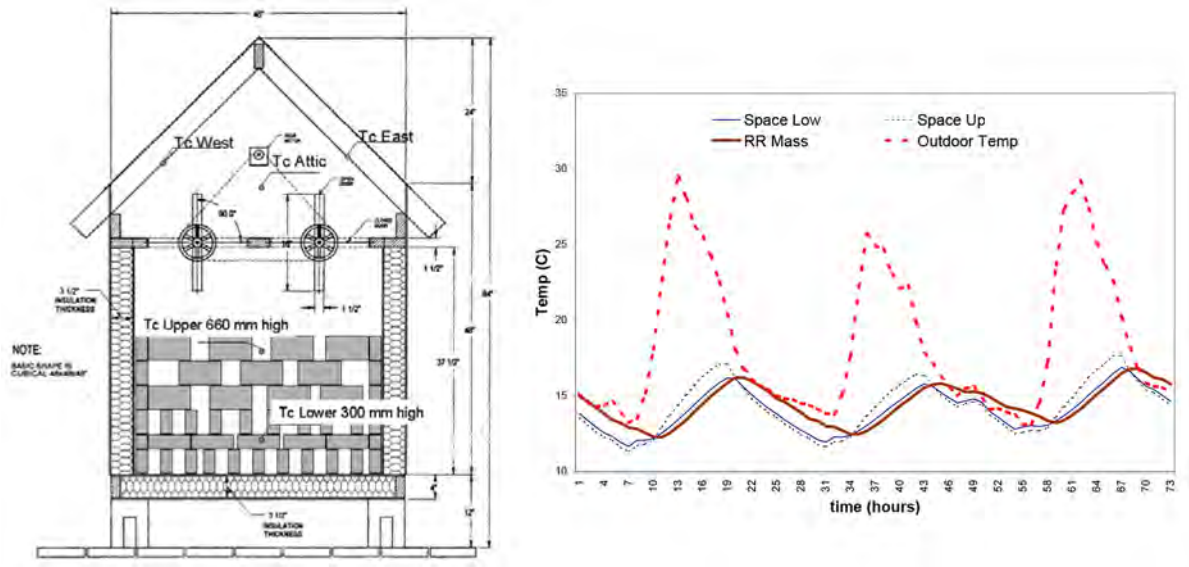

Figure 1.6 – Effect of Radiant Cooling on Indoor Air Temperature. Left: Indoor air temperatures are measured at 300 mm and 660 mm from floor level, and are indicated in the section of the La Roche test chamber with operable radiant cooling roof. Right: Results of closed chamber indoor air temperature at different heights compared to outdoor air temperature. (La Roche and Givoni, 2002, p. 2)

One study focused entirely on the use of appropriate materials and construction techniques directly preceded this thesis research. It was conducted by CEPT University Masters student Veerendranath Satrasala in collaboration with the Hunnarshala Foundation in Bhuj, India. In this study, eight 1 m by 1 m by 2 m

test chambers were outfitted with various roof assemblies (Figure 1.7), and performance was measured by comparing interior and exterior air and roof surface temperatures (Satrasala, 2014). Aside from one corrugated metal sheet variation, all roof assemblies, though composed of different materials were similarly thermally massive. Test chamber walls were shaded with burlap sacks and an access window in each chamber remained constantly open. The results of this study (Figure 1.8) indicate that the amount of thermal mass and the single, constantly open window in each test chamber prohibited the space from effectively cooling at night.

This past work suggest that further improvements can be obtained by establishing the framework for and conducting a rigorous experimental study that explores not only materials and assemblies appropriate to context, but also evaluates the effect of proven passive cooling techniques on those assemblies.

Figure 1.7 – Bhuj Test Chambers with Thermally Massive Roof Assemblies. (Satrasala, 2014, p. 43)

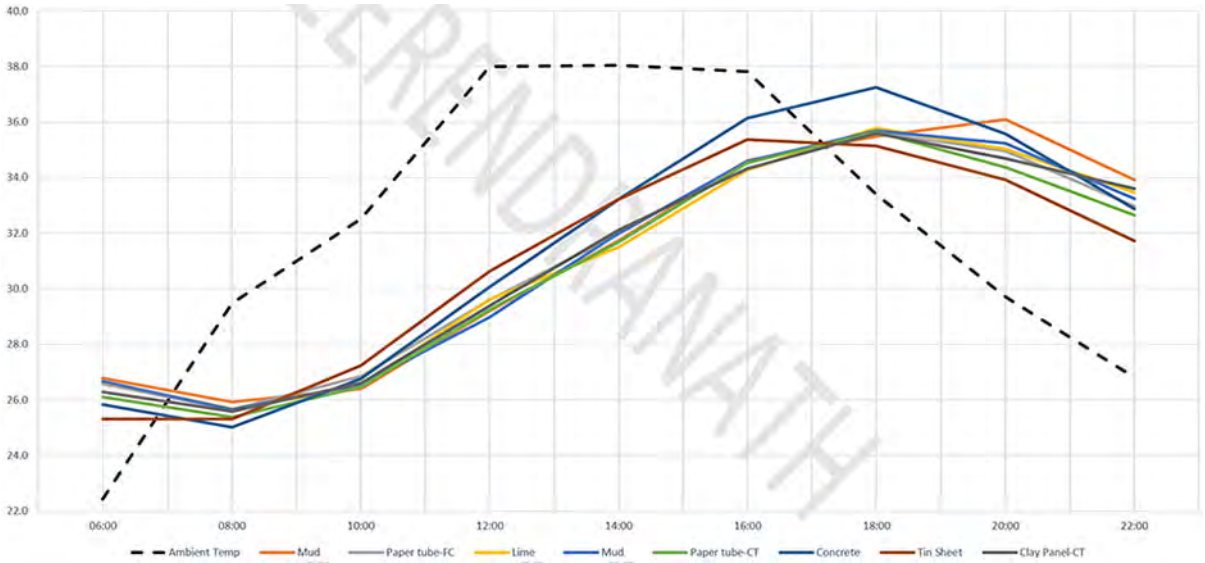

Figure 1.8 – Satrasala test chamber indoor air temperature results. (Satrasala, 2014, p. 58)

1.2 Design for Development

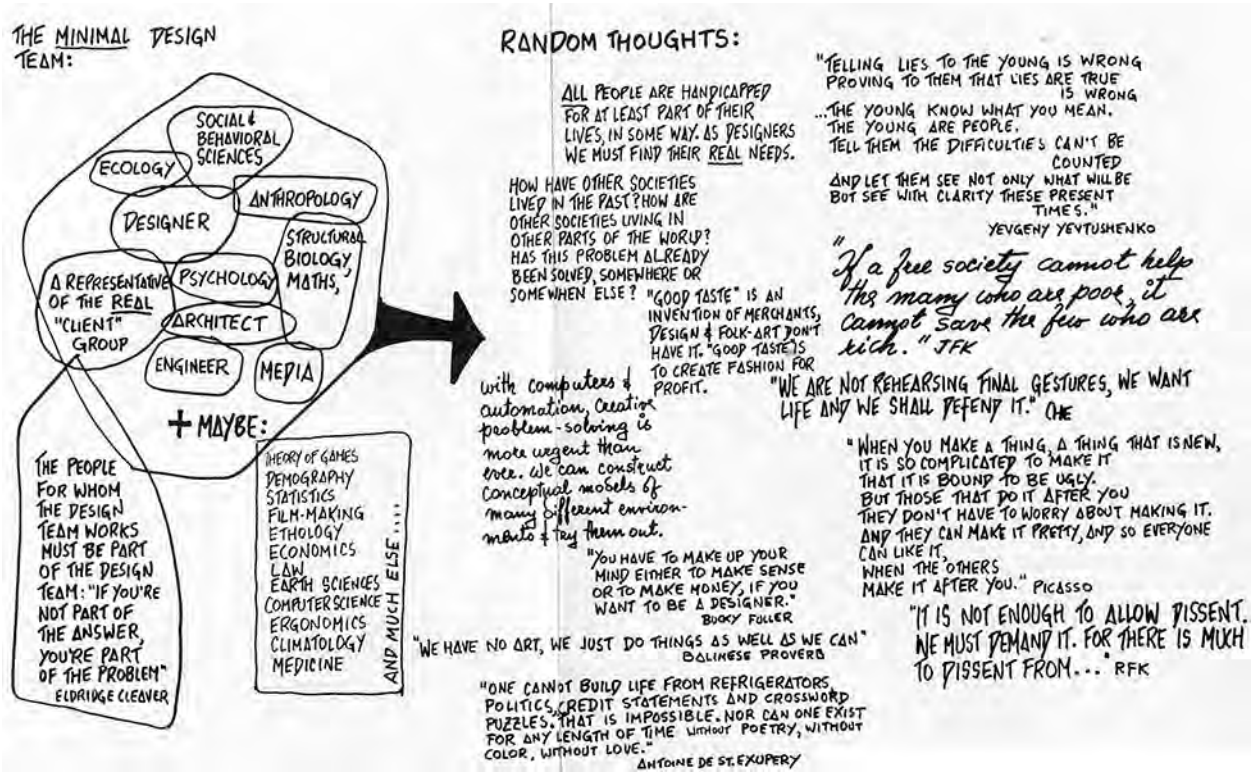

Figure 1.9 – Papanek Design for Development diagram. (Papanek, 1972)

In their thermal analysis of pre-fabricated aid houses supplied to thousands immigrants in Israel in the 1990's, Pearlmutter and Meir highlight a recurring misdirection of good intentions toward development by designers, organizations, and governments; solutions fail to function because designers fail to prioritize the climate and culture for which they design solutions. Emergency relief housing is not the focus of this thesis. However, the methods and the decisions behind the work contained in the thesis aim to pro-actively address the so often seen mismatch of solution to context. The purpose of this section is not make blanket criticisms of past development efforts or to comprehensively address the expansive issues that the affordable housing crisis presents. Instead, design for development theories are briefly discussed to establish the framework by which this thesis work was conducted.

The 1972 *Design for the Real World* by Victor Papanek sounded the "earliest alarm bell" (Morelli, 2007, p. 3) for Design for Development with his polemic call to revolutionize design thinking such that it prioritize social and moral responsibilities to those in need. Eight years later, Papanek was one of the many international attendees at the UNIDO-ICSID 79 (United Nations Industrial Development Organization and International Council of Societies of Industrial Design) meeting in Ahmedabad India. UNIDO-ICSID 79, organized by India's National Institute of Design (NID) marked a milestone for progress in the definition and coalition of the Design for Development movement, producing the *Ahmedabad Declaration on Industrial Design for Development* which included a plan of action and recommendations for the promotion of industrial design for development (Balaram, 2009). The following is a series of ex-

cerpts from the declaration which help to frame the overarching theory to which this thesis work intends to address:

"The Meeting for the Promotion of Industrial Design in Developing Countries . . . to satisfy urgent needs in this field . . . [s]olemnly declares"

> "Its firm conviction that design can be a powerful force for the improvement of the quality of life in the developing world"
>
> "That design in the developing world must be committed to a search for local answers to local needs, utilizing indigenous skills, materials and traditions while absorbing the extraordinary power that science and technology can make available to it"
>
> "That designers in every part of the world must work to evolve a new value system which dissolves the disastrous divisions between waste and want, preserves the identity of peoples and attends the priority areas of need for the vast majority of mankind" (National Institute of Design, 1979).

The new conditions this declaration called for required design methodologies which differed from traditional paradigms (Morelli, 2007). In the more than thirty years since UNIDO-ICSID 79, *participatory design* or *co-design* strategies gained momentum as a way toward successful design for development. Defined as "the collective . . . creativity of designers and people not trained in design" or as an approach that "puts together the expertise of systems designers/researchers and the situated expertise of the people whose work was to be impacted by the change [in the system]" (Sanders and Stappers, 2008), the co-design process emphasizes the role of the professional designer as *facilitator*, who is especially effective at the front end, or pre-design phase of the design process. According to Elizabeth Sanders and Jan Stappers, "[t]he goal of the explorations in the front end is to determine what is to be designed and sometimes what should not be designed and manufactured" (Sanders and Stappers, 2008). Also, the co-design process tends toward a shift "from the provision of finite solutions (products) which often *relieve* people of their own tasks and responsibilities to the provision of semi-finished platforms, including products and services, that will *enable* people to create value according to their individual needs" (Morelli, 2007). Non-profit design organization IDEO outlines this new design methodology by breaking it into the three phases of "inspiration, ideation, and implementation" to be thought of as "a system of overlapping spaces rather than a sequence of orderly steps" (Brown and Wyatt, 2008). The three spaces of IDEO design thinking emphasize iterative engagement between user, researcher and designer through field observation, review or brainstorming sessions, and prototyping.

The methods of this thesis project qualify as co-design in many ways. It should be noted that the roles of *user*, *researcher* and *designer* all overlap in this project. The Hunnarshala Foundation, as the Indian organization that is regularly engaged with end users, local artisans and national agencies, assumes all three roles in this project to varying degrees and is the primary facilitator when it comes to the scope of the Slum Free Bhuj project. My role is best classified as researcher and co-designer. Though the overall goal of the project is to arrive at a material solution for the end user, my role has also simultaneously been to establish a committed relationship with Hunnarshala to foster co-design thinking through the transfer of ideas. This is discussed throughout Chapters 3, 4, 5 and 6.

1.3 Thesis Scope, Objectives and Structure

This project documents the formation and critical points of the co-design process during the first one and a half years in a continuing partnership with the Hunnarshala Foundation. This co-design method uses energy simulation as a predictive tool, as well as field research and experimentation, to develop a material solution that addresses the pressing need of indoor thermal health in informal housing. The objectives of this research are:

- Define criteria for Thermal Autonomy according to local perception as well as accepted standards for thermal comfort and health.
- Understand climate conditions so passive cooling potential of housing is maximized.
- Analyze rule of thumb Design with Climate strategies to determine their relationships and to predict their impact on indoor thermal conditions in common Bhuj construction types.
- Compare traditional and contemporary Bhuj building typologies to establish and quantify thermal performance.
- Measure the cooling potential of Night Flush Ventilation.
- Establish a local thermal field lab to validate design decisions and enable the transfer of ideas between co-design partners.
- Co-Design building envelope modifications that improve indoor thermal conditions in hot and arid environments.
- Collaborate with Hunnarshala to focus design decisions on appropriate, implementable, scalable solutions.

This thesis is structured as follows:

Chapter 2 defines standardized as well as perceived thermal comfort and health metrics to establish a framework for thermal autonomy. The chapter also briefly introduces the reader to Bhuj, India, by describing typical climate conditions, and existing vernacular, as well as proposed Rajiv Awas Yojana *Slum Free Bhuj* re-development housing construction types. Chapter 3 is an analysis of temperature data collected from seven existing buildings in Bhuj to further develop an understanding of context. It establishes a method to use predictive digital energy modeling as well as field data collection to establish a local thermal performance database. Data collection methods are discussed, then the seven case study buildings' thermal performance is directly compared and evaluated. Chapter 4 describes the first year of the co-design process. It documents the methods and results of three pre-design digital energy analysis iterations, as well as the feedback and recommendations between partners that informed the design of a thermal field lab in Bhuj and the first round of roof assembly prototypes. Chapter 5 describes the designs for five roof assembly prototypes. It also describes the co-design and construction of a thermal field lab in Bhuj. It then presents the methods and results from a series of field experiments to determine the effect of roof design and natural ventilation on indoor thermal conditions. Chapter 6 concludes the thesis by providing recommendations for improving thermal conditions in informal housing, based on research findings.

Chapter 2

Background

Section 2.1 describes the established outdoor thermal comfort and health metrics used in this thesis to define thermal autonomy. The typical Bhuj annual climate conditions are analyzed according to these metrics. Indoor thermal comfort metrics used in this thesis are then described. These metrics are countered with a discussion of differing views of thermal comfort based on field observation and informal interviews with Bhuj inhabitants. The discussion leads to the third part of the chapter, the purpose of which is to introduce the reader to the built context of Bhuj, India, by describing the vernacular Mistri caste Madhapar courtyard house typology that Hunnarshala has modeled the Slum Free Bhuj houses after (Section 2.2) contrasted with typical informal house construction found in the area (Section 2.3).

2.1 Thermal Criteria for Healthy Housing

The human body must maintain a core body temperature of 37 °C (98.6 °F) to 38 °C (100 °F) to survive. Heat stress occurs when body temperature exceeds 38 °C for an extended period of time. (Brake and Bates, 2002; Epstein and Moran, 2006) According to the United States Department of Labor Occupational Safety and Health Administration (OSHA), people should not be permitted to work when their core temperature exceeds 38 °C. In its technical manual, OSHA outlines heat disorders and health effects that range in severity from Heat Fatigue, signified by impaired sensorimotor and mental performance, to Heat Stroke, a medical emergency, potentially leading to death. Core body temperature thresholds are well defined, but the causes of rises in body temperature to unhealthy levels are unpredictable. A body's ability to thermoregulate depends on many internal factors: an individual's level of physical fitness and exertion, medical condition, age, degree of acclimatization, and clothing, among others (OSHA, 1999). These factors cannot be completely controlled by our external environment. However it is possible to create spaces which minimize the risk of thermal stress to occupants. To minimize this risk, we must first understand the thermal criteria that exist to which we can measure thermal performance of our built environment. We must consider outdoor as well as indoor environmental conditions.

2.1.1 Outdoor Conditions and Thermal Stress

What conditions are necessary to meet the WHO call for housing to provide adequate protection from extreme heat? Epidemiological research identifies exposure to high ambient temperatures as a significant factor of increased morbidity and mortality in developed and developing communities (Azhar et al., 2014; Basu, 2009; Dube and Rao, 2005; Medina-Ramón and Schwartz, 2007; O'Neill et al., 2005). The research uses varied empirical methods to define extreme heat in terms of outdoor temperature. Many of these empirical methods establish a threshold Apparent Temperature (T_{app})[1] above average historical daily maximum temperatures. As an example, according to Indian Meteorological Department (IMD):

> "[A] heat wave in India is declared when either there is an excess of 5 °C over a normal daily historical maximum temperature (30 year average) of less than 40°C; or an excess of 4 °C over a normal historical maximum temperature of more than 40 °C. If the actual maximum temperature is above 45 °C, is a heat wave is declared irrespective of the normal historical maximum temperature" (Azhar et al., 2014).

The IMD method for classifying extreme heat accounts for some degree of acclimatization, but none of the other factors pertinent to increase of thermal stress risk to an individual. Figure 2.1 shows this extreme outdoor temperature classification applied to Bhuj average historical daily maximums. The figure shows that there is a high potential for heatwaves to affect Bhuj from mid March through late September. This indicates that, at a minimum, buildings should protect occupants during these months.

There are two outdoor thermal standards that translate outdoor weather conditions to thermophysiological stress; the OSHA Threshold Limit Values for Thermal Stress and the Universal Thermal Climate Index (UTCI). Figure 2.2 shows how typical annual climate conditions compare to both these standards. An online program containing a number of Visual Basic macros was used to calculate WBGT for the OSHA standard and UTCI given climatic variables of temperature, humidity, solar radiation and wind speed (Climate CHIP, 2015). These variables were provided by a Typical Mean Year EnergyPlus Weather file for Bhuj, India in following the Liljegren model (Liljegren et al., 2008).

OSHA Threshold Limit Values for Thermal Stress
In 1992 The American Conference on Governmental Industrial Hygienists (ACGIH) established Threshold Limit Values (TLVs) for outdoor as well as indoor environments, in an effort to reduce environmental risk of thermal stress on workers. TLVs are set according to a Wet Bulb Globe Temperature (WBGT) Index (Finucane, 2006):

For outdoors with solar load:

$$WBGT = 0.7NWB + 0.2GT + .1DB \tag{2.1}$$

For indoor and outdoor conditions with no solar load:

$$WBGT = 0.7NWB + 0.3GT \tag{2.2}$$

[1]The United States National Weather Service defines Apparent Temperature as "the perceived temperature in degrees Fahrenheit derived from either a combination of temperature and wind (Wind Chill) or temperature and humidity (Heat Index) for the indicated hour. When the temperature at a particular grid point falls to 50 °F [10 °C] or less, wind chill will be used for that point for the Apparent Temperature. When the temperature at a grid point rises above 80 °F [27 °C], the heat index will be used for Apparent Temperature. Between 51 and 80 °F, the Apparent Temperature will be the ambient air temperature. (source:http://www.nws.noaa.gov/ndfd/definitions.htm

where:

$WBGT$	=	Wet Bulb Globe Temperature Index
NWB	=	Natural Wet-Bulb Temperature
GT	=	Globe Temperature
DB	=	Dry-Bulb Temperature

The WBGT index classifies permissible heat exposure TLVs relative to a range of a work/rest ratios as shown in Table 2.1. These TLVs are based on the assumptions that workers are fully acclimatized and that the spaces for work and rest have the same WBGT (**?**).eee

Work/Rest Regimen, Each Hour	Work Load [WGBT]		
	Light	Moderate	Heavy
100% Work	30.0°C (86°F)	26.7°C (80°F)	25.0°C (77°F)
75% Work, 25% Rest	30.6°C (87°F)	28.0°C (82°F)	25.9°C (78°F)
50% Work, 50% Rest	31.4°C (89°F)	29.4°C (85°F)	27.9°C (82°F)
25% Work, 75% Rest	32.2°C (90°F)	31.1°C (88°F)	30.0°C (86°F)

source: ACGIH 1992, OSHA 1999

Table 2.1 – ACGIH Permissible Heat Exposure Limit Value

Universal Thermal Climate Index
The Universal Thermal Climate Index (UTCI) is an accepted outdoor thermal health standard that is an translation of outdoor conditions to physiological thermal stress levels. The UTCI has been accepted as "valid in all climates, seasons and scales", and "independent of person's characteristics (age, gender, specific activities and clothing etc" (UTCI, 2015). Table 2.2 shows the UTCI heat stress classifications relative to a series of ranges of temperatures, measured in °C (UTCI, 2003).

UTCI Range [°C]	Stress Category
Above +46	Extreme Heat Stress
+38 to +46	Very Strong Heat Stress
+32 to +38	Strong Heat Stress
+26 to +32	Moderate Heat Stress
+9 to +26	Not Thermal Stress
+9 to 0	Slight Cold Stress
0 to -13	Moderate Cold Stress
-13 to -27	Strong Cold Stress
-27 to -40	Very Strong Cold Stress
Below -40	Extreme Cold Stress

source: UTCI 2003

Table 2.2 – UTCI Assessment Scale: UTCI categorized in terms of thermal stress

Figure 2.1 – Heatwave risk for Bhuj, India.

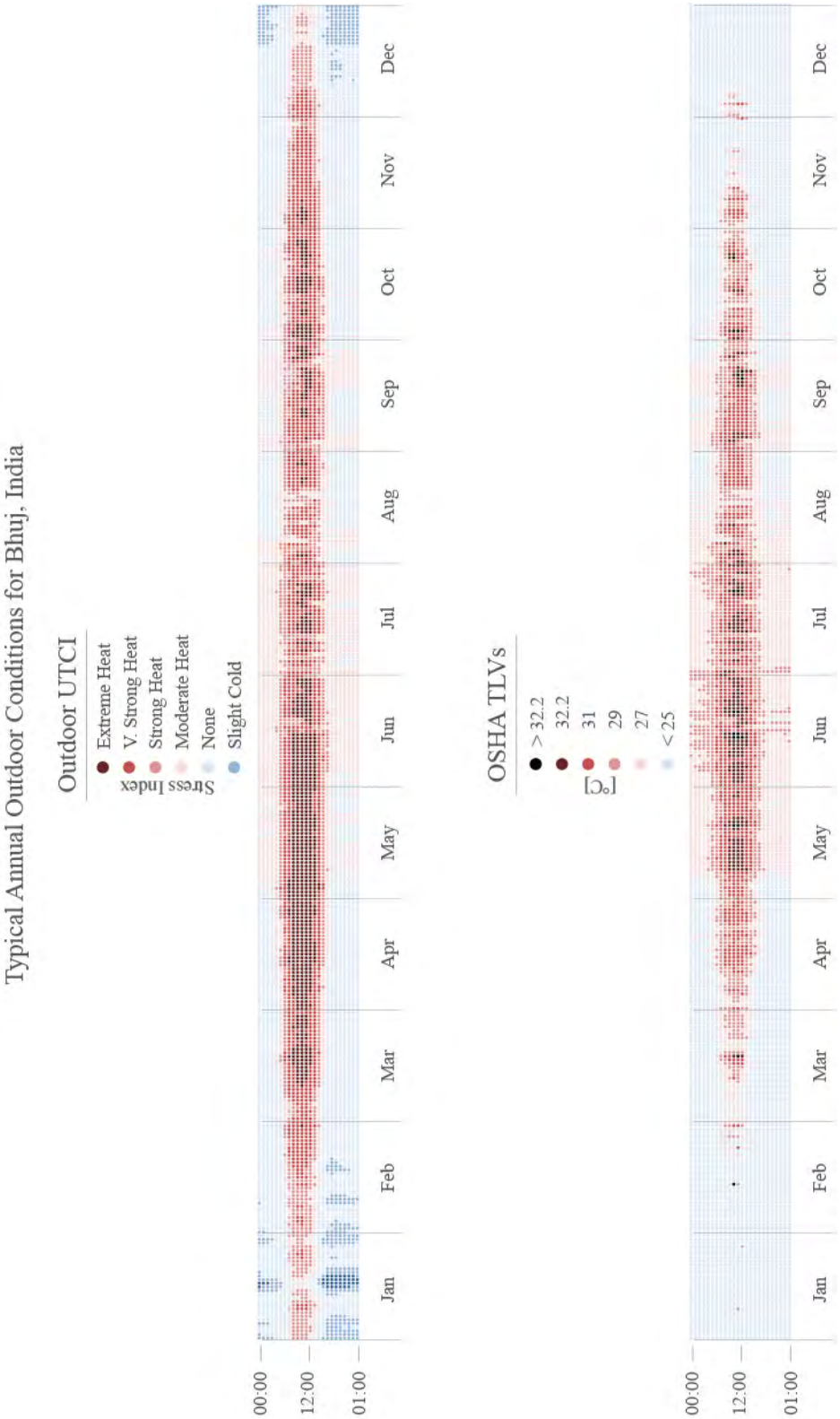

Figure 2.2 – Annual hourly map of Bhuj Typical Mean Year compared against UTCI (top) and OSHA (bottom) outdoor heat stress indices.

2.1.2 Indoor Conditions: Thermal Stress and Thermal Comfort

The question about what constitutes a thermally safe interior environment is still unanswered. And, it should be noted here, that a goal of this research is not only to improve indoor thermal conditions during periods of extreme heat, but to increase thermal health and comfort conditions year round. There are a number of standards that address acceptable limits of indoor thermal comfort, or "that condition of mind that expresses satisfaction with the thermal environment and is assessed by subjective evaluation". (ANSI/ASHRAE, 2013). For this research, indoor thermal performance is evaluated against two metrics that support passive cooling strategies: ASHRAE Standard 55-2013, "Thermal Environmental Conditions for Human Occupancy" (ANSI/ASHRAE, 2013), and the EN 15251 European Indoor Environmental Criteria (Nicol and Wilson, 2010).

ASHRAE 55 Adaptive Thermal Comfort Model
The American Society of Heating, Refrigerating, and Air-Conditioning Engineers Standard 55-2013 (ASHRAE-55) follows an adaptive model, defined as "a model that relates indoor design temperature ranges to outdoor meteorological or climatological parameters" at the 80% acceptability limit, where the thermal environment is one that "more than 80% of occupants find thermally acceptable" (ANSI/ASHRAE, 2013). Note that the unit used for acceptability limits is operative temperature, which is the average between air temperature and Mean Radiant Temperature (MRT). Equations 2.3 and 2.4 are used to determine acceptability limits.

$$Upper\ 80\%\ Acceptability\ Limit\ (^{\circ}C) = .31t_{pma(out)} + 21.3 \tag{2.3}$$

$$Lower\ 80\%\ Acceptability\ Limit\ (^{\circ}C) = .31t_{pma(out)} + 14.3 \tag{2.4}$$

Where:

$t_{pma(out)}$ = Prevailing Mean Outdoor Temperature*

* According to ASHRAE $t_{pma(out)}$ "shall be a simple arithmetic mean of all the mean daily outdoor temperatures" for 30 sequential days previous to the day in question.

EN 15251 European Indoor Environmental Criteria
The Comité Européen de Normalisation (CEN) Standard EN 15251 also follows an adaptive model, and was adopted to define acceptable indoor conditions to determine building energy use levels. Instead of % acceptability limits, the EN 15251 determines acceptability ranges based on building type and expectations of occupants (Nicol and Wilson, 2010). Category III limits reflect moderate expectations, and is generally used for existing buildings. Note that the unit used for acceptability limits is also operative temperature, which is the average between air temperature and Mean Radiant Temperature (MRT). Methods for calculating Category III operative temperature ranges are similar to ASHRAE-55 but result in a more "heat tolerant" set of limits. Equations 2.5 and 2.6 are used to determine Category III acceptability limits.

$$Upper\ Category\ III\ Limit\ (^{\circ}C) = .33t_{rm} + 22.8 \tag{2.5}$$

$$Lower\ Category\ III\ Limit\ (^{\circ}C) = .33t_{rm} + 14.8 \tag{2.6}$$

Where:

t_{rm} = running mean of the outdoor operative temperature

* This research calculates t_{rm} as the simple arithmetic mean of all the mean daily outdoor temperatures for 30 sequential days previous to the day in question.

Note about IMAC, the India Model for Adaptive (thermal) Comfort
An initiative is currently underway at CEPT University's Centre for Advanced Research in Building Science and Energy (CARBSE) to develop and standardize an Adaptive thermal comfort model specifically for India. Though this standard is not currently published, a significant finding of the initial study is that "occupants in Indian offices are more adaptive and tolerant of warmer temperatures" (Manu et al., 2014). The initial study then goes on to suggest that calculations for the IMAC uses the EN 15251 standard as a base but is "contextualized for the Indian dataset" (Manu et al., 2014).

Established vs Perceived Thermal Comfort Standards
For the purposes of measuring thermal autonomy in this research, it is necessary to rely on the established and accepted thermal comfort standards previously described. It is worthy to note, however, that through discussions with Hunnarshala Directors and various un-structured interviews with Bhuj residents, thermal comfort limits seem to be more tolerant not only of warmer temperatures than either the ASHRAE or EN 15251 standards dictate, but also of a greater fluctuation of temperatures and conditions during the day. In interviews Bhuj residents tended to agree that the months of April, May and June were generally uncomfortably to unbearably hot indoors because there was little to no reprieve from the heat during the day. They also agreed that short periods of the day during the rest of the year were uncomfortable. Many of those interviewed expressed that when it was too hot for short periods of time, they found ways to spatially adapt, by moving to a cooler room in the house, or by resting under a ceiling fan. Some mentioned the desire to live without mechanical cooling because a stark contrast between outdoor and indoor conditions felt like they were being separated from their sense of place. As an anecdote, during a co-design meeting I attended, (with only a few days of adaptation to climate behind me) at Hunnarshala in March 2015, when outdoor temperatures exceeded 40°C, indoor air temperatures reached 36°C, the meeting proceeded without being disrupted by the heat. The four Hunnarshala Directors in attendance commented during this meeting that temperatures of up to 36°C *might* be within acceptable limits, but that lower temperatures would be preferable. Though not quantifiable, these observations are important to acknowledge.

2.2 Madhapar Mistri Caste and Rajiv Awas Yojana Slum Free Bhuj Courtyard House Typologies

The Mistri caste is known for its master craftsman, artisans and builders that migrated to the Kutch region in the early 7th century (Mevada, 2008). The Mistris built a number of settlements near Bhuj that are in many ways typical to vernacular hot and arid house typologies worldwide (described in Section 1.1). In Madhapar, a Mistri neighborhood built around the time of the construction of the railroad in Kutch that still thrives near Bhuj City, rule of thumb Design with Climate strategies are manifest in the buildings. Row after row of clustered courtyard houses are oriented with their short walls facing east/west, so their long walls are shared with adjacent buildings and so that the upper floors of the houses

can take advantage of cool evening breezes coming from the southwest. Streets are narrow so the houses protect each other from solar radiation during the day. Houses are generally constructed from thick (30-40 cm) sandstone walls and are traditionally plastered with a mud and straw mixture to increase the walls' thermal resistance. The courtyard serves to protect interior environments from hot outside breezes during the day but doors and windows can be opened to them at night to allow for night flush ventilation. The courtyards are also where many of the wet functions occur such as washing, laundry and cleaning. This programmatic function of the courtyard aids in evaporative cooling of the houses' micro-climates. Building interiors are low-lit by small openings and many houses have high ceilings and high ventilator windows (Figure 2.4).

Figure 2.3 – Mistri Madhapar neighborhood site plan (left) and three variations of the house typology (right). Drawings by Shilpa Mevada (Mevada, 2008, p. 26, 52, 58, 62)

Figure 2.4 – Images of Madhapar Neighborhood and House Typology. Left: Narrow alleyway typical to Madhapar. Center: Typical programmatic functions of courtyard. Right: Typically dark house interiors with high ceilings and high ventilator windows.

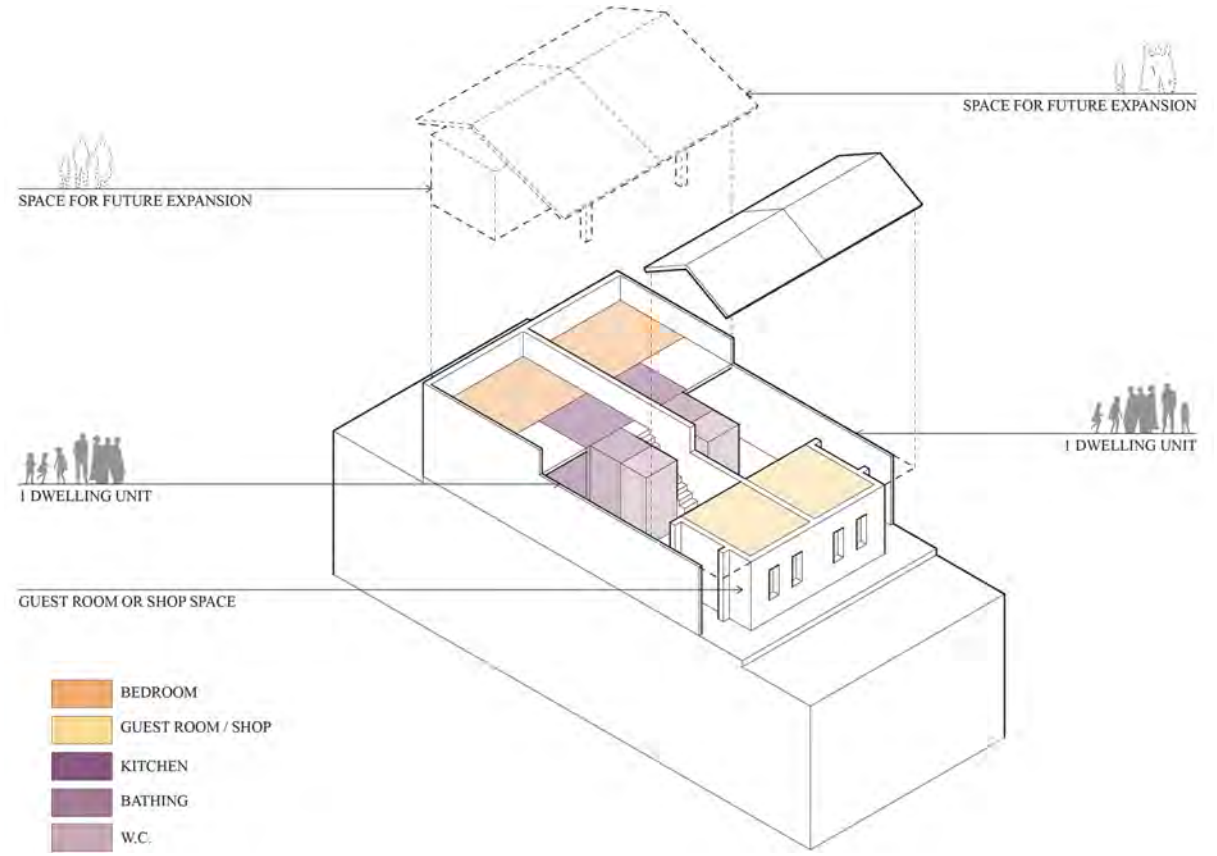

Figure 2.5 – Example of one Hunnarshala RAY house typology, based on the traditional Madhapar house. Drawn by David Moses.

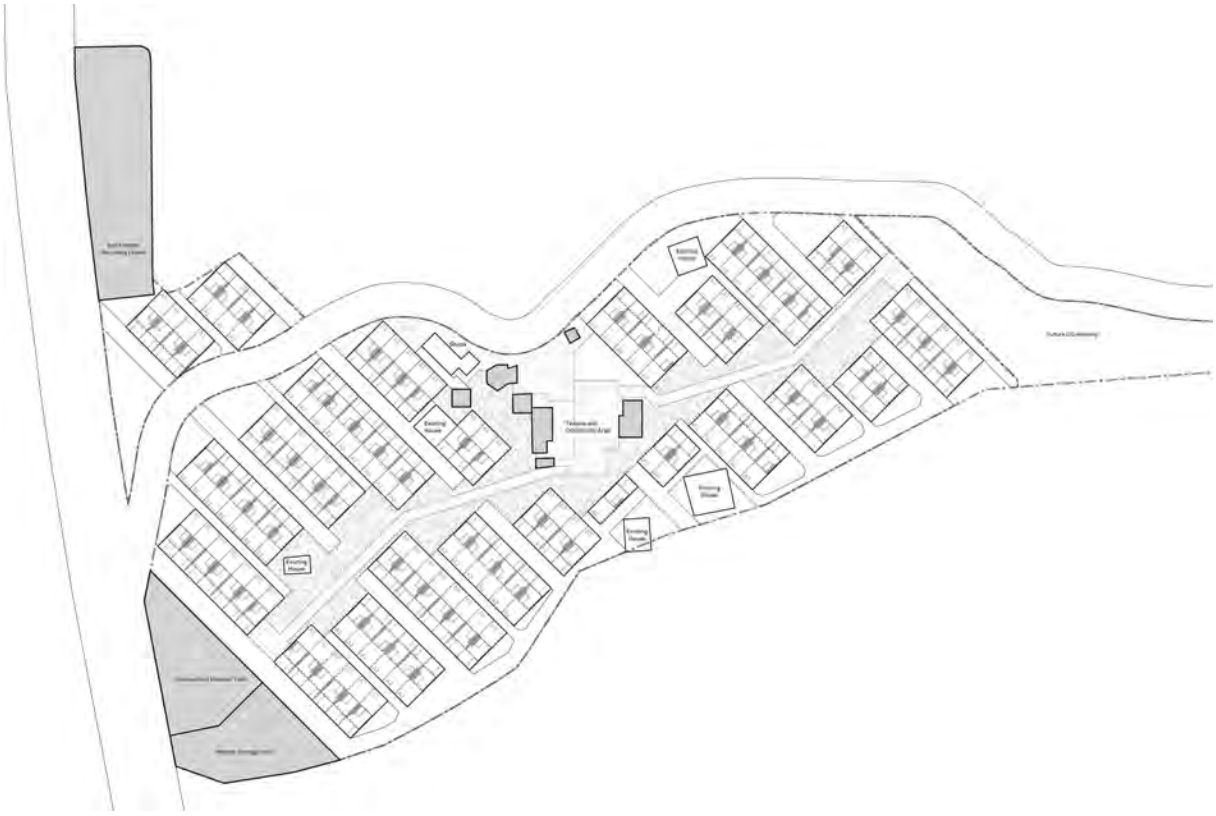

Figure 2.6 – Initial site plan for the Ramdevnagar community RAY re-development. Site Plan re-drawn by David Moses.

Hunnarshala's designs for the Rajiv Awas Yojana (RAY) *Slum Free Bhuj* house typology follow some of the Design with Climate Strategies that are manifest in the Madhapar houses. Where possible these courtyard houses share long axis walls (Figure 2.5) and are clustered along narrow streets for self-shading. These houses have been designed to be built with 23 cm local sandstone block walls, and with framed clay tile or sheet material roofs. Figure 2.6 shows one proposed site plan for the Ramdevnagar community re-development.

2.3 Typical Bhuj Informal and Slum Re-Development Construction

Figure 2.7 – Common Bhuj Informal Housing Construction Types. Examples of temporary to more permanent construction types are pictured from left to right.

Based on observations from field visits to slum and slum re-development sites near Bhuj City in January and August 2014, low cost housing construction types are generally classified for this study according to roof and wall materials. These types set the context for initial simulations which are detailed in Chapter 4. Dwellings are commonly stand-alone, single or double room structures where members of one to three generations of a family live together and perform a variety of daily tasks, thus the dwellings are usually occupied at all hours of the day. Common outdoor spaces are shared between multiple dwellings and in denser settlements, where dwellings are clustered together, it is common for multiple structures to share walls and/or be in close enough proximity to shade each other in various orientations. Of the temporary structures observed in the villages of Bhachau, Ramdevnagar and Bhimraonagar, walls and roofs are typically constructed from one or a combinations of found or purchased metal, asbestos cement, or plastic sheet materials. Semi-permanent structures can be identified by walls that are sandstone, clay brick, concrete masonry unit (CMU) block, or are earthen, and roofs tend to be constructed from the aforementioned sheet materials or from thin layers of thatch protected by plastic sheets. The most permanent of the typologies were found in the Gujarat Industrial Development Corporation (GIDC) relocation site, as well as the villages of Ramdevnagar, Bhimraonagar, and Anjar. These permanent structures can be identified by their masonry, earth, or cast reinforced cement concrete (RCC) walls and roofs are generally framed with clay tile or sheet material as an outer material. RCC slab roofs are also seen, though tile and sheet roofs are more common. Though existing construction types of slum re-development housing vary, generally the roofs of more permanent types are uninsulated and provide very little resistance to heat gain due to intense solar radiation. Openings of all types are rarely glazed, but are usually outfitted with manually operable shutters, dampers, or opaque panels. Ceiling fans are common in structures with RCC slab or framed roofs. Residents who were asked about fan and window operation all reported that during the summer, windows remain open and fans remain on during occupied hours (through the day and night), and operation during cooler winter months varies.

Note that three informal house types were included in the existing building case study set, which is detailed in Chapter 3.

Chapter 3

Existing Building Analysis and Energy Model Simulation Methods

Five existing buildings, typical to Bhuj, but of varied construction types, are case studies in a series of digital and physical thermal performance analyses. There are four overlapping objectives for existing building thermal analysis. The first objective was to develop an understanding of context, by studying typologies that reflect both the vernacular and contemporary building practices of Bhuj, to inform future design decisions, which are discussed in detail in chapters 4, 5 and 6. The second, detailed in sections 3.1, 3.3 and 3.4, was to develop a method to use existing buildings for energy modeling, to first predict thermal performance using typical mean year climate data, then validate those predictions by calibrating the models to actual climate conditions, and comparing the digital model outputs with actual measured data. The third objective, detailed in section 3.2 was to test the experimental set up of thermal sensors and data loggers that would be employed in a series of prototype thermal performance experiments detailed in 5. The fourth objective is to acquire a thermal performance data set on which Hunnarshala can build future thermal research and use to influence slum redevelopment building guidelines.

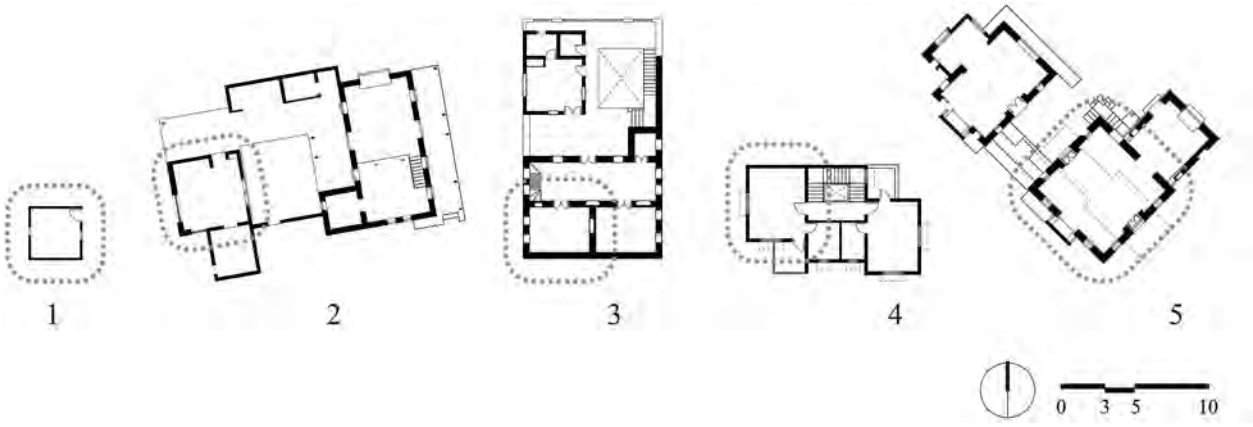

Figure 3.1 – Key plans showing case study buildings B1, B2, B3, B4 and B5. Dashed bubbles indicate simulated thermal zones.

3.1 Initial Predictions of Existing Building Thermal Performance

Figure 3.1 is a keyplan for five existing Bhuj buildings that were chosen as representative of traditional to contemporary, as well as slum and non-slum typologies. Construction and treatment of walls and roofs vary widely between the five buildings, which is described in further detail below. Ventilation practices also varied according to occupant preference. Each building was drawn and surveyed to determine a) building size, geometry, orientation, site placement relative to adjacent structures, and other shading elements, b) wall materials, finishes and thicknesses, c) roof materials, finishes, and insulation levels, and d) opening, size, placement, shading elements and whether it was glazed or un-glazed. Building occupants were informally interviewed to estimate a) number of occupants, b) occupancy schedule c) appliance use that could contribute to internal gains and d) general operation of windows to determine ventilation schedules. This information was then input into uncalibrated energy models to predict annual performance of each type for a typical mean year in Bhuj. All models were simulated using EnergyPlus as the engine and DesignBuilder as the GUI using the Bhuj Typical Mean Year .epw file from previous climate analysis. Because average wind data in TMY.epw files is unreliable, the wind factor in each model was set to 0, and a best guess was made for infiltration rate settings based on a visual assessment of each space and informal interviews. It is also important to note that while shade producing site elements and building elements were modeled, vegetation was not. These initial models serve as a ballpark estimate of relative performance between types. Tables 3.1 through 3.10 show the material and schedule properties that were inputs for EnergyPlus where:

for material properties:

L	=	Average Wall Thickness	(cm)
U	=	Overall U Value for the Assembly	(W/m^2 °K)
k	=	Outermost Material Conductivity	(W/m °K)
ρ	=	Density	(kg/m^3)
C_p	=	Specific Heat	(J/kg °K)
ε	=	Emissivity	(-)
α	=	Solar Absorptance	(-)

and for other properties:

If any of the zone's walls are shared with adjacent structures, wall orientation is indicated.
If un-shared walls are shaded by nearby site elements or roof overhangs, wall orientation is indicated.
If openings are shaded by shutters or curtains, operation schedule is indicated in days and hours.

Constant infiltration rate in air changes per hour, (ac/h)
Occupancy Schedule during days of week and hours of day.
Occupant Density, in people per m^2, (p/m^2)
Ventilation Schedule during days of week and hours of day where window operation is possible.
Ventilation type during span of schedule (i.e. windows constantly open, or only when $T_{in} > T_{out}$).

In the following subsections, these properties are defined for each of the five case study buildings in table form. Then for each, three annual hourly temperature maps are shown for comparison of annual thermal performance (Figures 3.3, 3.5, 3.7, 3.9 and 3.11). The maps show hourly indoor air temperatures in °C as well as hourly operative temperatures which are compared to two adaptive thermal comfort standards: the ASHRAE-55 80% Acceptability Limits in addition to the more "heat tolerant" EN 15251 Category III Acceptability Limits (described in Section 2.1). The captions for these figures list thermal performance statistics for each building type, including the percent of the year indoor air temperatures exceed 34 °C, the maximum air temperature reached, the maximum operative temperature reached, and the percent of the year when operative temperatures exceed ASHRAE or EN 15251 Limits.

It is important to evaluate the models in this way because the five types are so diverse in their materials and schedules, one metric will not suffice to determine thermal performance. For example, one can assume, without any simulation, that B1, a building with no shared or shaded 15 cm thick thermal mass walls, and uninsulated roof, will be much warmer during the day than B5, which has shared, well shaded 30 cm walls, and a highly insulated roof. When we compare Figure 3.3 to Figure 3.11 though, we see that the uncalibrated predictive models show that B1 reaches a maximum air temperature of 41 °C and a maximum operative temperature of 47 °C, while B5 reaches a higher maximum air temperature of 44 °C, likely due to the fact that it is constantly ventilated, but a maximum operative temperature of 41 °C, due to much lower radiant temperatures from protected, thermally massive, and highly insulative materials. Furthermore, the predictions show that B1 exceeds EN 15251 Acceptability Limits 33% of the year as opposed to 14% for B5, a difference which is equivalent to about 70 days of the year of cooler operative temperatures. In two other cases, B3, and B4, the maximum air and operative temperatures for both match, reaching 38 °C, but this is not necessarily a good indication of relative thermal performance either, because the models indicate that B3 exceeds ASHRAE limits 44% of the year as opposed to B4's 33% a difference which is equivalent to about 40 days of the year of cooler operative temperatures.

One still might argue that because the case study houses are so different from each other, it is impossible to make comparisons that lead to valid and definitive conclusions to prioritize one Design with Climate strategy over the other. For this reason, it is important to look at the daily and seasonal trends for each building as they compare to each other. Daily and seasonal trends are noted for each building in the subsections below. Here, in the initial stages of building performance analysis, we can make analogous comparisons between building types. The visualizations help to answer important questions about trends in a building's thermal behavior such as:

Do indoor temperatures reflect or moderate outdoor conditions?
Does the building gain heat rapidly or slowly during the day?
Does the building lose heat rapidly at night or retain it?
Does the building maintain acceptable temperatures during hot as well as cold seasons?

Section 3.4 will show how the initial models vary, sometimes widely in absolute temperatures, from measured data. But for each case, these initial, uncalibrated simulations establish appropriate daily and seasonal trends that are upheld by measured data. Though these models cannot be relied on for conclusive comparisons, they are a necessary step in the development of a method to dissect, measure, and validate long accepted rules of thumb for Design with Climate strategies.

Building 1 - Description, Energy Plus Parameters, and Initial Thermal Performance Predictions

Figure 3.2 – Exterior images of Building 1. Left: Looking at the building from the northeast. Right: close view of exterior roof to wall connection on the southwest wall.

Description

Building 1 (B1) is a single room dwelling with 15 cm thick solid CMU walls and an uninsulated asbestos cement corrugated sheet roof. It is largely unprotected from direct solar gain. Though of typical construction to informal housing communities, this particular dwelling is unoccupied for all but a few hours during mid-day. The house is equipped with an electric ceiling fan, used when occupied on warm days. Two small un-glazed windows on the east and west facades are kept open on a similar schedule. Building performance statistics are listed in the caption of Figure 3.3. The figure shows that air and operative indoor temperatures generally reflect outdoor conditions. B1 cools quickly at night, and at times over-cools well below thermal comfort limits.

Construction Type Properties																
Walls		E+ Wall Total U Value	E+ Wall Outer Material Properties					Roof		E+ Roof Total U Value	E+ Roof Outer Material Properties					
Material	L	U	k	ρ	c_p	ε	α	Material	L	U	k	ρ	c_p	ε	α
	[cm]	[W/m^2°K]	[W/m°K]	[kg/m^3]	[J/kg°K]				[cm]	[W/m^2°K]	[W/m°K]	[kg/m^3]	[J/kg°K]		
Solid CMU	15	2.16	0.79	1950	840	0.9	0.6	AC corr Sheet	0.1	6.38	0.36	1500	1050	0.9	0.7

Table 3.1 – Wall and roof construction type properties for B1, used as inputs for initial EnergyPlus models.

Non-Construction Type Properties													
Walls Shared w/ Adj Bldgs				Shaded Un-Shared Walls				Window Shading	Infilt. Rate	Occupancy		Ventilation		Int Gains	Notes
N	S	E	W	N	S	E	W	schedule	[ac/h]	schedule	[p/m^2]	schedule	type	[W/m^2]	
none				none				Mon-Sun 0:00-24:00	0.5	Mon-Sun 11:00-14:00	0.2	Mon-Sun 11:00-14:00	constant	20	*oriented 32° NE. *typical low cost house type *all surfaces unprotected *irregular schedules

Table 3.2 – Occupancy, Ventilation, and Shading Schedules for B1, used as inputs for initial EnergyPlus models.

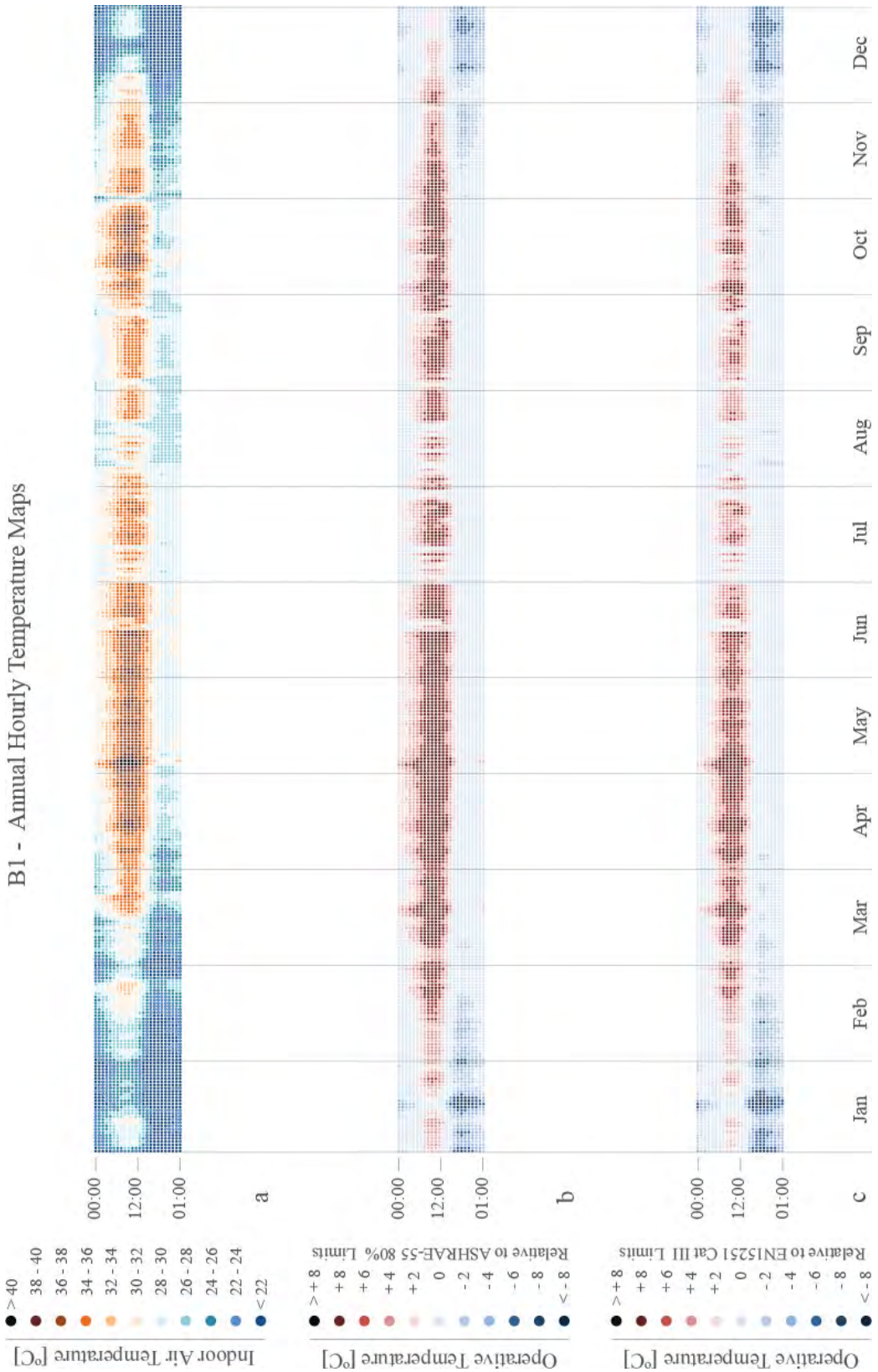

Figure 3.3 – Annual hourly temperature maps plotting thermal performance predictions for B1. Top: Map a is an annual hourly plot of predicted indoor temperatures for every hour of the year. The model predicts indoor temperatures will exceed 34 °C 16% of the year (equivalent to about 58 days) and the maximum air temperature reached is 41 °C. Middle: Map b is an hourly plot of operative temperatures as they compare to the ASHRAE-55 80% Acceptability Limits. The model predicts that indoor operative temperatures will exceed 80% limits 46% of the year and will reach up to 47 °C. Bottom: Map c is an hourly plot of operative temperatures as they compare to the more "heat tolerant" EN 15251 Category III Acceptability Limits. The model predicts that indoor operative temperatures will exceed category III limits 33% of the year (equivalent to about 120 days).

Building 2 - Description, Energy Plus Parameters, and Initial Thermal Performance Predictions

Figure 3.4 – Exterior images of Building 2. Left: Looking at a portion of the building from the west. Right: close view of exterior roof country tile detail.

Description

Building 2 (B2) is a multi-room dwelling with +/- 30 cm thick sandstone block walls, some light in color, and an a single-layer country tile roof. All walls are well shaded by adjacent structures, site elements, and/or large roof overhangs. The modeled thermal zone in this dwelling is generally occupied by two people during evening hours. The zone is equipped with an electric ceiling fan, used on warm days. All windows are un-glazed and well shaded by operable louvered shutters. Building performance statistics are listed in the caption of Figure 3.5. The figure shows that air temperatures generally reflect outdoor conditions, but that operative temperatures are more moderate than B1.

Construction Type Properties																
Walls		E+ Wall Total U Value	E+ Wall Outer Material Properties					Roof		E+ Roof Total U Value	E+ Roof Outer Material Properties					
Material	L	U	k	ρ	c_p	ε	α	Material	L	U	k	ρ	c_p	ε	α
	[cm]	[W/m^2°K]	[W/m°K]	[kg/m^3]	[J/kg°K]				[cm]	[W/m^2°K]	[W/m°K]	[kg/m^3]	[J/kg°K]		
Sndstn Block	30	2.44	1.30	2200	712	0.9	0.2	Cntry Tile	1.50	2.25	0.81	1700	840	0.9	0.6

Table 3.3 – Wall and roof construction type properties for B2, used as inputs for initial EnergyPlus models.

Non-Construction Type Properties													
Walls Shared w/ Adj Bldgs				Shaded Un-Shared Walls				Window Shading	Infilt. Rate	Occupancy		Ventilation		Int Gains	Notes
N	S	E	W	N	S	E	W	schedule	[ac/h]	schedule	[p/m^2]	schedule	type	[W/m^2]	
								Mon-Sun 0:00-24:00	3	Mon-Sun 19:00-6:00	0.1	Mon-Sun 19:00-6:00	constant	10	*all walls well shaded, west wall white *single layer country tile roof *generally for sleep *windows are screened, not glazed

Table 3.4 – Occupancy, Ventilation, and Shading Schedules for B2, used as inputs for initial EnergyPlus models.

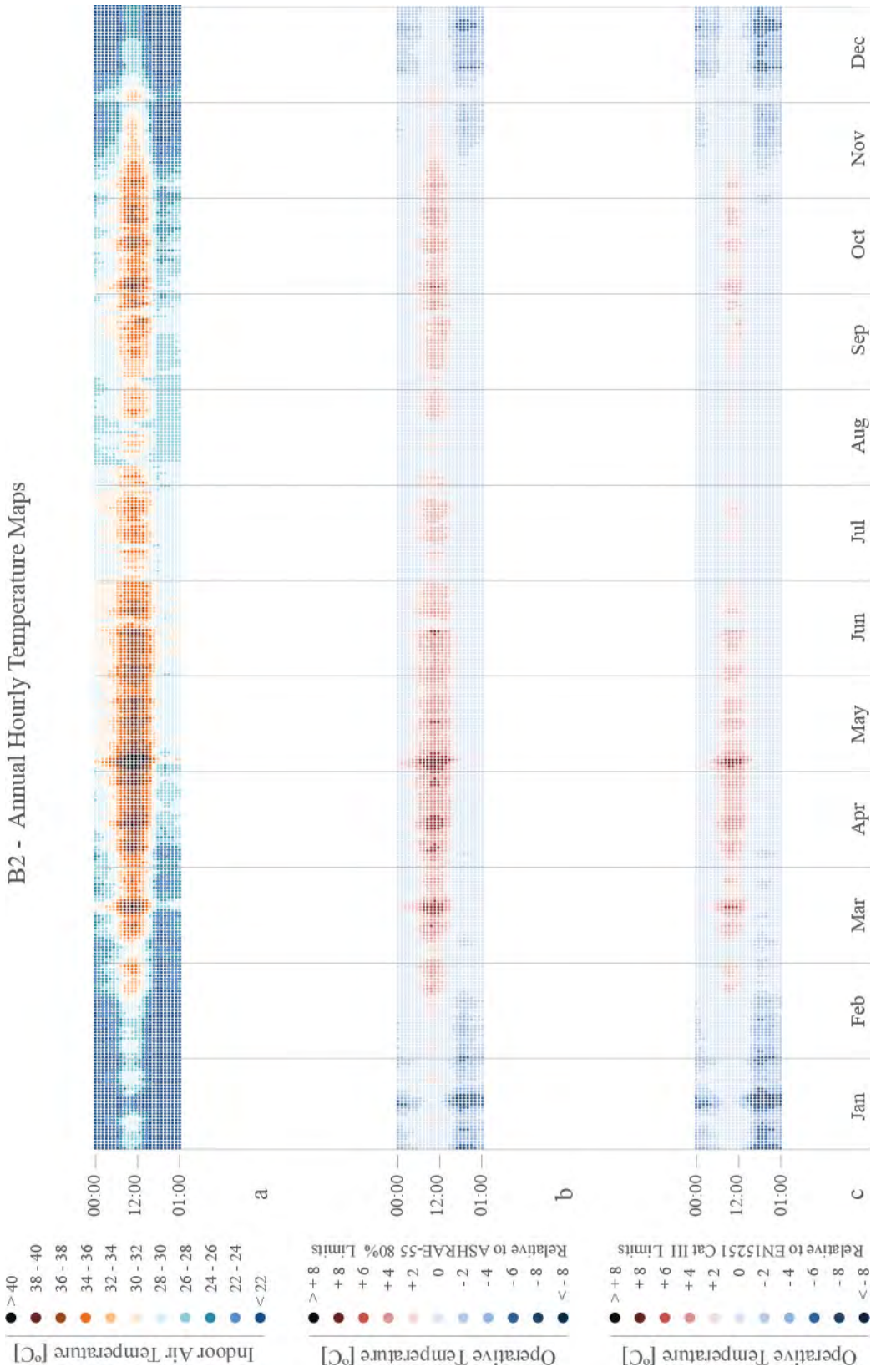

Figure 3.5 – Annual hourly temperature maps plotting thermal performance predictions for B2. Top: Map a is an annual hourly plot of predicted indoor temperatures for every hour of the year. The model predicts indoor temperatures will exceed 34 °C 10% of the year (equivalent to about 37 days) and the maximum air temperature reached is 43 °C. Middle: Map b is an hourly plot of operative temperatures as they compare to the ASHRAE-55 80% Acceptability Limits. The model predicts that indoor operative temperatures will exceed 80% limits 29% of the year and will reach up to 41 °C. Bottom: Map c is an hourly plot of operative temperatures as they compare to the more "heat tolerant" EN 15251 Category III Acceptability Limits. The model predicts that indoor operative temperatures will exceed category III limits 16% of the year (equivalent to about 58 days).

Building 3 - Description, Energy Plus Parameters, and Initial Thermal Performance Predictions

Figure 3.6 – Exterior images of Building 3. Left: View of the north facade. Right: View into courtyard during mid-day.

Description

Building 3 (B3) is typical of the vernacular Madhapar courtyard house. It is a multi-room, multi-floor dwelling with light colored 35 cm thick plastered sandstone block walls and a double-layer country tile roof with an interior false ceiling. All walls are protected by adjacent structures, site elements, and/or roof overhangs. The modeled thermal zone is on the top floor and is rarely occupied. It is equipped with an electric ceiling fan, used when occupied on warm days. All windows are un-glazed and well shaded by operable opaque panel shutters. Performance statistics are listed in the caption of Figure 3.7. The figure shows that both air and operative temperatures moderate outdoor conditions throughout the year.

Construction Type Properties

Walls		E+ Wall Total U Value	E+ Wall Outer Material Properties					Roof		E+ Roof Total U Value	E+ Roof Outer Material Properties				
Material	L	U	k	ρ	c_p	ε	α	Material	L	U	k	ρ	c_p	ε	α
	[cm]	[W/m^2°K]	[W/m°K]	[kg/m^3]	[J/kg°K]				[cm]	[W/m^2°K]	[W/m°K]	[kg/m^3]	[J/kg°K]		
Sndstn Block	35	2.64	1.83	2200	712	0.9	0.2	Cntry Tile	3.00	1.09	0.81	1700	840	0.9	0.6

Table 3.5 – Wall and roof construction type properties for B3, used as inputs for initial EnergyPlus models.

Non-Construction Type Properties

Walls Shared w/ Adj Bldgs				Shaded Un-Shared Walls				Window Shading	Infilt. Rate	Occupancy		Ventilation		Int Gains	Notes
N	S	E	W	N	S	E	W	schedule	[ac/h]	schedule	[p/m^2]	schedule	type	[W/m^2]	
								Mon-Sun 0:00-24:00	0.5	Mon-Sun 19:00-6:00	0.05	rare	none	0	*all walls well shaded, e/w wall white *dbl layer country tile roof - false ceil *rarely occupied *windows are screened, not glazed, opaque panel shutters

Table 3.6 – Occupancy, Ventilation, and Shading Schedules for B3, used as inputs for initial EnergyPlus models.

Figure 3.7 – Annual hourly temperature maps plotting thermal performance predictions for B3. Top: Map a is an annual hourly plot of predicted indoor temperatures for every hour of the year. The model predicts indoor temperatures will exceed 34 °C 6% of the year (equivalent to about 22 days) and the maximum air temperature reached is 38 °C. Middle: Map b is an hourly plot of operative temperatures as they compare to the ASHRAE-55 80% Acceptability Limits. The model predicts that indoor operative temperatures will exceed 80% limits 44% of the year and will reach up to 38 °C. Bottom: Map c is an hourly plot of operative temperatures as they compare to the more "heat tolerant" EN 15251 Category III Acceptability Limits. The model predicts that indoor operative temperatures will exceed category III limits 11% of the year (equivalent to about 40 days).

Building 4 - Description, Energy Plus Parameters, and Initial Thermal Performance Predictions

Figure 3.8 – Exterior images of Building 4. Left: View of the south facade. Right: View into side yard during mid-day.

Description

Building 4 (B4)is a contemporary multi-room, multi-floor dwelling with white 23 cm thick reinforced cast concrete (RCC) walls and a 12 cm thick white RCC slab roof. All walls are protected by adjacent structures, site elements, and/or roof overhangs. The modeled thermal zone is on the top floor and is occupied by three people during evening hours. It is equipped with an electric ceiling fan, and the occupants practice night flush ventilation. All windows are glazed and well shaded by nearly opaque interior curtains. Performance statistics are listed in the caption of Figure 3.9. The figure shows that both air and operative temperatures moderate outdoor conditions throughout the year.

Construction Type Properties

Walls		E+ Wall Total U Value	E+ Wall Outer Material Properties					Roof		E+ Roof Total U Value	E+ Roof Outer Material Properties				
Material	L	U	k	ρ	c_p	ε	α	Material	L	U	k	ρ	c_p	ε	α
	[cm]	[W/m^2°K]	[W/m°K]	[kg/m^3]	[J/kg°K]				[cm]	[W/m^2°K]	[W/m°K]	[kg/m^3]	[J/kg°K]		
Cast RCC	23	3.43	1.90	2300	840	0.9	0.25	Cast RCC	12	2.80	1.4	2100	840	0.9	0.2

Table 3.7 – Wall and roof construction type properties for B4, used as inputs for initial EnergyPlus models.

Non-Construction Type Properties

Walls Shared w/ Adj Bldgs				Shaded Un-Shared Walls				Window Shading	Infilt. Rate	Occupancy		Ventilation		Int Gains	Notes
N	S	E	W	N	S	E	W	schedule	[ac/h]	schedule	[p/m^2]	schedule	type	[W/m^2]	
								Mon-Sun 0:00-24:00	0.5	Mon-Sun 19:00-6:00	0.3	windows open when $T_{in} > T_{out}$		15	*all walls well shaded, bright white *RCC roof with white tile exterior *night flush vent practiced *windows covered during the day and glazed

Table 3.8 – Occupancy, Ventilation, and Shading Schedules for B4, used as inputs for initial EnergyPlus models.

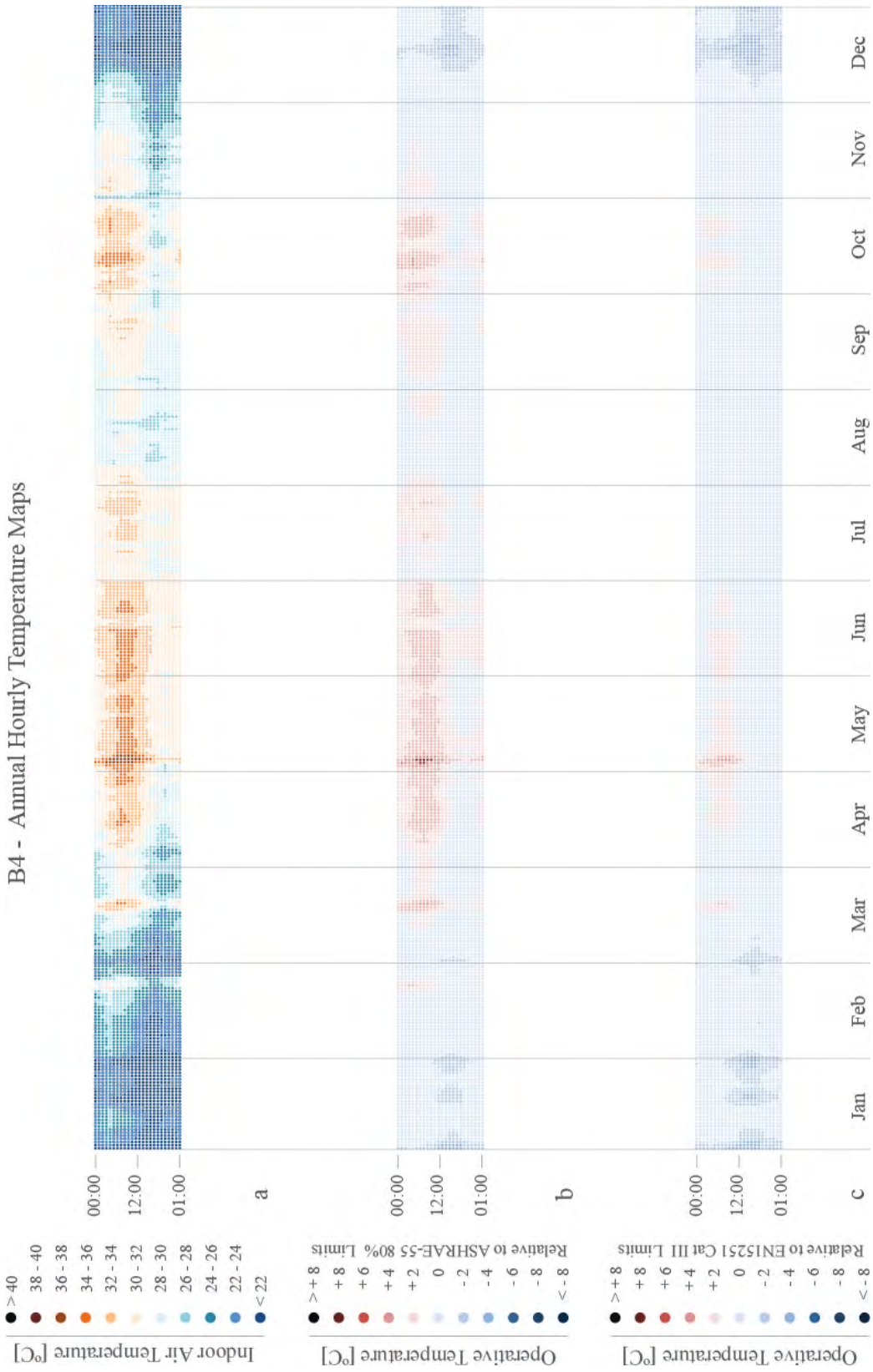

Figure 3.9 – Annual hourly temperature maps plotting thermal performance predictions for B4. Top: Map a is an annual hourly plot of predicted indoor temperatures for every hour of the year. The model predicts indoor temperatures will exceed 34 °C 1% of the year (equivalent to about 4 days) and the maximum air temperature reached is 38 °C. Middle: Map b is an hourly plot of operative temperatures as they compare to the ASHRAE-55 80% Acceptability Limits. The model predicts that indoor operative temperatures will exceed 80% limits 33% of the year and will reach up to 38 °C. Bottom: Map c is an hourly plot of operative temperatures as they compare to the more "heat tolerant" EN 15251 Category III Acceptability Limits. The model predicts that indoor operative temperatures will exceed category III limits 7% of the year (equivalent to about 26 days).

Building 5 - Description, Energy Plus Parameters, and Initial Thermal Performance Predictions

Figure 3.10 – Exterior images of Building 5. Left: View of the southwest facade. Right: Interior view of thatch roof overhang and open-air clerestory window.

Description

Building 5 (B5) is an open plan studio space, with +/- 30 cm thick adobe and CSEB block walls and a +/- 40cm thatch roof. All walls are generally protected by adjacent structures, site elements, and/or roof overhangs. B4 is occupied by anywhere from 4 to 20 people at irregular times during weekday office hours. It is equipped with five electric ceiling fans, which are used during warm days. Lower and southwest windows are glazed and well shaded roof by overhangs or interior shutters. Upper clerestories are open to the air constantly. Performance statistics are listed in the caption of Figure 3.9. The figure shows that air temperatures reflect outdoor conditions, but that operative temperatures are more moderate.

Construction Type Properties																
Walls		E+ Wall Total U Value	E+ Wall Outer Material Properties					Roof		E+ Roof Total U Value	E+ Roof Outer Material Properties					
Material	L	U	k	ρ	c_p	ε	α	Material	L	U	k	ρ	c_p	ε	α
	[cm]	[W/m²°K]	[W/m°K]	[kg/m³]	[J/kg°K]				[cm]	[W/m²°K]	[W/m°K]	[kg/m³]	[J/kg°K]		
Adobe + CSEB	30	2.99	1.83	2200	710	0.9	0.6	Thatch	40	0.17	0.07	240	180	0.9	0.6

Table 3.9 – Wall and roof construction type properties for B5, used as inputs for initial EnergyPlus models.

Non-Construction Type Properties													
Walls Shared w/ Adj Bldgs				Shaded Un-Shared Walls				Window Shading	Infilt. Rate	Occupancy		Ventilation		Int Gains	Notes
N	S	E	W	N	S	E	W	schedule	[ac/h]	schedule	[p/m²]	schedule	type	[W/m²]	
								Mon-Sat 8:00-6:00	5	Mon-Sat 8:00-6:00	0.1	Mon-Sat 8:00-6:00	constant	15	*oriented 45° NW *all walls well shaded *some eindows glazed, upper windows open

Table 3.10 – Occupancy, Ventilation, and Shading Schedules for B5, used as inputs for initial EnergyPlus models.

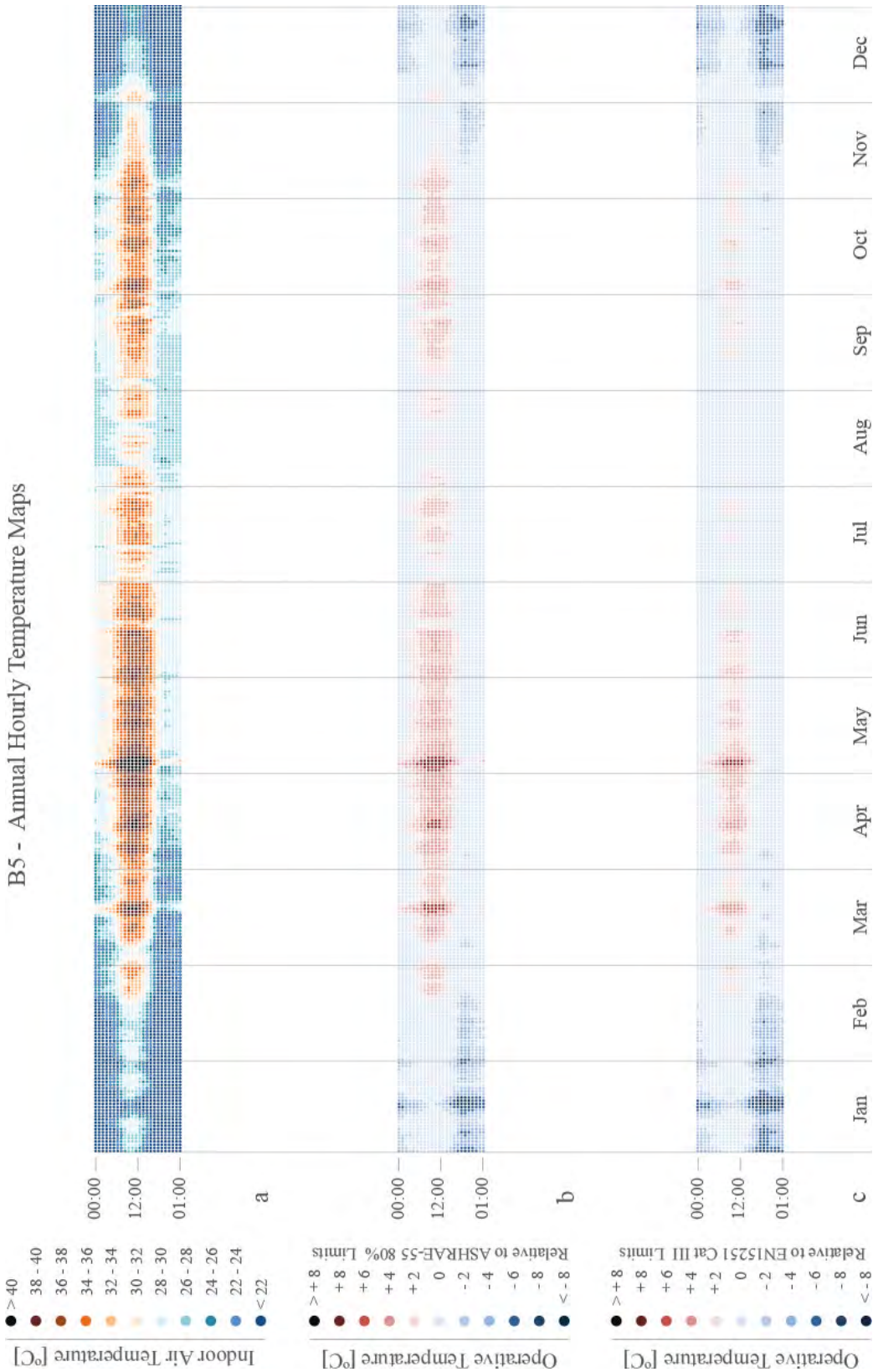

Figure 3.11 – Annual hourly temperature maps plotting thermal performance predictions for B5. Top: Map a is an annual hourly plot of predicted indoor temperatures for every hour of the year. The model predicts indoor temperatures will exceed 34 °C 16% of the year (equivalent to about 58 days) and the maximum air temperature reached is 44 °C. Middle: Map b is an hourly plot of operative temperatures as they compare to the ASHRAE-55 80% Acceptability Limits. The model predicts that indoor operative temperatures will exceed 80% limits 30% of the year and will reach up to 41 °C. Bottom: Map c is an hourly plot of operative temperatures as they compare to the more "heat tolerant" EN 15251 Category III Acceptability Limits. The model predicts that indoor operative temperatures will exceed category III limits 14% of the year (equivalent to about 51 days).

3.2 Data Collection

Exterior and interior sensors and data loggers record hourly air and surface temperature, relative humidity, and solar radiation data for the purposes of direct comparison of Bhuj existing building thermal performance (Section 3.3), validation of the initial uncalibrated models (shown in Section 3.1), as well as energy model calibration (shown in Section 3.4) for annual thermal autonomy predictions. This section describes the equipment, setup and data collection periods. Figures 3.12 through 3.16 show the locations and images of the sensors in each of the five buildings.

3.2.1 Interior Data Collection

Interior Surface Temperature Equipment and Setup
Each of the existing Bhuj buildings were outfitted with three surface temperature sensors (HOBO TMC6-HD), connected to a HOBO UX120 4-Channel Analog Data Logger (UX120-006M), to measure hourly temperatures of the ceiling, south wall, and west wall. In each wall, the sensors were coated with thermal paste and inserted into a 3 cm deep, .5 cm diameter drilled hole, so that the entire surface of the sensor was in contact with the wall. The hole with the sensor inserted was then fixed in place with a minimal application of silicon caulk at the exposed end. Ceiling sensors were mounted in the same fashion in building 4 (concrete slab roof) and were sandwiched between the innermost roof assembly layers of buildings 1, 2, 3, and 5.

Interior Air Temperature/Relative Humidity Equipment and Setup
Interior air temperature and relative humidity hourly values were recorded using a HOBO UX100 Temp/RH 3.5% Data Logger (UX100-003). Initially the data loggers were hung on strings in the middle of the room, just above head height, but soon after installation this position proved to be obtrusive to occupants. Where possible, data loggers were kept in the center of the room but were moved up to within 1 m of the ceiling. It was noted that this practical installation measure might show increased temperatures due to stratification of hot air, especially in B5, the design studio, which has the highest ceilings of the group.

Interior Data Collection Period
Due to staggered shipments of equipment, interior data collection began at various times between August 14 and September 25 2014, and will record hourly data through late August 2015. As the project progressed, additional sets of sensors were installed in a house with an uninsulated Mangalore tile roof and CMU walls, and second reinforced concrete building, both of which are briefly described at the end of Section 3.3. While data from these types are not included to the same extent as the initial five in this thesis analysis, a direct comparison of all seven case study buildings is shown for measurements from February 24th through March 23rd and a full cross analysis of all seven buildings is planned to be completed in fall of 2015.

3.2.2 Exterior Data Collection

Exterior Air Temperature/Relative Humidity Equipment and Setup
Exterior air temperature and relative humidity hourly values were recorded using a HOBO U23 Pro v2

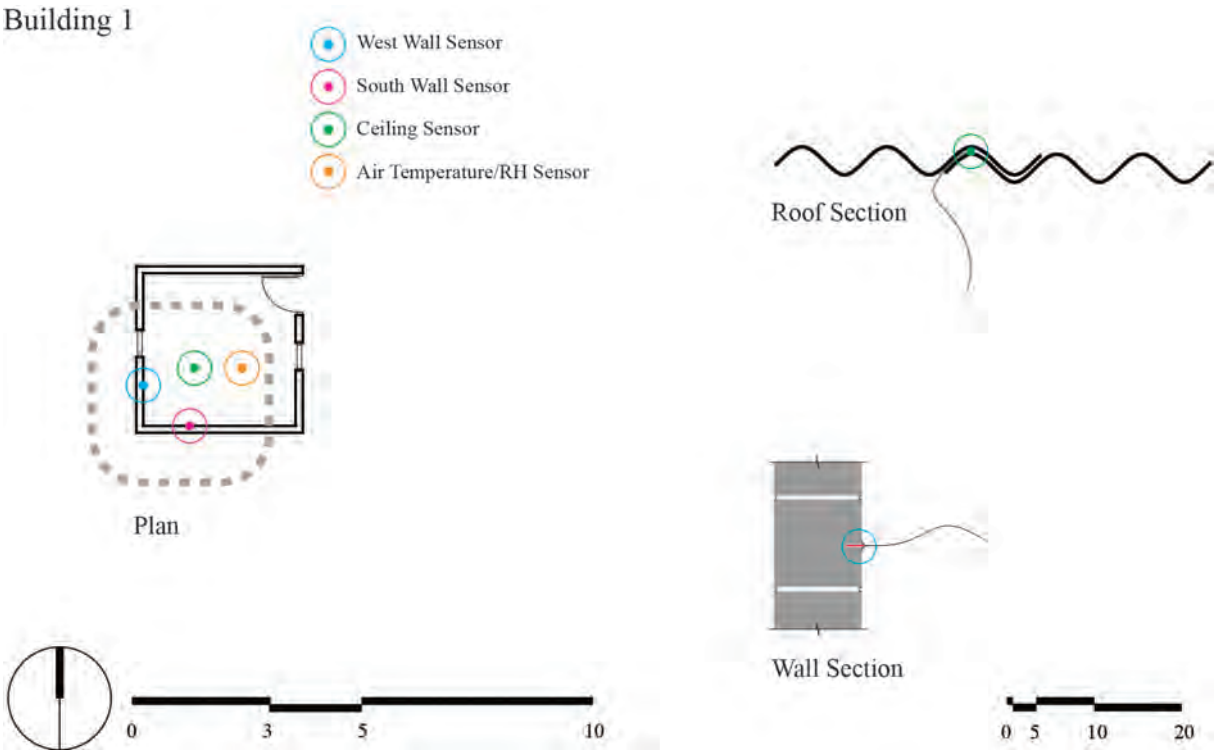

(a) Plan and Wall and Roof Sections Showing Sensor Locations in Building 1.

(b) Interior of Building 1 Showing Ceiling and Wall Materials.

Figure 3.12 – Building 1 Sensor Locations

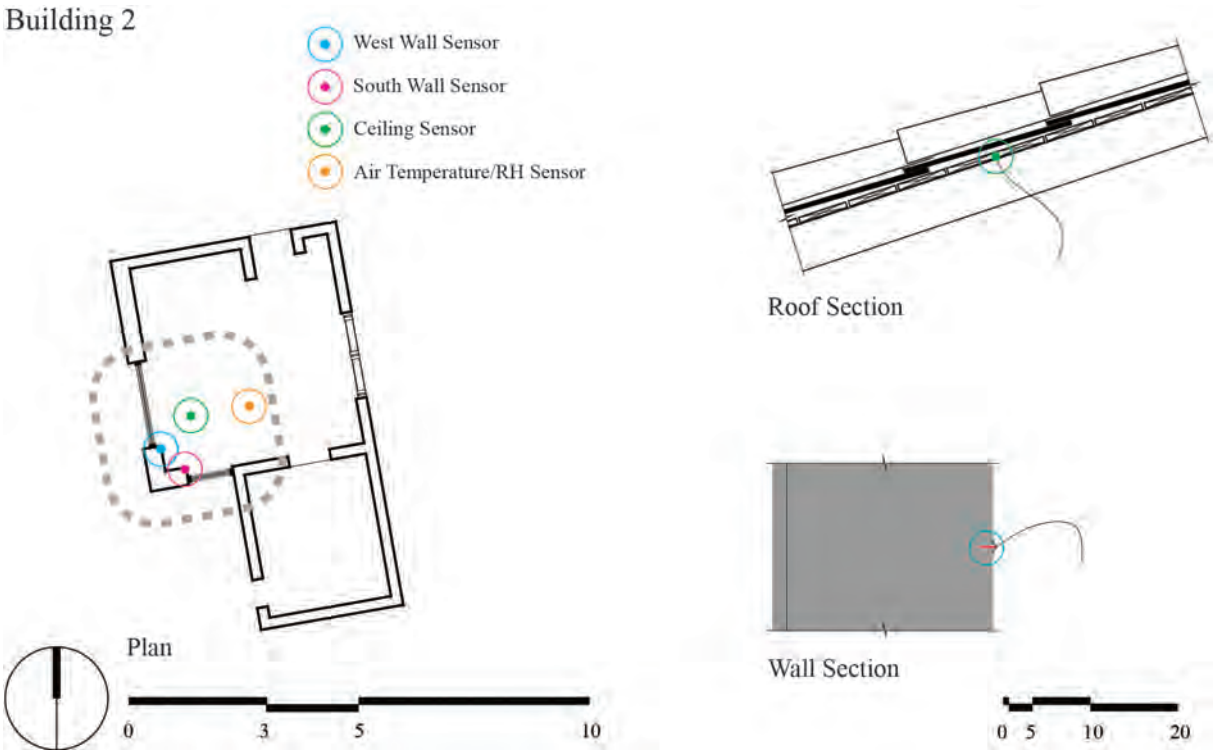

(a) Plan and Wall and Roof Sections Showing Sensor Locations in Building 2.

(b) Interior of Building 2 Showing Ceiling and Wall Materials.

Figure 3.13 – Building 2 Sensor Locations

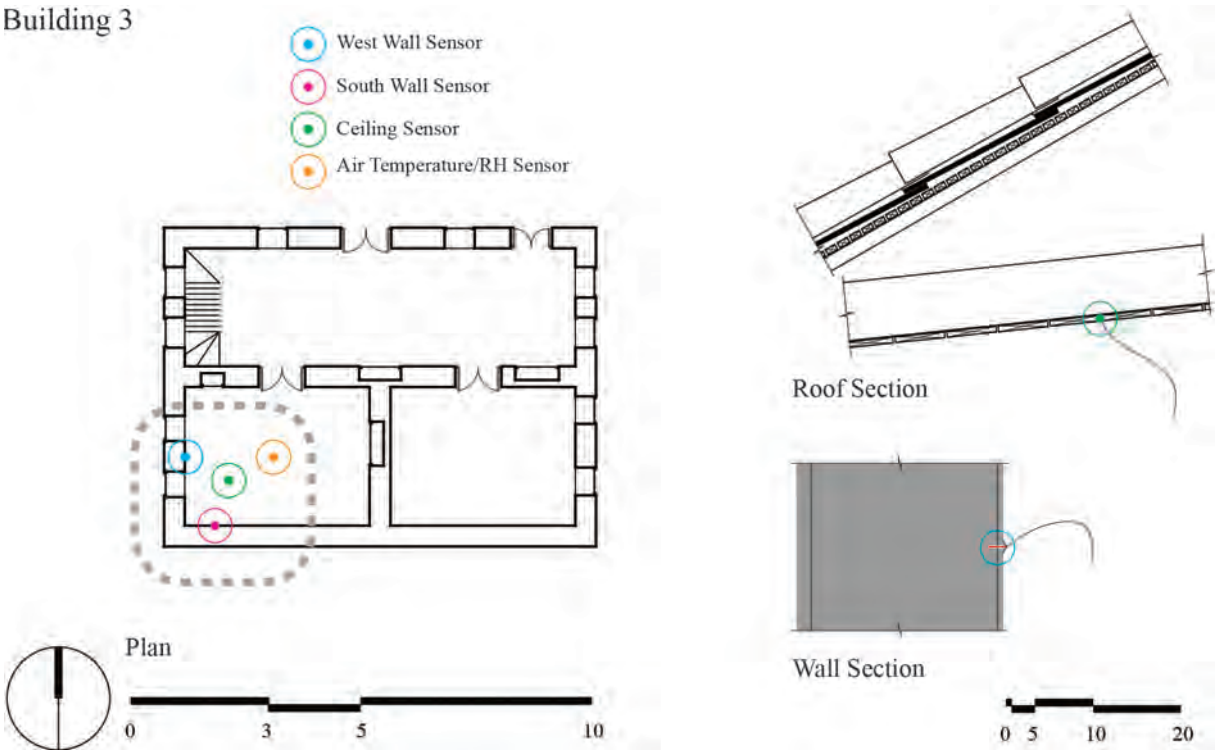

(a) Plan and Wall and Roof Sections Showing Sensor Locations in Building 3.

(b) Interior of Building 3 Showing Ceiling and Wall Materials.

Figure 3.14 – Building 3 Sensor Locations

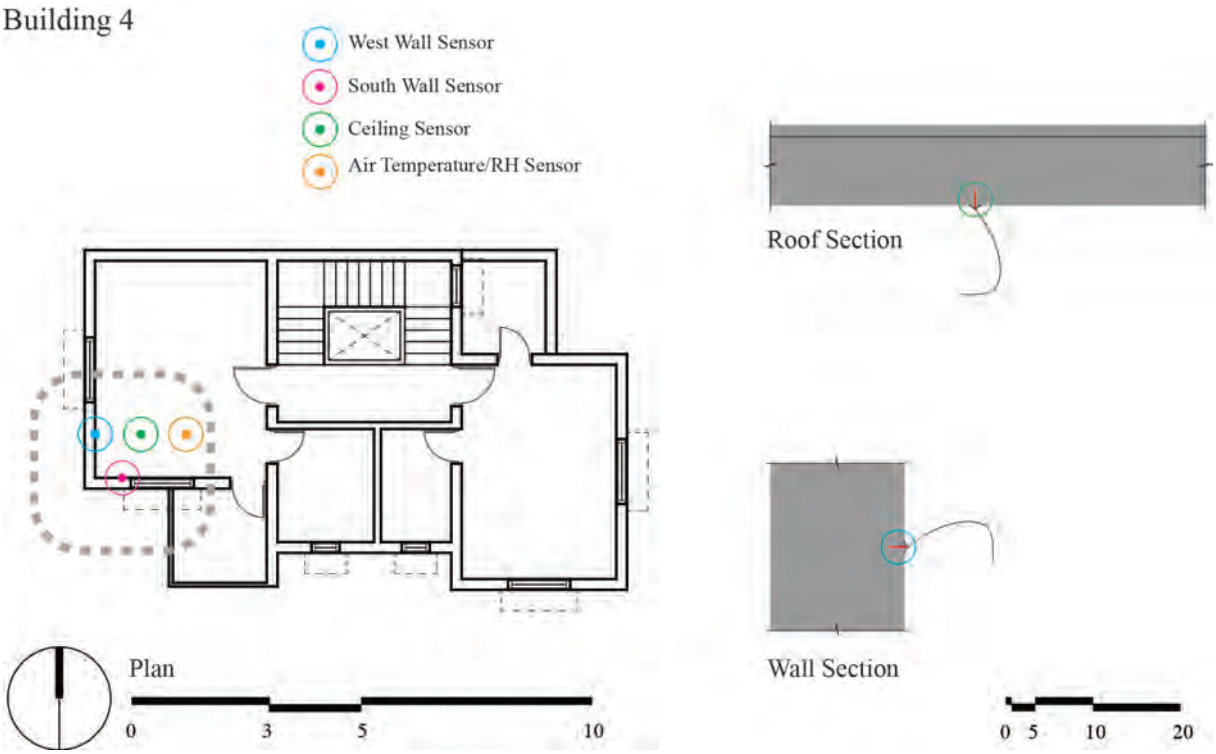

(a) Plan and Wall and Roof Sections Showing Sensor Locations in Building 4.

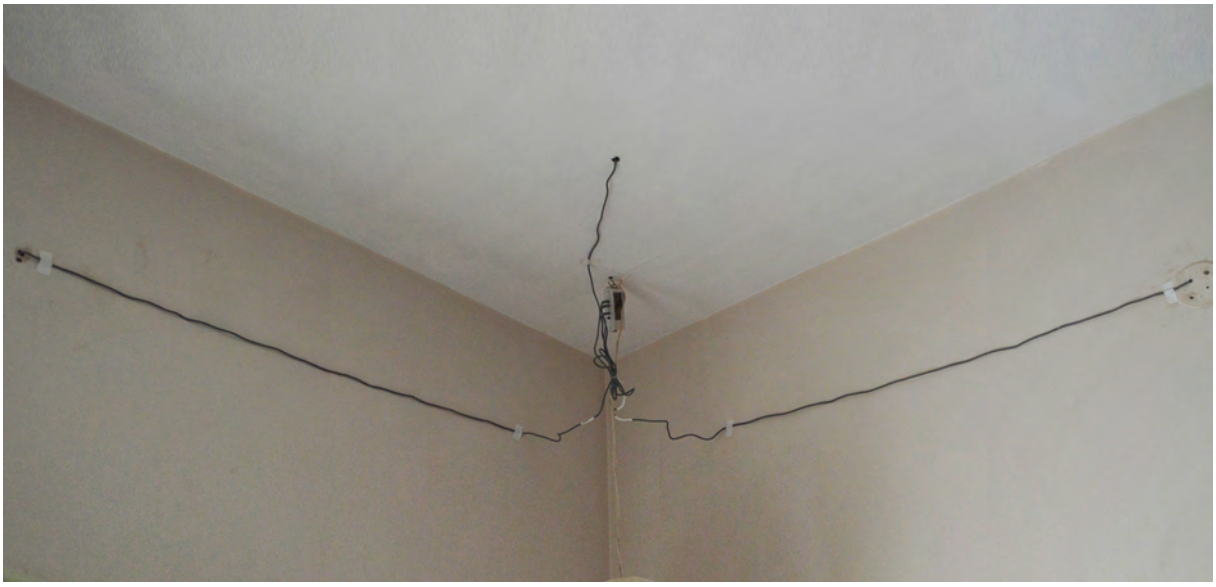

(b) Interior of Building 4 Showing Ceiling and Wall Materials.

Figure 3.15 – Building 4 Sensor Locations

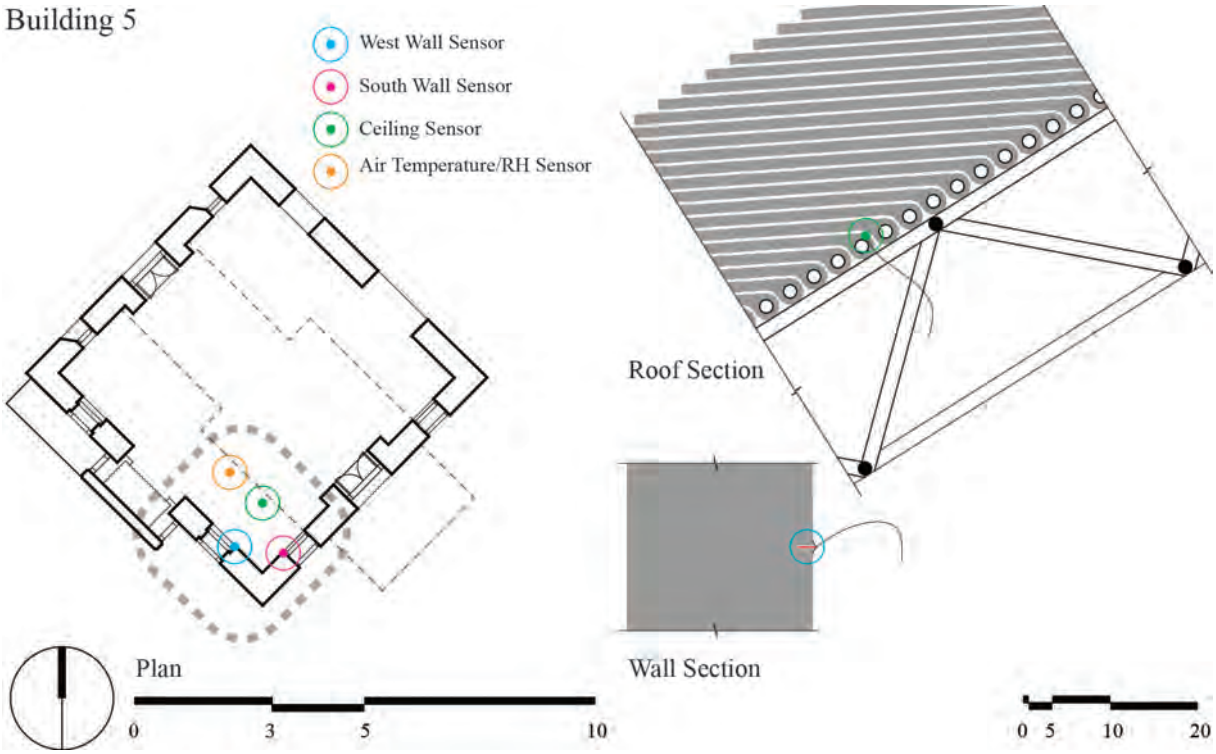

(a) Plan and Wall and Roof Sections Showing Sensor Locations in Building 5.

(b) Interior of Building 5 Showing Ceiling and Wall Materials.

Figure 3.16 – Building 5 Sensor Locations

(U23-00) data logger. The data logger was mounted under an eave on a Hunnarshala campus building to ensure protection from direct solar radiation.

Global Horizontal Irradiance Equipment and Setup
Global Horizontal Irradiance hourly values were recorded using an ONSET Silicon Pyranometer (S-LIB-M003) connected to a HOBO Micro Station Data Logger (H21-002). The pyranometer was mounted to a horizontal bracket on top of the roof of a Hunnarshala campus building that is not shaded by trees or overhead obstructions.

Exterior Data Collection Period
Outdoor air temperature and relative humidity data collection began on September 26, 2014, and will record hourly data through late August 2015. Solar radiation data collection began on January 15, 2015 and is planned to continue until at least January 2016.

3.3 Direct Comparison of Measured Temperatures

The following section simply catalogs measured indoor air temperatures and ceiling, south and west wall surface temperatures for the five case study buildings. Figure 3.17 shows indoor air temperatures measured from from September 25th, 2014 through March 24th 2015. Figures 3.18 through 3.20 show indoor surface ceiling, south and west wall temperatures measured from August 26th, 2014 through March 24th 2015. Measurement of these temperatures will continue through August 2015 so that one full year of thermal performance can be compared between the five case study buildings. Though the measurements available for this thesis do not span the hottest summer months in Bhuj, note that for the period of time from August 26th, 2014 to March 24th 2015, outdoor air temperatures reached 34 °C or above for 496 out of the 4395 hours logged (11%) and 40 °C or above for 27 hours. These higher temperatures occurred mid-day during October and March. Note that in Figures 3.18 through 3.20, the data collection time is shorter for B2 due to equipment malfunction. A few statistics are listed in Table 3.11 below to quickly summarize temperature comparisons between Buildings 1 through 5.

	B1	B2	B3	B4	B5
% Hours Air Temperature ≥ 34 °C	19	4	< 1	< 1	5
# Hours Air Temperature ≥ 34 °C	836	189	55	8	200
Max Air Temperature Recorded [°C]	43	37	36	34	38
Max Ceiling Temperature Recorded [°C]	52	41	37	36	39
Max South Wall Temperature Recorded [°C]	43	34	33	35	34
Max West Wall Temperature Recorded [°C]	46	34	34	35	34

Table 3.11 – Direct comparison data for Buildings 1-5.

Upon examination of the results we quickly see a great difference in thermal performance between Building 1 and the rest. Though to varying degrees, B2 - B5 show much more moderate air and surface temperatures than B1. B3, the traditional Madhapar house, and B4, the contemporary RCC house, are the most moderate of the group.

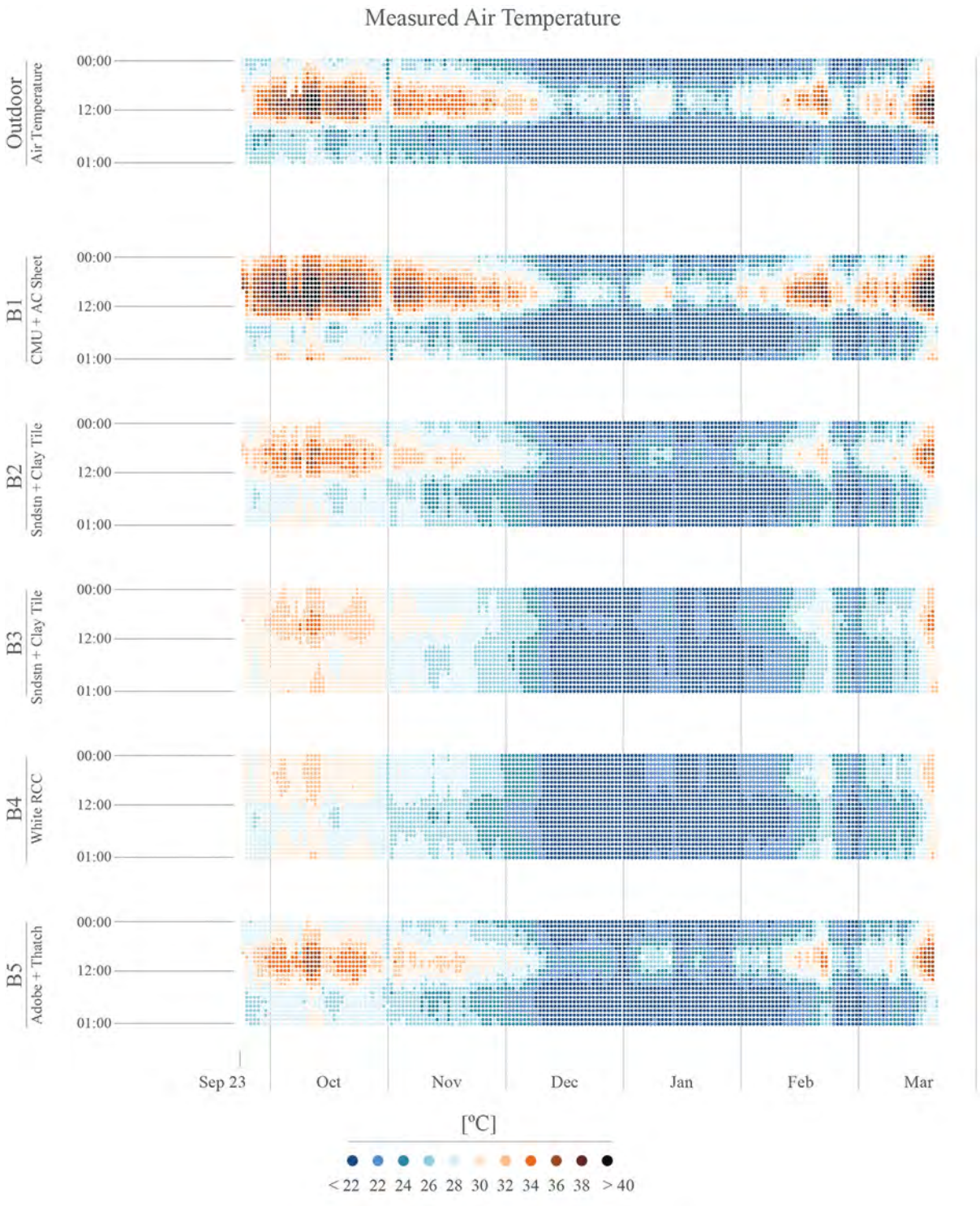

Figure 3.17 – Direct comparison of indoor measured air temperatures for Buildings 1 - 5.

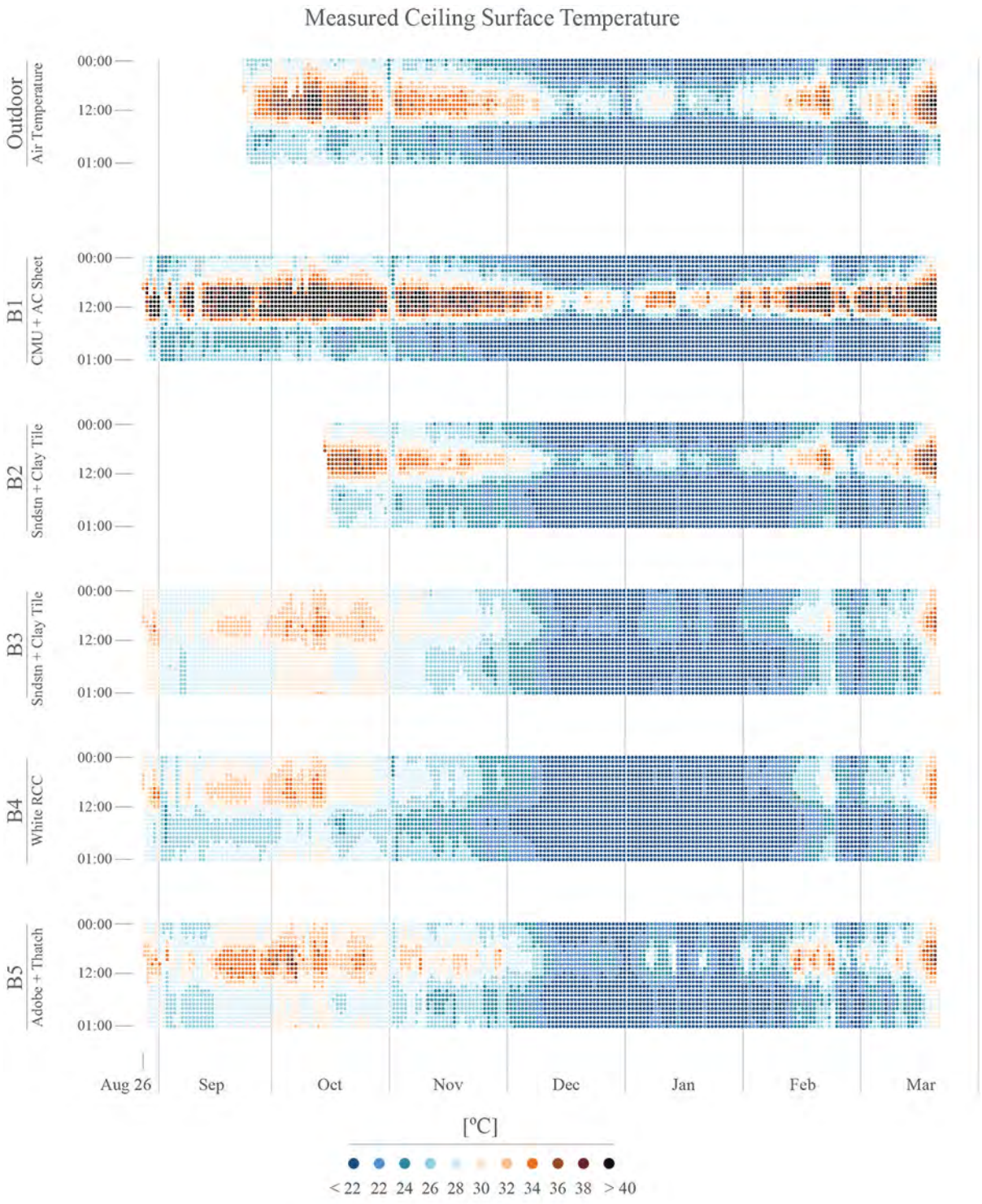

Figure 3.18 – Direct comparison of indoor measured ceiling surface temperatures for Buildings 1 - 5.

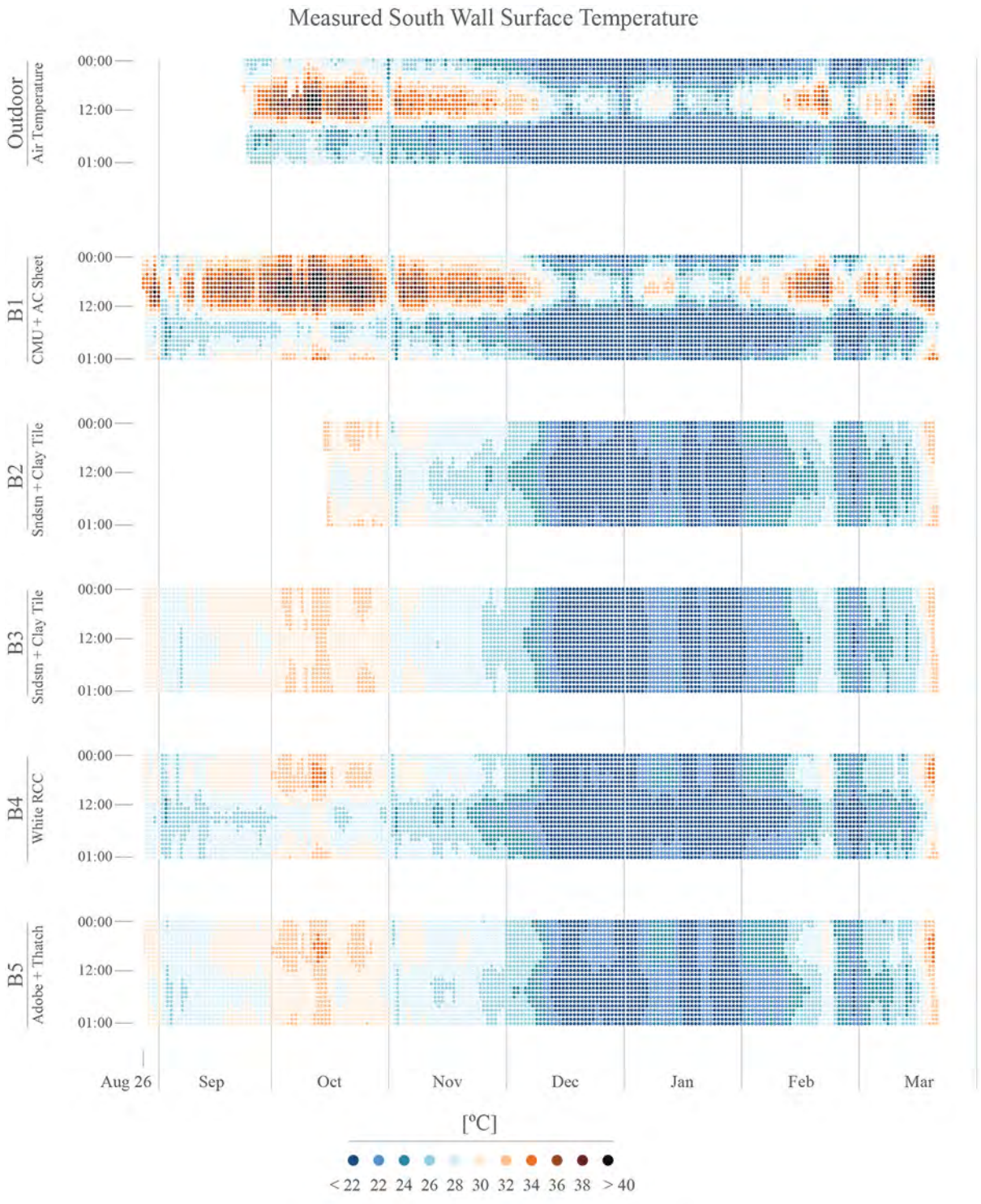

Figure 3.19 – Direct comparison of indoor measured south wall interior surface temperatures for Buildings 1 - 5.

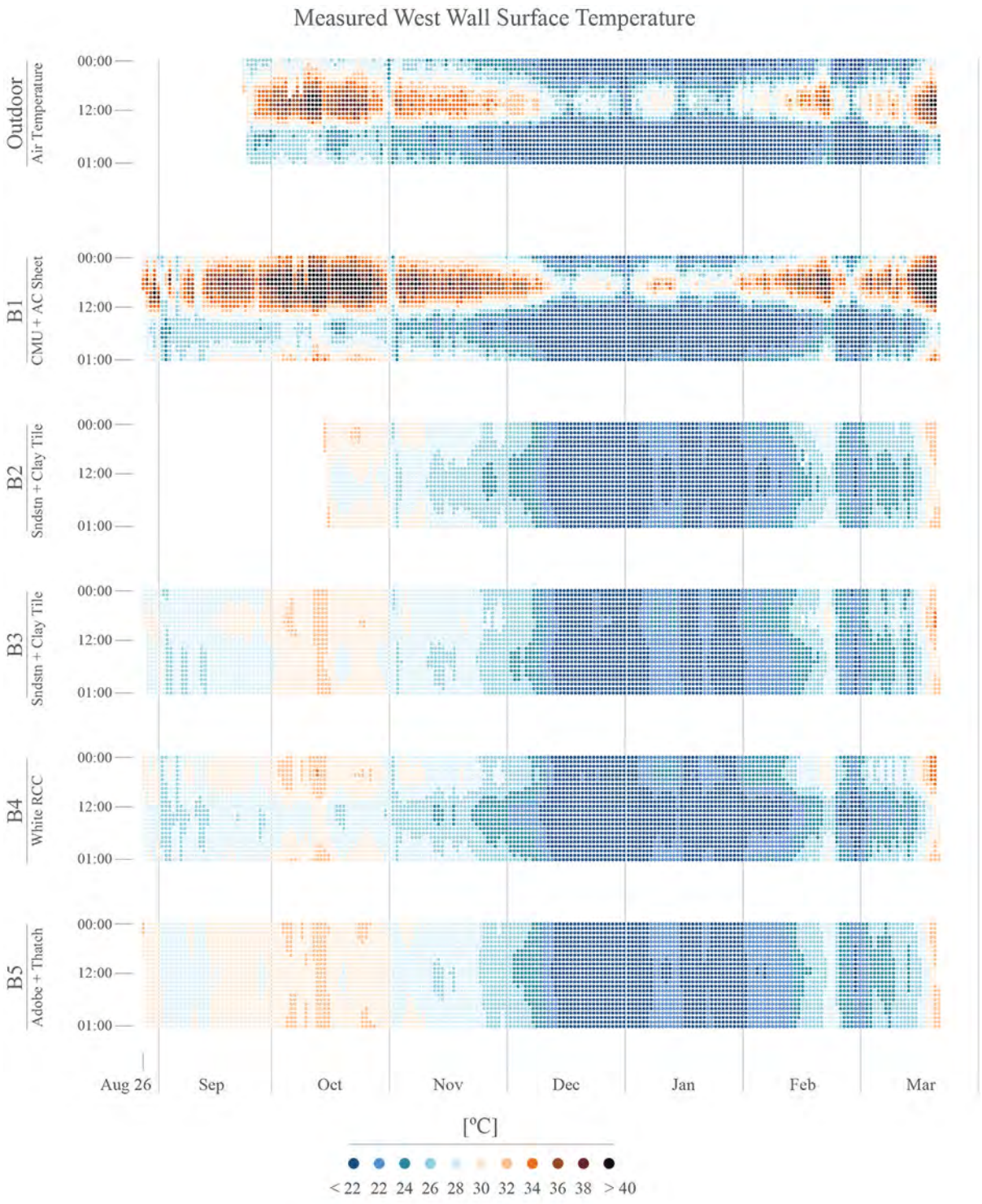

Figure 3.20 – Direct comparison of indoor measured west wall interior surface temperatures for Buildings 1 - 5.

On a field trip to Bhuj in November 2014, after the first set of measurements were plotted relative to each other and similarities between four of the five houses became apparent, it was decided to add two more buildings to the case study group that reflected additional informal house construction typologies. It was on the subsequent trip in January 2015 that data logger equipment was installed in the additional typologies, Building 6 and Building 7. All seven buildings are compared February 24th through March 24th 2015 in the next sub-section. This comparison including two additional informal house types lead to the division of the seven case study houses into two groups: a *higher performance* group and a *lower performance* group. The results were presented to the Hunnarshala Directors in late March 2015. In that meeting, Design with Climate strategies were discussed and prioritized according to the analysis. These conclusions are presented in Chapter 6, Section 6.1.

Additional Case Study Buildings 6 and 7

Building 6 Description
Similar to Building 1, Building 6 (B6) is a commonly found permanent informal house type in Bhuj. It is a stand alone two room dwelling with 15 cm thick uninsulated CMU walls and a single-layer Mangalore Pattern tile roof. The south wall is protected by a deep overhang. All other walls are exposed and unfinished. The room where thermal sensors are installed is equipped with an electric ceiling fan, used when occupied during warm days and nights. All windows are un-glazed and have operable opaque panel shutters that normally remain open. The house is occupied throughout the day and windows and doors are usually left open throughout the day for daylight and ventilation. Figure 3.21 depicts an exterior and interior view of Building 6.

Building 7 Description
Building 7 (B7) is part of a series of clustered buildings on the Gujarat Industrial Development Corporation (GIDC) 2001 earthquake re-development site outside of Bhuj City. It is a one room dwelling with 23 cm thick uninsulated Compressed Stabilized Earth Block (CSEB) walls and 12 cm RCC slab roof. The dwelling shares its north wall with its mirrored neighbor. Otherwise, wall surfaces are generally exposed to solar radiation. The CSEB walls are plastered and are light in color, but not as bright as Building 4. The room where thermal sensors are installed is equipped with an electric ceiling fan, used when occupied during warm days and nights. All windows are un-glazed and are covered by sheets of paper and interior curtains. The house is irregularly during the day by three family members. Figure 3.22 depicts an exterior and interior view of Building 7.

Discussion

Figure 3.27 is a series of graphs that qualitatively rank each of the seven case study buildings according to the extent to which they follow the rule of thumb Design with Climate strategies (outlined in Chapter 2). The plots are based off qualitative field observation and discussions with Hunnarshala Foundation Directors, not quantifiable data. Information from these graphs are then further compiled to create a "Relative Cumulative Design with Climate Score" (presented in Section 6.1) for each of the case study buildings as a way to begin a discussion about how to prioritize passive cooling strategies for low cost housing. When compared to measure data, the graphs show that the cooler buildings (shown with blue circles) generally manifest more instances of rule of thumb passive cooling strategies more frequently.

Figure 3.21 – Images of Building 6. Left: View of the south facade. Right: Interior view of uninsulated Mangalore Tile roof.

Figure 3.22 – Images of Building 7. Left: View of the southwest facade. Right: Interior view of the uninsulated CSEB walls and RCC slab roof.

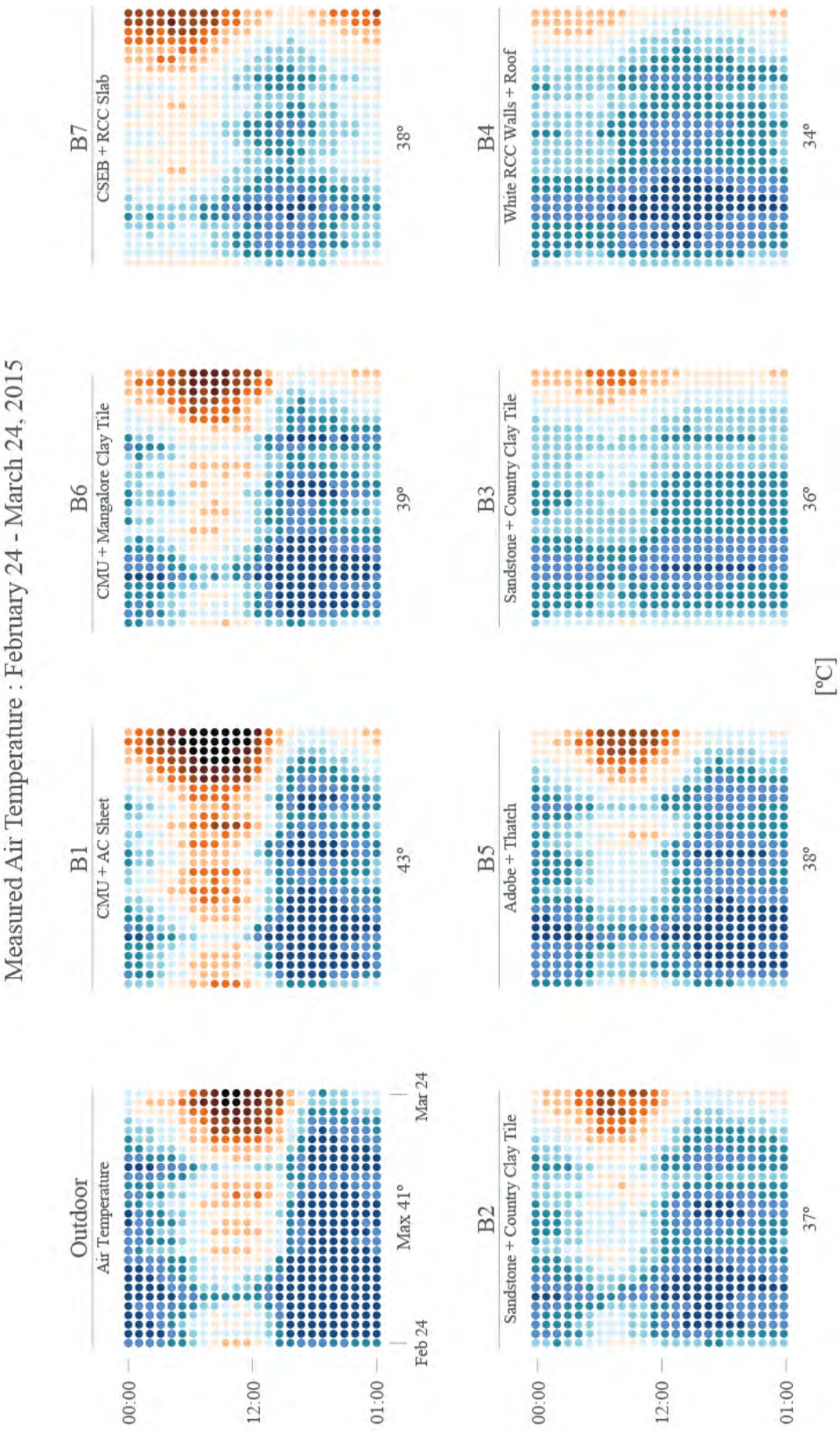

Figure 3.23 – Direct comparison of measured indoor air temperatures for Buildings 1-7 for February 24th through March 23th, 2015. Maximum recorded temperatures are listed underneath each map.

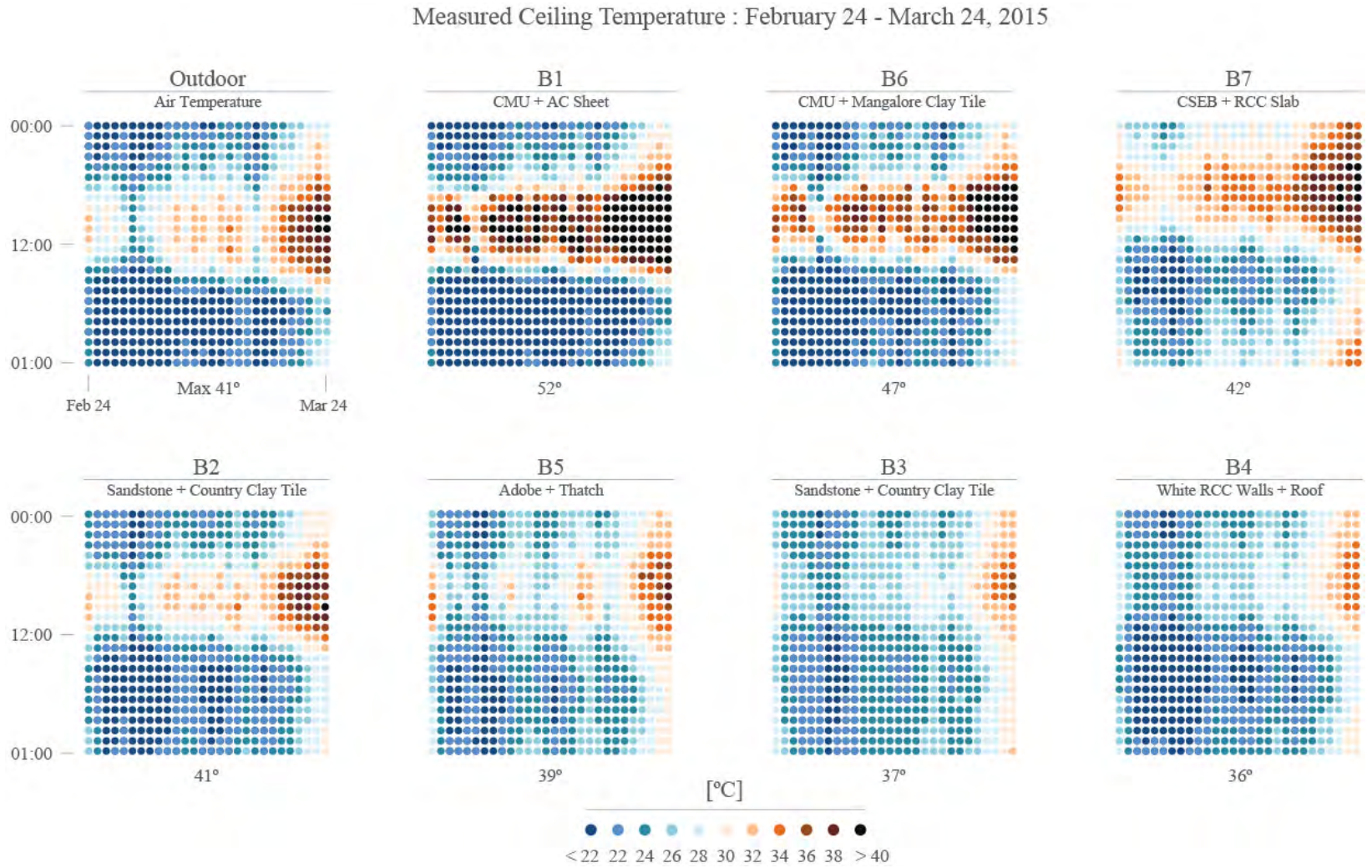

Figure 3.24 – Direct comparison of measured ceiling surface temperatures for Buildings 1-7 for February 24th through March 23th, 2015. Maximum recorded temperatures are listed underneath each map.

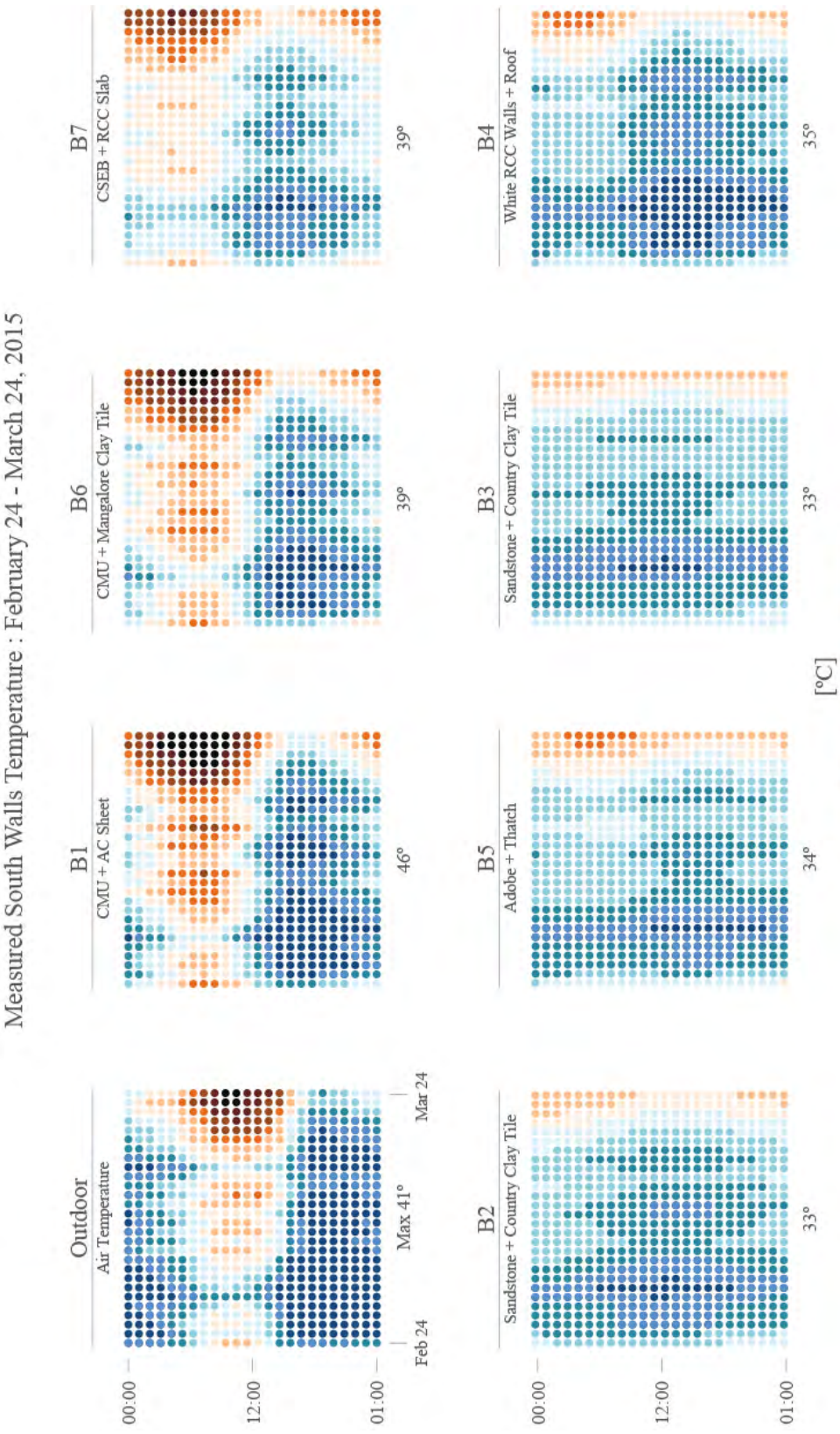

Figure 3.25 – Direct comparison of measured indoor south wall surface temperatures for Buildings 1-7 for February 24th through March 23th, 2015. Maximum recorded temperatures are listed underneath each map.

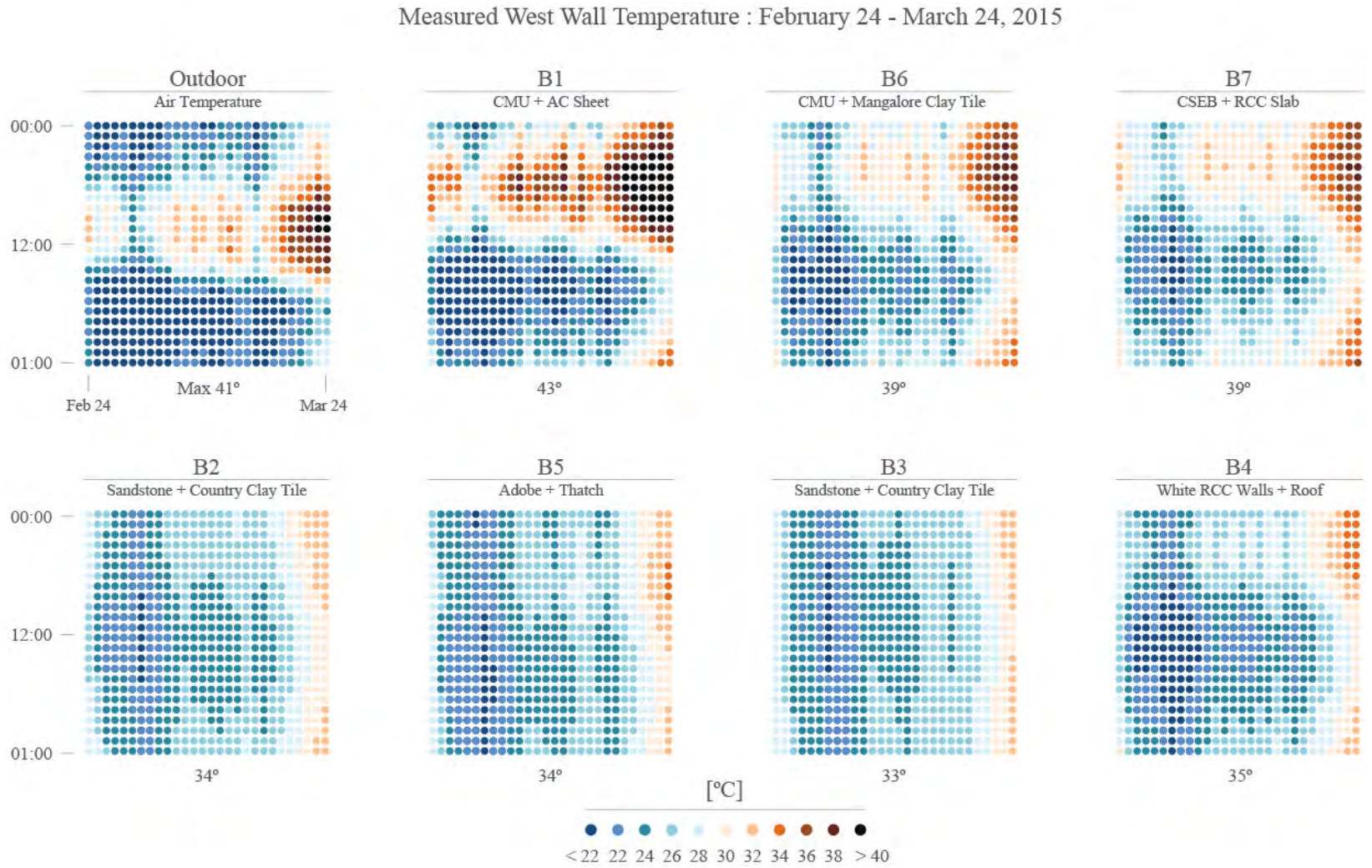

Figure 3.26 – Direct comparison of measured indoor west wall surface temperatures for Buildings 1-7 for February 24th through March 23th, 2015. Maximum recorded temperatures are listed underneath each map.

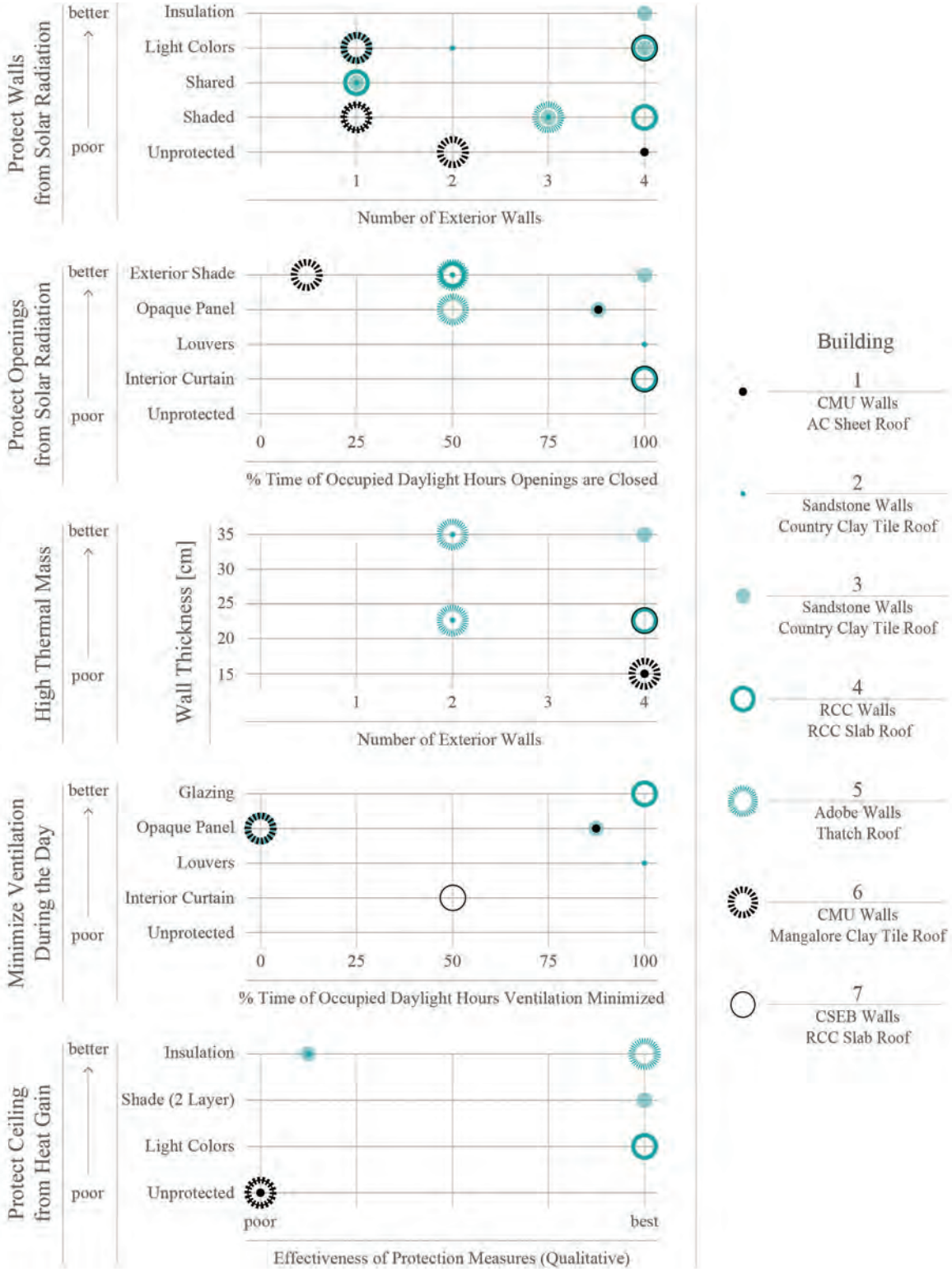

Figure 3.27 – Qualitative Mapping of Observed Design with Climate Strategies for Case Study Buildings 1-7. Buildings 1-7 are ranked by level of effectiveness, y-axis and frequency, x-axis.

3.4 Building 1 Energy Model Calibration

This section explains the methods by which the initial digital model from section 3.1 for Building 1 was calibrated, using measured temperature data from late August 2014 through late March 2015. Calibrating the B1 digital energy model enabled it to become a tool to more accurately predict thermal performance of common informal house types with roof modifications. Section 5.5 details the variations made to and resulting outputs from the calibrated B1 model.

EnergyPlus Weather File Modifications

In order to calibrate the model, the .epw file needed to be changed to reflect the actual outdoor conditions in Bhuj from late August 2014 to late March 2015. The Indian Meteorological Department (IMD) confirmed early in the project that validated hourly weather data for Bhuj would not be available. Thus, a series of inputs from both measured and interpolated data sets were used to construct an EnergyPlus weather file to accurately reflect actual Bhuj weather conditions during the span of the project. The Weather Analytics Typical Mean Year EnergyPlus weather (.epw) file from previous climate analysis was used as the base file, then measured and interpolated data was substituted for the period of September 25th through March 25rd for existing building calibration. Table 3.12 depicts the base .epw inputs that were modified.

Tag	Description	Units
T_{air}	Dry Bulb Temperature	°C
T_{dew}	Dewpoint Temperature	°C
RH	Relative Humidity	%
P_{sfc}	Atmospheric Pressure	Pa
GHI	Global Horizontal Irradiation	Wh/m^2
DNI	Direct Normal Irradiation	Wh/m^2
DHI	Diffuse Horizontal Irradiation	Wh/m^2
W_{spd}	Wind Speed	m/s
W_{dir}	Wind Direction	°

Table 3.12 – EnergyPlus Weather File Inputs

Weather Analytics Daily Current and Forecast Weather Data
Weather Analytics (WA) provides daily current and forecast weather data that can be purchased and downloaded as a comma separated values (.csv) file. The file contains hourly data that satisfies all of the inputs listed in Table 3.12. Before the outdoor air temperature/RH sensors were purchased, the intention was to use the Weather Analytics current weather files for all data. However, after comparing the Weather Analytics files' daily temperature highs and lows to those provided by the IMD online for the Bhuj area,[1] it was decided the WA files were too dissimilar to the available IMD data for the hourly

[1] http://www.imd.gov.in/section/nhac/distforecast/kutch.htm provides district level 5 day forecast information and http://imdahm.gov.in/cwo.htm provides daily minimum and maximum temperatures.

dry bulb temperature (T_{air}), relative humidity (RH), and global horizontal irradiance (GHI) data to be useful to construct an accurate .epw file. Figure 3.28 shows an example comparison of the WA hourly data to measured data for all hours between October 8th, 2014 06:00 to March 5th, 2015 11:00. The root-mean-square deviation between the example WA and measured values is 2.14 °C with a maximum discrepancy of 7.33 °C.

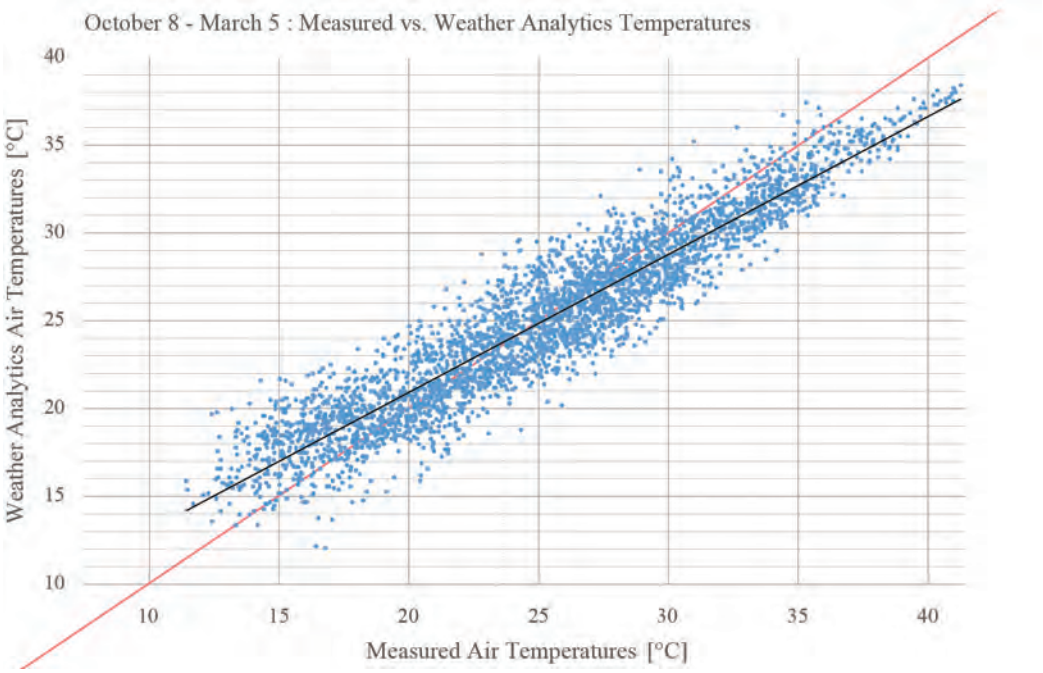

Figure 3.28 – Measured air temperature values plotted against Weather Analytics air temperature values.

The WA current weather files proved useful for hourly data that could not be estimated using measured data, which is discussed in the next subsection. EnergyPlus inputs that show little variation, such as atmospheric pressure (P_{sfc}), were used from the WA files. The WA values for wind speed and direction (W_{spd} and W_{dir}) were also used.

Calculated Dewpoint Temperatures from Measured Data

Equations 3.1, 3.2 and 3.3 show how psychrometrics were used as a model to calculate dewpoint temperature (T_d) from measured (T_{air}) and RH data.

$$\ln p_{ws_1} = \frac{C_1}{T_{air}} + C_2 + C_3 T + C_4 T^2 + C_5 T^3 + C_6 \ln T_{air} \tag{3.1}$$

$$p_w = \frac{\phi}{100} p_{ws_2} \tag{3.2}$$

$$T_d = 6.54 + 14 \ln P_w + 0.7389 \left(\ln p_w^2\right) + 0.09486 \left(\ln p_w^3\right) + 0.4569 \left(p_w^{0.1984}\right) \tag{3.3}$$

where:

p_{ws_1}	=	Water Vapor Saturation Pressure	(Pa)
T_{air}	=	Dry Bulb Temperature	(°K)
p_{ws_2}	=	Water Vapor Saturation Pressure	(kPa)
p_w	=	Water Vapor Partial Pressure	(kPa)
ϕ	=	Relative Humidity	(%)
T_d	=	Dewpoint Temperature	(°C)
C_1	=	-5.800 220 6 E+03	(-)
C_2	=	1.391 499 3 E+00	(-)
C_3	=	-4.864 023 9 E-02	(-)
C_4	=	4.176 476 8 E-05	(-)
C_5	=	-1.445 209 3 E-08	(-)
C_6	=	6.545 967 3 E+00	(-)

To test the accuracy of these psychrometrics equations, T_d was calculated using given T_{air} and ϕ values from WA Bhuj TMY3 .epw file. Those calculated values were then compared to the given T_d values of that same file. The scatter plot in Figure 3.29 shows the overall accuracy for 8670 hourly values. The root-mean-square deviation between the given and calculated values is 0.24 °C with a maximum discrepancy of 3.40 °C.

Calculated Direct Normal and Diffuse Horizontal Irradiation from Measured Data

Figure 3.30 plots Weather Analytics' Global Horizontal Irradiation (GHI) values against Measured values for January 15th through March 25th, 2015. Though the measured and WA values closely follow the same linear trendline, it was decided to continue to measure GHI with the pyranometer for the remainder of the project due to the vast differences in individual values. Then gen-reindl, an executable file that comes as part of the Radiance suite of tools, was used to calculate hourly direct and diffuse solar irradiation levels from measured GHI. Gen-reindl uses a site's time zone, latitude, and longitude along with hourly GHI levels to interpret direct and diffuse values.

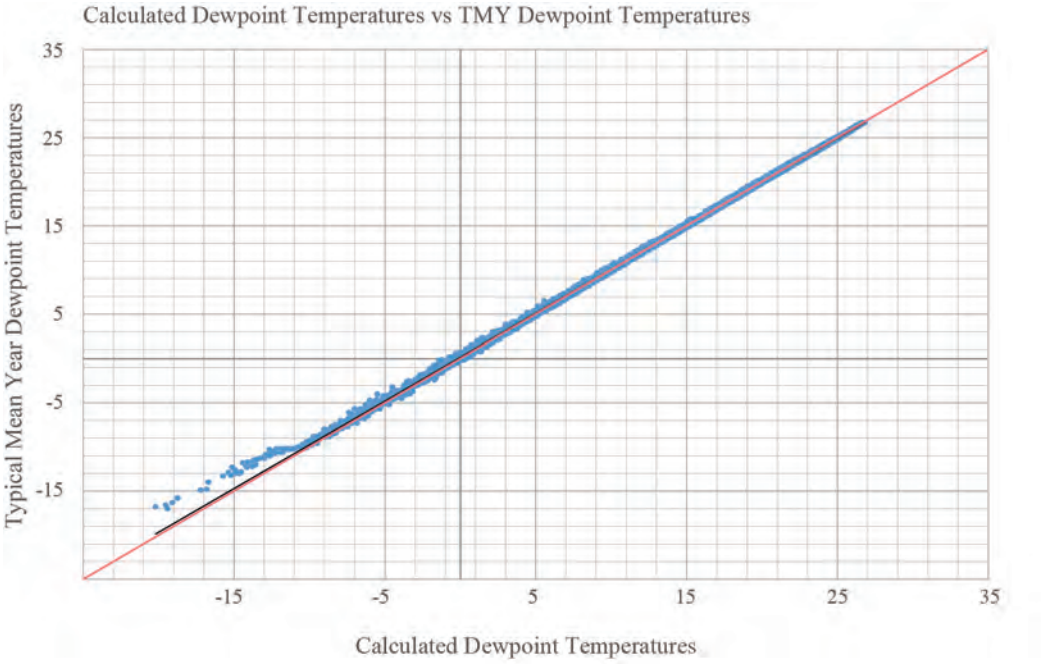

Figure 3.29 – Calculated dewpoint temperature values plotted against Typical Mean Year .epw dewpoint temperature values.

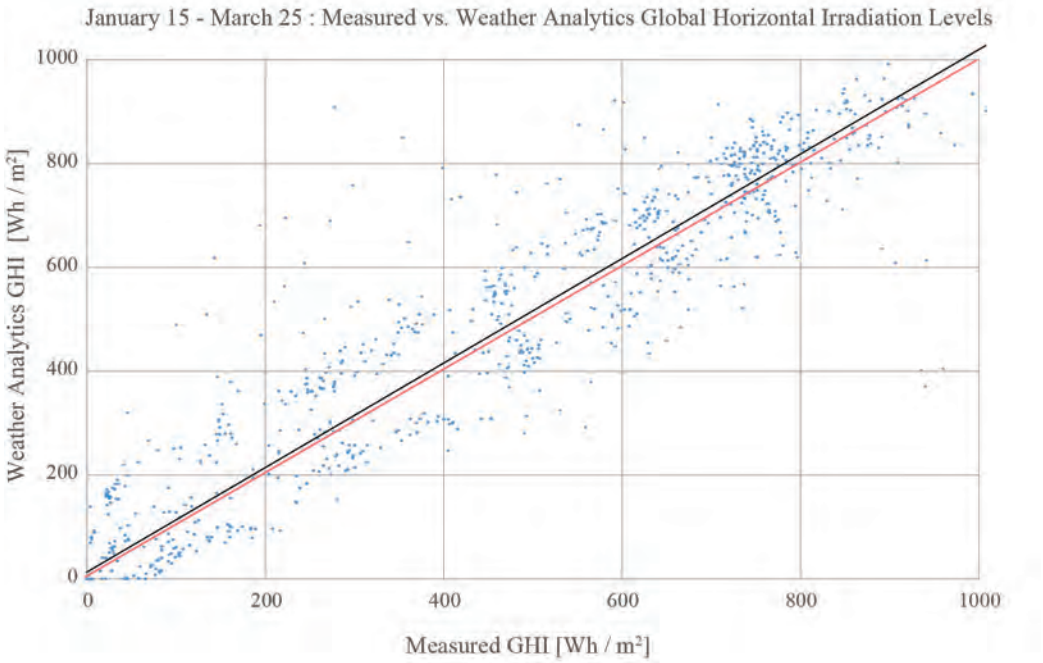

Figure 3.30 – Measured Global Horizontal Irradiation Values Plotted Against Weather Analytics Global Horizontal Radiation Values for January 15th through March 25th, 2015

3.4.1 Energy Model Modifications and Model Calibration Results

Tables 3.13 and 3.14 show the slight changes made to the initial B1 digital energy model to better reflect actual occupation and internal gains. Though the uncalibrated B1 model followed the same trends as the measurements, the models deviations between simulated and measured temperatures were generally high. Figures 3.31 through 3.37 show measured versus simulated temperatures for both the calibrated and uncalibrated models, both in hourly temperature map and scatter plot forms.

Though deviations between simulated and measured temperatures varied widely, measured indoor air temperatures tended to be lower during the day and higher during the night than the uncalibrated model predicted (Figure 3.32), as were the wall surface temperatures (Figures 3.36 and 3.38). This indicated that the walls of the uncalibrated model might not be thermally massive enough, so the density, specific heat capacity, and the conductivity of the CMU wall material was increased. This modification to the walls attributed to a slightly lower average deviation between between measured and simulated wall and air temperatures. Ceiling surface temperature deviations were further off than wall or air temperature deviations, so much so that the simulated ceiling temperatures generated a much higher slope trendline than measured values (top, Figure 3.34). Average deviations were lowered and trends were fit better by lowering the absorptivity of the outer roof material from .7 to .43 and increasing the emissivity from .9 to .98. Because there was a higher deviation between daily high measured versus simulated temperatures for both the air and ceiling, the interior surface convective heat transfer coefficient for the ceiling was fixed in DesignBuilder to a relatively high 5.0 W/m^2 $^\circ$C to effectively decouple the hot ceiling surface from interior air.

Construction Type Properties															
Walls		E+ Wall Total U Value	E+ Wall Outer Material Properties					Roof		E+ Roof Total U Value	E+ Roof Outer Material Properties				
Material	L	U	k	ρ	c_p	ε	α	Material	L	U	k	ρ	c_p	ε	α
	[cm]	[W/m²°K]	[W/m°K]	[kg/m³]	[J/kg°K]				[cm]	[W/m²°K]	[W/m°K]	[kg/m³]	[J/kg°K]		
Uncalibrated Model															
Solid CMU	15	2.16	0.79	1950	840	0.9	0.6	AC corr. Sheet	0.1	6.38	0.36	1500	1050	0.9	0.7
Modifications															
Solid CMU	15	3.61	1.40	1900	840	0.92	0.5	AC corr. Sheet	0.1	6.38	0.36	1900	1050	0.98	0.43

Table 3.13 – Wall and roof construction type property modifications for B1 calibrated EnergyPlus model.

Non-Construction Type Properties																
Walls Shared w/ Adj Bldgs				Shaded Un-Shared Walls				Window Shading	Infilt. Rate	Occupancy		Ventilation		Int Gains	Notes
N	S	E	W	N	S	E	W	schedule	[ac/h]	schedule	[p/m²]	schedule	type	[W/m²]	
Uncalibrated Model															*oriented 32° NE *typical low cost house type *all surfaces unprotected *irregular schedules *to lower roof temps during day, fixed interior surface convective heat transfer coefficient to 5 W/m°K, decreased α to .43 *increased ε to .98 to lower ceiling temps at night
none				none				Mon-Sun 0:00-24:00	0.5	Mon-Sun 11:00-14:00	0.2	Mon-Sun 11:00-14:00	constant	20	
Modifications															
none				none				Mon-Sun 0:00-24:00	1	Mon-Sun 11:00-14:00	0.05	Mon-Sun 11:00-14:00	constant	0	

Table 3.14 – Occupancy, Ventilation, and Shading Schedules modifications for B1 calibrated EnergyPlus model.

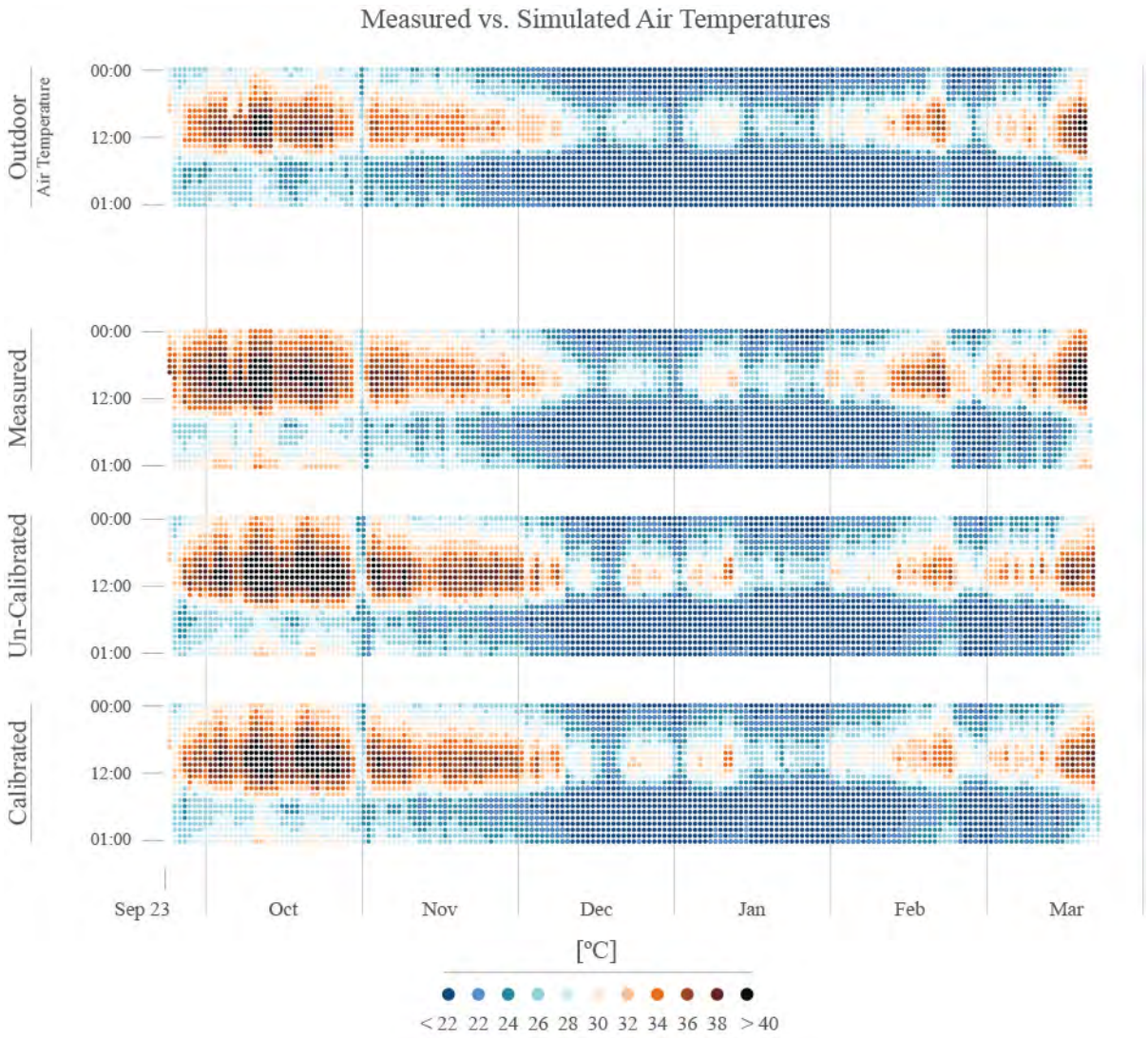

Figure 3.31 – Temperature maps comparing Building 1 measured indoor air temperatures to uncalibrated and calibrated models.

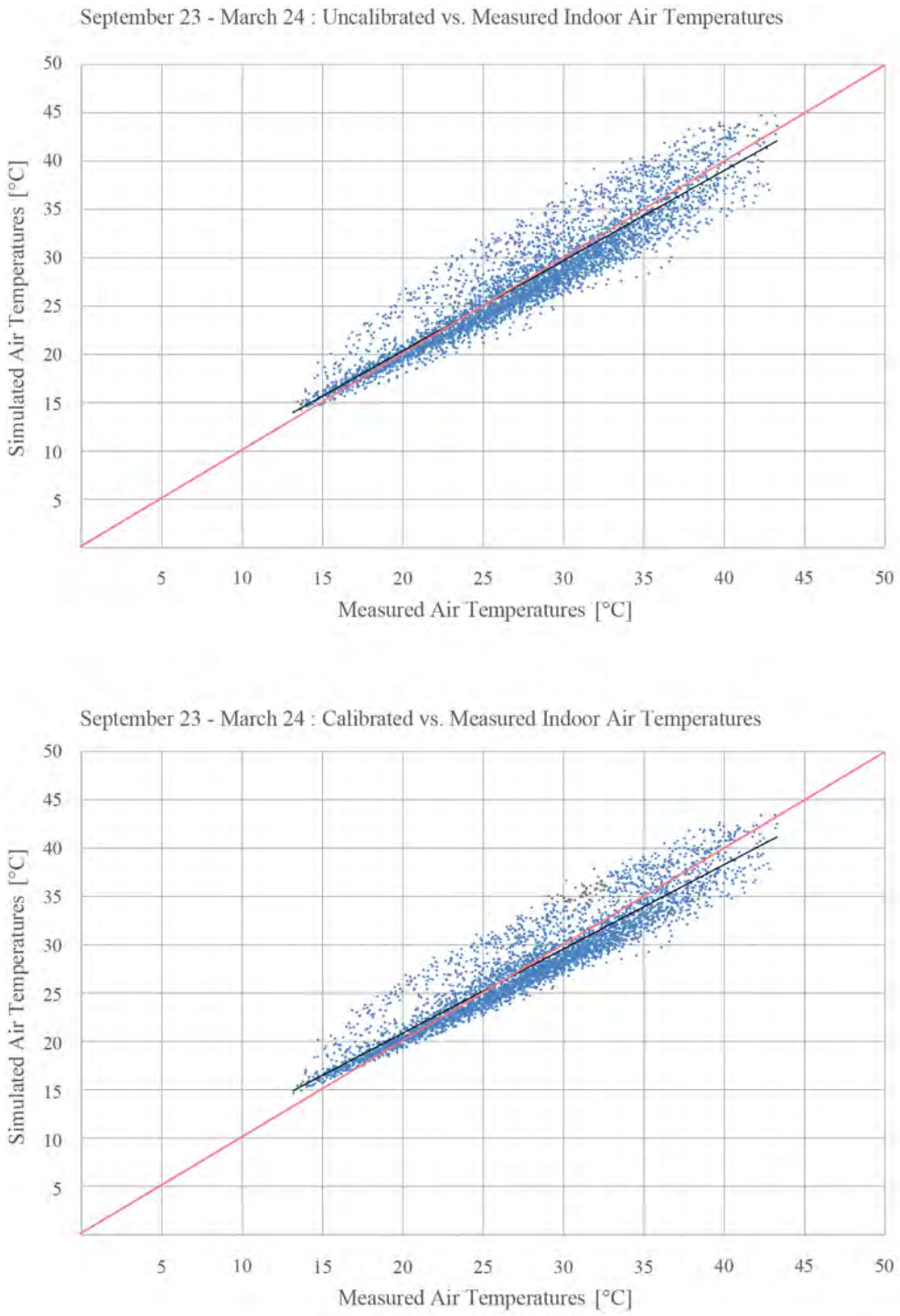

Figure 3.32 – Scatter plots show deviations in individual hourly temperatures as well as trends between simulated and measured indoor air temperatures for September 23rd through March 24th. Top: Measured temperatures plotted against uncalibrated model temperatures. Root mean square temperature deviation is 2.2 °C with a maximum deviation of 7.5 °C. Bottom: Measured temperatures plotted against calibrated model temperatures. Root mean square temperature deviation is 2 °C with a maximum deviation of 6.7 °C.

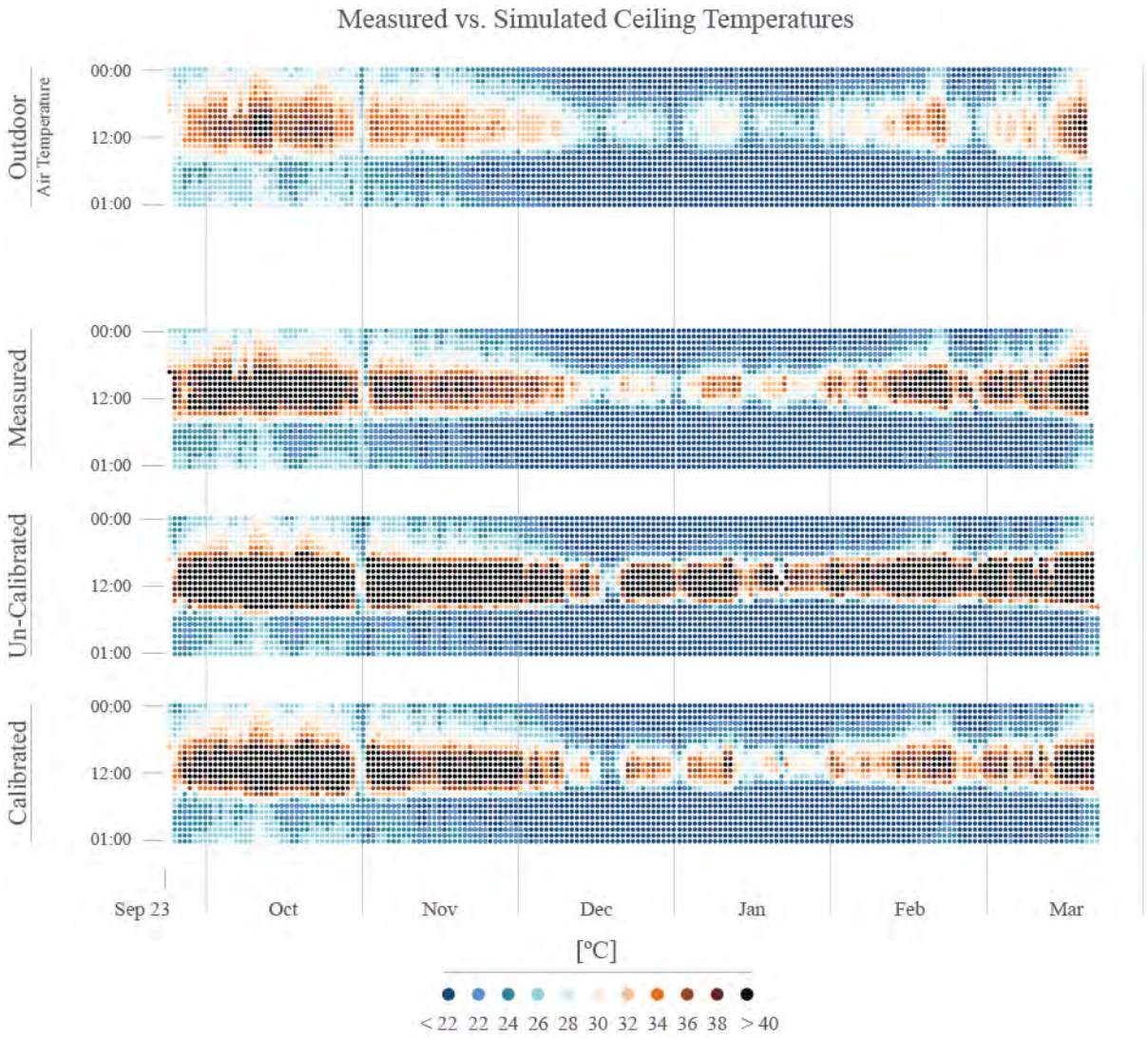

Figure 3.33 – Temperature maps comparing Building 1 measured ceiling temperatures to uncalibrated and calibrated models.

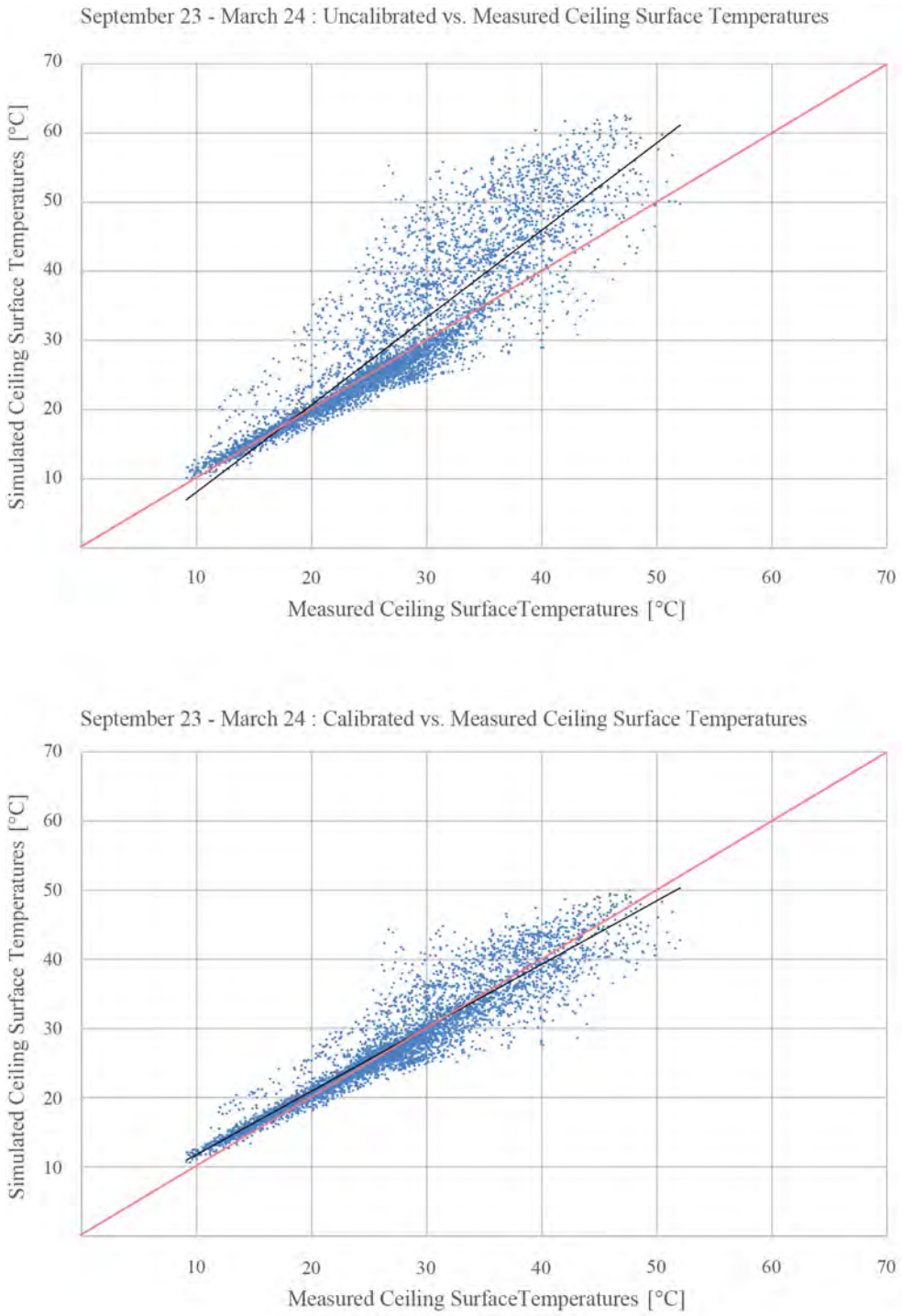

Figure 3.34 – Scatter plots show deviations in individual hourly temperatures as well as trends between simulated and measured ceiling surface temperatures for September 23rd through March 24th. Top: Measured temperatures plotted against uncalibrated model temperatures. Root mean square temperature deviation is 6.1 °C with a maximum deviation of 21 °C. Bottom: Measured temperatures plotted against calibrated model temperatures. Root mean square temperature deviation is 2.5 °C with a maximum deviation of 9.8 °C.

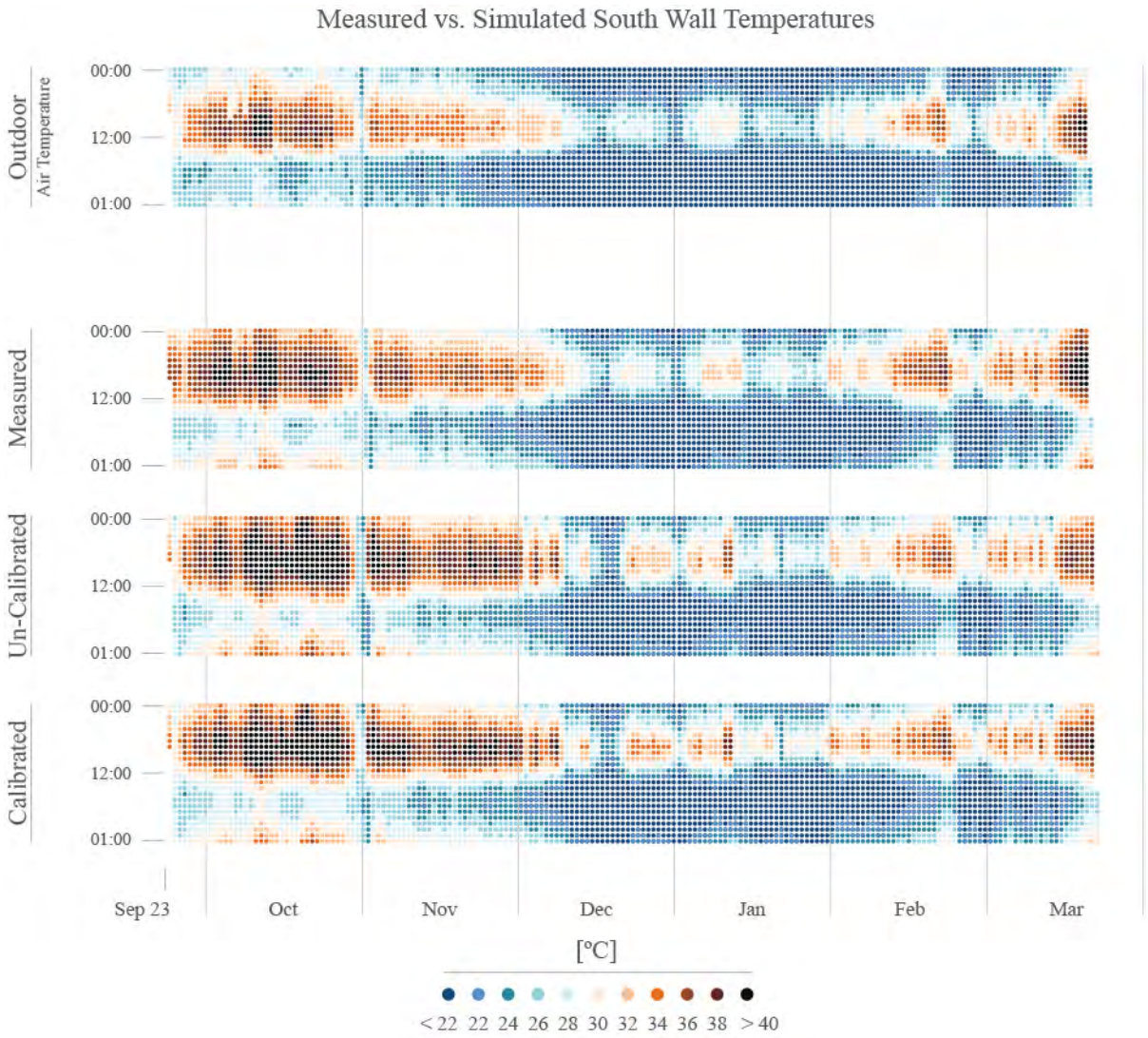

Figure 3.35 – Temperature maps comparing Building 1 measured indoor south wall surface temperatures to un-calibrated and calibrated models.

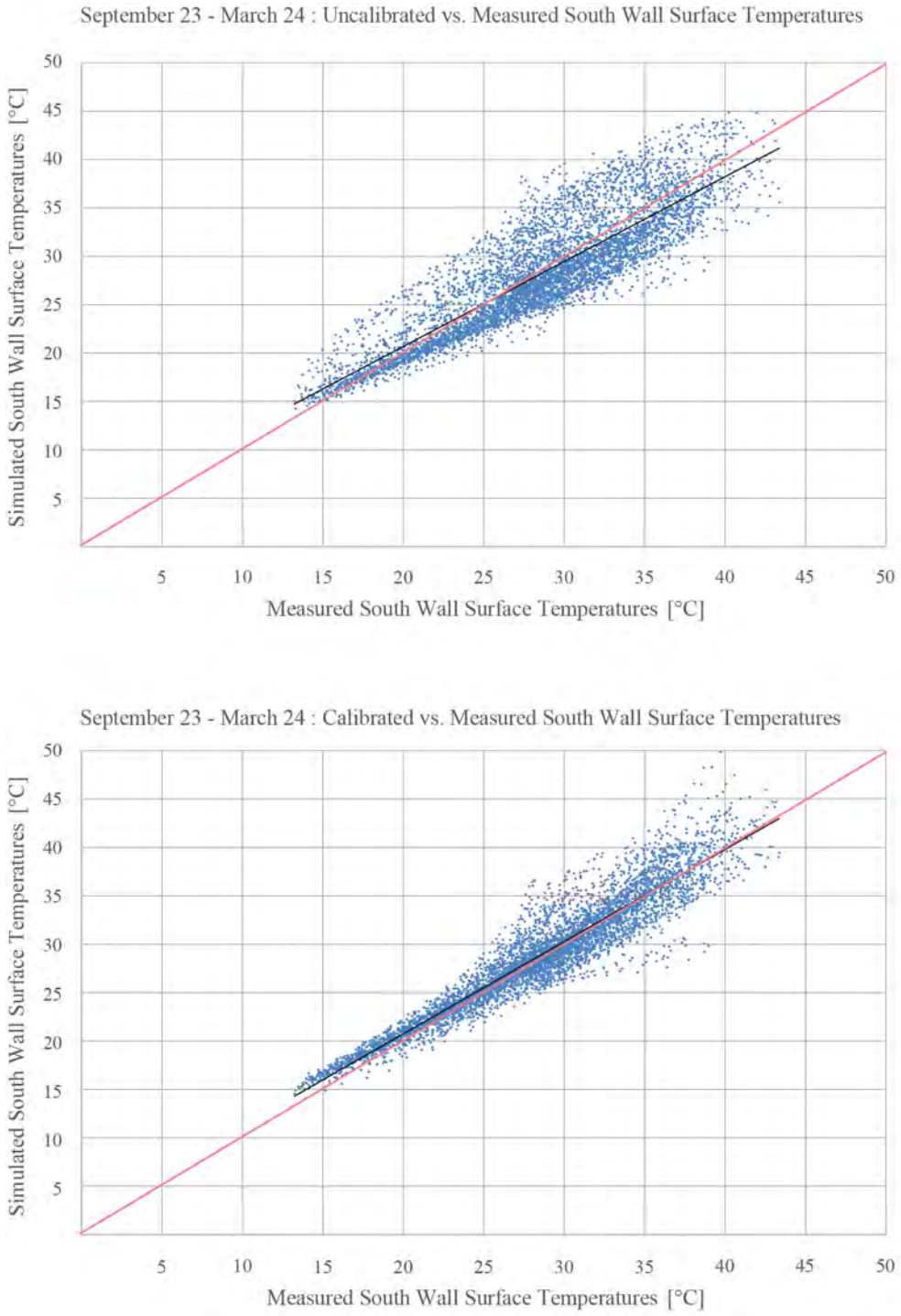

Figure 3.36 – Scatter plots show deviations in individual hourly temperatures as well as trends between simulated and measured south wall surface temperatures for September 23rd through March 24th. Top: Measured temperatures plotted against uncalibrated model temperatures. Root mean square temperature deviation is 2 °C with a maximum deviation of 7.8 °C. Bottom: Measured temperatures plotted against calibrated model temperatures. Root mean square temperature deviation is 2.2 °C with a maximum deviation of 7.3 °C.

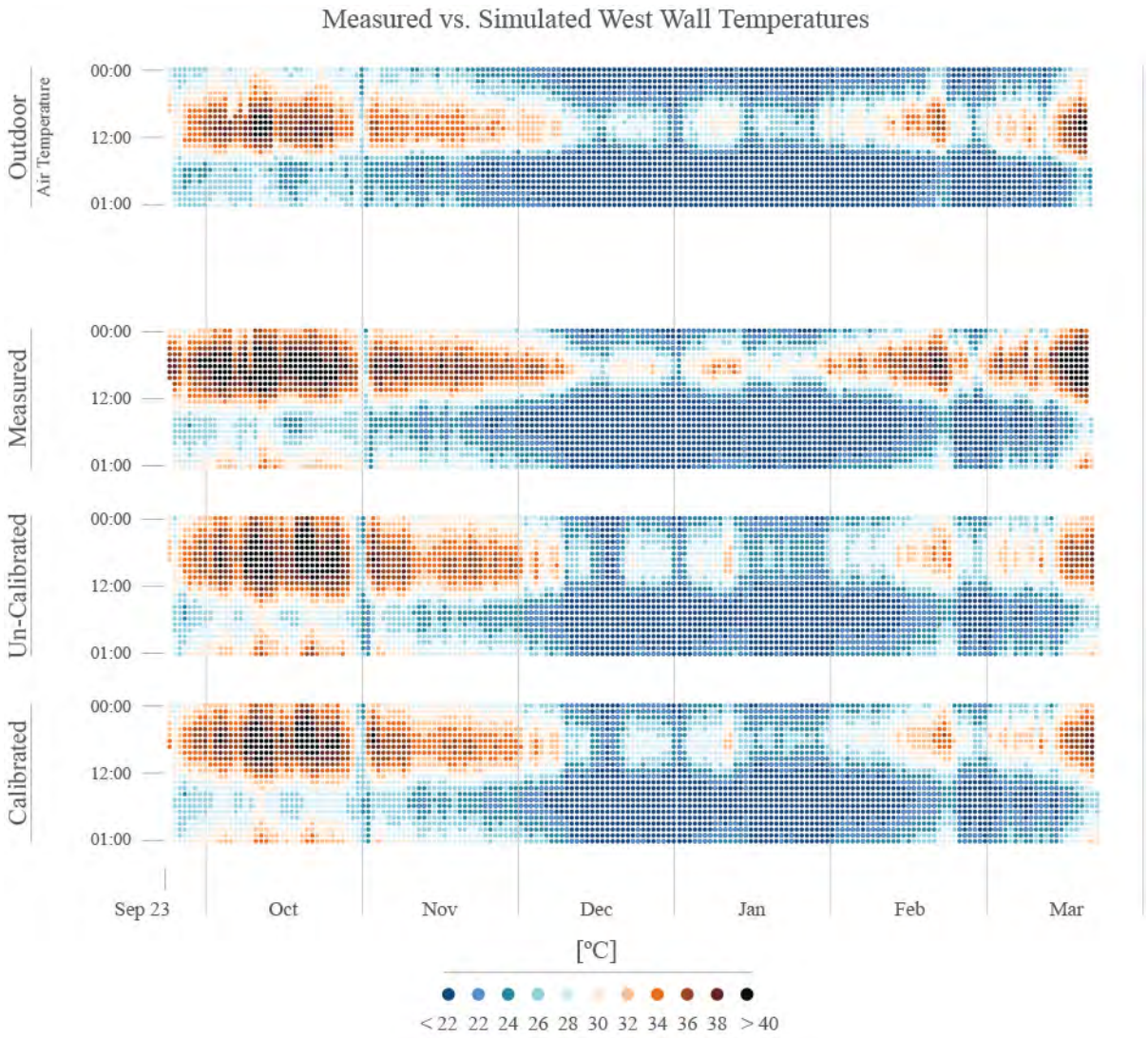

Figure 3.37 – Temperature maps comparing Building 1 measured indoor west wall surface temperatures to uncalibrated and calibrated models.

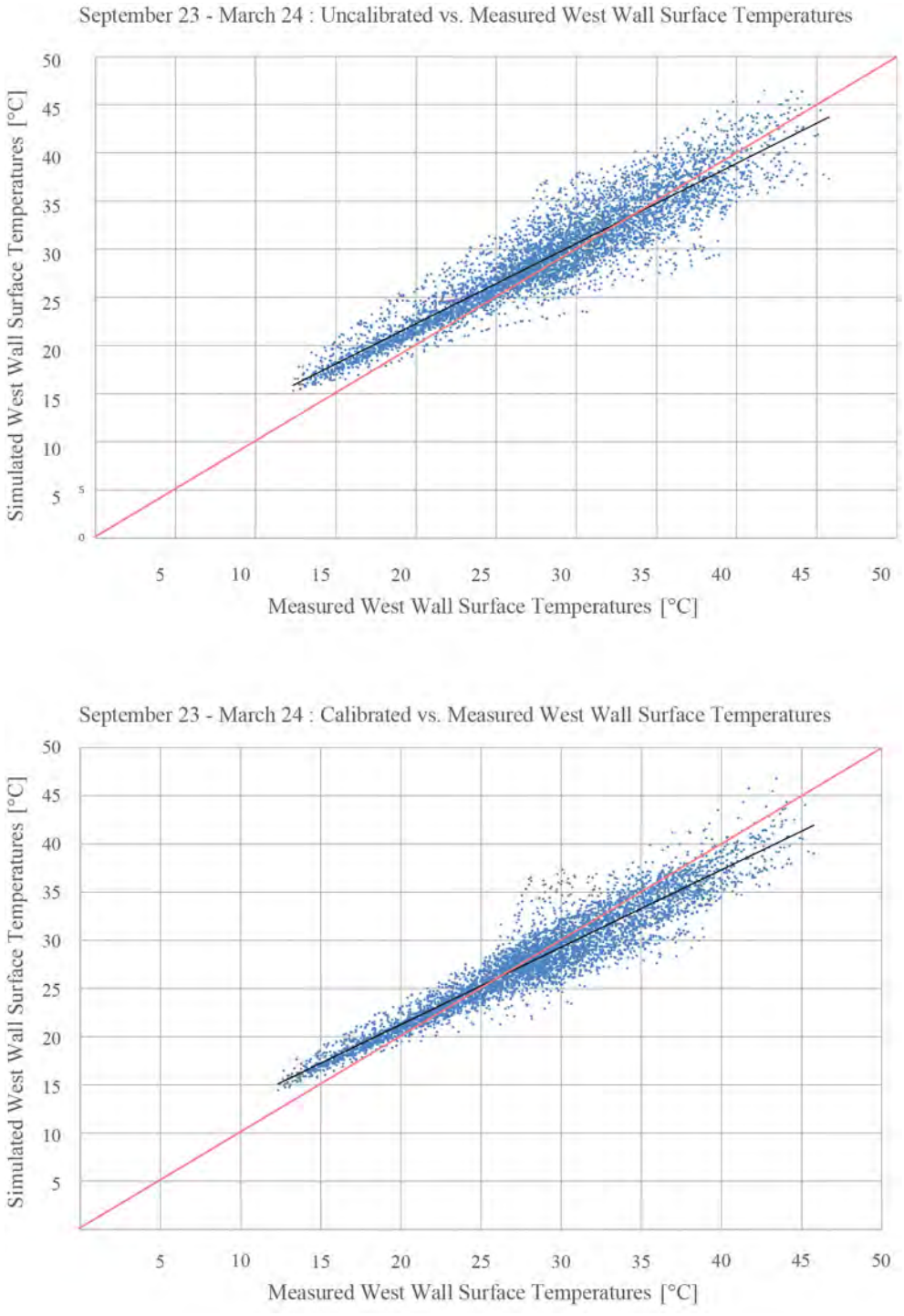

Figure 3.38 – Scatter plots show deviations in individual hourly temperatures as well as trends between simulated and measured west wall surface temperatures for September 23rd through March 24th. Top: Measured temperatures plotted against uncalibrated model temperatures. Root mean square temperature deviation is 2.5 °C with a maximum deviation of 6 °C. Bottom: Measured temperatures plotted against calibrated model temperatures. Root mean square temperature deviation is 2 °C with a maximum deviation of 4.4 °C.

Chapter 4

Role of Energy Simulation in Co-Design

The purpose of this chapter is to chronicle early digital simulation methods and results that guided co-design decisions for the first round of test chamber field experiments, detailed in chapter 5. Single zone digital energy models formed the basis for a series of iterative studies to analyze rule of thumb Design with Climate strategies and identify relationships between the building envelope, natural ventilation using building materials, construction types and climate conditions typical to Bhuj, India.

Section 4.1 describes the methods and results of the first iteration of simulation, where models parametrically varied in construction types as well as in size and position of operable openings, so that the effect of rule of thumb Design with Climate strategies, such as thermal mass and night flush ventilation, could be assessed using a controlled set of independent variables. These results were then used to refine simulation methods, remove certain variables, and introduce new parameters to include construction materials atypically seen in Bhuj, such as exterior wall insulation. Section 4.2 defines these variables and is an analysis of the resulting annual thermal performance outputs. Section 4.3 details the collaborative design feedback that lead to the final shift in simulation variables, yielding the third and final iteration of pre-design energy simulations. The refinements and results of this iteration are presented in section 4.4. Finally, the chapter concludes with the presentation of project design and roof prototype design recommendations for the thermal field lab experiments.

4.1 Iteration 1 - 24 Hour Simulations

As discussed in Chapter 3, it is difficult to precisely determine the effectiveness of singular Design with Climate strategies or assess their subtle dependencies on each other by only monitoring and modeling existing buildings. The multi-dimensional variation of size, orientation, building materials, construction quality and occupancy and ventilation schedules in the existing buildings makes quantitative assessment of and equivalent thermal performance metrics difficult. Thus, the objective of the first iteration of simulations was to quickly identify the influence of several controlled variables on the effectiveness of night flush ventilation. It is well known that night flush ventilation works well as a passive cooling measure in hot and arid climates with high diurnal swings, and that to be most effective it be coupled with "high thermal mass". This first study aimed to not only to determine how thermal mass affected

night flush ventilation, but also to quickly but parametrically determine the integrated effects of roof insulation level, window size and window position on indoor operative temperature of a single thermal zone in a hot and arid environment.

4.1.1 Modeling Assumptions, Inputs and Parameters

All models were simulated using EnergyPlus as the engine and DesignBuilder as the GUI using the Bhuj Typical Mean Year (TMY) EnergyPlus weather (.epw) file from previous climate and existing building analysis, to define outdoor conditions. To test the largest potential passive cooling effects of night flush ventilation, weather file conditions were chosen for a 24 hour period reflecting a typical day in April for Bhuj. April was chosen as a the best fit month to test the effectiveness of night flush ventilation because, according to the TMY weather file, the average day in April experiences high daily outdoor temperatures in conjunction with a large diurnal swing. April 6^{th} was the 24 hour period that best reflected a the average April day, reaching a high temperature of 40 °C and experiencing a diurnal temperature swing of more than 20 °C.

To focus the comparison on the impacts of heat transfer through wall and roof materials on indoor operative temperature (T_{op}), direct solar gain through openings was eliminated by orienting the windows north/south and specifying virtual exterior shading devices. To obtain a base comparison of the effect of window size and position on natural ventilation, the wind factor in DesignBuilder was set to 0.00 so that only buoyancy-driven was calculated. It is important to note here that night flush ventilation was not scheduled. To understand maximum cooling effects of natural ventilation on T_{op}, settings in DesignBuilder were configured such that the windows were open only when indoor temperature exceeded outdoor air temperature.

In all variations, the overall building geometry was a cube enclosing a 3 m by 3 m by 3 m volume of air which is similar in size to many of the single room informal houses observed in the field. The floor was input as a non-heated, 15 cm thick concrete slab on grade. Internal heat gains were assumed constant at 20 W/m^2. Infiltration settings were set to "poor" for all variations allowing a constant .5 air changes per hour (ac/h). As mentioned above, airflow due to natural ventilation was additional to this constant infiltration rate, and varied throughout the day according to temperature difference between interior and exterior air temperatures, and opening size, and position. Specifications for window size and position variations are shown in Figure 4.1.

The test volume was modeled as a free standing zone with walls exposed to the four cardinal directions. To ascertain the effect of uninsulated thermal mass on heat transfer wall material was either input as 10 cm brick or 50 cm concrete. These two thickness reflected the thinnest and thickest thermal mass walls observed in the informal housing settlements. All roof assembly variations used a single layer of clay tile as an exterior material. To ascertain the effect of roof insulation on thermal performance, variations included insulation levels with thermal resistances in the range of .16 m^2 °C/W RSI (R-1) to 7 m^2 °C/W RSI (R-40). Specific material properties for the roof and wall variations are shown in Table 4.1.

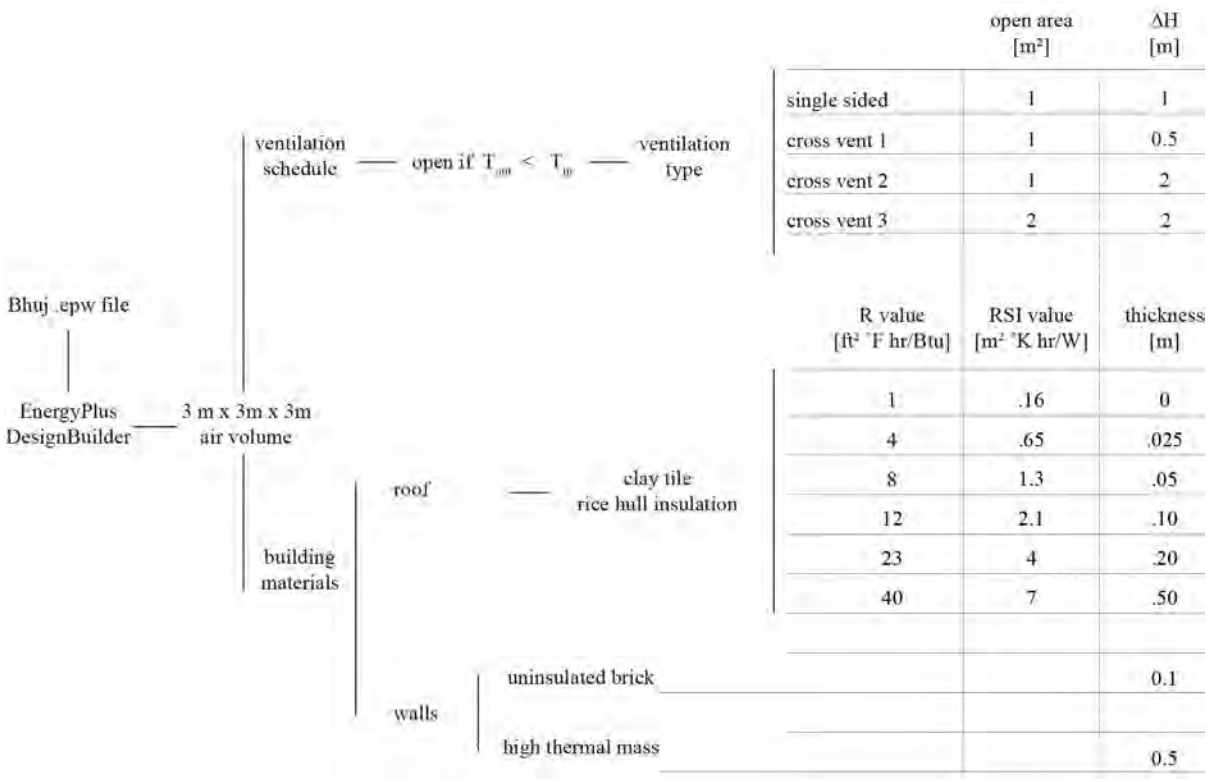

Figure 4.1 – Building material and ventilation variables for April 6th simulations. Note that windows open only when indoor air temperatures exceed outdoor air temperatures.

Construction Type Properties

Walls		**E+ Total U Value**	**E+ Material Properties**				
Material	L [cm]	U [W/m²°K]	k [W/m°K]	ρ [kg/m³]	c_p [J/kg°K]	ε	α
Clay Brick	10	3.39	0.72	1920	840	0.9	0.6
Concrete, Medium Weight	50	1.26	0.81	1500	840	0.9	0.6
Roof							
Material	L [cm]	U [W/m²°K]	k [W/m°K]	ρ [kg/m³]	c_p [J/kg°K]	ε	α
Clay Tile	1	6.41	0.81	1700	840	0.9	0.6
Rice Hull Insulation	2.5	1.55	0.05	120	1000	0.9	0.6
	5	0.88					
	10	0.47					
	35	0.14					

Table 4.1 – EnergyPlus building material properties for April 6th simulations.

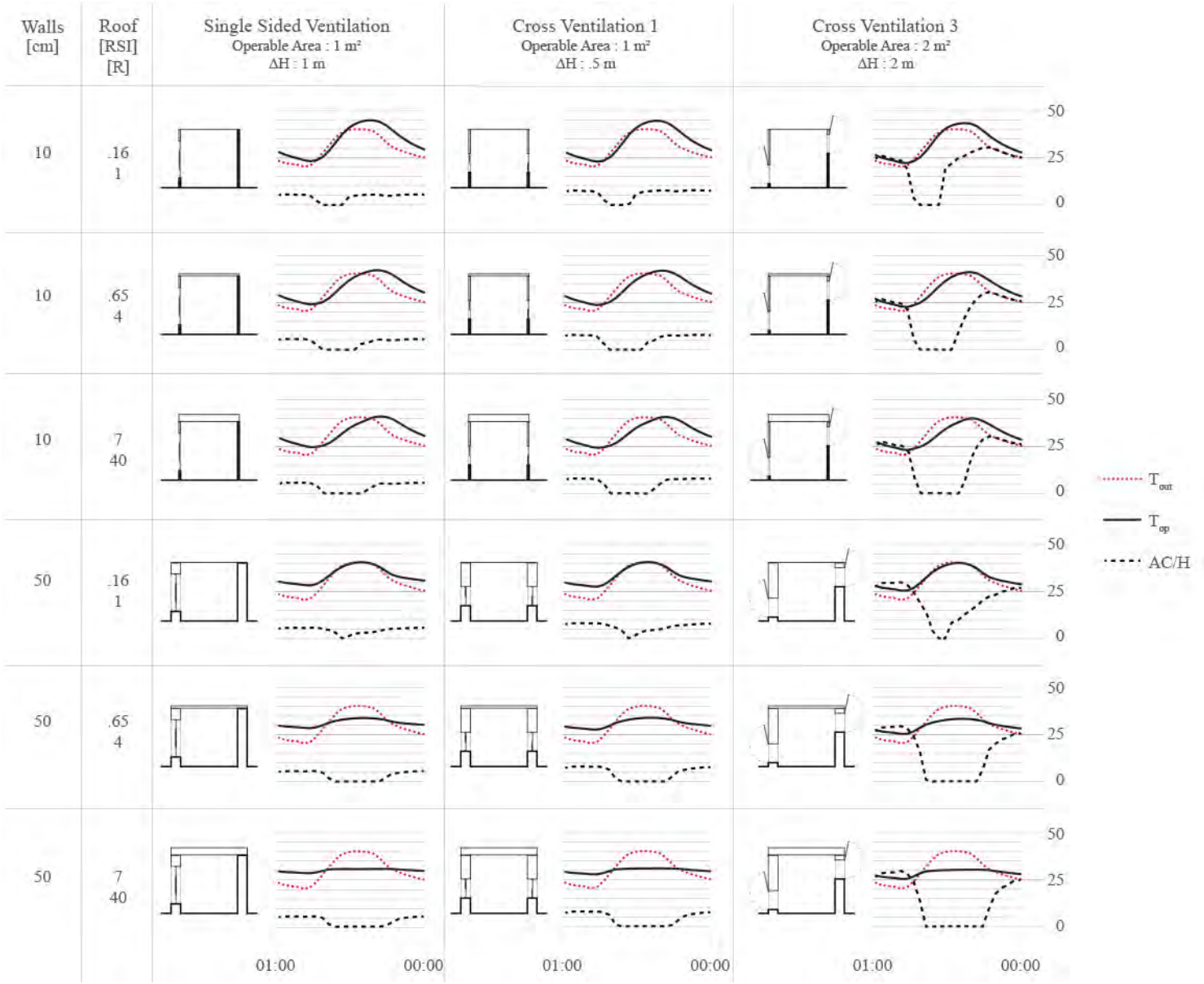

Figure 4.2 – Iteration 1, sample results of 18 out of 72 variations. Window size and position changes along the x-axis, and roof and wall materials change along the y-axis.

4.1.2 Results

Figure 4.2 is a snapshot of 18 of the 72 variations tested for the April 6th 24 hour period. Icons of each test volume variation are situated next to line graphs that show outdoor air temperature, indoor operative temperature, and air changes per hour as they progress through 24 hours. This set of results is useful to see the effect of building materials and openings on natural ventilation schedules and rates. As roof insulation levels increase, the pattern of natural ventilation begins to assume a night flush schedule on its own. This indicates that increased roof insulation levels, openings are shut for longer periods of time during the day. This means that indoor T_{op} is kept lower than outdoor air temperatures for a longer period of time than in spaces with uninsulated roofs. The 50 cm wall variations show a similar trend to a greater effect (bottom row, Figure 4.2). The periods when T_{op} in the insulated high thermal mass variations is less than outdoor air temperature is extended on average 6 hours longer than their 10 cm wall counterparts (third row). The size and position of windows then effects the air change per hour rate in the space (x-axis). Increasing the operable area, A_{eff} from 1 m^2 to 2 m^2 has a greater impact on increase of air changes per hour than changing ΔH from .5 m to 2 m. An increase in nightly air changes per hour does not appear to greatly affect daily maximum indoor operative temperatures in this simulation set. It does, however, decrease nightly temperatures by 2 °C to 5 °C. This is especially important in the high thermal mass variations. The high thermal mass walls have the greatest impact on moderating indoor operative temperature, but in order for it to cool at night, more airflow is needed.

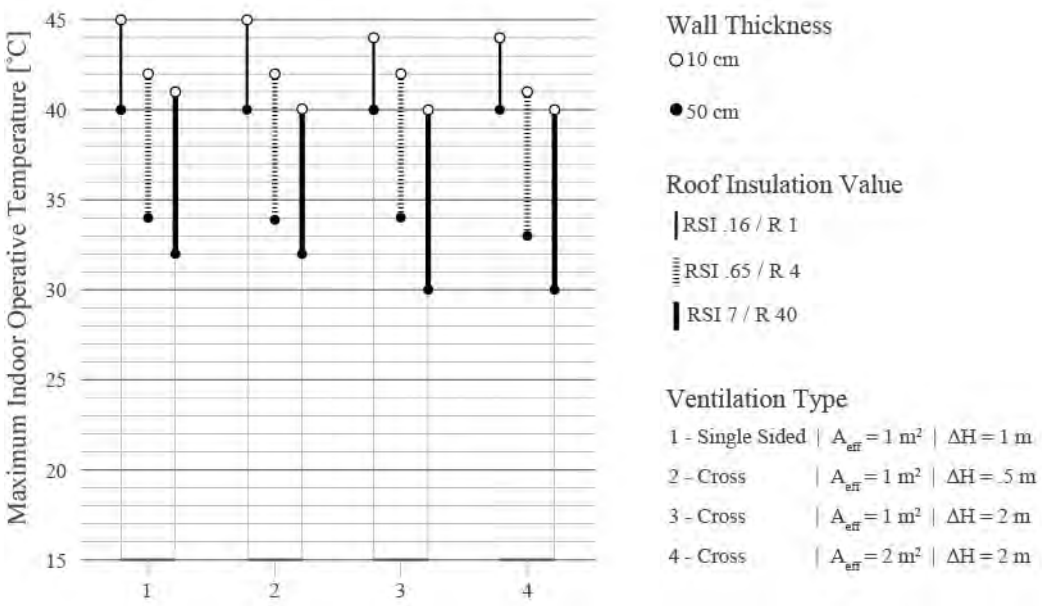

Figure 4.3 – Plot of maximum daily indoor operative temperatures for 24 Iteration 1 variations.

As a quick reference of effect on wall thickness, roof insulation level, and ventilation type on operative temperature, Figure 4.3 shows us primarily two things. First, roof insulation levels have the greatest impact on daily maximum indoor T_{op}. The addition of .65 m^2 °C/W RSI (R-4) to roofs of 10 cm wall variations causes a T_{op} drop of 2 °C to 3 °C, and in the 50 cm variations, a drop of 6 °C to 7 °C. However, the simulations show that there are diminishing returns on lowering daily maximum T_{op} with the addition

of insulation past .65 m^2 °C/W RSI (R-4). With the addition of more than ten times the insulation, Figure 4.3 shows that T_{op} only drops an addition 1 °C to 4 °C. The variation that resulted in the lowest maximum indoor T_{op} of 30 °C was comprised of the .5m thermal mass wall, 7 m^2 °C/W RSI (R-40) insulated roof, 2 m^2 A^{eff} and a ΔH of 2m between openings. The 10 cm wall counterpart out put its daily maximum T_{op} of 40 °C.

4.1.3 Discussion

It is a widely accepted general rule that night flush cooling is effective in buildings with high thermal mass in arid environments with high diurnal temperature swings, and this is corroborated by the results of these initial simulations. However these results show that in buildings without thermally massive roofs, such as those commonly seen in the field, night flush ventilation by manual operation (opening windows after sunset and closing them after sunrise) though certainly possible, will be effective only when there is both a sufficient amount of thermal mass in the building envelope as well as sufficient thermal resistance from solar radiation from the roof. The April 6^{th} simulations show that with resistance levels as little as .65 m^2 °C/W RSI (R-4), equivalent to a roof with +/- 3.5 cm of rice hull insulation, maximum indoor T_{op} can potentially reduce by 5 °C or more.

The results also show that small changes in window size and height differences affected nighttime air change rates but did not have as great an impact on daily high T_{op}. For this reason, window size and position variations were removed from the varying parameter set. In all subsequent iterations, window size (effective area, or A_{eff}) was kept constant at 1 m^2 per window and positions were set with a ΔH of 2 m between north and south windows.

This study made it possible to quickly visualize several subtle relationships between all these parameters. The next step in pre-design assessment was to build the variation set by taking most influential parameters forward, such as insulation and thermal mass.

4.2 Iteration 2 - Annual Simulations

To assess the influence of thermal mass, thermal resistance to solar radiation, and natural ventilation on the overall annual thermal autonomy of a single zone, a second series of energy models with refined parameters are evaluated against three metrics. Annual hourly indoor T_{op} is evaluated against both the ASHRAE-55 2013 adaptive thermal comfort model at the 80% Acceptability Limits and the EN 15251 Category III acceptability limits. Operative temperatures are also plotted irrespective of an established standard so that the information can be directly compared in a familiar way, relieved of biases one standard might have over the other.

4.2.1 Modeling Assumptions, Inputs and Parameters

Figure 4.4 shows modifications made to the single thermal zone model variations to include additional wall assembly types, which are described in this section. Building size, orientation and geometry, as well as thermal gains, wind factor and infiltration inputs remained the same from Iteration 1. Also

similar to Iteration 1, settings in DesignBuilder were configured such that the windows were only open when indoor air temperature exceeded outdoor air temperature. It is important to note here that because passive cooling is the focus of this research, the ventilation settings remain this way regardless of time of year. Thus, during the cooler months, the test volumes tend to over-cool at night. In addition to the conditional ventilation settings, and second ventilation was input to the simulation set to determine indoor T_{op} resulting from a scenario where the windows constantly remained open. This "constant" ventilation setting better reflects actual conditions in Bhuj informal settlements. As mentioned in the previous section, to maximize the effects of natural ventilation, windows in all variations enabled buoyancy-driven cross ventilation with a 2 m^2 A_{eff} and 2 m ΔH opening offset parameter.

Wall material inputs were augmented to include a 20 cm two wythe uninsulated brick option, as well as one and two wythe options outfitted with exterior rice husk insulation at a total 1.3 m^2 °C/W RSI (R-8). The reason behind the introduction of the new wall assembly variables is that, as mentioned in previous sections, night flush ventilation is most effective in hot and arid climates only if there exists sufficient thermal mass heat sink. The purpose of adding exterior insulation to brick walls was to find a minimum thickness of thermal mass in conjunction with minimum level of thermal resistance necessary for the wall to be most effective with night flush ventilation. Specific material properties for the roof and wall variations are shown in Table 4.2.

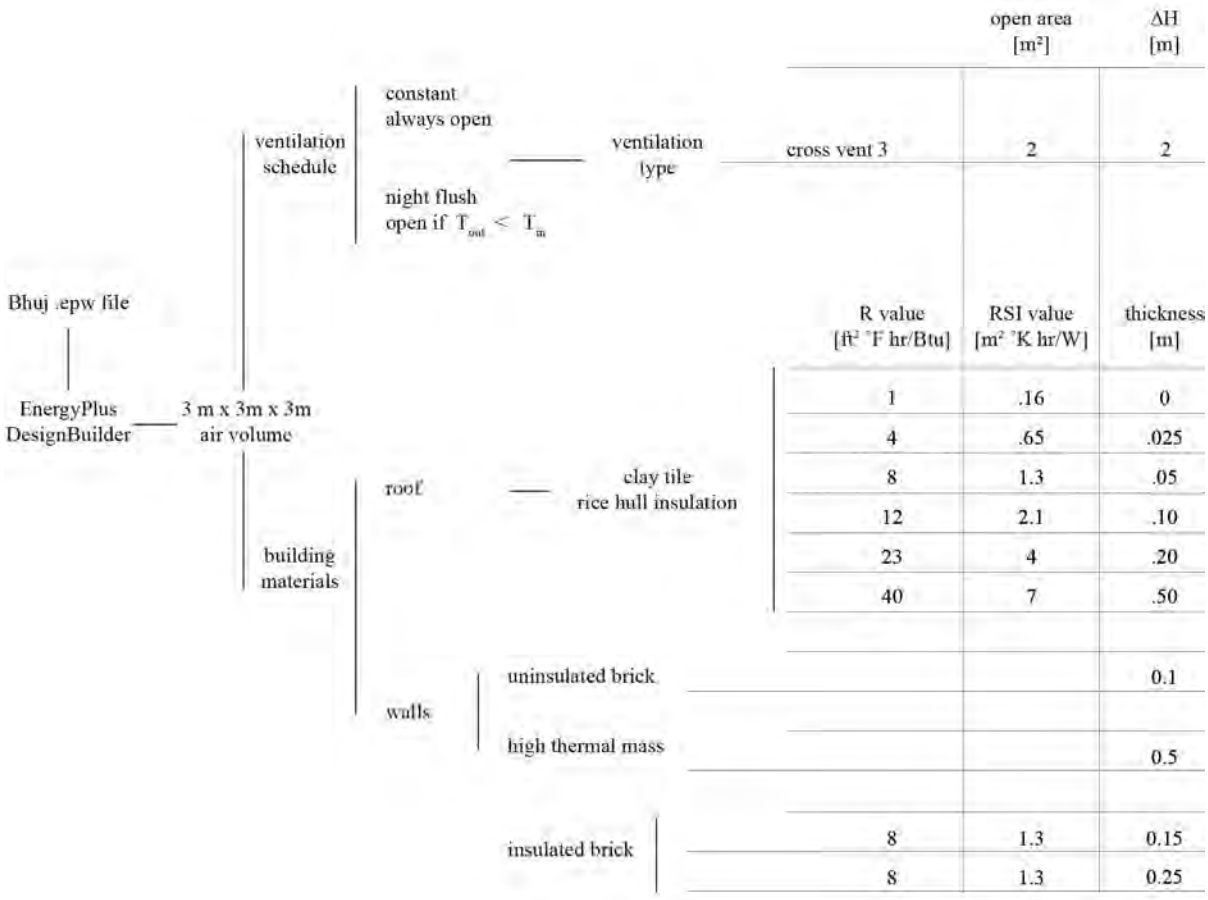

Figure 4.4 – Building material and ventilation variables for Iteration 2 simulations.

Construction Type Properties							
Walls		**E+ Total U Value**	**E+ Material Properties**				
Material	L	U	k	ρ	c_p	ε	α
	[cm]	[W/m²°K]	[W/m°K]	[kg/m³]	[J/kg°K]		
Clay Brick - Uninsulated	20	2.1	0.72	1920	840	0.9	0.6
Clay Brick - with 5 cm ext. Rice Hull Insulation	15	0.78	0.05	120	1000	0.9	0.6
	25	0.69					
Concrete, Medium Weight	50	1.26	0.81	1500	840	0.9	0.6
Roof							
Material	L	U	k	ρ	c_p	ε	α
	[cm]	[W/m²°K]	[W/m°K]	[kg/m³]	[J/kg°K]		
Clay Tile	1	6.41	0.81	1700	840	0.9	0.6
Rice Hull Insulation	2.5	1.55	0.05	120	1000	0.9	0.6
	5	0.88					
	10	0.47					
	35	0.14					

Table 4.2 – EnergyPlus building material properties for Iteration 2 simulations.

4.2.2 Results

Figure 4.5 shows the percent hours indoor operative temperatures exceed ASHRAE-55 80% and EN 15251 Category III acceptability limits for all resulting 32 Iteration 2 variations. Figures 4.6 through 4.8 Hourly T_{op} are more detailed annual hourly maps for three of the 32 variables. Outputs for these temperature maps are plotted in °C values as base comparison as well as against ASHRAE-55 80% and EN 15251 Category III acceptability limits. Performance statistics are listed in the caption of Figures 4.6 through 4.8.

Upon analysis of each of the 32 variables, it is apparent that though none of the variables tested were 100% thermally autonomous relative to the ASHRAE-55 80% acceptability limits, certain modifications to model parameters reduced high operative temperatures more than others. According to these predictions and the ASHRAE standard, thermal autonomy can be increased from 59% to 71% of the year with the addition of roof and exterior wall insulation if the space is constantly ventilated. If the models are simulated with inputs that allow for night flush ventilation, the model predicts the potential for thermal autonomy for 89% of the year according to ASHRAE standards and 100% for EN 15251 standards.

In variations with uninsulated roofs, wall insulation level or thickness has little effect on thermal performance according to both the ASHRAE and EN 15251 standards. Regardless of ventilation schedule, thermal autonomy is only increased from 59% to 63% of the year by ASHRAE standards and from 75% to 76% by EN 15251 standards.

Even with sufficient levels of thermal mass in the walls, the efficacy of night flush ventilation also depends on the level of insulation in the roof. When as little as 5 cm of roof insulation (equivalent to RSI .65) is added to the roof, significant increases in thermal autonomy occur. As wall thicknesses increase and exterior wall insulation is added, hours above acceptability limits drop even further. In the constantly ventilated variations with RSI .65 roofs, thermal autonomy increases from 62% to 69% of the year by ASHRAE standards and from 81% to 84% by EN 15251 standards. If the models are simulated with

inputs that allow for night flush ventilation for RSI .65 variations, the model predicts the potential for thermal autonomy for 65% to 74% of the year according to ASHRAE and 87% to 95% according to EN 15251.

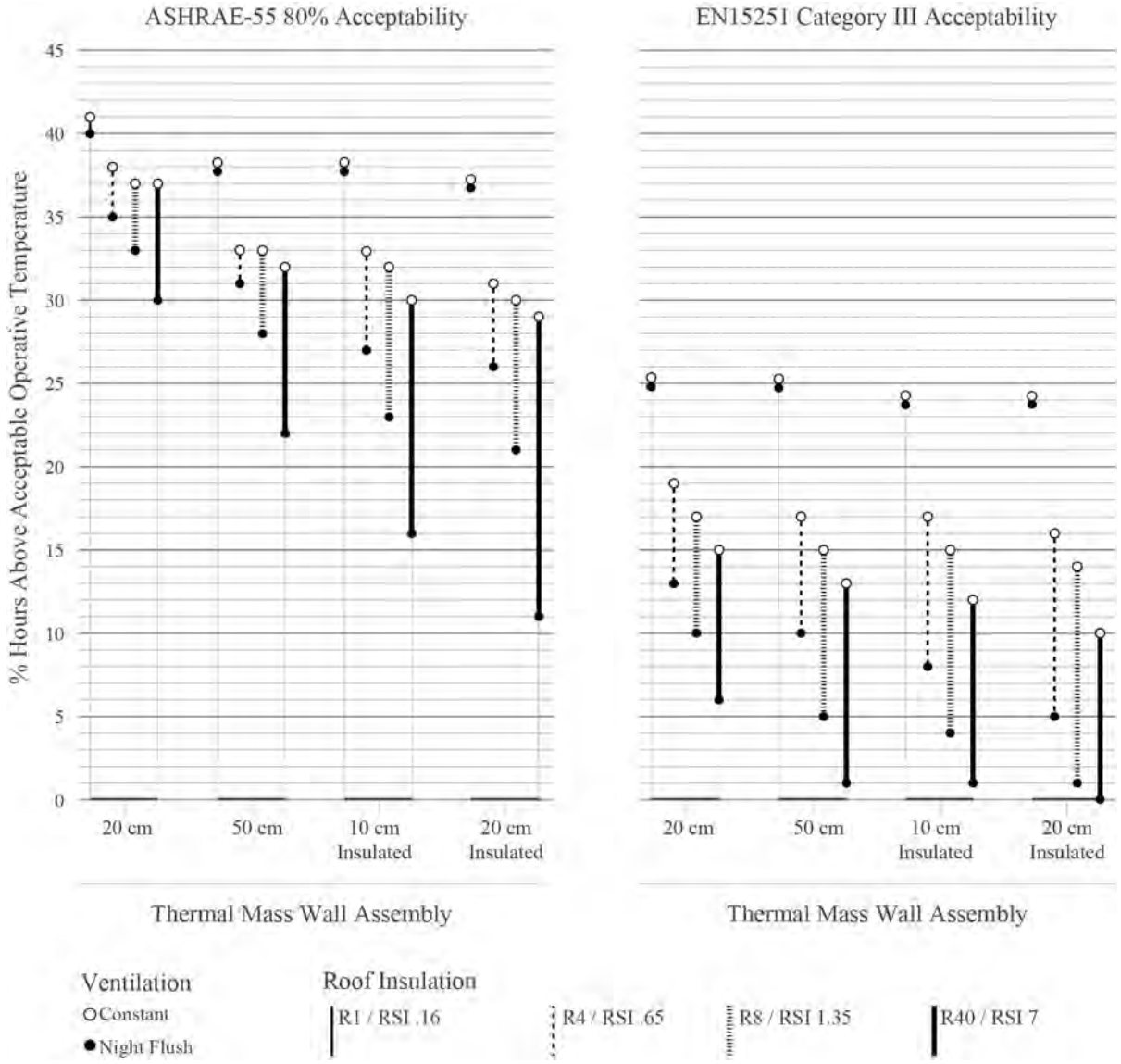

Figure 4.5 – Plot of operative temperatures for Iteration 2 variations relative to ASHRAE-55 and EN 15251 Acceptability Limits.

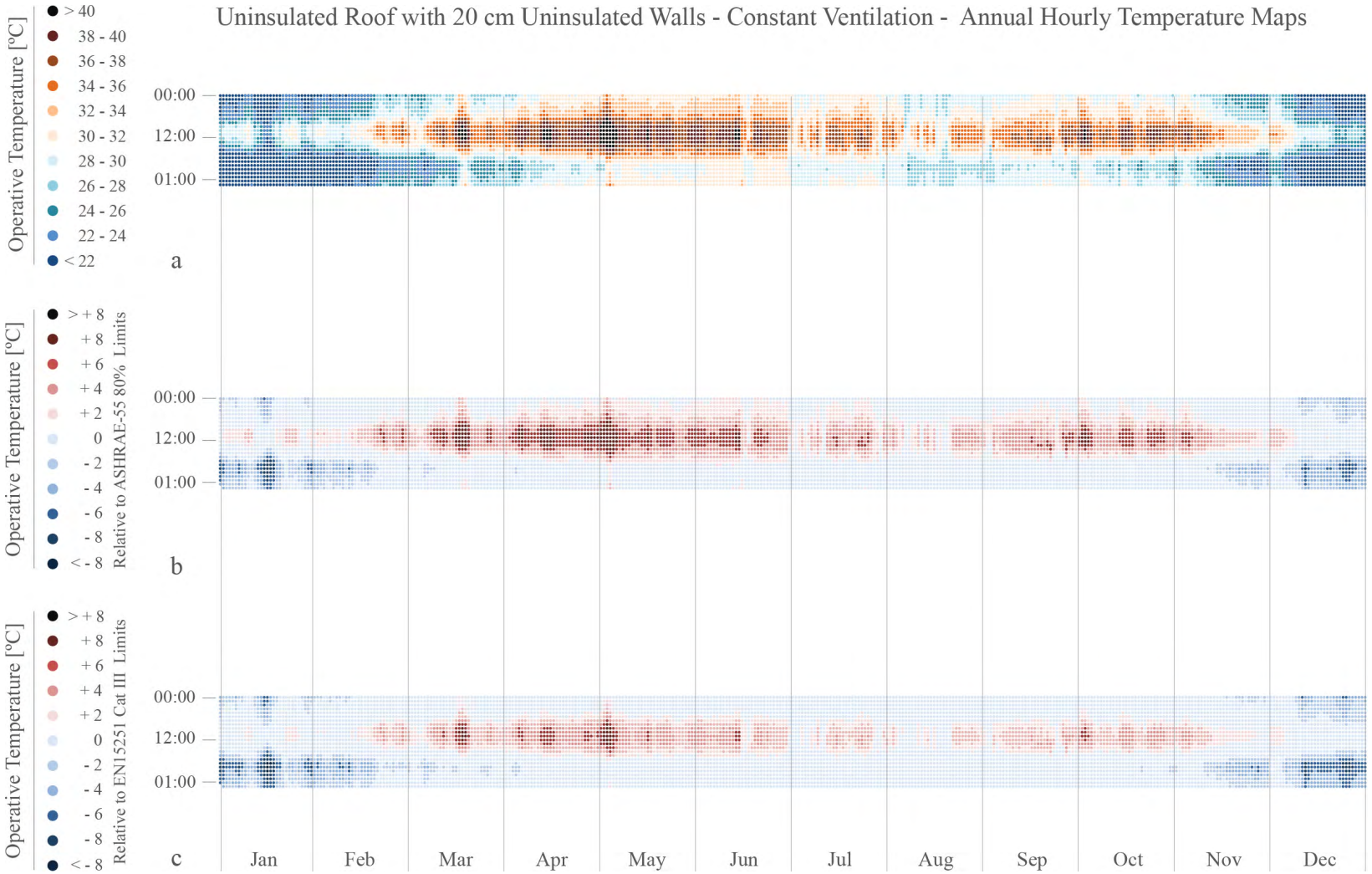

Figure 4.6 – Annual hourly temperature maps plotting thermal performance predictions for a constantly ventilated 3 m by 3 m by 3 m building with exposed uninsulated walls and clay tile roof. Top: Map a is an annual hourly plot of predicted operative temperatures for every hour of the year. The model predicts indoor temperatures will exceed 34 °C 20% of the year (equivalent to about 73 days) and the maximum operative temperature reached is 44 °C. Middle: Map b is an hourly plot of operative temperatures as they compare to the ASHRAE-55 80% Acceptability Limits. The model predicts that indoor operative temperatures will exceed 80% limits 41% of the year. Bottom: Map c is an hourly plot of operative temperatures as they compare to the more "heat tolerant" EN 15251 Category III Acceptability Limits. The model predicts that indoor operative temperatures will exceed category III limits 25% of the year (equivalent to about 91 days).

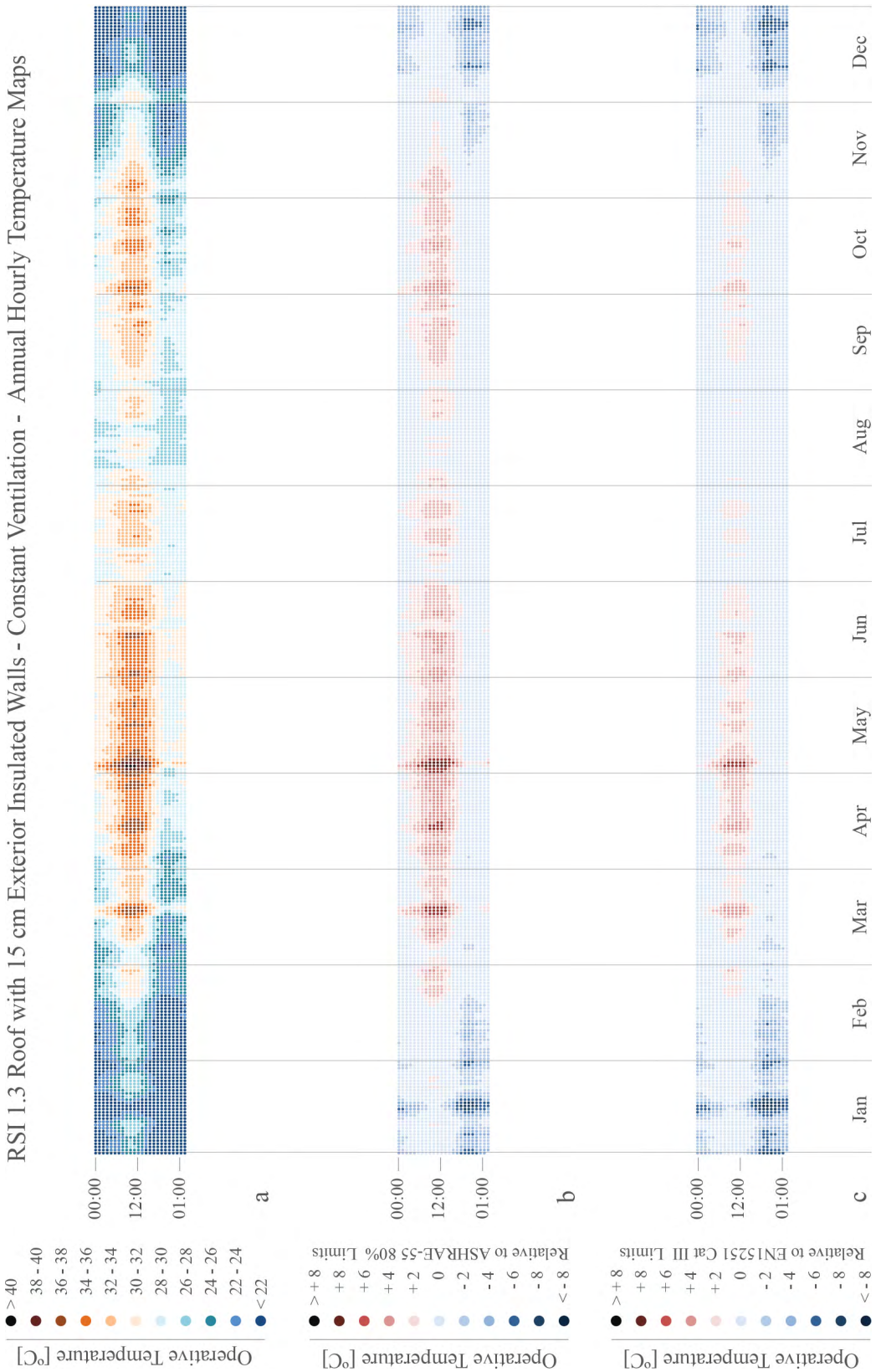

Figure 4.7 – Annual hourly temperature maps plotting thermal performance predictions for a constantly ventilated 3 m by 3 m by 3 m building with 15 cm exterior insulated walls and RSI 1.3 insulated clay tile roof. Top: Map a is an annual hourly plot of predicted operative temperatures for every hour of the year. The model predicts indoor temperatures will exceed 34 °C 8% of the year (equivalent to about 29 days) and the maximum operative temperature reached is 40 °C. Middle: Map b is an hourly plot of operative temperatures as they compare to the ASHRAE-55 80% Acceptability Limits. The model predicts that indoor operative temperatures will exceed 80% limits 32% of the year. Bottom: Map c is an hourly plot of operative temperatures as they compare to the more "heat tolerant" EN 15251 Category III Acceptability Limits. The model predicts that indoor operative temperatures will exceed category III limits 15% of the year (equivalent to about 55 days).

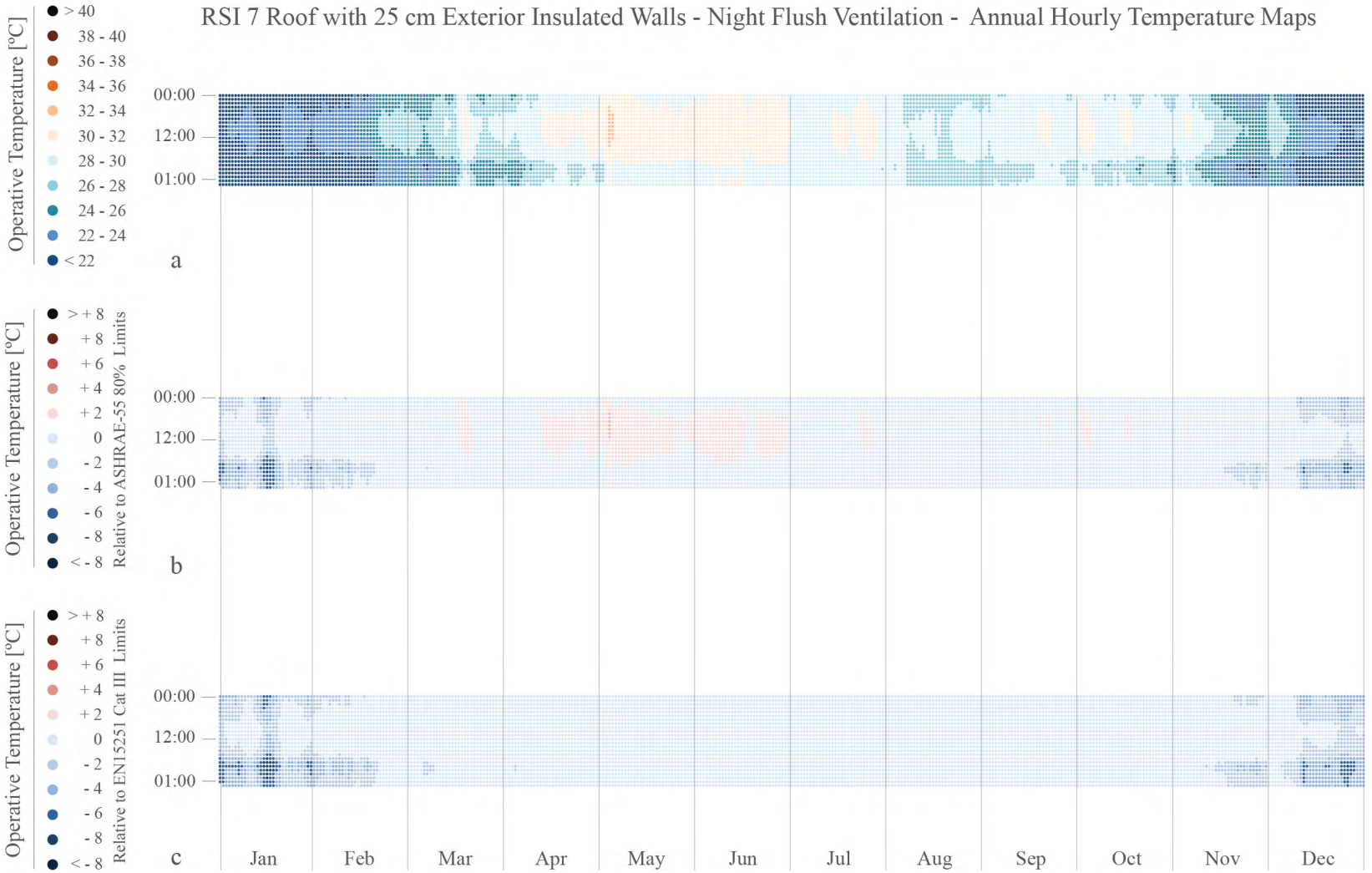

Figure 4.8 – Annual hourly temperature maps plotting thermal performance predictions for a night flush ventilated 3 m by 3 m by 3 m building with 25 cm exterior insulated walls and RSI 7 insulated clay tile roof. Top: Map a is an annual hourly plot of predicted operative temperatures for every hour of the year. The model predicts indoor temperatures will exceed 34 °C 0% of the year and the maximum operative temperature reached is 32.5 °C. Middle: Map b is an hourly plot of operative temperatures as they compare to the ASHRAE-55 80% Acceptability Limits. The model predicts that indoor operative temperatures will exceed 80% limits 11% of the year. Bottom: Map c is an hourly plot of operative temperatures as they compare to the more "heat tolerant" EN 15251 Category III Acceptability Limits. The model predicts that indoor operative temperatures will exceed category III limits 0% of the year.

4.3 Impact of Initial Simulations on Co-Design

The co-design process is a fluid one: its success is dependent on whether it responds to technical, practical, social and cultural concerns. This beginning research phase yielded results, not solutions. Appropriate solutions are only possible when they not only function well or are optimized, but when they are implementable and are responsive to the context for which they are designed.

Though design constraints and preferences changed as the project progressed, the purpose of this section is to document the recommendations and feedback between co-design partners that resulted from initial digital simulation analysis. The initial analysis resulted in an set of recommendations, presented to Hunnarshala in August 2014. It was recommended that Hunnarshala incorporate roof as well as exterior wall insulation at 1.3 m^2 °C/W RSI (R-8). Discussion also began with foundation directors about the potential benefits of night flush ventilation and methods by which information about natural ventilation might be effectively diffused to the residents of the upcoming Rajiv Awas Yojana (RAY) housing re-development.

This meeting marked a critical point in project formation. Hunnarshala agreed that the results of the simulations looked promising enough to embark on an extensive project to include not only further iterations of digital model analyses, but to add existing building analysis (the methods and results of which are detailed in Chapter Ch3), as well as the design and testing of innovative roof assemblies to improve thermal comfort in slum re-development communities.

During the meeting Hunnarshala directors offered valuable feedback about traditional building methods and operation, as well as recommendations based on findings from its own past research, experiences and expertise. The Slum Free Bhuj house will be the first site of application, so it was decided to first focus on the component that would have the most impact on thermal performance and was specific to that house typology. Hunnarshala's feedback re-routed and focused subsequent iterations in the following ways:

Prioritization of roof assemblies over wall assemblies.
The Slum Free Bhuj courtyard house typology is oriented such that it shares walls on its long axis with neighboring houses (Section 2.2). Walls facing the courtyard space in each house are shaded by +/- 2 m overhangs and during periods of low sun, will be shaded by adjacent courtyard perimeter walls. Thus the majority of the surfaces of the houses will be largely protected from direct solar radiation. The part that remains un-protected is the roof.

Establishment of wall and outer roof material.
Hunnarshala previously established that the Slum Free Bhuj house walls be constructed from 23 cm thick sandstone block that is locally available and widely used in the region. The outer roof material is set to be built from Mangalore Pattern, or flat, clay tiles; another material that is widely used and accepted in the region. Not only are these materials readily available, Hunnarshala staff are technical experts with the materials, have established that the materials are the aesthetically preferred choices by future residents of RAY re-developments.

Inclusion of thermal mass in the roof as a digital model simulation parameter.
Hunnarshala developed an innovation that incorporates mud, a traditional roofing material, into rolls that are used simultaneously as structural members and heat sinks for clay tile roofs. The rolls are made by coating burlap sacks with mud, surkhi, or lime slurry, then wrapping the sacks tightly around a batten with

its ends exposed. Those ends are then mechanically fastened to main roof rafters such that they provide support for roof tiles above. In an attempt to increase the rolls' insulative value, straw is incorporated. Hunnarshala performed load and soil tests to determine the durability and strength of the rolls (Satrasala, 2014), and based thermal design decisions empirically from vernacular building traditions as well as their own expertise in earth building. To foster the continued development of the mud rolls as to compare thermal performance of insulative to thermally massive roof construction, the rolls were added to the list of roof "insulation" parameters for digital modeling.

4.4 Iteration 3 - Annual Simulations

A third set of annual performance simulations incorporated Hunnarshala's feedback and refine building envelope assemblies to further improve thermal performance in low cost housing.

4.4.1 Modeling Assumptions, Inputs and Parameters

Figure 4.9 shows modifications made to the single thermal zone model to better reflect the RAY house typology's shared walls and courtyard design. Zone size, orientation, geometry, window placement and position, as well as internal gains, wind factor, infiltration, and window operation settings remained the same from the previous iteration. The wall material input was set to 23 cm sandstone block. Outer roof materials were set to exposed clay tile, and exposed clay tile shaded by an opaque plane of solid material. It is important to note here that in DesignBuilder, it is not possible to assign thermal properties to a shading component. The component is input as a 100% opaque surface, devoid of conductive or radiative properties. Thus, the shaded roof variations are models of an ideal condition where no heat transfer via radiation occurs between the upper and lower layers. This limitation of the model lead to the inclusion of a double-layer uninsulated roof design with a radiant barrier, which is discussed later in this chapter and in detail in Chapter Ch6.

Roofs were simulated without insulation, with a 10 cm interior layer of mud, to approximate the Hunnarshala mud roll, and finally a 10 cm layer of rice husk insulation (2.1 m^2 °C/W RSI, or R-12). Specific material properties for the roof and wall variations are shown in Table 4.3.

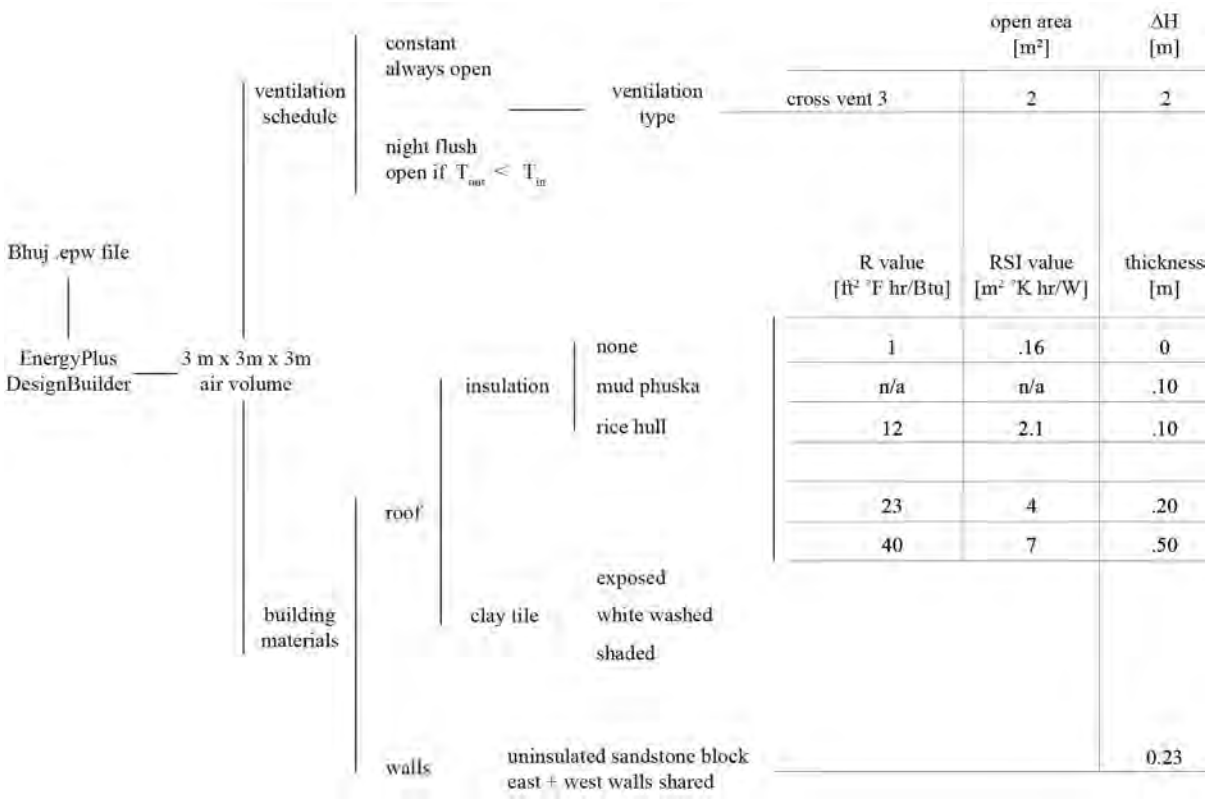

Figure 4.9 – Building material and ventilation variables for Iteration 3 simulations.

Construction Type Properties

Walls		**E+ Total U Value**	**E+ Material Properties**				
Material	L [cm]	U [W/m²°K]	k [W/m°K]	ρ [kg/m³]	c_p [J/kg°K]	ε	α
Sandstone Block	23	2.76	1.30	2200	712	0.9	0.6
Roof							
Material	L [cm]	U [W/m²°K]	k [W/m°K]	ρ [kg/m³]	c_p [J/kg°K]	ε	α
Exposed Clay Tile	1	6.41	0.81	1700	840	0.9	0.6
Whitewashed Clay Tile	1	6.41	0.81	1700	840	0.9	0.2
Mud Phuska	10	2.87	0.52	1622	880	0.9	0.6
Rice Hull Insulation	10	0.47	0.05	120	1000	0.9	0.6

Table 4.3 – EnergyPlus building material properties for Iteration 3 simulations.

4.4.2 Results

Figure 4.10 shows the % hours indoor operative temperatures exceed ASHRAE-55 80% and EN 15251 Category III acceptability limits for all resulting 18 Iteration 3 variations. Figures 4.11 through 4.13 Hourly T_{op} are more detailed annual hourly maps for three of the 18 variables. Outputs for these temperature maps are plotted in °C values as base comparison as well as against ASHRAE-55 80% and EN 15251 Category III acceptability limits. Performance statistics are listed in the caption of Figures 4.11 through 4.13.

Upon analysis of each of the 18 variables, it is apparent that though none of the variables tested were 100% thermally autonomous relative to the ASHRAE-55 80% acceptability limits, certain modifications to model parameters reduced high operative temperatures more than others. In comparison to Iteration 2 results, just the addition of shared walls increases thermal autonomy from 59% to 65% of the year according to ASHRAE standards and from 75% to 79% by EN 15251 standards.

Shading or otherwise protecting the roof from solar radiation hast he greatest impact on indoor T_{op} in constantly ventilated spaces with high thermal mass. According to these predictions, thermal autonomy can be increased from 65% to 76% by the ASHRAE standard and from 79% to 96% by the EN 15351 standard with roof modification alone if the space is constantly ventilated. If the models with roof modifications are simulated with inputs that allow for night flush ventilation, predictions show the potential for thermal autonomy from 77% to 96% of the year according to ASHRAE standards and 81% to 100% for EN 15251 standards.

4.4.3 Discussion

The results of this final pre-design simulation suggest that in order to significantly decrease temperatures in RAY house interiors, it is necessary to modify roof assemblies by increasing their resistance to heat transfer via conduction and/or radiation. Because the RAY house is well shaded and shares walls with adjacent structures, the results further suggest that a number of different roof modifications will lead to near thermal autonomy if the spaces are properly night flush ventilated during hot periods of the year.

This series of simulations shows little difference in performance between constantly ventilated whitewashed and shaded roof variations, suggesting that painting a roof white, for instance, will have virtually the same impact on indoor T_{op} as would a separate, opaque sun shade at the exterior of the roof. While in principle both solutions drastically reduce radiative heat gain at the roof's surface, practically, the physical shading option should function more consistently that the whitewashed/painted option, as its reflection of solar radiation will not decrease as the surface degrades or becomes dirty. The decoupling of layers in the shaded option also reduces heat transfer via conduction. In an ideal scenario, as the model predicts, if the upper roof layer reflects 100% of solar radiation, the temperature of the air space would be the same as the the outside air, thereby reducing interior roof layer surface temperatures significantly.

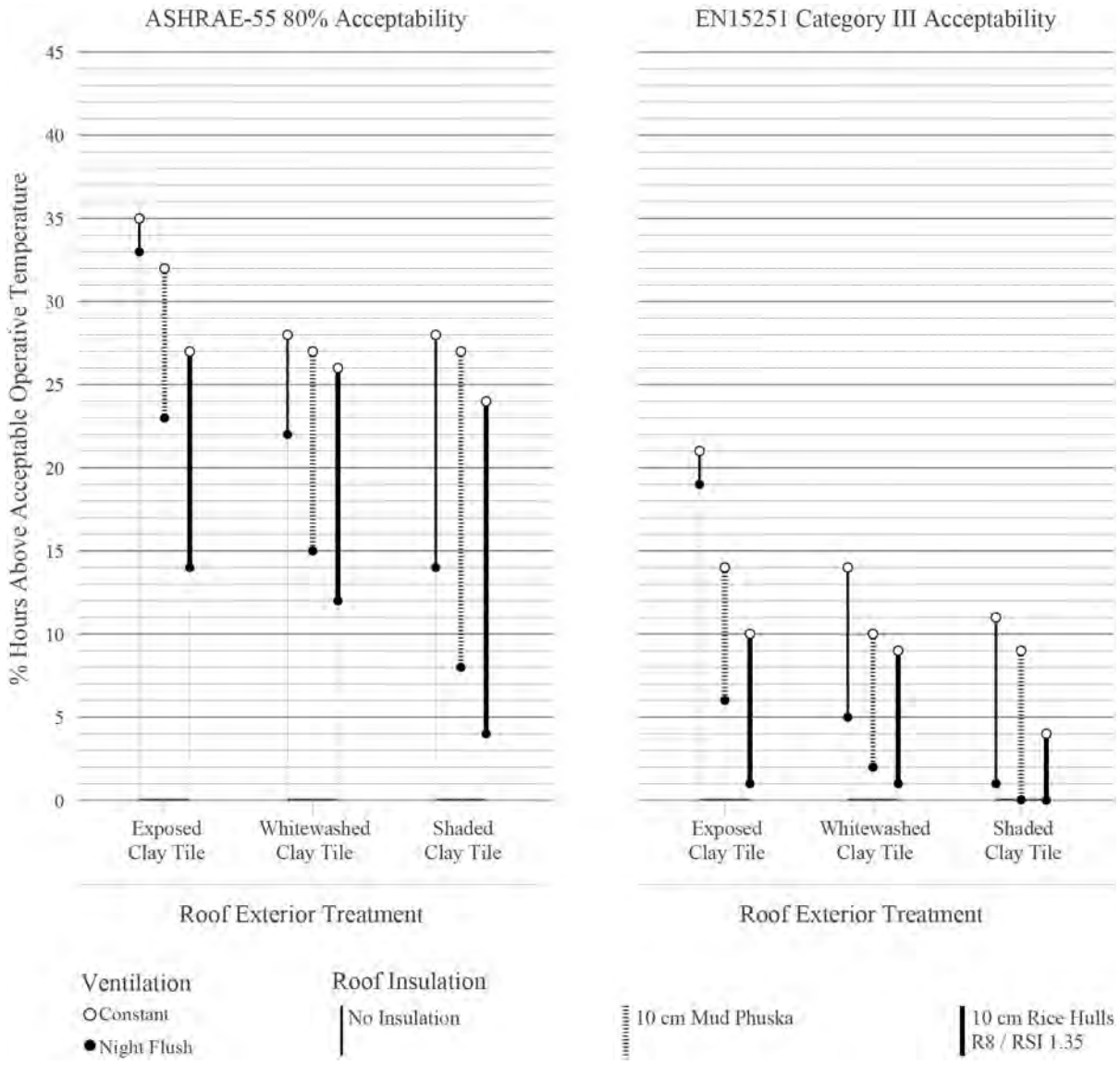

Figure 4.10 – Plot of operative temperatures for Iteration 3 variations relative to ASHRAE-55 and EN 15251 Acceptability Limits.

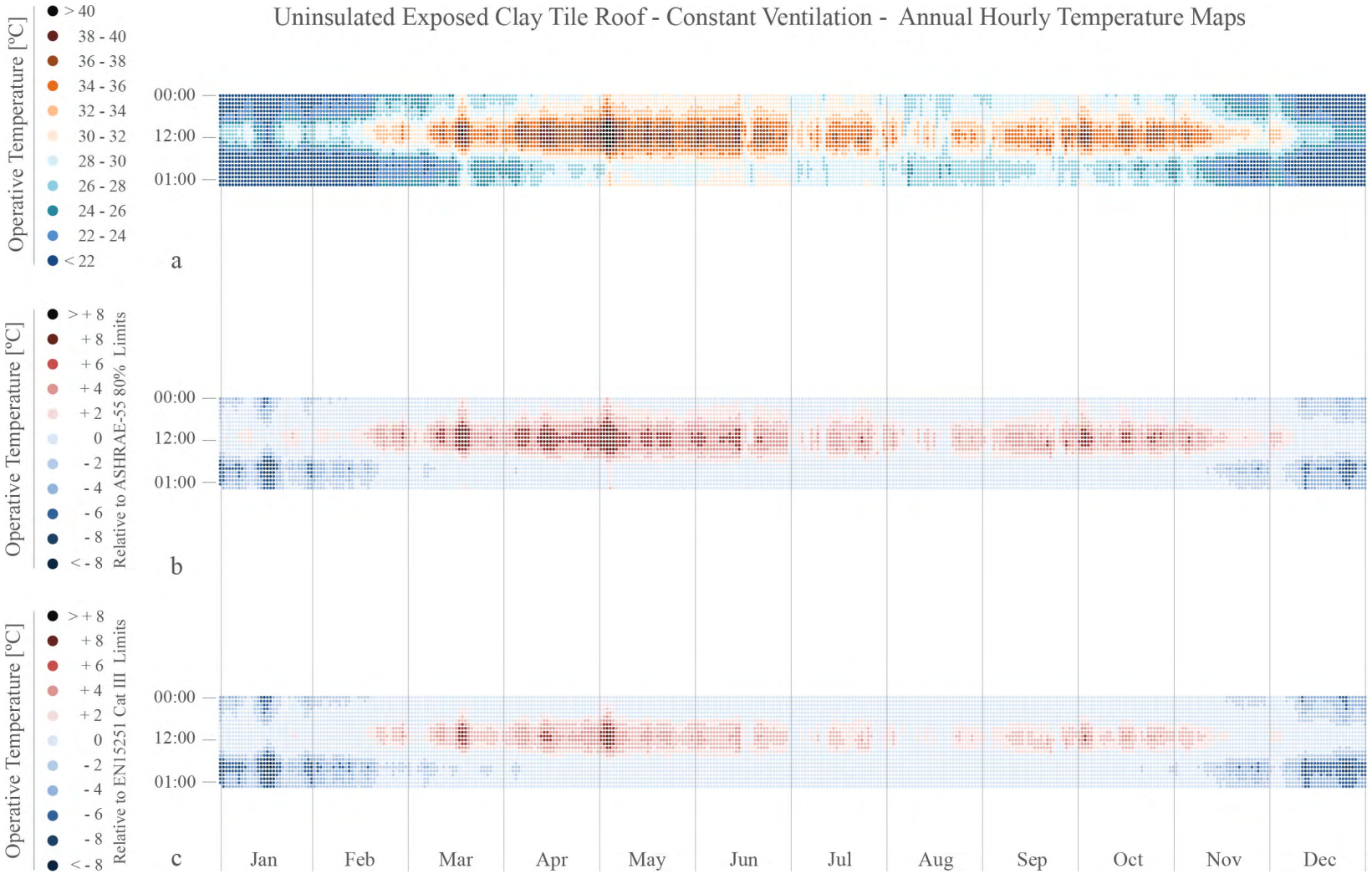

Figure 4.11 – Annual hourly temperature maps plotting thermal performance predictions for a constantly ventilated 3 m by 3 m by 3 m building with shared uninsulated walls and uninsulated exposed clay tile roof. Top: Map a is an annual hourly plot of predicted operative temperatures for every hour of the year. The model predicts indoor temperatures will exceed 34 °C 15% of the year (equivalent to about 55 days) and the maximum operative temperature reached is 43 °C. Middle: Map b is an hourly plot of operative temperatures as they compare to the ASHRAE-55 80% Acceptability Limits. The model predicts that indoor operative temperatures will exceed 80% limits 35% of the year. Bottom: Map c is an hourly plot of operative temperatures as they compare to the more "heat tolerant" EN 15251 Category III Acceptability Limits. The model predicts that indoor operative temperatures will exceed category III limits 21% of the year (equivalent to about 77 days).

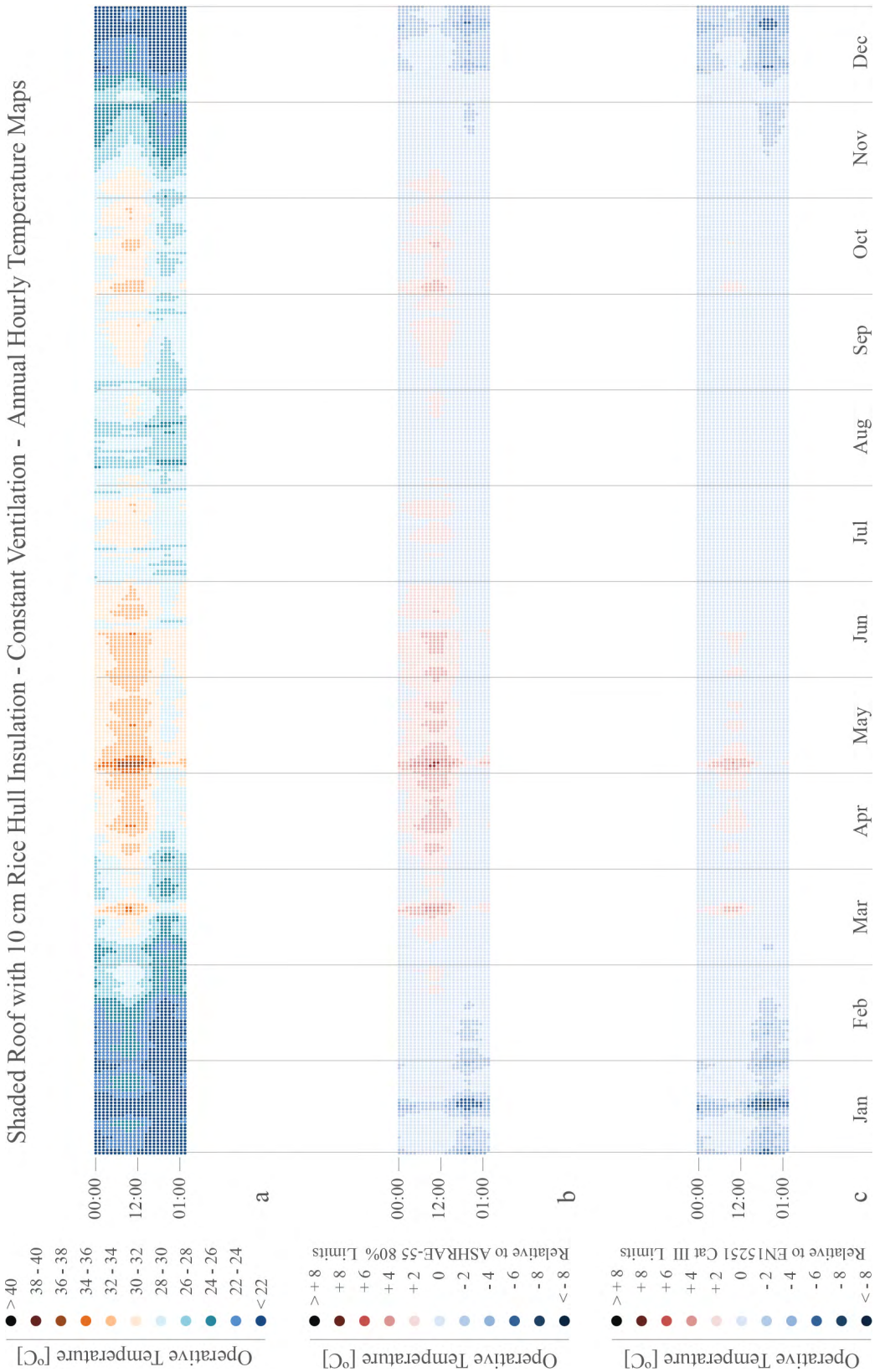

Figure 4.12 – Annual hourly temperature maps plotting thermal performance predictions for a constantly ventilated 3 m by 3 m by 3 m building with shared uninsulated walls and shaded clay tile roof with 10 cm rice hull insulation. Top: Map a is an annual hourly plot of predicted operative temperatures for every hour of the year. The model predicts indoor temperatures will exceed 34 °C 1% of the year (equivalent to about 4 days) and the maximum operative temperature reached is 37 °C. Middle: Map b is an hourly plot of operative temperatures as they compare to the ASHRAE-55 80% Acceptability Limits. The model predicts that indoor operative temperatures will exceed 80% limits 24% of the year. Bottom: Map c is an hourly plot of operative temperatures as they compare to the more "heat tolerant" EN 15251 Category III Acceptability Limits. The model predicts that indoor operative temperatures will exceed category III limits 4% of the year (equivalent to about 15 days).

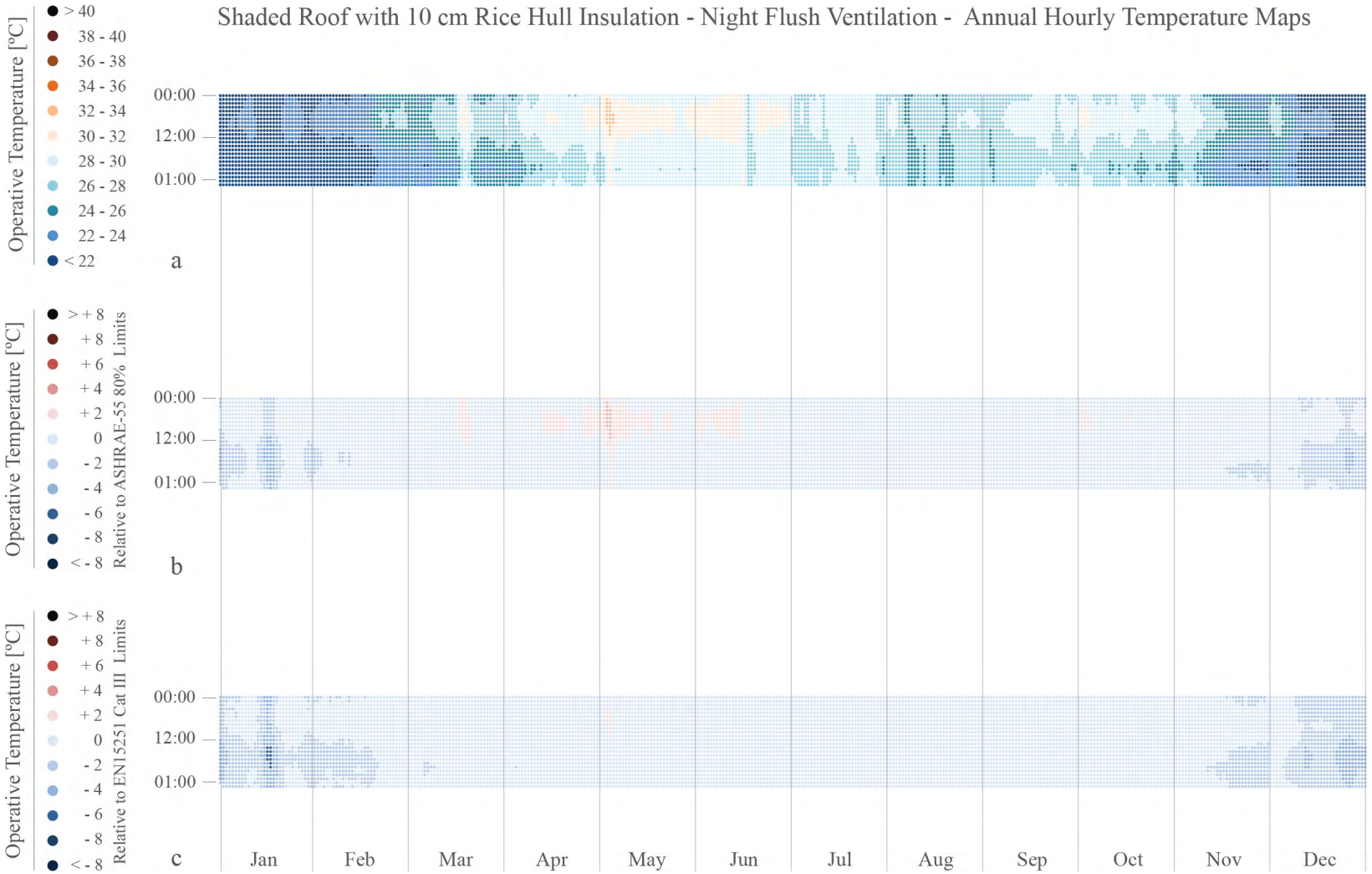

Figure 4.13 – Annual hourly temperature maps plotting thermal performance predictions for a night flush ventilated 3 m by 3 m by 3 m building with shared uninsulated walls and shaded clay tile roof with 10 cm rice hull insulation. Top: Map a is an annual hourly plot of predicted operative temperatures for every hour of the year. The model predicts indoor temperatures will exceed 34 °C less than 0% of the year and the maximum operative temperature reached is 33 °C. Middle: Map b is an hourly plot of operative temperatures as they compare to the ASHRAE-55 80% Acceptability Limits. The model predicts that indoor operative temperatures will exceed 80% limits 4% of the year. Bottom: Map c is an hourly plot of operative temperatures as they compare to the more "heat tolerant" EN 15251 Category III Acceptability Limits. The model predicts that indoor operative temperatures will exceed category III limits less than 1% of the year.

4.5 Recommendations

Iteration 3 results lead to the schematic design of six roof assemblies that mimicked the better performing simulation variations in one or more ways. The design recommendations aimed to improve thermal performance of the RAY house roofs by using low-cost, readily available materials, assembled into forms aesthetically and tectonically appropriate to the construction typology. Figures 4.14 through 4.16 give a broad overview of the six initial roof design recommendations. The recommendations were to prototype double layer roof assemblies in three groups. The first group contains two variations to improve upon Hunnarshala's mud roll design (Figure 4.14). The second group contains two variations that introduced rice husk insulation panels as the interior layer (Figure 4.15). The third group contains two variations of is an exterior shaded roof proposal using burlap and lime slurry to create rigid shading plates (Figure 4.16).

Interestingly, when these designs were proposed, Hunnarshala opted to move forward with the uninsulated shaded roof group and the insulated roof group. It is important to note here that the partners did not decide to table the double-layered thermally massive roofs because they are de facto inferior to insulated or shaded versions. On the contrary, Iteration 3 results predict that the mud roll variations perform similarly to insulated variations. The reason for the shift away from double-layer thermally massive roofs at that juncture in the project had to do with one of the director's visions for the potential to scale the project past Hunnarshala's own RAY re-development in the future. This marked another critical point in the project formation. Chapter 5 details the resulting prototypes that were developed as a result of this co-design process. The thought was that roof assembly prototypes follow the simulation recommendations but be made from clay tile, as originally discussed, as well as from corrugated tin sheet, which is very commonly seen in informal housing settlements, and potentially easier to scale to a panel product that could be implemented in various informal construction types. Furthermore, as the design ideas were very different than what is currently constructed, Hunnarshala recommended to first rigorously test the double-layer roof concept in the field with simplified versions of the proposed designs. The burlap and lime shade variation changed into an uninsulated double-layer tin sheet prototype with a radiant barrier. And, after several insulation conductivity tests, the rice hull and fabric insulation panel variation was replaced with a lighter weight rigid insulation panel made from cardboard and shredded waste plastic.

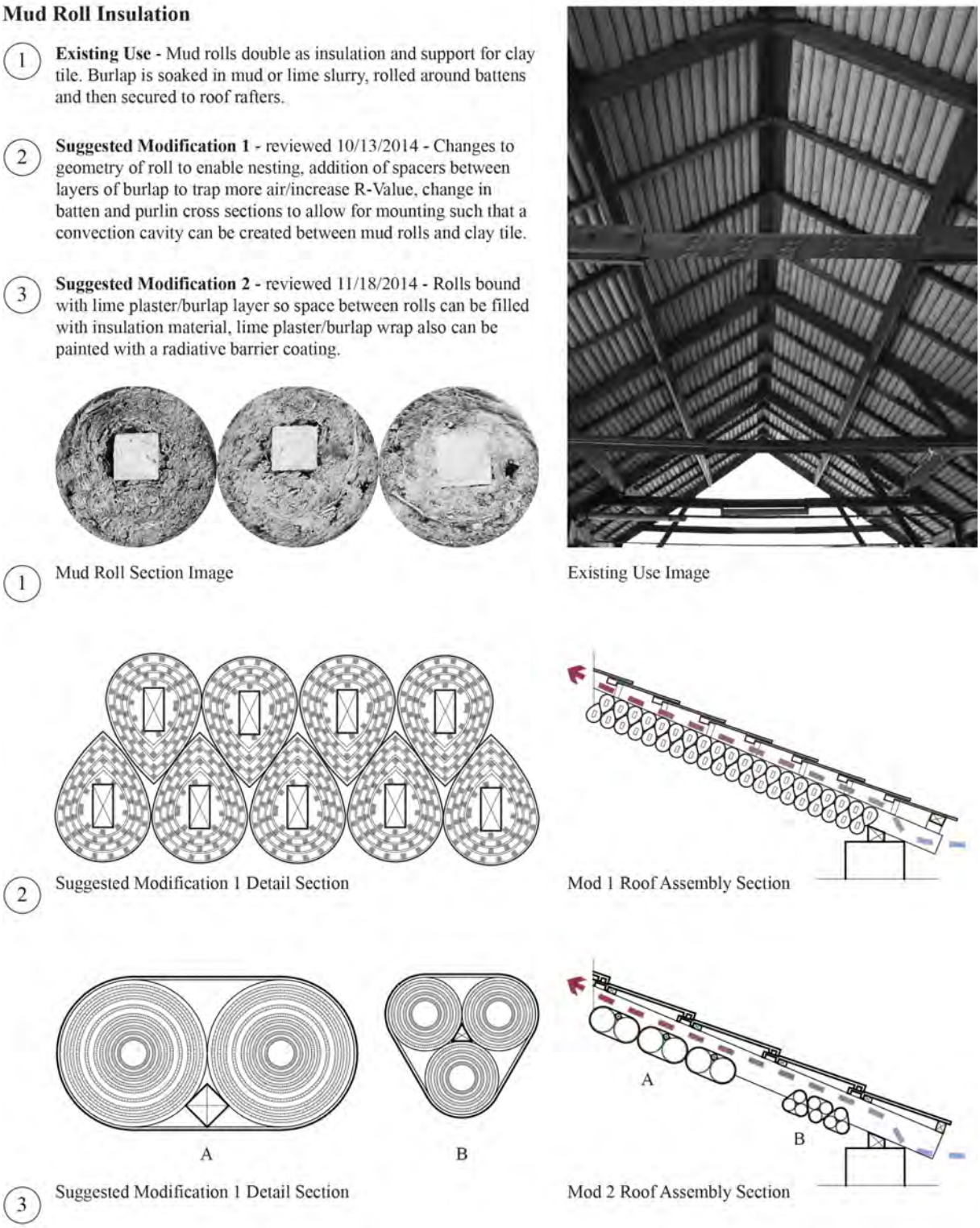

Figure 4.14 – Schematic design for modifications to existing mud roll insulation system.

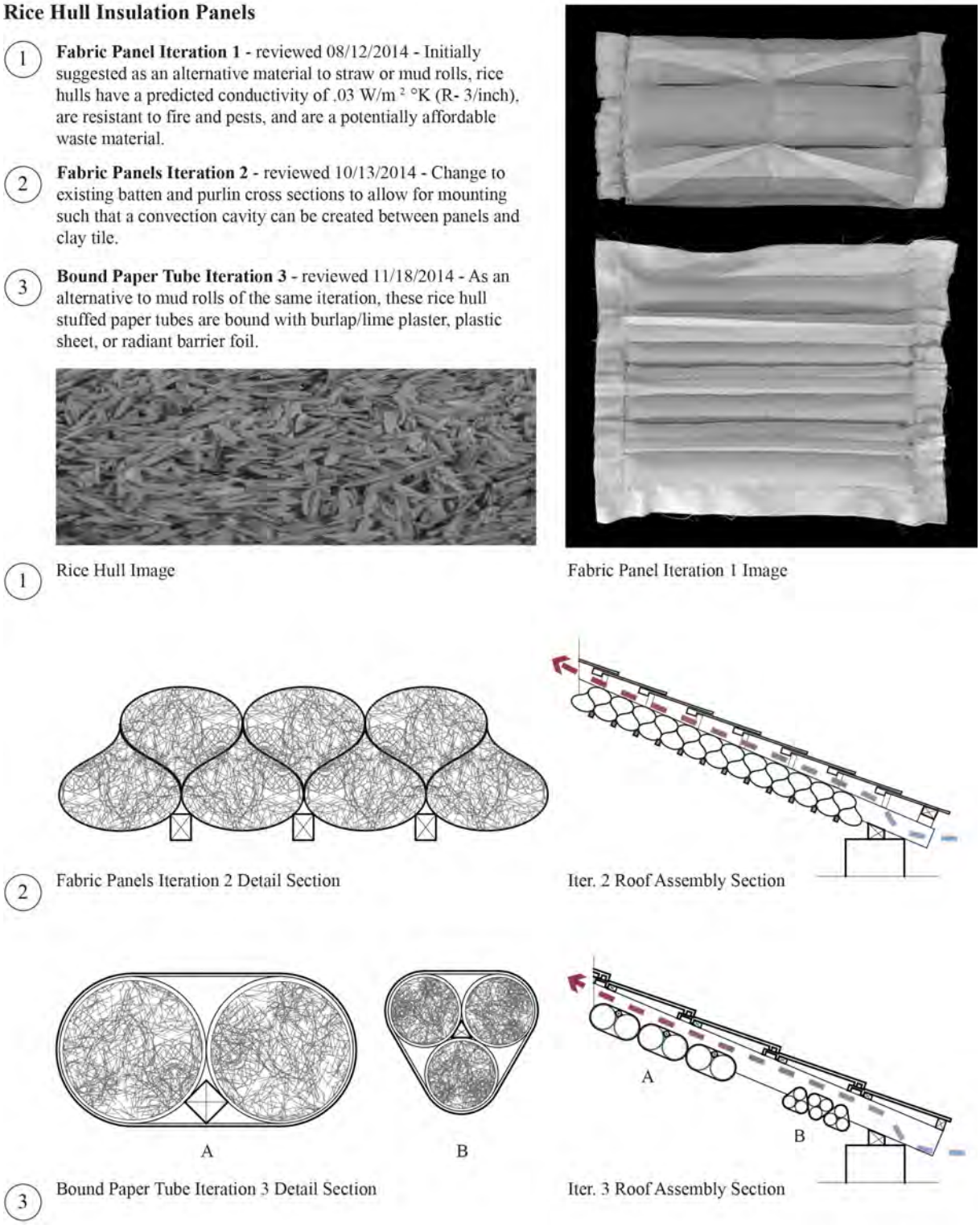

Figure 4.15 – Schematic design ideas for rice hull and fabric insulation panels.

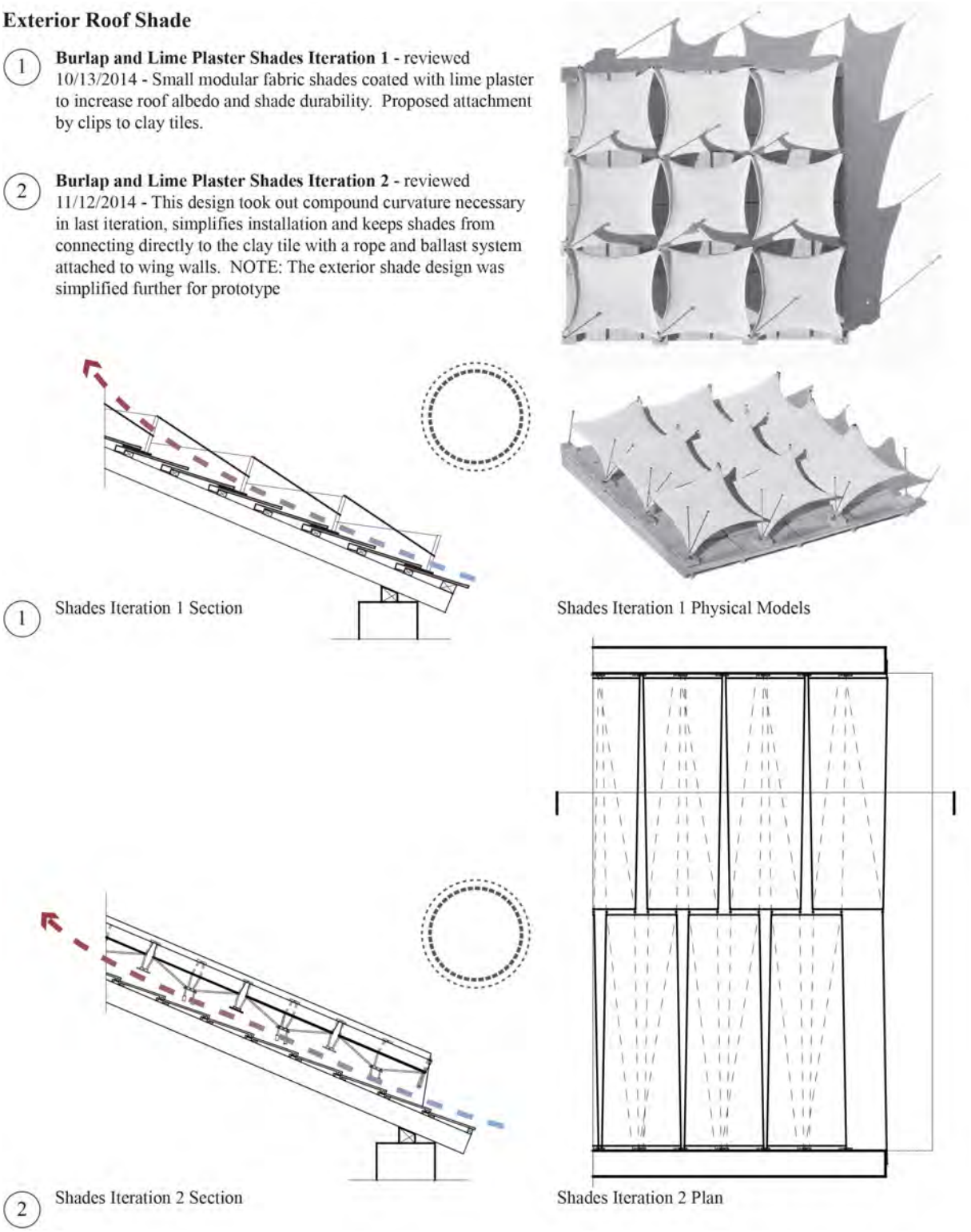

Figure 4.16 – Schematic design ideas for burlap and lime plaster exterior shade panels.

Chapter 5

Thermal Field Lab Experiments

This chapter describes the motivation, construction, research methods and results of the first round of an ongoing series of passive cooling field experiments conducted in Bhuj, India that began in November 2014. There are three main objectives of this part of the project. The first is to test prototypes to validate, prove, or disprove design decisions based on design with climate rules of thumb. Second, the construction of full-scale physical prototypes inevitably advances understanding of local construction materials and techniques. In that vein, physical construction also highlights potential unintended consequences of design decisions well before implementation. The third objective is to build the foundation for a thermal building technology lab in the field for continuous iterative future research.

5.1 Test Chamber Experimental Setup

After initial digital simulations, then prototype and experiment co-design review sessions, construction for a thermal research field lab began on a small farm, called *Paraspar*, a Gujarati word meaning *symbiotic*, southwest of the Bhuj city center. The foundation for the lab consists of five 2.4m by 2.4m by approximately 2.4m chambers, modeled after similarly sized chambers from previous digital simulations. Construction of all chambers are identical, save the roof assemblies. Chamber walls are constructed from 23 cm thick local sandstone block and mud mortar, and are externally insulated with approximately 15 cm of straw thatch. The insulated block walls are further protected from direct solar radiation – and cows' mouths – with an outer layer of burlap fabric coated with lime plaster. Each chamber is oriented to the four cardinal directions, having one .75 m wide by .5m high screened opening on the north and south facing walls. Each opening has an outer hinged solid panel, that can be manually operated according to desired ventilation schedules. The openings are oriented north/south for two reasons. The first is so that the hinged panels can provide full shade to the southern opening, to minimize direct solar gain to the interior. The second is to take advantage of Bhuj's summer evening prevailing winds from the southwest. These openings are offset vertically by 1.5m so that at times of little or no wind, buoyancy-driven ventilation can be maximized for the volume. The identical chambers were then outfitted with five variations of roof prototypes, which are detailed in sections 5.1.1 and 5.2.1 through 5.2.5. Finally, each chamber was instrumented with a series of thermal sensors to monitor thermal performance (section 5.1.2) during multiple ventilation schedules (section 5.1.3).

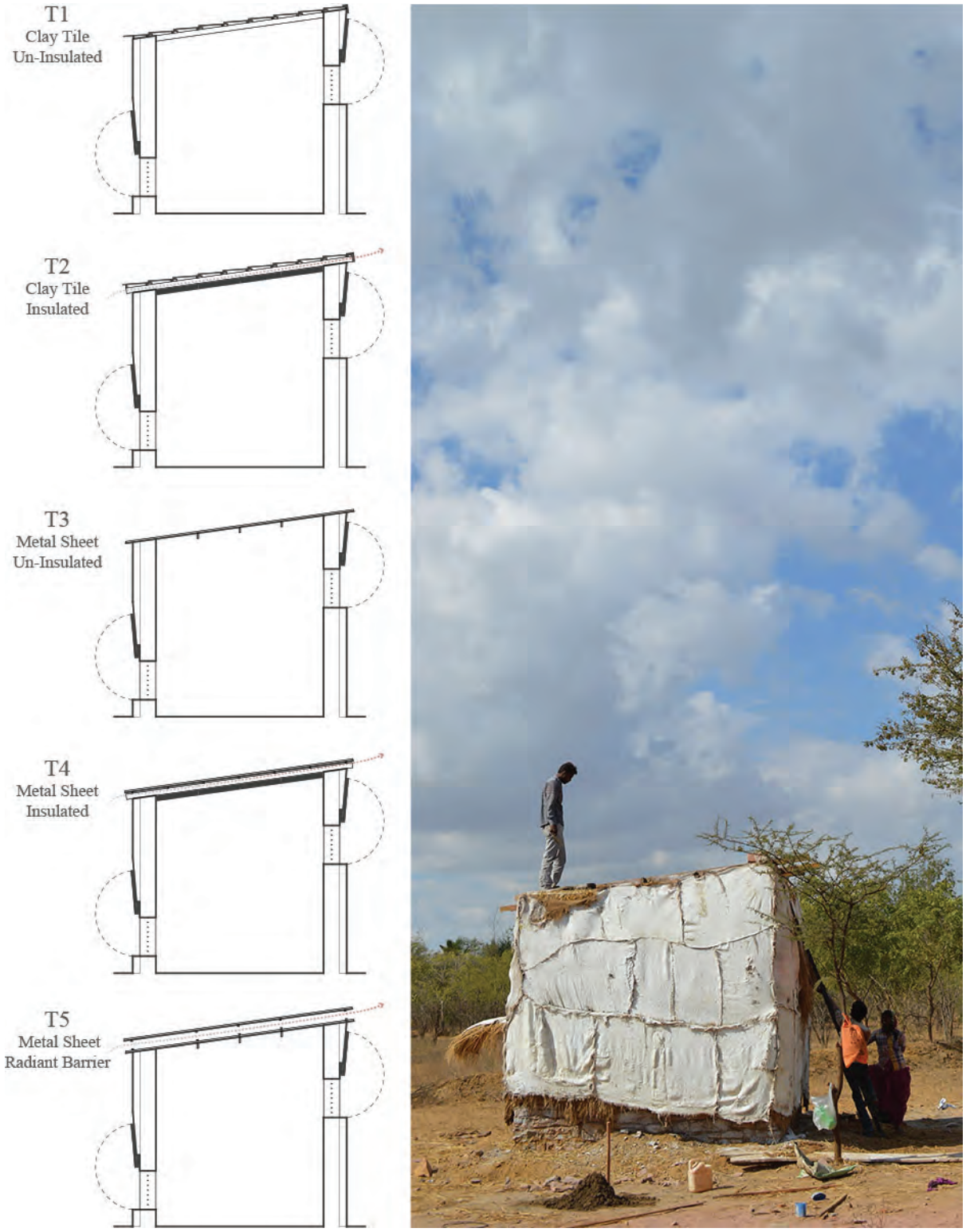

Figure 5.1 – Left: Five test chamber types for reference. Right: Chamber construction at Paraspar.

5.1.1 Single and Double-Layer Roof Protoype Overview

Section 4.5 explains the process by which the five roof designs developed for the field experiment described in this chapter differ from initial recommendations. Broadly, the designs were chosen to compare performance of typical single-layer Bhuj roofs to double-layered roofs with convective cavities, made from readily available, widely used materials. There are two reasons for designing the double-layer roofs to have a convective cavity. First, the relatively wide 7.5cm gap allows for ventilation of air heated via radiation from the upper roof layer that is exposed to the sun. Second, the gap effectively decouples the upper and lower layers to minimize heat transfer to the interior via conduction.

Corrugated metal and asbestos cement sheet, as well as clay tile are the most widely used for low cost housing in Bhuj and thus became the three likely candidates for the first round of prototypes. However, Hunnarshala Directors were concerned about the negative health and ecological effects of asbestos so it was removed from the list of candidates for outer roof material. Co-design discussions in November 2014 resulted in an agreement to move forward with flat Mangalore pattern clay tile or corrugated tin sheet as the outer skin materials for all prototypes (Figure 5.5). Though the digital simulations predicted that the uninsulated exposed clay tile and tin sheet would perform similarly to each other, we chose to build them both as controls, to assess subtle differences in thermal performance. The uninsulated single layer clay tile roof (which we are calling T1, and is shown in greater detail in figure 5.6) is the control for an insulated double-layer clay tile prototype (T2, figure 5.9). Similarly, the uninsulated single layer tin sheet roof (T3, figure 5.12) is the control for an insulated double-layer tin sheet prototype (T4, figure 5.15). Insulation panels are specified in sections 5.2.2 and 5.2.4. Finally, inspired by the digital predictions of the uninsulated, shaded clay roof type (Section 4.4), T5 (5.18) is a double-layer, tin sheet assembly with an aluminum foil radiant barrier affixed to the underside of the upper layer in lieu of an insulation panel (Figure 5.5).

5.1.2 Instrumentation and Data Collection

In addition to the exterior weather data measurements described in section 3.2.2 interior temperature sensors and data loggers for the purposes of direct comparison of test chamber thermal performance. Figure 5.3 shows the locations of the sensors in each of the five chambers.

Each chamber was outfitted with two, two-channel waterproof HOBO U23 Pro External Temperature Data Logger (U23-003), to measure hourly air, ceiling, west and south wall temperatures. A fourth sensor was placed in the air gap of the double-layer roofs (T2, T4, T5) or on the west wall of the single-layer roofs (T1, T3). Wall sensors were coated with thermal paste and inserted into a 3 cm deep, .5 cm diameter drilled hole, so that as much as possible the entire surface of the sensor was in contact with the wall. The hole with the sensor inserted was then fixed in place with a minimal application of silicon caulk at the exposed end. The sensors were located in centroid of the the center block in each wall. Ceiling sensors were sandwiched between the innermost roof assembly layers. Air temperature sensors were hung in the center of each chamber zone.

Operative Temperature Estimate
Globe thermometers were not available for these tests, so mean radiant temperature was approximated by taking the average of ceiling, ground, and wall surface temperatures. Wall surface temperatures were assumed to be similar to each other as and the ground, because, as it will be seen in results analysis,south

and west wall temperature measurements were nearly identical to each other throughout the chambers. Nearly identical inter-chamber wall temperatures indicated that walls were sufficiently protected from heat gain through solar radiation.

5.1.3 Ventilation Schedules

Test chamber data collection began on January 31, 2015. Windows were operated according to the following schedules:

No Ventilation: January 31 - February 14, 2015
Openings are covered by hinged panels 24 hours a day.

Constant Ventilation: February 15 - March 3, 2015
Hinged panels are propped open 24 hours a day.

Night Flush Ventilation: March 4 - March 23, 2015
Openings are covered by hinged panels from 7am to 7pm. Hinged panels are propped open from 7pm to 7am.

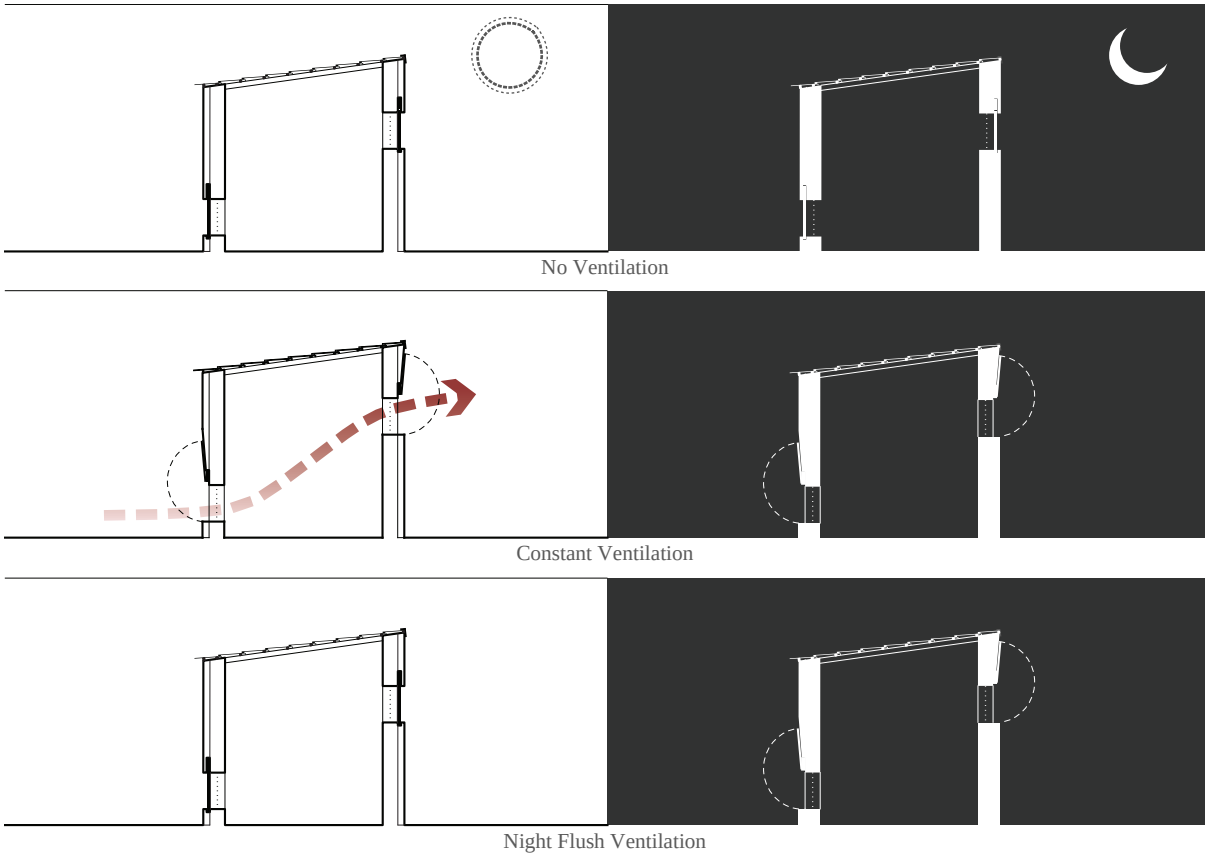

Figure 5.2 – Three Ventilation Schedule Types.

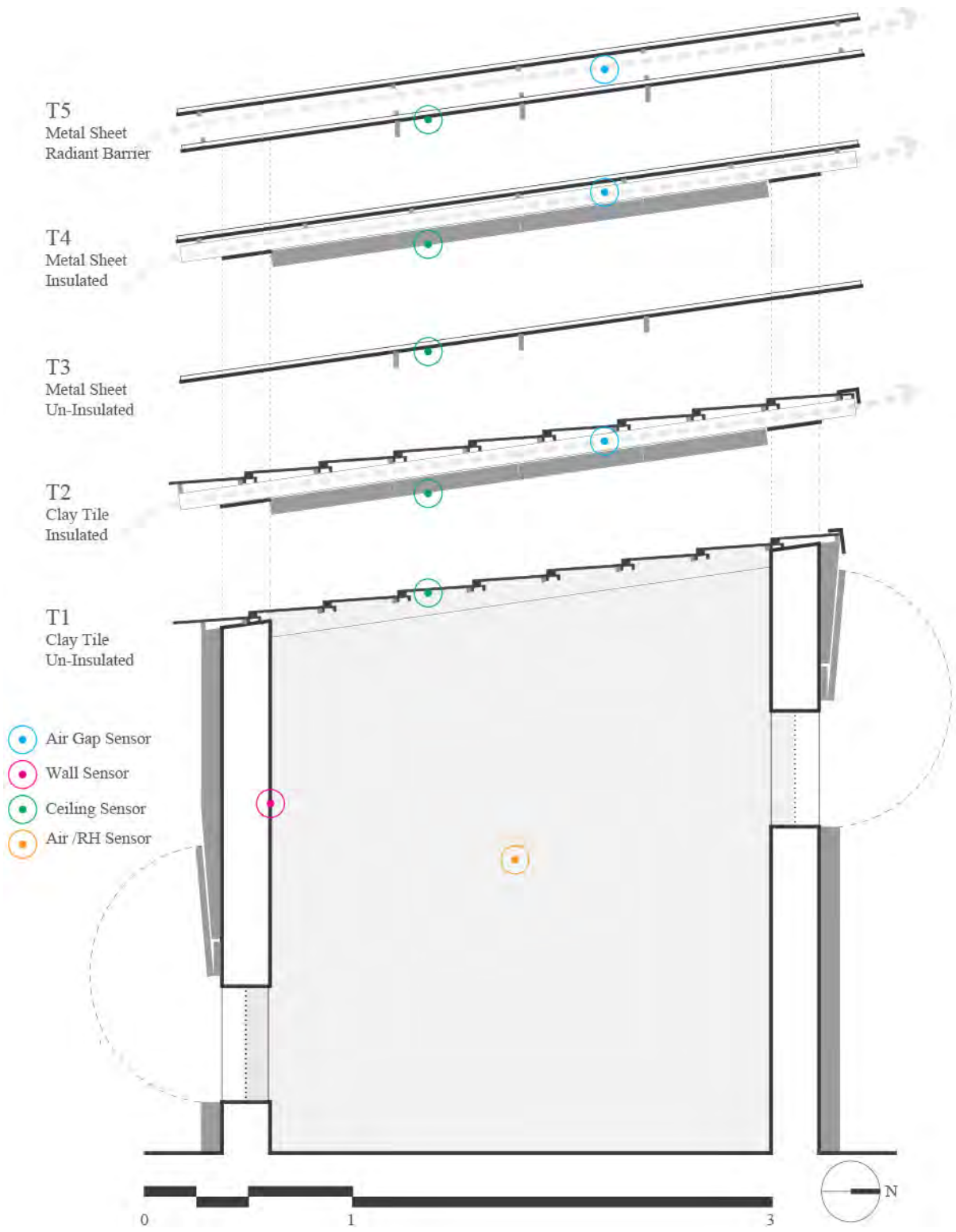

Figure 5.3 – Chamber section, sensor locations and roof types.

Figure 5.4 – Test Chambers in Various Stages of Construction. Chamber walls are constructed from 23 cm local sandstone block (top) and then insulated on the exterior with straw thatch panels (middle). Walls are further protected from the sun and outdoors with an outer finishing of burlap sacks coated with lime plaster (bottom).

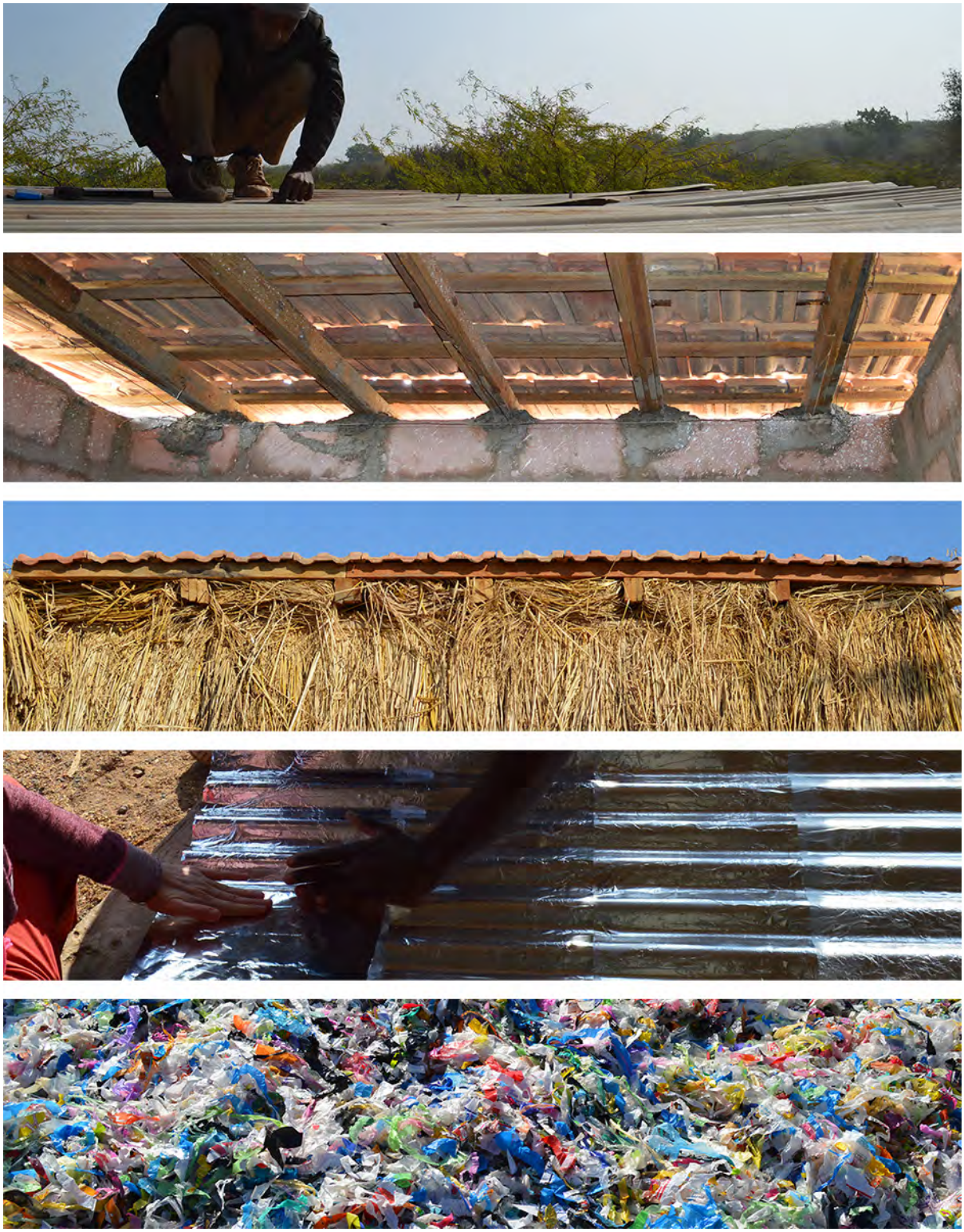

Figure 5.5 – Chamber building materials. From top to bottom: corrugated tin sheet roof, Mangalore Pattern clay tile roof with sandstone block walls, exterior straw insulation, aluminum foil as radiant barrier, shredded waste plastic for insulation panels.

5.2 Intra-Chamber Comparisons

This sections details the results of measured air and surface temperatures, and estimated operative temperatures for three representative one week periods during each ventilation schedule. Because outdoor daily high temperatures ranged widely, from 29 °C to 41 °C, intra-chamber comparisons are not made using absolute temperature values, but rather the comparison average deviation of indoor temperatures from outdoor highs and lows.

5.2.1 T1: Uninsulated Clay Tile

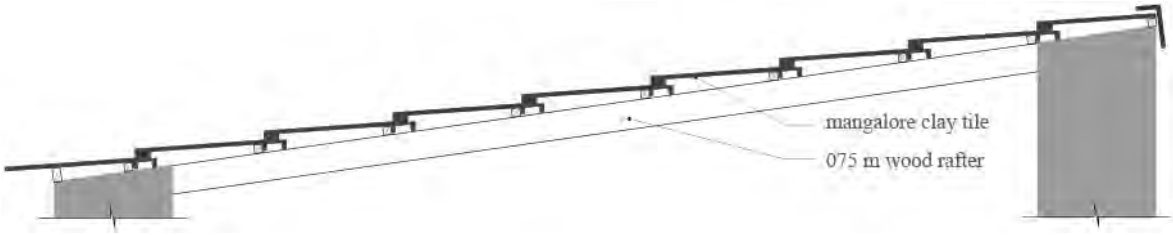

Figure 5.6 – T1 Roof Section.

This roof type is composed of 7.5 cm wood rafters at 50 cm O.C., with an outer single layer of exposed, un-coated, flat Mangalore pattern roof tiles that are resting on battens approximately 2 cm by 5 cm. Air gaps between the wall and roof (as seen in figure 5.5 are filled with mud mortar.

Figure 5.7 shows that there is generally less than 1 °C difference between thermal performance of *no ventilation* and *night flush ventilation* schedules. Daily high operative, air and wall temperatures for these two schedules are 2 to 3 °C cooler than those in the constantly ventilated chamber. Of note are ceiling temperature measurements. Nightly ceiling temperatures drop more rapidly in the un-ventilated chamber (Figure 5.8), due to a decrease in the convective heat transfer coefficient at the underside of the roof. All ceiling temperatures drop below outside air temperature at night, with lowest temperatures occurring just before dawn. Average nightly deviation in ceiling temperature ranges from 3.7 to 5.8 °C.

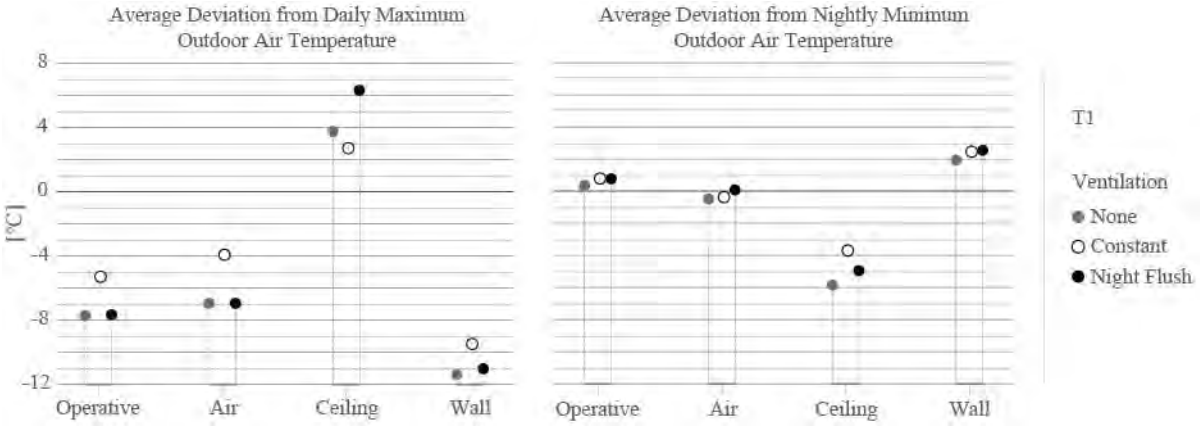

Figure 5.7 – T1 intra-chamber night and day average deviations for three ventilation schedules.

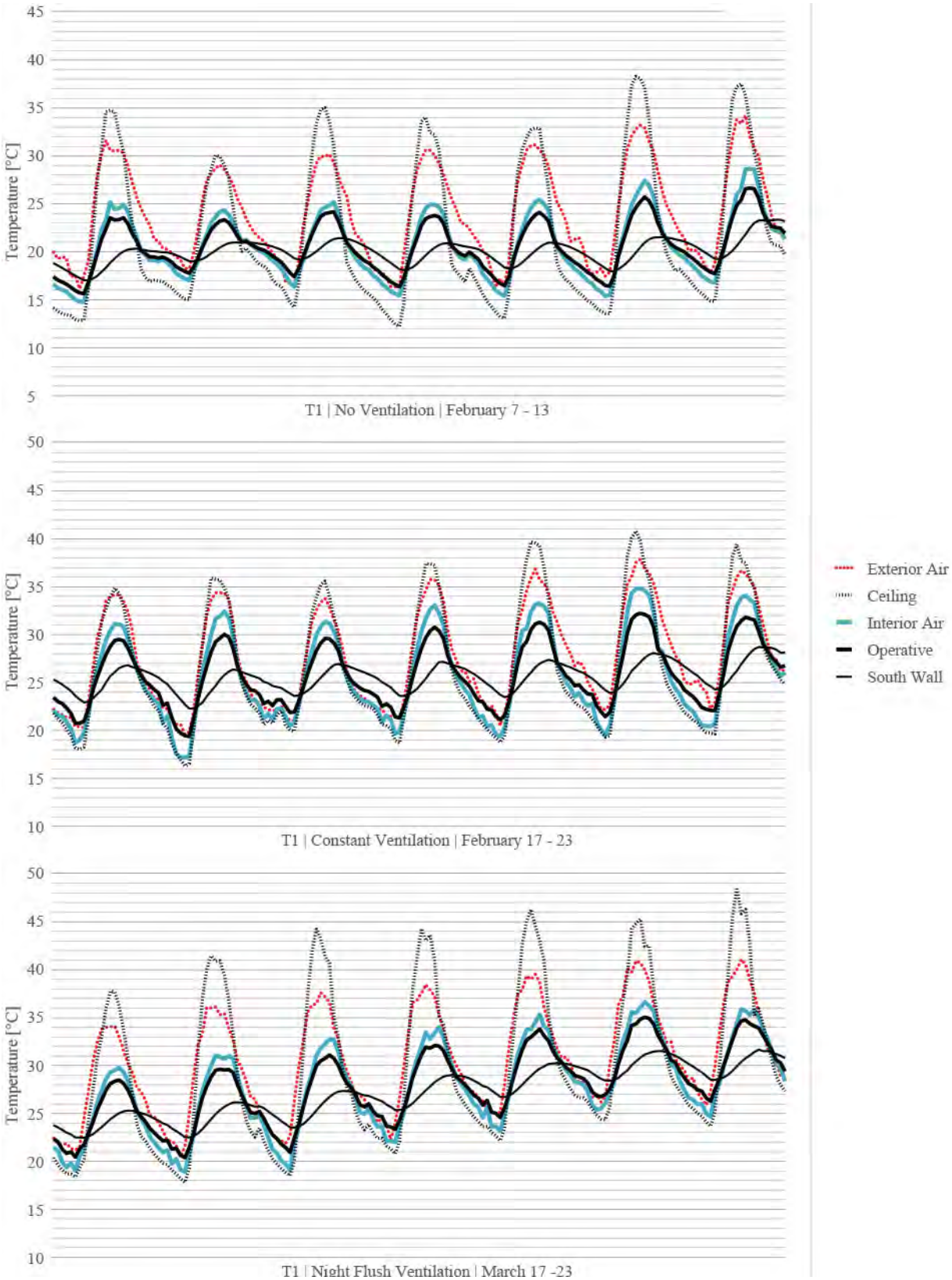

Figure 5.8 – T1 measured data comparison for selected weeks of various ventilation schedules.

5.2.2 T2: Insulated Clay Tile

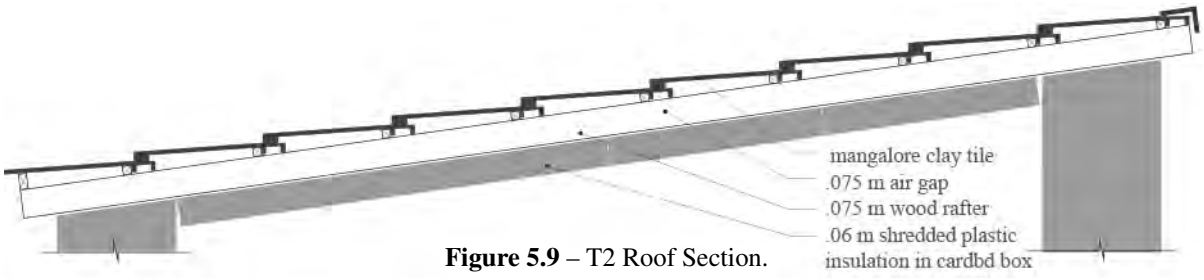

Figure 5.9 – T2 Roof Section.

The outer layers of this roof are constructed identically to T1. Rafters are mortared to the top of the sandstone walls to create a 7.5 cm continuous air gap between tiles and lower insulation panels. Insulation panels were made from 6 cm deep cardboard boxes filled with shredded waste plastic (Figure 5.5) at a density of 65 kg/m^3 to achieve the desired total RSI value.[1] Panels were affixed tightly to the rafters, under a continuous plastic vapor barrier, and fill the entire area of the ceiling to minimize infiltration from the chamber interior to ceiling air gap.

Similar to T1, measurements for T2 show generally less than a 1 °C difference between thermal performance of *no ventilation* and *night flush ventilation* schedules. Daily high operative, air and surface temperatures for these two schedules are 2 to 3 °C cooler than those in the constantly ventilated chamber. Ceiling temperatures are within 2 °C of chamber air temperatures. The 8 to 11 °C difference between ceiling gap and surface temperatures indicates that the insulation panels effectively block heat transfer via convection and conduction from the gap to the interior. Similar daily high air gap and outside temperatures, shown best in figure 5.11, indicates a)the gap is sufficiently wide to ventilate heated air from the roof to the outside and/or b)cooler air enters the gap from below. The latter cause may explain occurrences where the gap temperature falls below outdoor temperatures during the day. This phenomenon occurs most in the un-ventilated chamber results (Figure 5.11). The minimal differences between air gap temperatures for all three schedules may correlate with similar differences in corresponding ceiling temperatures.

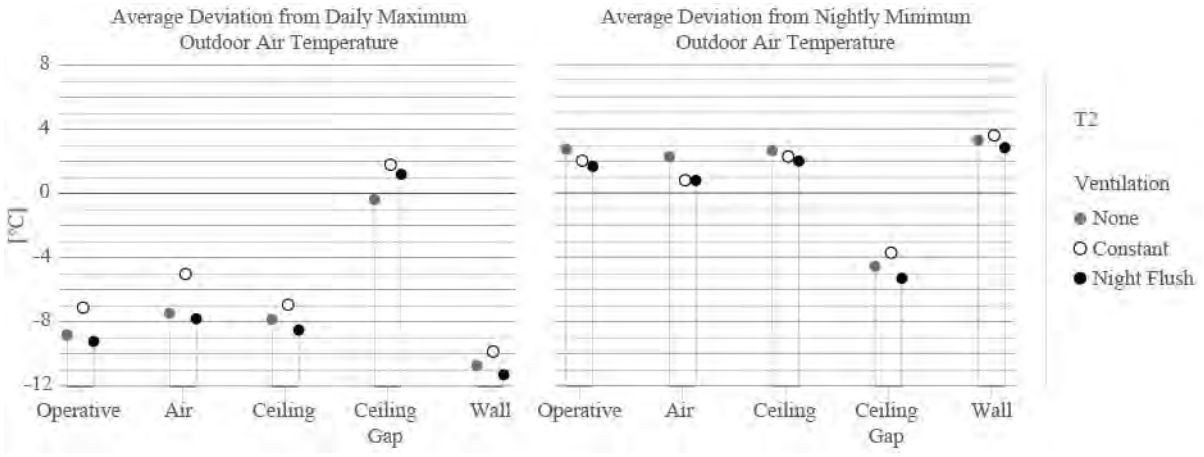

Figure 5.10 – T2 intra-chamber night and day average deviations for three ventilation schedules.

[1] A total RSI value of 1.4m^2°C/W (R-8) was chosen based on digital simulations detailed in Chapter 4. A smaller the field experiment was performed to estimate insulation material conductivity, thus, total RSI value.

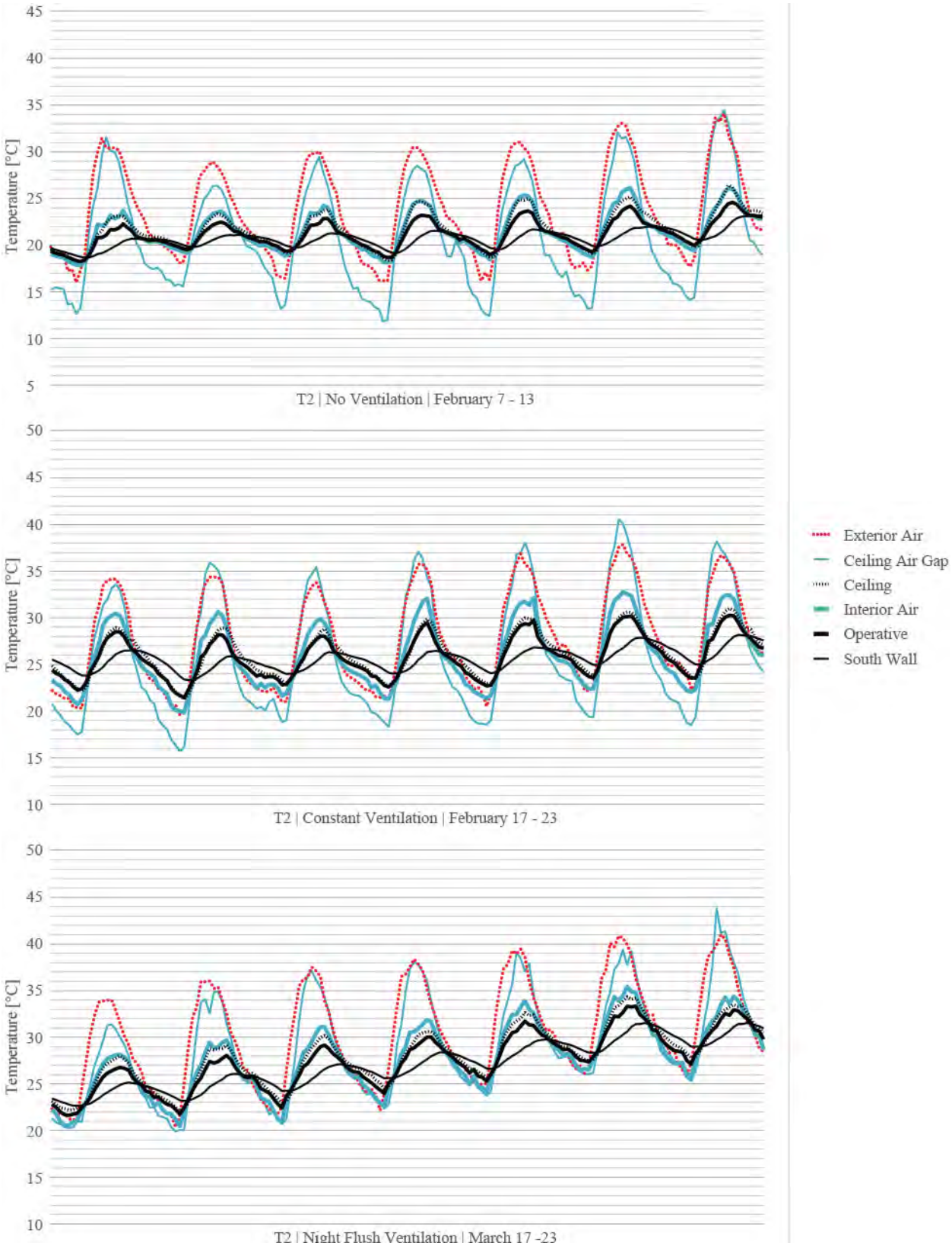

Figure 5.11 – T2 measured data comparison for selected weeks of various ventilation schedules.

5.2.3 T3: Uninsulated Metal Sheet

Figure 5.12 – T3 Roof Section.

This roof type is composed of 7.5cm wood rafters at 60cm O.C., with an outer single layer of corrugated tin sheet with its exterior painted white. Air gaps between the wall and roof are filled with mud mortar.

Figure 5.13 shows that there is generally less than 1 °C difference between thermal performance of *no ventilation* and *night flush ventilation* schedules. Daily high operative, air and wall temperatures for these two schedules are about 3 °C cooler than those in the constantly ventilated chamber. Results from all three schedules for this chamber highlight the cooling power of the insulated thermal mass walls as well as the effects of nocturnal radiant cooling. Though ceiling temperatures rise to averages of 5.3 to 6.3 °C above high outdoor air temperatures during the day, walls stay at averages of 9.5 to 11.8 °C below daily temperatures. This is due to insulation efficacy as well as the fact that ceiling temperatures drop rapidly after sunset, to averages of about 5 °C below nightly lows for the constant and night flush ventilated schedules, to 9.9 °C for the un-ventilated schedule. These results, as well as the similar albeit less dramatic results from T1, show that it is still possible to achieve lower indoor temperatures during the day without the use of roof insulation, if the walls are properly insulated. However, the low indoor night air temperature results shown figure 5.13, indicate that, regardless of ventilation schedule the uninsulated roof will possibly pose the problem of *over-cooling* the space during winter nights. Cross-chamber comparisons of nightly low temperatures in section 5.3 further demonstrate this risk.

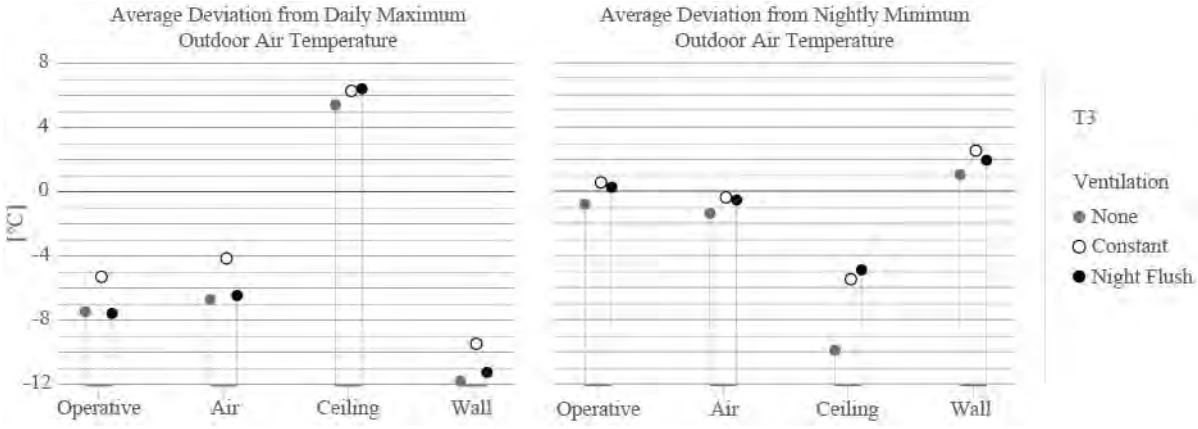

Figure 5.13 – T3 intra-chamber night and day average deviations for three ventilation schedules.

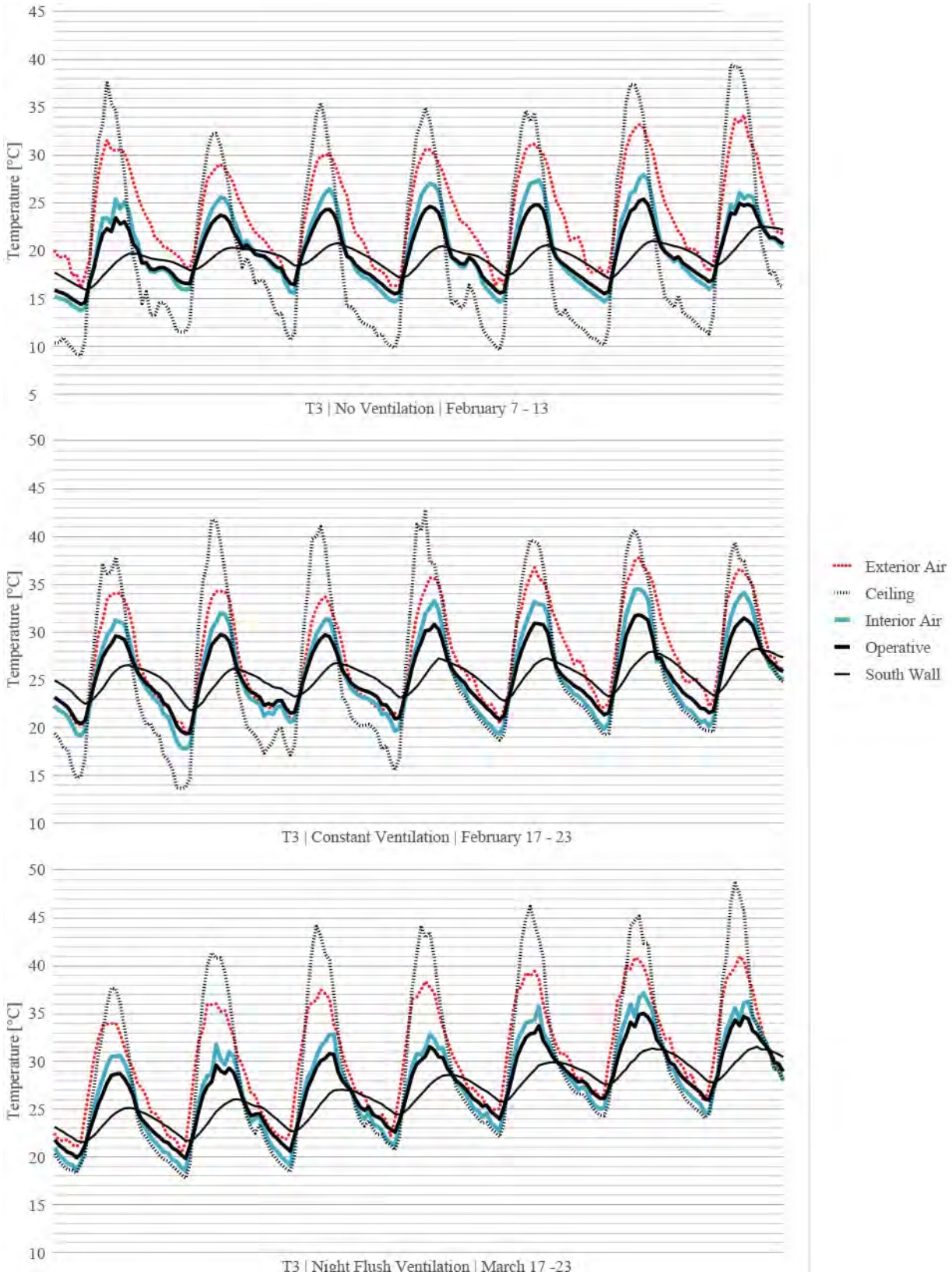

Figure 5.14 – T3 measured data comparison for selected weeks of various ventilation schedules.

5.2.4 T4: Insulated Metal Sheet

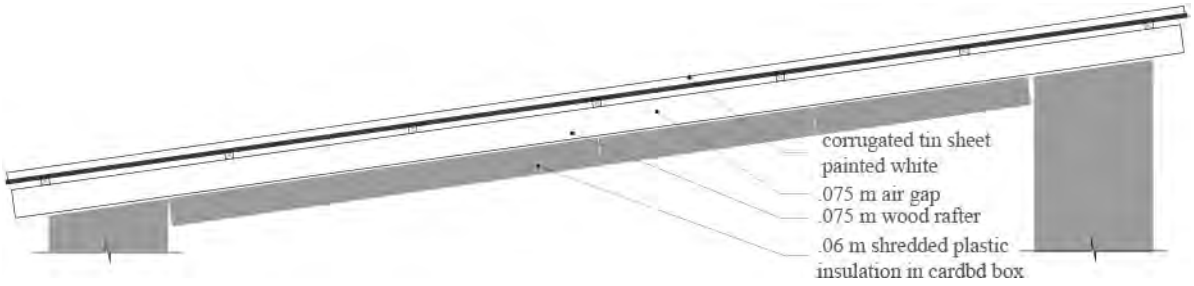

Figure 5.15 – T4 Roof Section.

The layers of this roof are constructed identically to T2 - the insulated clay tile version, with the tiles replaced by a single layer of corrugated tin sheet with its exterior painted white.

Thermal performance is also very similar to that of T2. Measurements for T4 show generally less than a 1 °C difference between thermal performance of *no ventilation* and *night flush ventilation* schedules. Daily high operative, air and surface temperatures for these two schedules are 2 to 4 °C cooler than those in the constantly ventilated chamber. Ceiling temperatures are within 2 °C of chamber air temperatures. The 7 to 9.5 °C difference between ceiling gap and surface temperatures indicates that the insulation panels effectively block heat transfer via convection and conduction from the gap to the interior. Similar daily high air gap and outside temperatures, shown best in figure 5.17, indicates a)the gap is sufficiently wide to ventilate heated air from the roof to the outside and/or b)cooler air enters the gap from below. The latter cause may explain occurrences where the gap temperature falls below outdoor temperatures during the day. This phenomenon occurs most in the un-ventilated chamber results (Figure 5.17). The minimal differences between air gap temperatures for all three schedules may correlate with similar differences in corresponding ceiling temperatures.

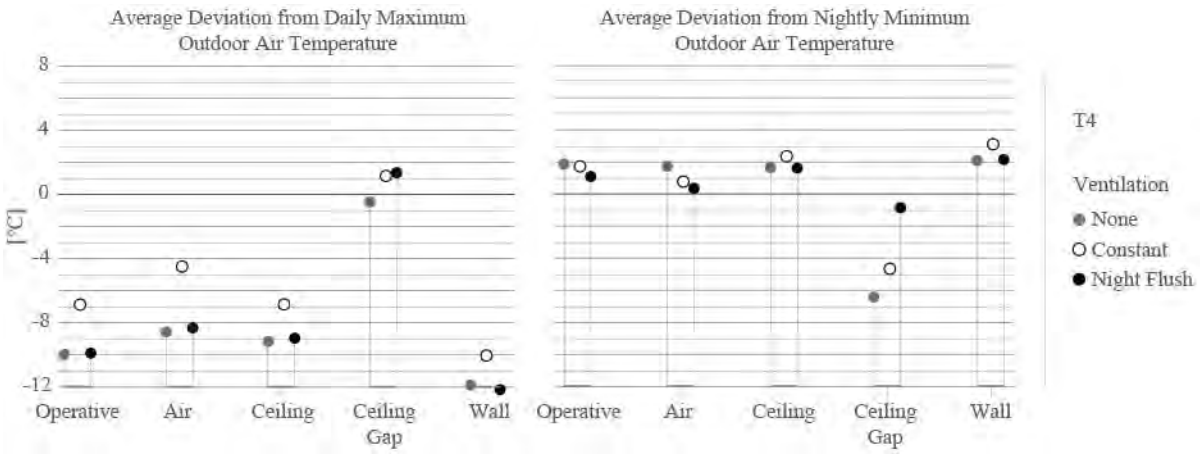

Figure 5.16 – T4 intra-chamber night and day average deviations for three ventilation schedules.

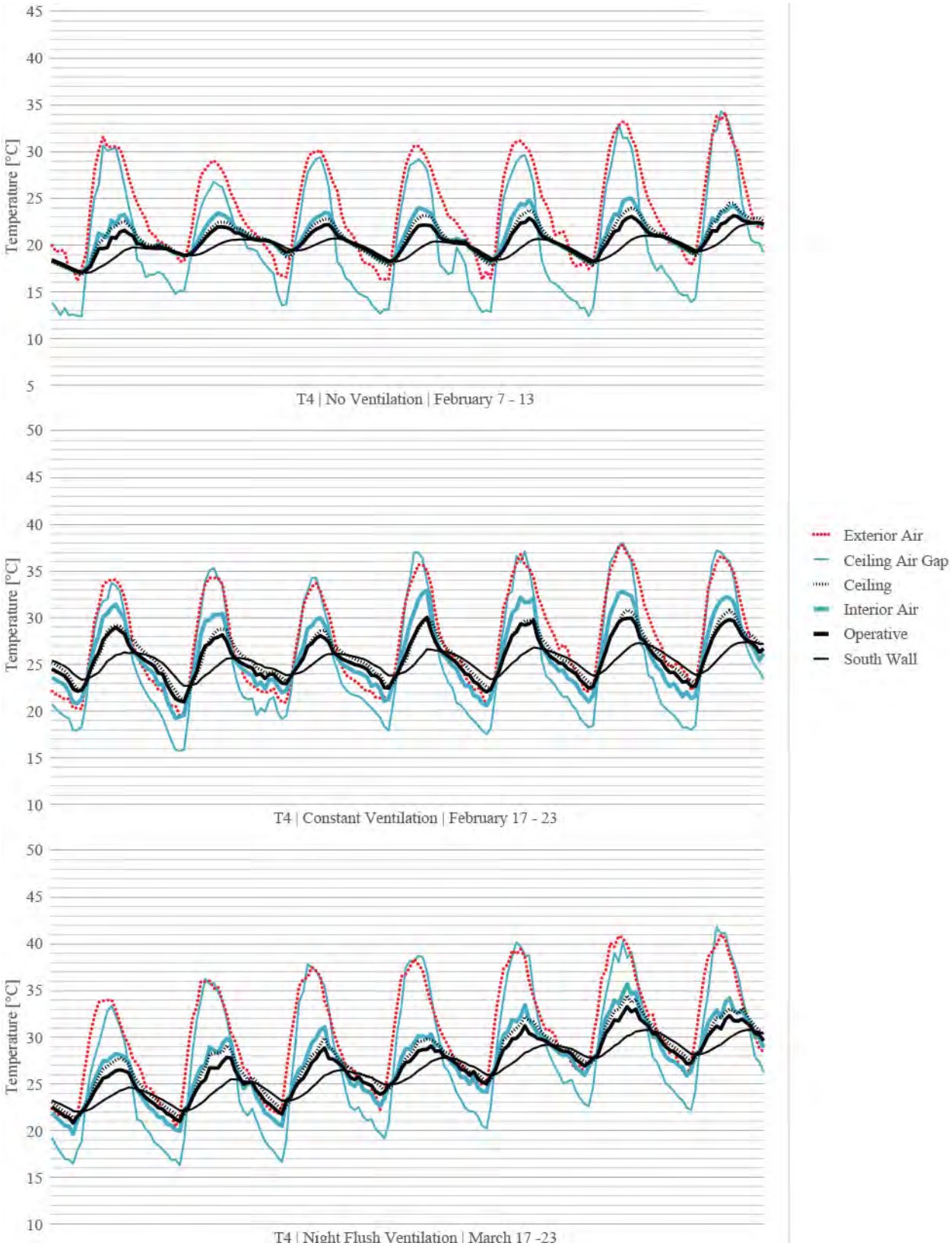

Figure 5.17 – T4 measured data comparison for selected weeks of various ventilation schedules.

5.2.5 T5: Metal Sheet with Radiant Barrier

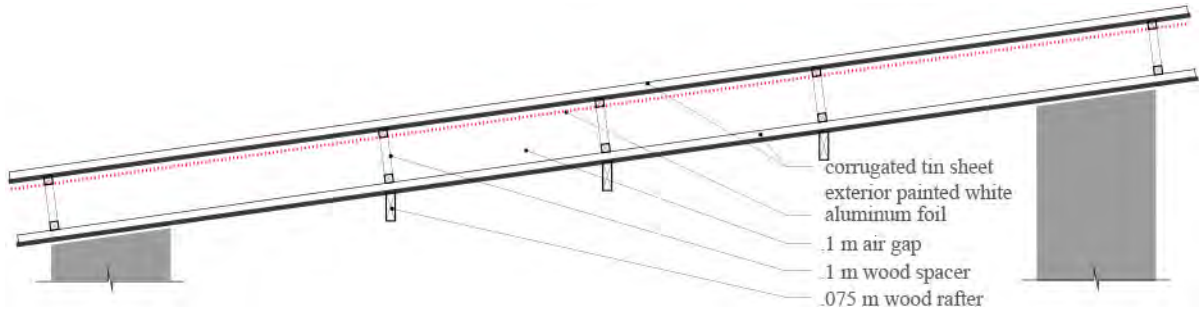

Figure 5.18 – T5 Roof Section.

This roof is constructed from two layers of corrugated tin sheet separated by a 100cm wooden spacers to make a continuous airgap. The outer tin sheet is painted white on its exterior face and an aluminum foil radiant barrier is affixed to its interior face with epoxy. The double-layer with radiant barrier assembly is attached to 7.5cm wood rafters at 60cm O.C., which are built into the sandstone walls of the chamber.

Thermal performance follows the trends of the other double-layer roofs. Similar to all chambers there is less than a 1 °C difference between thermal performance of *no ventilation* and *night flush ventilation* schedules. Daily high operative, air and surface temperatures for these two schedules are 2 to 3 °C cooler than those in the constantly ventilated chamber. Ceiling temperatures are within 2 °C of chamber air temperatures, and 4 °C of chamber operative temperatures. Average temperature differences between ceiling surface and gap ranges from 3.6 to 6.4 °C, indicating that radiant barrier blocks enough heat from solar radiation to allow the insulated thermal mass walls to effectively keep the ceiling surface temperature slightly above indoor air temperature. Similar daily high air gap and outside temperatures, shown best in figure 5.20, indicates a)the gap is sufficiently wide to ventilate heated air from the roof to the outside.

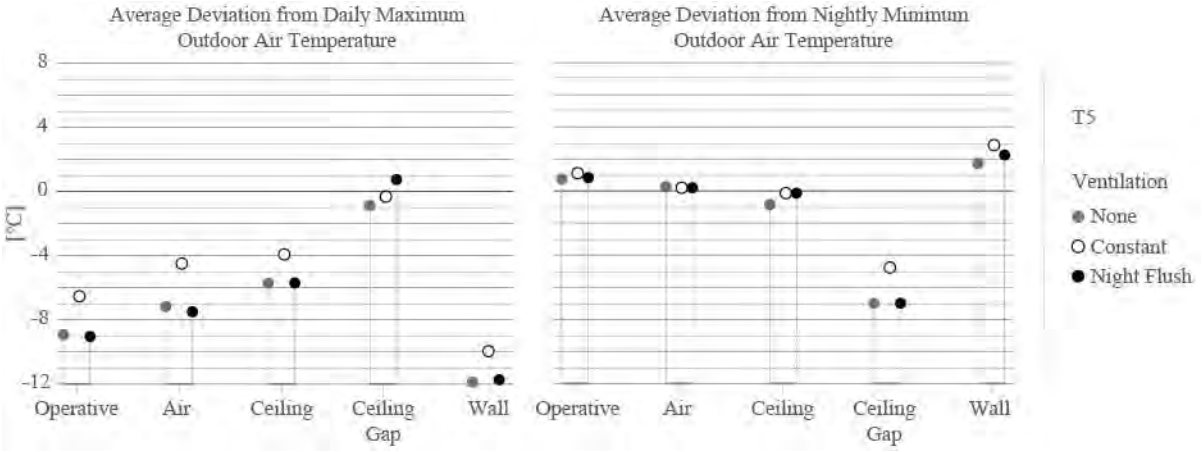

Figure 5.19 – T5 intra-chamber night and day average deviations for three ventilation schedules.

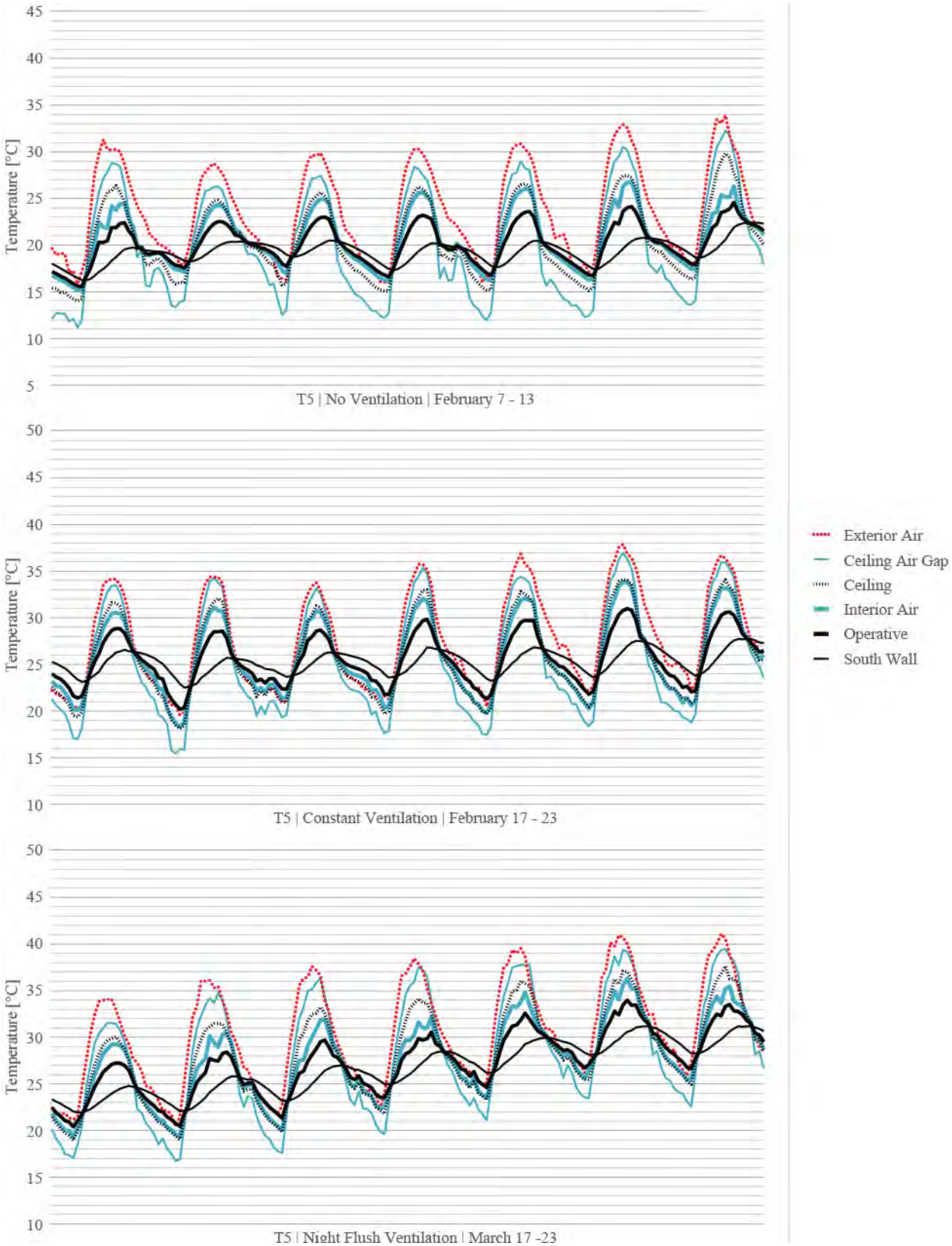

Figure 5.20 – T5 measured data comparison for selected weeks of various ventilation schedules.

5.3 Chamber Cross Comparisons

5.3.1 Comparison of All Chambers During No Ventilation Period

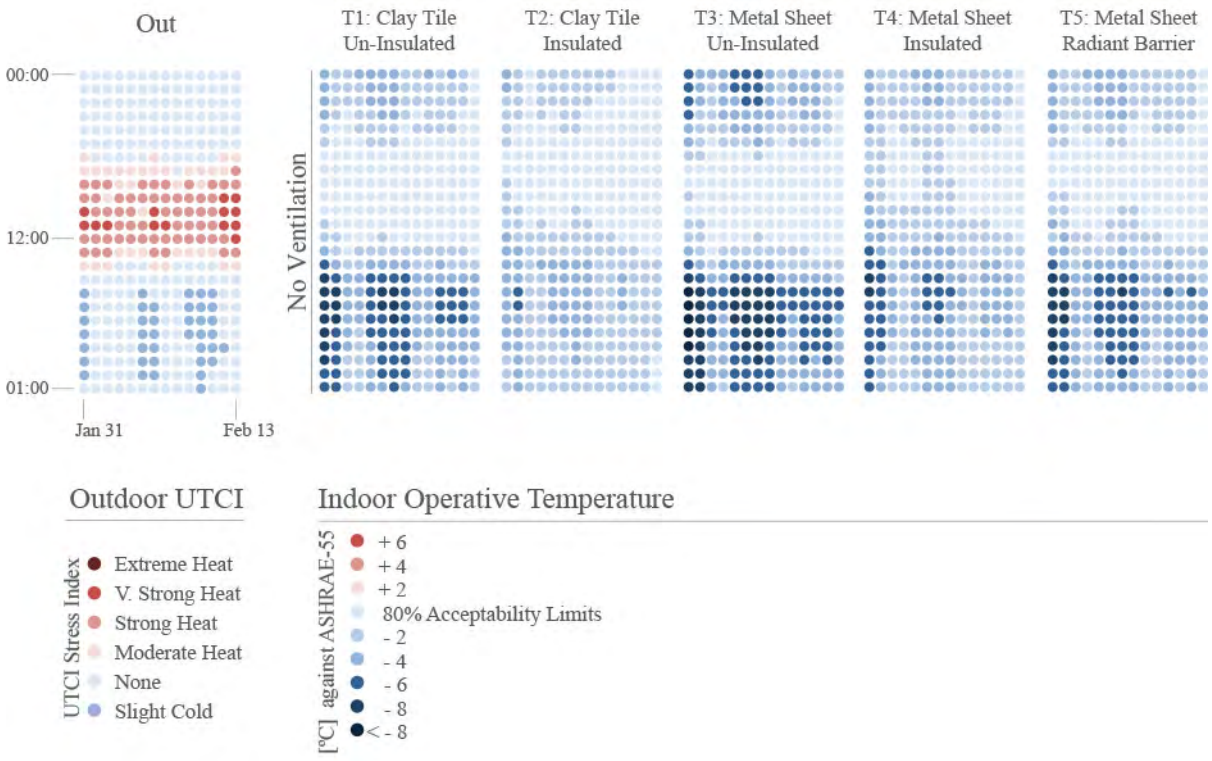

Figure 5.21 – Operative temperature comparison for all chambers during *no ventilation* testing period. Indoor operative temperatures are plotted against the ASHRAE-55 Eighty Percent Acceptability Limits and outdoor temperature is plotted against the UTCI thermal stress index. Note that the indoor and outdoor thermal limits are calculated differently. For an explanation behind the calculations, refer to Section **??**TCHH)

Figure 5.21 depicts a cross-chamber comparison of estimated operative temperatures for a two week *no ventilation* period. The un-ventilated chambers show the cooling power of the insulated thermal mass walls for all chambers, as well as of nocturnal radiant cooling of the uninsulated roofs (T1, T3, and T5). It is important to note that this ventilation schedule is not a realistic solution, as people will inevitably open and close windows and doors, either on regular or irregular schedules. It is also important to note the predicted cooling performance of a closed volume will decrease if internal gains are present and the resulting heat is not able to sufficiently escape.

This set of results is useful to understand the risk of over-cooling a space at night when roof insulation is not present. In all cases, early morning temperatures fall below outdoor UTCI temperatures and well below 80% acceptability limits. Though all chambers maintain similar operative temperatures within the acceptable range during the day, chambers T1, T3, and T5 often reach early morning temperatures of 6 to greater than 8 °C below ASHRAE 80% limits.

5.3.2 Comparison of All Chambers During Constant Ventilation Period

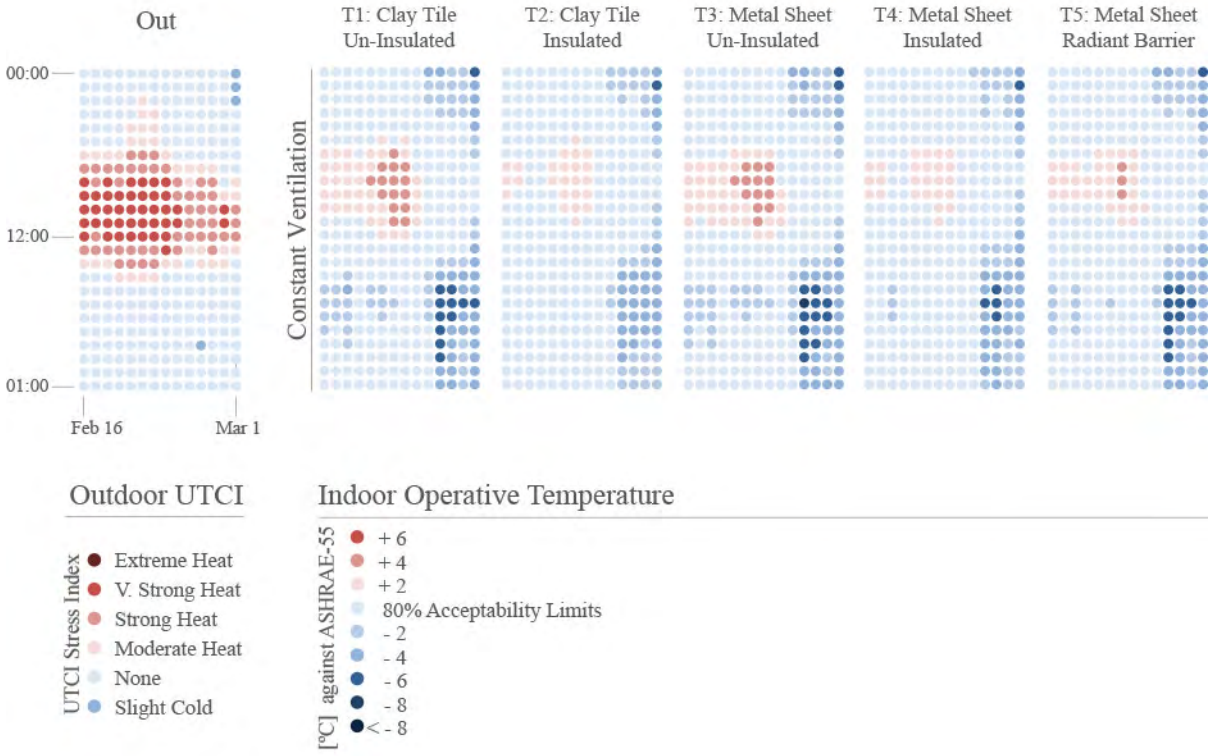

Figure 5.22 – All chamber operative temperature comparison for *constant ventilation* testing period. Indoor operative temperatures are plotted against the ASHRAE-55 Eighty Percent Acceptability Limits and outdoor temperature is plotted against the UTCI thermal stress index.Note that the indoor and outdoor thermal limits are calculated differently. For an explanation behind the calculations, refer to Section **??**TCHH)

Figure 5.22 depicts a cross-chamber comparison of estimated operative temperatures for a two week *constant ventilation* period. Outdoor daily temperature limits ranged from nightly conditions posing no thermal risk to afternoon conditions posing strong or very strong heat risk. For reference, indoor operable temperatures that fall within the 80% ASHRAE Acceptability Limits for this time period range from 21.5 to 28.5°C. Chambers with uninsulated roofs, T1 and T3, each logged nine days with three or more hours 0 to 2 °C above 80% Acceptability Limits and three days with three or more hours 2 to 4 °C above 80% Acceptability Limits. T5, with the double-layer radiant barrier roof, logged nine days with three or more hours 0 to 2 °C above 80% Acceptability Limits and one day with three or more hours 2 to 4 °C above 80% Acceptability Limits. Chambers with insulated roofs, T2 and T4, each logged six days with three or more hours 0 to 2 °C above 80% Acceptability Limits.

5.3.3 Comparison of All Chambers During Night Flush Period

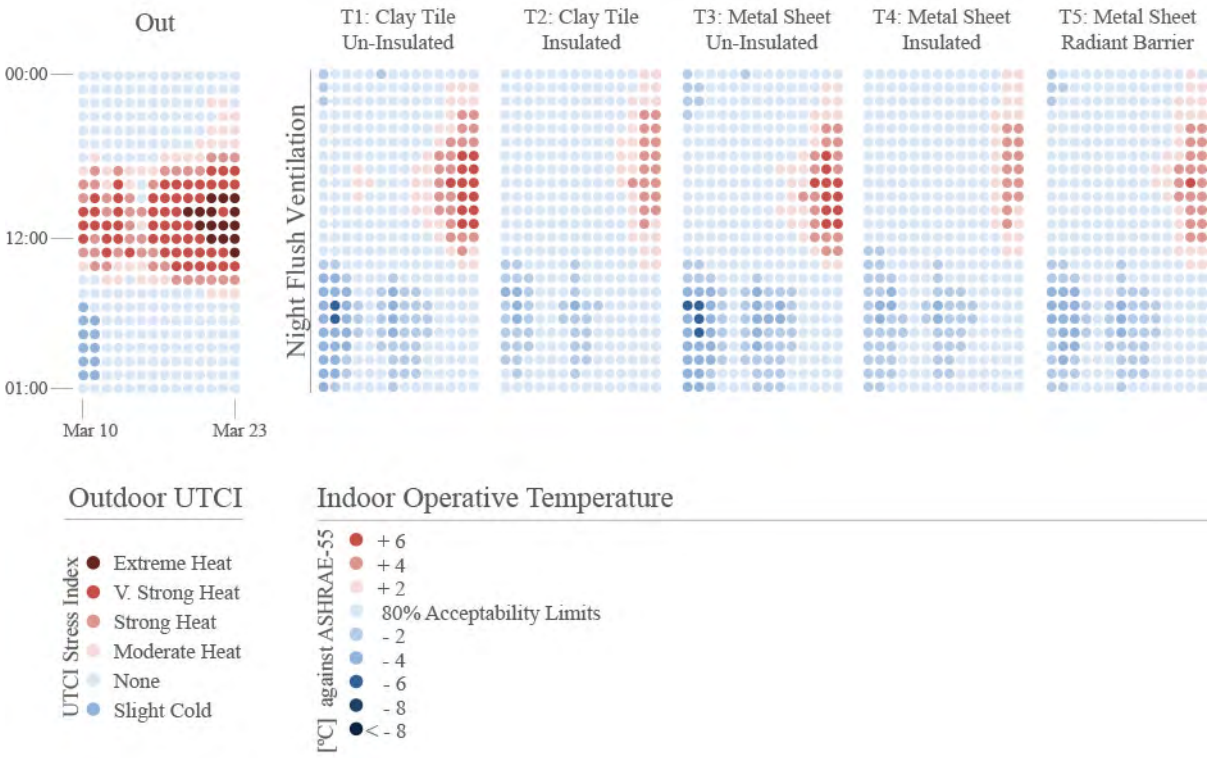

Figure 5.23 – All chamber operative temperature comparison for *night flush ventilation* testing period. Indoor operative temperatures are plotted against the ASHRAE-55 Eighty Percent Acceptability Limits and outdoor temperature is plotted against the UTCI thermal stress index. Note that the indoor and outdoor thermal limits are calculated differently. For an explanation behind the calculations, refer to Section **??**TCHH)

Outdoor daily temperature limits during the *night flush ventilation* period ranged from nightly conditions posing no thermal risk to afternoon conditions posing very strong or extreme heat risk (5.23). Indoor operable temperatures within ASHRAE 80% Limits for this period ranged from 22.5 to 29.5°C. The following results are listed from warmest to coolest chambers. T1 logged seven days with three or more hours 0 to 2 °C above, four days with three or more hours 2 to 4 °C above and two days with three or more hours 4 to 6 °C above 80% Acceptability Limits. T3 logged six days with three or more hours 0 to 2 °C above, three days with three or more hours 2 to 4 °C above and two days with three or more hours 4 to 6 °C above 80% Acceptability Limits. T5 logged four days with three or more hours 0 to 2 °C above, and two days with three or more hours 2 to 4 °C above 80% Acceptability Limits. T2 logged four days with three or more hours 0 to 2 °C above, and two days with three or more hours 2 to 4 °C above 80% Acceptability Limits. T4 logged three days with three or more hours 0 to 2 °C above, and two days with three or more hours 2 to 4 °C above 80% Acceptability Limits.

The relative efficacy of night flush ventilation over constant ventilation in all cases is shown in figure 5.24, which compares average deviations of indoor temperatures to daily maximum and nightly minimum outdoor air temperatures. Figure 5.24 shows that there is a lowering of daily high operative temperatures by 1.5 °C from warmest to coolest constantly ventilated chambers, and the lowering of an additional 2 to 2.5 °C with the use of night flush ventilation.

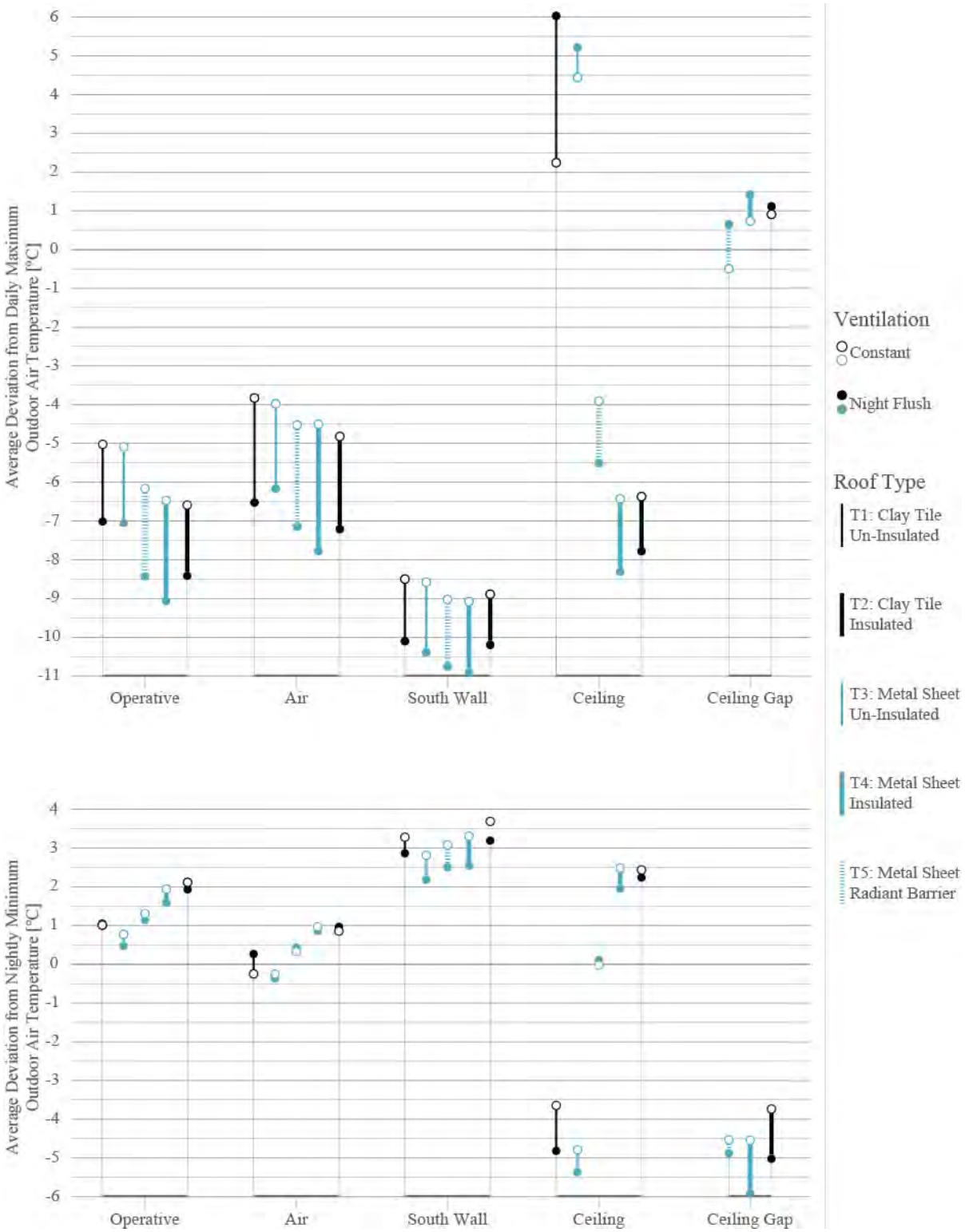

Figure 5.24 – Comparison of average deviations of indoor temperatures from extreme day and night outdoor temperatures for constant and night ventilation schedules.

5.3.4 Discussion

Figure 5.24 shows the potential for daily high average air and operative temperatures to decrease by 4 °C between an constantly ventilated space with an uninsulated roof to a night ventilated space with an insulated roof. It also shows that T5 – the double-layer metal sheet roof with upper radiant barrier – performs similarly to the coolest performing insulated roof types. During both constant and night ventilation periods, the average maximum daily and minimum nightly operative, air, and walls temperatures are within 1 °C of the insulated roof chambers. The ceiling of the radiant barrier roof maintains high daily surface temperatures within 1 °C of indoor air temperature and is anywhere from 9 to 11.5 °C cooler than its uninsulated counterparts. Nightly air gap temperatures fall below air temperature, and because there are no insulation panels to prohibit heat transfer, the ceiling contributes to some amount of nocturnal radiative cooling, staying at outdoor air temperature, but below wall and operative temperatures. This radiative cooling effect, however, might pose less of a risk of over-cooling during winter months, as the nightly low ceiling temperature of T5 is between 2 and 4 °C warmer than the uninsulated roofs. Balancing resistance to solar radiation during the day and radiative cooling during the night allows for the insulated walls to discharge heat during the night and remain relatively cool during the day.

5.4 Comparison of Chamber to Existing Building Performance

Regardless of roof type, it is apparent that wall insulation plays a critical part to maintaining lower indoor temperatures. None of the test chambers had uninsulated walls, as the purpose of the experiment was to ascertain roof performance. Figures 5.25 through 5.27 show a vast difference in performance between volumes with insulated and uninsulated walls. Existing building 1 (B1, described in more detail in Chapter 3) is a single thermal zone with a larger air volume, approximately 27 m^2 than the test chambers' 16 m^2 but identical in roof to wall proportions. The house is constructed from uninsulated, solid CMU block walls and has an uninsulated, corrugated asbestos cement sheet roof. The house is largely un-occupied: it is used by one person to nap in during approximately one hour each afternoon. During the times the house is occupied, the windows and door are opened on an irregular schedule, though the occupant reported that he tends to open the windows during the summer. A ceiling fan is also operated during the summer. Because of these differences it is not possible to make completely analogous comparisons between B1 and the chambers. However, because the B1 measurements are so drastically different from the T1-T5 measurements, the benefits of wall and roof protection can be relatively, if not equivalently deduced.

No Ventilation Results (Figure 5.25)
Test chamber air temperatures highs were lower than B1 indoor air temperatures by 7 to 11 °C. Test chamber ceiling temperature highs were lower than B1 ceiling temperatures by 4 to 18 °C. Test chamber wall temperature highs were lower than B1 wall temperatures by 13 to 14 °C.

Constant Ventilation Results (Figure 5.26)
Test chamber air temperature highs were lower than B1 indoor air temperatures by 4 to 6 °C. Test chamber ceiling temperature highs were lower than B1 ceiling temperatures by 5 to 15 °C. Test chamber wall temperature highs were lower than B1 wall temperatures by 10 to 12 °C.

Night Flush Ventilation Results (Figure 5.27)
Test chamber air temperature highs were lower than B1 indoor air temperatures by 6 to 7 °C. Test chamber ceiling temperature highs were lower than B1 ceiling temperatures by 4 to 18 °C. Test chamber wall temperature highs were lower than B1 wall temperatures by 11 to 12 °C.

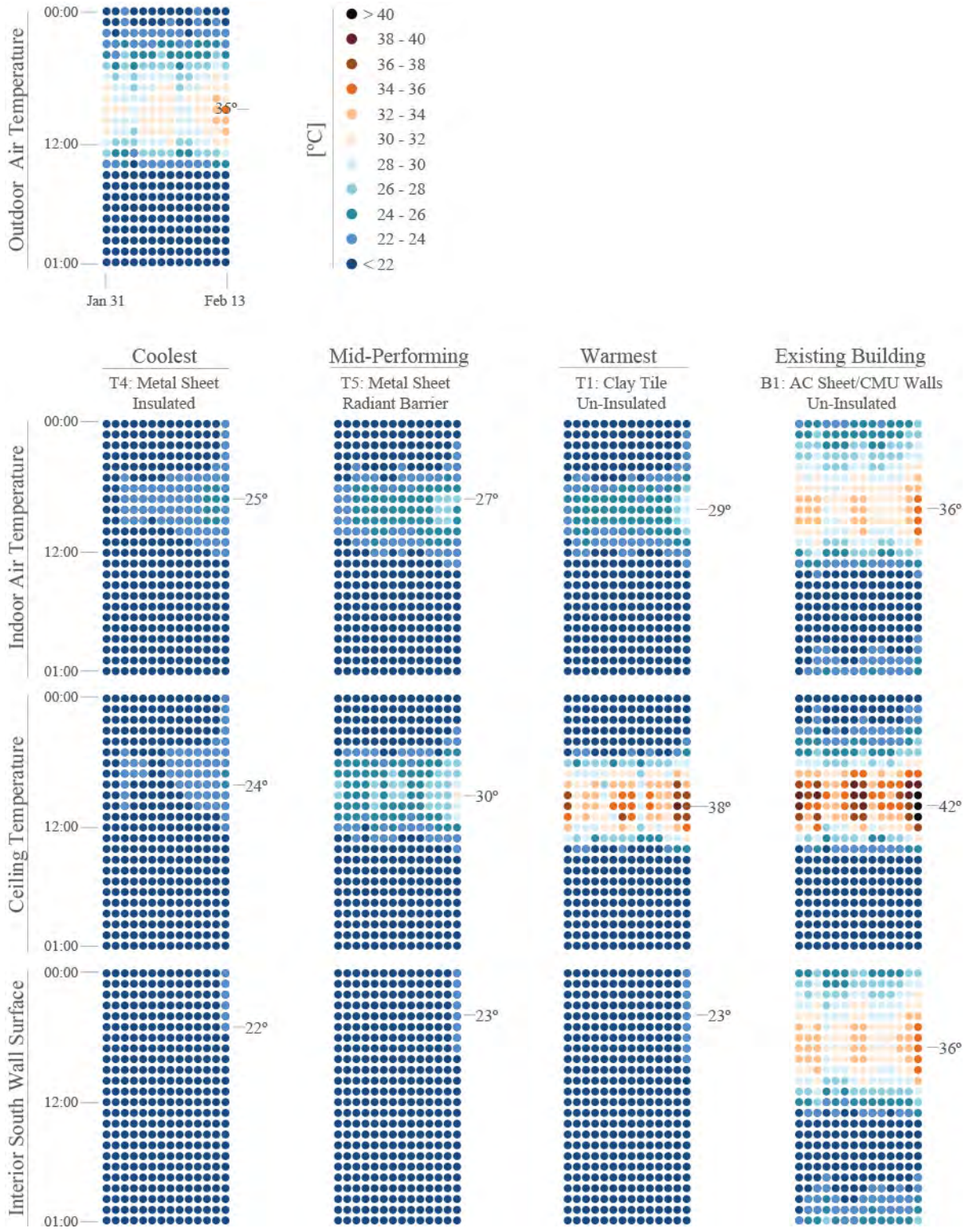

Figure 5.25 – Measured temperature comparison for *no ventilation* period, of coolest, mid-performing and warmest chambers against typical uninsulated slum house type (B1). Highest recorded temperatures are called out for each section.

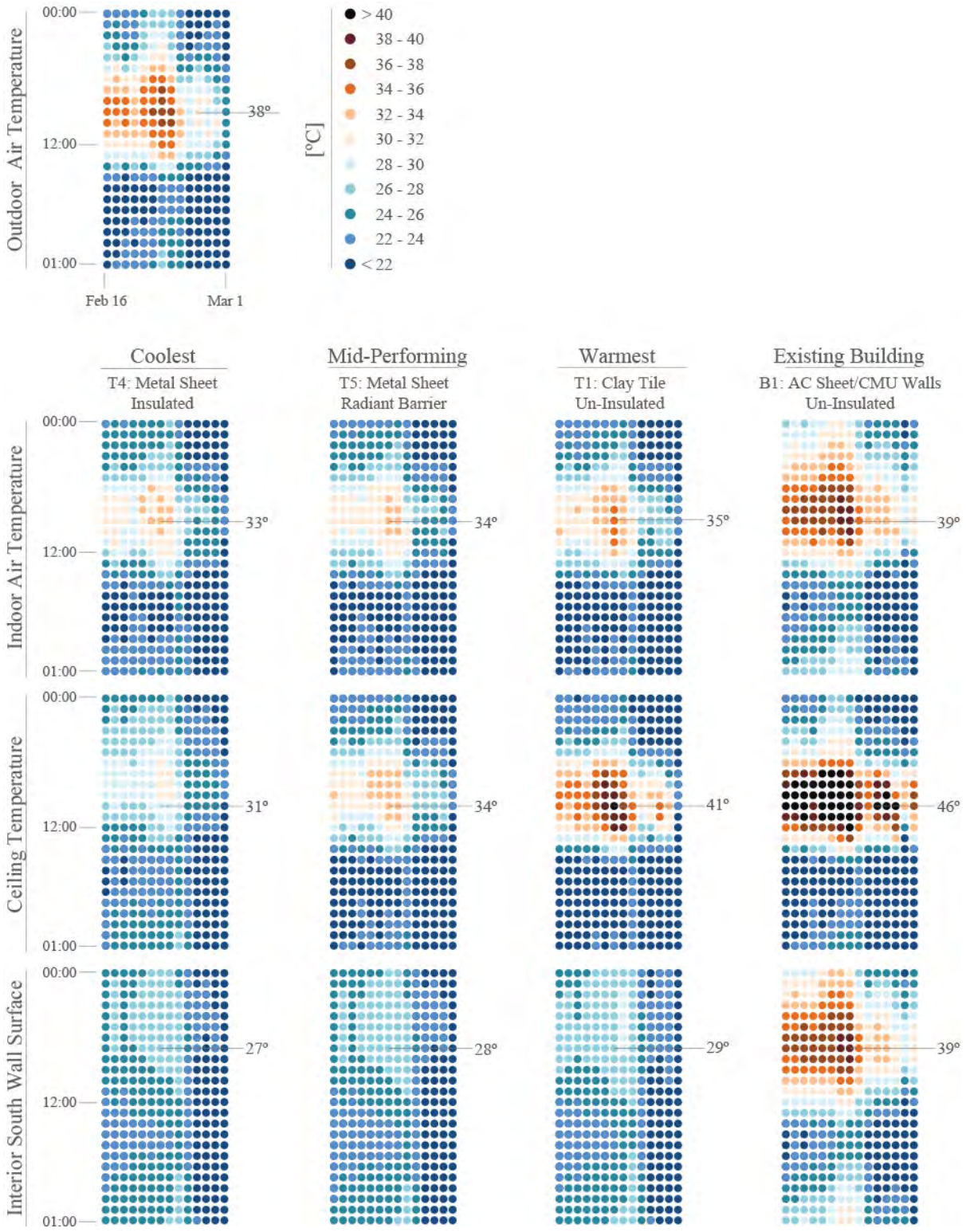

Figure 5.26 – Measured temperature comparison for *constant ventilation* period, of coolest, mid-performing and warmest chambers against typical uninsulated slum house type (B1). Highest recorded temperatures are called out for each section.

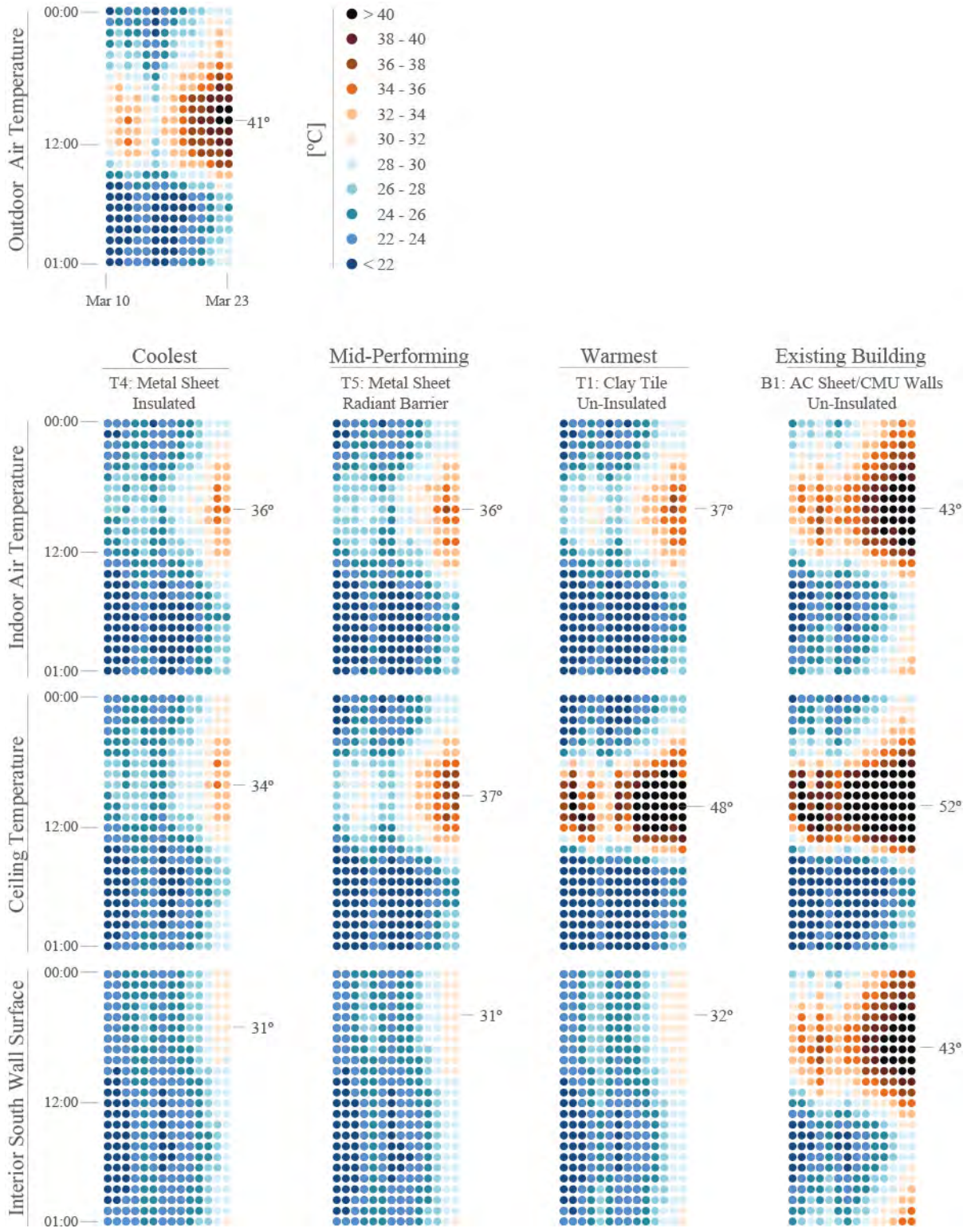

Figure 5.27 – Measured temperature comparison for *night flush ventilation* period, of coolest, mid-performing and warmest chambers against typical uninsulated slum house type (B1). Highest recorded temperatures are called out for each section.

5.5 Simulated Impact of Roof Modifications to Bhuj Slum House Type

Figures 5.25 through 5.27 show that when compared to the common existing slum typology, maximum indoor air temperatures decrease by up to 7 °C, regardless of roof type, with the addition of outer wall insulation. Then, insulated or double-layer roofs decrease maximum indoor air temperature further by up to 4 °C. From March 10 to March 23, when outdoor temperatures were hottest, wall insulation decreased indoor air temperature by 6 °C and roof type variation further decreased maximum indoor air temperatures by 1 °C. The results from the hot week thus show a relatively small change in air temperatures due to roof modification in the presence of wall insulation. It was unclear if roof type alone would significantly impact indoor temperatures of houses with uninsulated walls, as is commonly found in existing slum house typologies. So, a series of annual simulations were run using the calibrated model for Building 1 (detailed in Section 3.4.1) as a base. The series predicts annual thermal performance of variations on the uninsulated concrete masonry block walled typology with an uninsulated sheet roof. There were four wall type variations: a) exposed block, as is currently found in the existing building, b) two shared walls with adjacent buildings, as is commonly found in denser settlements, c) white-washed or white painted block, as is found in more permanent incremental settlements, and finally d) exterior insulated block, a variation that is not commonly found in informal communities. Roof variations included a) exposed asbestos cement corrugated sheet material, as is currently found in the existing building, b) double-layer corrugated sheet roof with radiant barrier, similar to the corrugated metal T5 prototype, and c) double-layer insulated corrugated sheet assembly, similar to prototypes T2 and T4.

Figure 5.28 shows the outputs of percent annual hours that indoor operative temperatures exceed acceptability limits according to two adaptive thermal comfort standards: ASHRAE-55 80% Acceptability and the more "heat tolerant" EN 15251 Category III Acceptability (described in more detail in Chapter 2). For the exposed wall variations, the simulations predict that roof type will decrease hours above acceptability limits by a range of 1% (88 hour, or 4 days) to 4% (350 hours, or 15 days) according to ASHRAE-55 80% acceptability limits, and from 6% (526 hours, or 22 days) to 8% (701 hours, or 29 days) according to EN 15251 Category III acceptability limits. For the shared wall variations, where the building was modeled attached to neighboring buildings on the south and north facades, the simulations predict that roof type will decrease hours above acceptability limits by a range of 4% (350 hours, or 15) to 7% (613 hours, or 26 days) according to ASHRAE-55 limits, and from 6% (526 hours, or 22 days) to 13% (1139 hours, or 47 days) according to EN 15251 limits. For the white wall variations, where the building stands alone with all wall surfaces having a solar absorptance, α, of 20%, the simulations predict that roof type will decrease hours above acceptability limits by a range of 5% (438 hours, or 18 days) to 8% (701 hours, or 29 days) according to ASHRAE-55 limits, and from 8% (701 hours, or 29 days) to 13% (1139 hours, or 47 days) according to EN 15251 limits. Though not commonly seen in Bhuj informal house types, the exterior wall insulation variations are shown for reference, and show the biggest potential drop in operative temperatures, with the models predicting that roof type will decrease hours above acceptability limits by a range of 13% (1139 hours, or 47 days) to 29% (2540 hours, or 106 days) according to ASHRAE-55 limits, and from 10% (876 hours, or 37 days) to 17% (1489 hours, or 62 days) according EN 15251 limits.

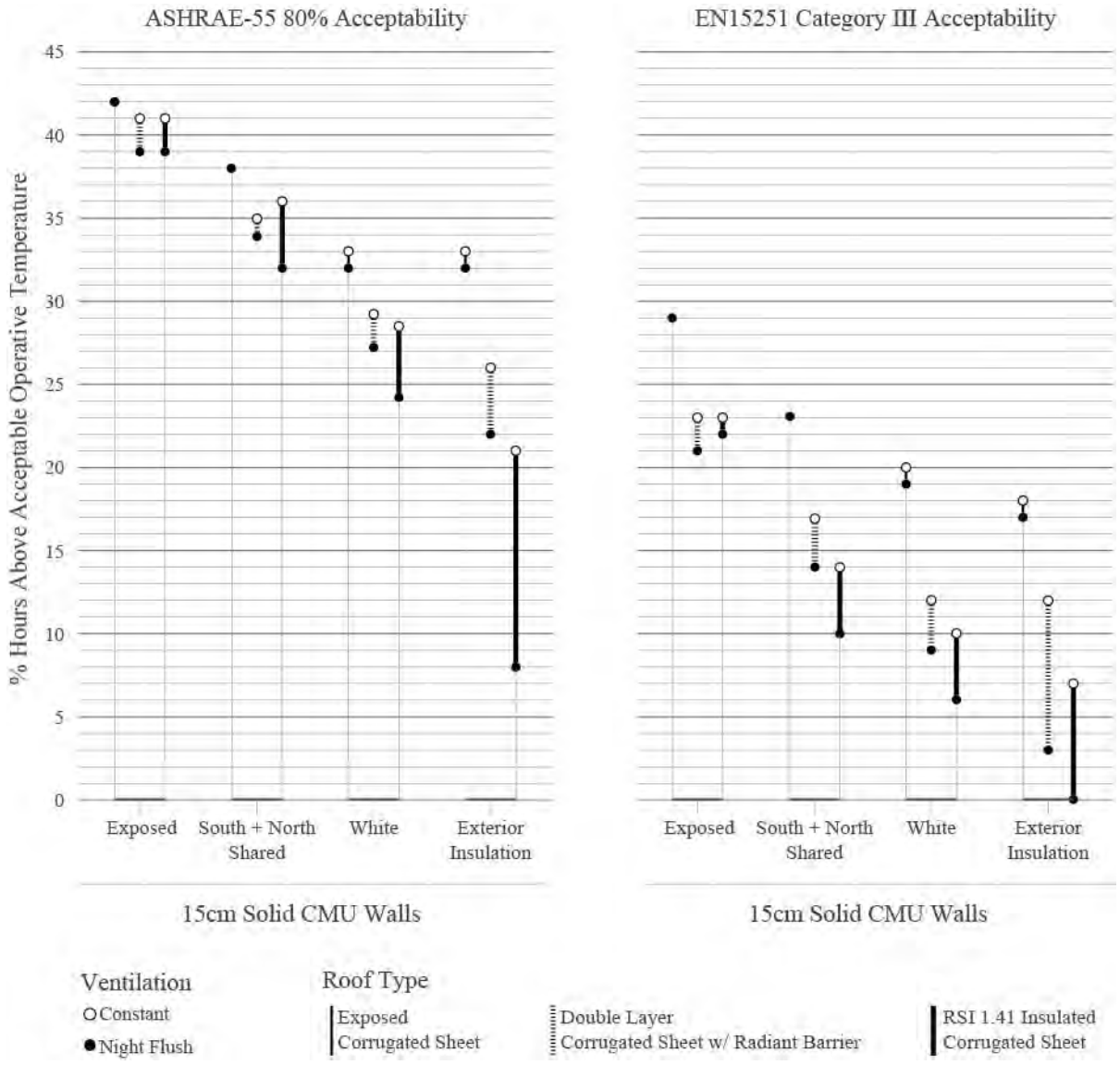

Figure 5.28 – Percent annual hours simulated indoor operative temperatures exceed ASHRAE-55 80% Acceptability Limits (left) and EN 15251 Category III Acceptability Limits (right).

Similar to initial simulations, discussed in Chapter 4, the dramatic drop in operative temperatures to reach full thermal autonomy for this type of building depends not only on the roof assembly, but largely on the wall assemblies as well. Though the versions with insulated walls perform the best, insulated walls are not commonly seen in informal housing. The exposed and shared wall variations, however, are very common. Both of these variations generally are equipped with a single-layer, corrugated sheet roof made from asbestos cement, tin or steel sheet, or clay tile. To further assess the potential impact of roof types on thermal conditions in these more common variations, the simulated operative temperatures of houses with unmodified roofs were plotted against those with modeled roof modifications.

Figure 5.29 shows deviations in annual hourly operative temperatures of a constantly ventilated house with exposed, uninsulated walls with two different roofs: the typical single-layer, uninsulated corrugated sheet(plotted on the x-axis) to the double-layer radiant barrier type (plotted on the y-axis). The graph shows that the roof modification causes a trendline shift, where temperatures below 28.75 °C generally increase, and temperatures above 28.75 °C generally decrease. As a reference, the minimum acceptable winter and maximum acceptable summer operative temperatures (21.26 °C and 33.72 °C, respectively) according to EN 15251 Category III standards, are plotted as a blue field on the graph. Though acceptable temperatures vary throughout the year, any dots that fall in the blue field can be considered within the extreme limits of the thermal comfort zone. Modifying the roof to the double-layer with radiant barrier increases temperatures below 21.26 °C by an average of 1.4 °C and a maximum of 2.5 °C. The modification decreases temperatures above 33.72 °C by an average of 2°C and a maximum of 5°C.

Figure 5.30 shows deviations in annual hourly operative temperatures of a night flush ventilated house that shares its south and north walls with adjacent buildings, with two different roofs: the typical single-layer, uninsulated corrugated sheet(plotted on the x-axis) to the double-layer insulated type (plotted on the y-axis). The graph shows that the roof modification causes a trendline shift, where temperatures below 28 °C generally increase, and temperatures above 28 °C generally decrease. Modifying the roof to the double-layer with insulation increases temperatures below 21.26 °C by an average of 1.9 °C and a maximum of 3.2 °C. The modification decreases temperatures above 33.72 °C by an average of 2.7 °C and a maximum of 5.5 °C.

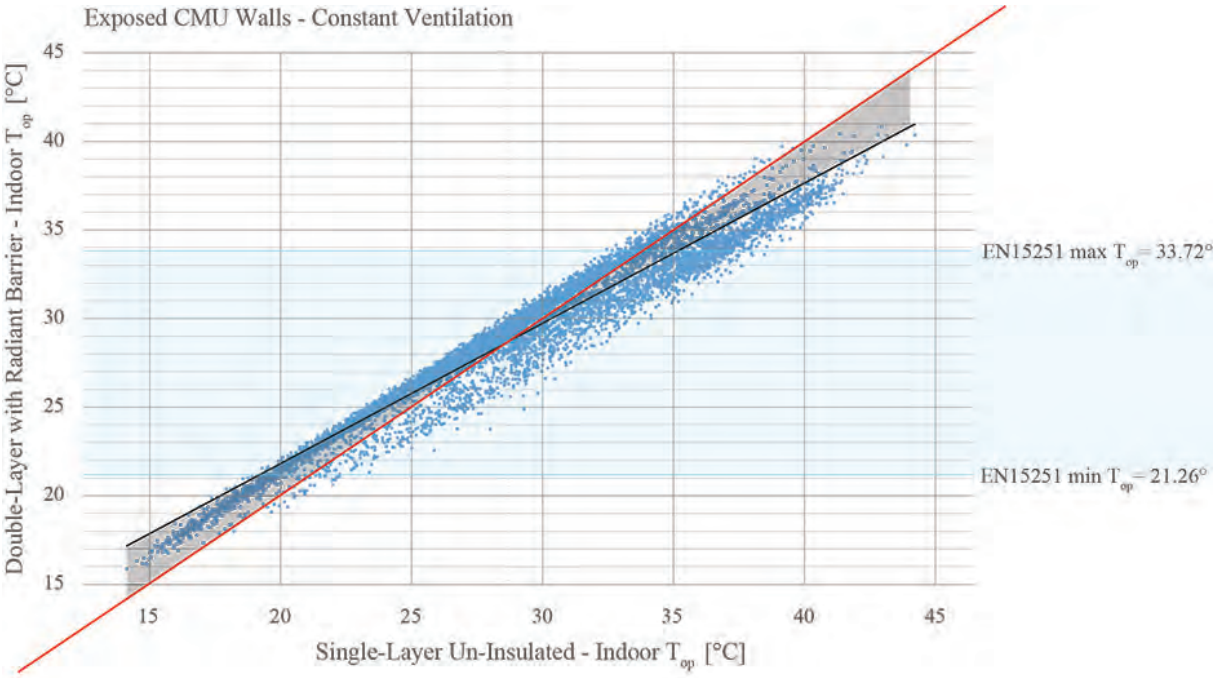

Figure 5.29 – Simulated Impact of Double-Layer Corrugated Sheet with Radiant Barrier Roof Modification to Hourly Operative Temperatures in Slum House Type with Exposed CMU Walls and Constant Ventilation.

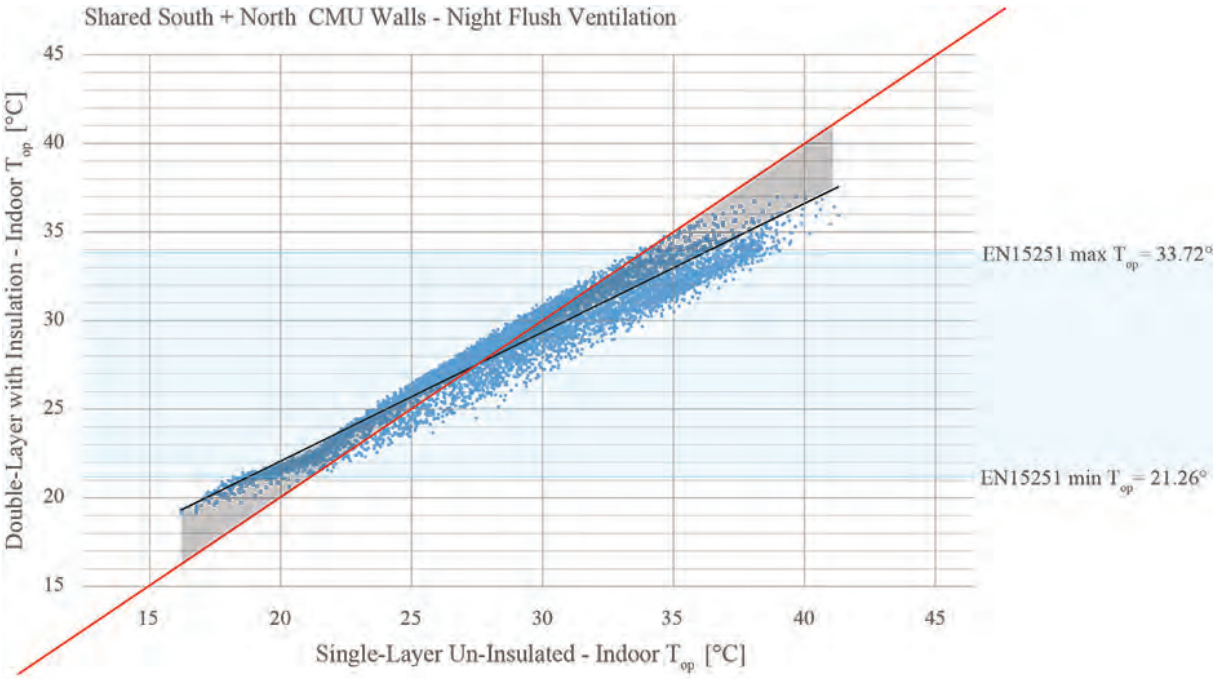

Figure 5.30 – Simulated Impact of Double-Layer Insulated Roof Modification to Hourly Operative Temperatures in Slum House Type with South and North Shared CMU Walls and Night Flush Ventilation.

Chapter 6

Conclusions and Recommendations

The conclusions and recommendations in this chapter are based off the co-design work, and the analysis of field data that was collected, between late August 2014 and late March 2015. To further verify the models, assumptions, and conclusions presented, data collection and analysis will continue through late August 2015 for the same seven existing Bhuj building types and the five roof prototypes documented in this thesis. This chapter serves three purposes. First, it serves to summarize research results that directly influence design decisions for both the Rajiv Awas Yojana (RAY) Slum Free Bhuj House design, as well as for general use outside of the RAY house typology application. Then, the latest iteration of roof panel prototypes are presented along with an initial set of cost estimates for further discussion. Finally, based off the thesis results, a series of new hypotheses are offered in preparation for future work and as a continuation the co-design process.

6.1 Recommendations Based off Existing Building Research Results

To summarize, seven existing buildings in Bhuj were chosen as typologies which mirror traditional to contemporary, as well as slum and non-slum typologies typical to Bhuj, India. Detailed analysis and results of the existing building research is presented in Chapter 3. In the cross-comparison of measured indoor air and surface temperatures for these seven typologies (Figures 3.23 through 3.26), it is apparent that a number factors contribute to thermal performance. We can conclude from these analyses that the rules of thumb for passive Design with Climate strategies, are upheld to various degrees. These strategies are listed again in this section but are ranked according to their commonality to the seven case study buildings. For the purposes of this section, the seven types are ranked relative to each other and are divided into two groups: a *higher performance* group and a *lower performance* group. Detailed building descriptions and individual analyses are available in Chapter 3.

Figure 6.1 is a graph that qualitatively scores each of the seven case study buildings according to the extent to which they follow these rule of thumb Design with Climate strategies. The plot is based off qualitative field observation and discussions with Hunnarshala Foundation Directors, not data analysis. Information from the individual graphs shown in Figure 3.27 were compiled to create a unit-less "Relative Cumulative Design with Climate Score" for each of the case study buildings. These qualitative scores

were calculated by multiplying the frequency of a certain strategy used (along the x-axis of Figure 3.27 graphs) by that strategy's overall effectiveness (along the y-axis of Figure 3.27 graphs) as a way to begin a discussion about how to prioritize passive cooling strategies for low cost housing. When compared to measured data, the graph shows that the *higher performance* buildings (shown with blue circles) generally also score higher according to the five Design with Climate strategies along the x-axis.

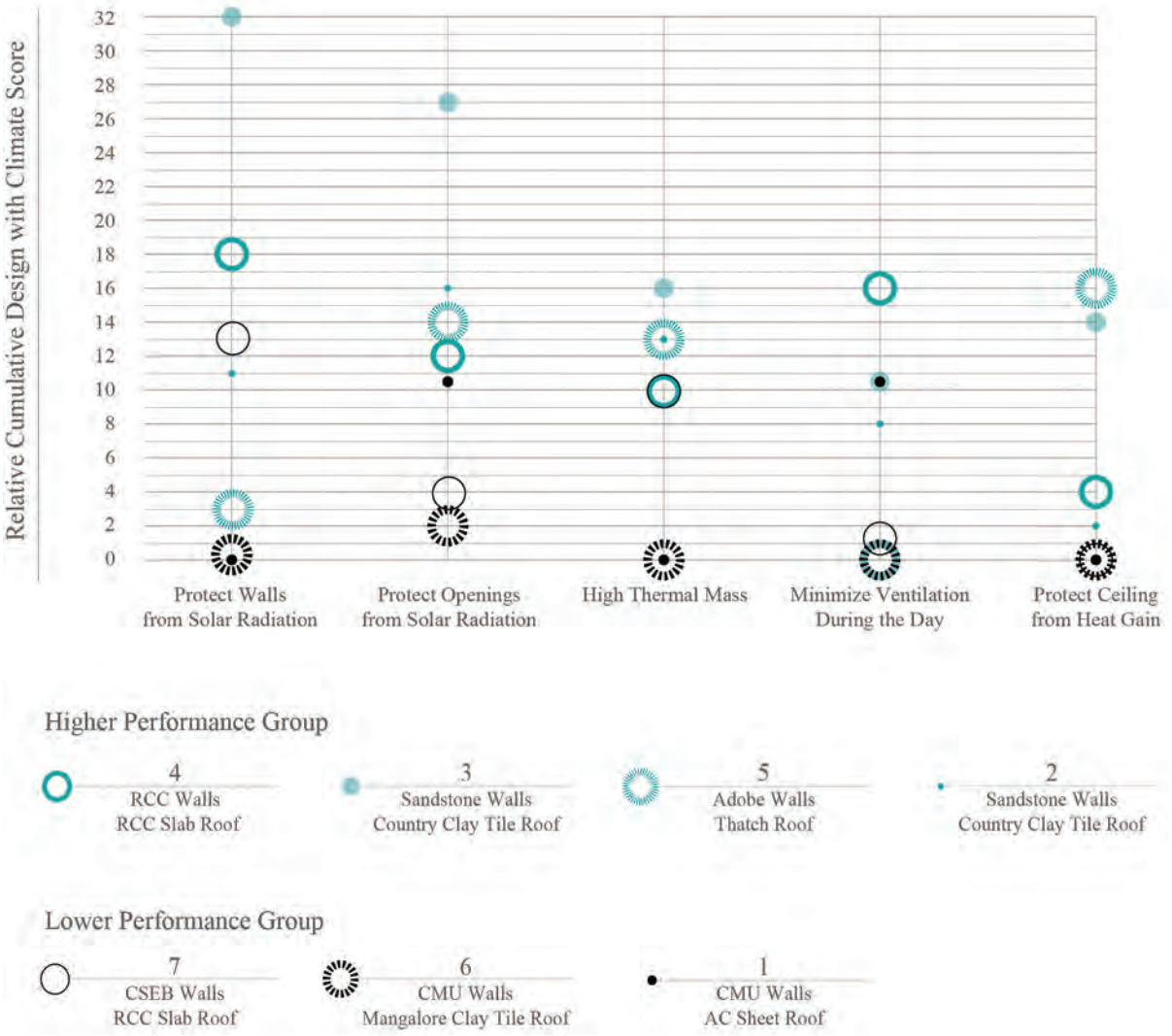

Figure 6.1 – Relative Cumulative Design with Climate Score Based from Observed Design with Climate Strategies for Case Study Buildings 1-7. Graphs plot ways which Buildings 1-7 utilize different passive cooling strategies. Buildings are grouped into a *higher performance* and *lower performance* group based on measured data presented in Figures 3.23 through 3.26). *Higher performance* buildings are shown in blue and *lower performance* buildings are shown in black.

Higher Performance Group - Common Traits and Resulting Recommendations

The following Design with Climate strategies are prioritized according to their commonality to the four buildings that comprise the higher performance group. It is important to note that though these strategies are prioritized, thermal performance will only improve with an amalgam of the strategies listed below. All four buildings are occupied at irregular schedules and have electric ceiling fans. The ceiling fans are used when the building is occupied and it is hot during the day and/or night.

Protect Walls from Direct Solar Radiation
All four buildings in the higher performance group had walls that were well shaded by neighboring trees, buildings, deep roof overhangs or adjacent buildings. Three of the four buildings shared walls with adjacent buildings, further protecting walls from the sun. In one building all the walls were un-shared, but plastered bright white. In two of the buildings, the south and/or west walls were plastered bright white.

Protect Windows from Direct Solar Radiation
All four higher performance buildings had all windows fully shaded from direct solar radiation during daylight hours. Shade types varied, but include fully opaque operable panels, operable louvered shutters, curtains, and exterior overhangs. Area of openings vary widely between the houses, and do not seem to correspond with better or worse performance within the group.

High Thermal Mass Walls
All four higher performing buildings benefited from having thermally massive walls thicker than the typical 15 cm block found in the lower performing slum house types. One has thermally massive walls on all sides approximately 40cm thick. Another two of the buildings have 30 cm to 40cm thick walls on the south and west facades, and 23 cm thick walls on the north and east facades. One building had all walls at 23 cm thick. However, in this building, cooler temperatures were attributed to the house's bright white plastered walls and ventilation schedule over wall thickness. That is to say, we cannot conclude that a non-white 23 cm thick wall will be sufficient to contribute to the building's passive cooling.

Minimize Natural Ventilation During the Day
Three of the four higher performing buildings minimized natural ventilation to the interior during the day. Two of these three observe a night flush ventilation schedule during hot periods. The third is ventilated on an irregular schedule. In the two best performing houses, air flow from the exterior is nearly to fully cut off during the heat of the day. In the highest performing building, windows were glazed and closed during daylight hours, and space is flushed at night, aided not only by window operation but use of an electric ceiling fan. One of the four buildings was an office and could not minimize ventilation during the day. It should be noted here that the use of ceiling fans during occupied hours, while potentially increasing infiltration of hot outside air to the interior, is not only customary in Bhuj but necessary for thermal comfort. Thus the recommendation is to equip houses with a variety of coverings for openings. Openings that are high up, or are otherwise not necessary for daylight, should have operable, opaque panels that close to be as air-tight as possible to minimize infiltration during the day but are able to be fully opened at night. If possible, openings that are required for daylight should be glazed or heavily screened and equipped with operable louvered shutters or curtains that prevent direct sunlight and some air from entering the building.

Protection of Ceiling Surface from Heat Gain due to Direct Solar Radiation

Roof types vary widely between all four higher performing buildings. However, though by different means, all four protected the interior ceiling surface from heat gain due to direct solar radiation to a better degree than those houses in the lower performance group. The best performer of the group has an uninsulated 15 cm thick concrete slab with bright white tile as an exterior surface. The second has a double layered clay tile roof. The third is the best insulated of the group; made of approximately 35 cm thick straw thatch. The fourth, which is the lowest performer of the high performance group, has what could be considered a double-layer clay tile roof. However, the space between the tiles and sub-structure that makes up the lower layer is too small to be properly ventilated.

Lower Performance Group - Common Traits and Resulting Recommendations

The following *anti*-Design with Climate strategies are prioritized according to their commonality to the three buildings that comprise the lower performance group. All three buildings in the lower performance group are typical Bhuj slum house types. All three buildings are occupied at irregular schedules and have electric ceiling fans. The ceiling fans are used when the building is occupied and it is hot during the day and/or night.

Surfaces not Protected from Direct Solar Radiation
Outer surfaces of buildings in the lower performing group were largely unprotected from direct solar radiation. One of the buildings has all four non-white facades and roof exposed, without any shade or protection from adjacent buildings. The two other buildings each have three facades and the roof exposed.

Constant or Irregular Natural Ventilation During the Day due to Building Occupation
One of the three buildings is constantly ventilated, regardless of time of day or season. This has to do with how the house is occupied, as well as its construction. It is interesting to note here that regardless of the air-tightness of the construction, if a house is comprised of a single room that is directly linked to the outside, where the majority of daily activities occur during the summer, doors are likely to be left open during the day. We may be able to design openings to maximize buoyancy-driven airflow, and design shutters and doors that can be tightly latched to minimize infiltration during the day, but effectiveness of such designs hinge on use as much as construction.

The other two houses are ventilated on an irregular schedule, similar to two of the houses in the higher performing group. It can be concluded here that ventilation schedule has little effect on houses that are unprotected from solar heat gain during the day.

6.2 Recommendations Based off Test Chamber Research Results

To summarize, five roof prototypes were co-designed and tested to determine the impact on roof modifications to thermal performance (section 5.1.1). Detailed analysis and results of the test chamber experiments is presented in Chapter 5. Broadly, the designs were chosen to compare performance of typical single-layer Bhuj roofs to double-layered roofs with convective cavities, made from readily available, widely used materials. The double-layered convective assemblies were either outfitted with interior insulation panels or a radiant barrier on the inner surface of the upper layer. Figure 5.24 is especially

helpful to see the overall predictions of the potential cooling effects of roof modifications. Figure 5.24 is re-printed on the following page as Figure 6.2 for clarity.

Impact of Roof Modification to Operative Temperature in Test Chambers

Average Cooling Effects of Roof Modifications to Constantly Ventilated Chambers
During the constant ventilation tests, double-layered, insulated roofs decreased daily high indoor operative temperatures by an average of 1.5 °C when compared to their single-layer, uninsulated counterparts. The double-layered, uninsulated roof with radiant barrier decreased daily high indoor operative temperatures by an average of 1.25 °C when compared to its single-layer, uninsulated counterpart.

Average Cooling Effects of Roof Modifications to Night Flush Ventilated Chambers
During the night flush ventilation tests, double-layered, insulated roofs decreased daily high indoor operative temperatures by an average of 2 °C to 2.5 °C when compared to their single-layer, uninsulated counterparts. The double-layered, uninsulated roof with radiant barrier decreased daily high indoor operative temperatures by an average of 2 °C when compared to its single-layer, uninsulated counterpart.

Day and Night Cooling Potential of Double-Layer Roofs with Radiant Barriers
The double-layer metal sheet roof with upper radiant barrier performed within 1 °C of the insulated types in the daytime. This type maintained high daily surface temperatures within 1 °C of indoor air temperature, anywhere from 9 to 11.5 °C cooler than its uninsulated counterparts. Nightly air gap temperatures fall well below outdoor air temperature, and because there are no insulation panels to prohibit heat transfer, the ceiling is able to contribute to some amount of nocturnal radiative cooling, staying at outdoor air temperature, but below wall and operative temperatures. This radiative cooling effect, however, might pose less of a risk of over-cooling during winter months, as the nightly low ceiling temperature of T5 is between 2 and 4 °C warmer than the uninsulated roofs. This balance of resistance to solar radiation during the day and mediated radiative cooling during the night still allows for the insulated walls to discharge heat during the night and remain relatively cool during the day.

Impact of Roof Modification to Common Bhuj Slum House Types

Similar to initial simulations, discussed in Chapter 4, the dramatic drop in operative temperatures necessary to reach full thermal autonomy for a wall-dominated building depends only in small part to the roof assembly, and in large part on the wall assemblies as well. From March 10 to March 23, when outdoor temperatures were hottest, wall insulation on the exterior of each test chamber decreased indoor air temperature by 6 °C, while the roof type variation further decreased indoor air temperatures by 1 °C. Because uninsulated or unprotected walls can reach temperatures above daily high outdoor temperatures (shown in Figures 5.25 through 5.27), that small but welcome decrease in temperature that the roof provides may be overpowered. Insulated walls are not commonly seen in informal housing and have not been proposed by Hunnarshala for any RAY house typology. The exposed and shared wall variations, however, are very common, and the current RAY house typologies are currently designed with shared and shaded walls. The results summary below show that roof modifications have the potential to significantly impact thermal conditions in these more common building types, as well as a version where walls are exposed but coated white. Figures 5.28 through 5.30 are especially helpful to see the overall predictions of the potential cooling effects of roof modifications to common existing Bhuj Slum House types. Figure 5.28 is re-printed as Figure 6.3 for clarity.

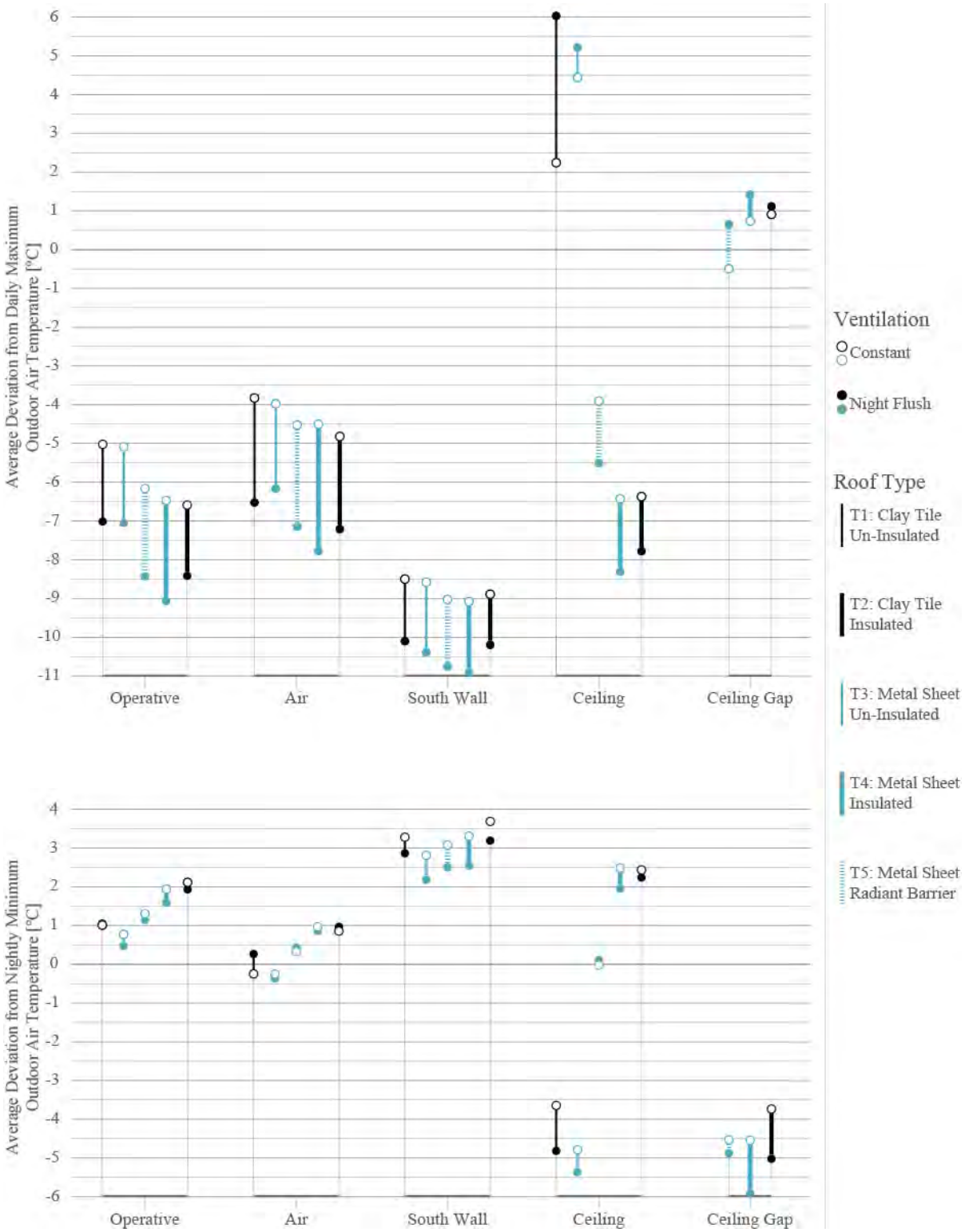

Figure 6.2 – Comparison of average deviations of indoor temperatures from extreme day and night outdoor temperatures for constant and night ventilation schedules.

Potential Cooling Effects of Roof Modifications to Buildings with Unprotected Walls
For wall dominated buildings that are not protected from direct solar radiation, double-layer roof modifications increase acceptable temperatures by a range of 6% (526 hours, or 22 days) to 8% (701 hours, or 29 days) according to EN 15251 Category III standards. When hourly temperatures are compared between buildings with single vs. double-layer roofs, the comparisons show that the modifications tend to increase operative temperatures below 21.26 °C by averages of 1.4 °C to 1.9 °C with a maximum increase of 3.2 °C. The modifications decrease operative temperatures above 33.72 °C by an average of 2 °C to 2.5 °C with a maximum decrease of 6 °C.

Potential Cooling Effects of Roof Modifications to Buildings with Some Shared Walls
When the building was modeled as attached to neighboring buildings on the south and north facades, the simulations predict that roof type will increase acceptable temperatures by a range of 6% (526 hours, or 22 days) to 13% (1139 hours, or 47 days) according to EN 15251 limits. When hourly temperatures are compared between buildings with single vs. double-layer roofs, the comparisons show that the modifications tend to increase operative temperatures below 21.26 °C by averages of .75 °C to 2 °C with a maximum increase of 3.2 °C. The modifications decrease operative temperatures above 33.72 °C by an average of 1.7 °C to 2.7 °C with a maximum decrease of 5.5 °C.

Potential Cooling Effects of Roof Modifications to Buildings with Exposed White Walls
For the white wall variations, where the building stands alone with all wall surfaces having a solar absorptance, α, of 20%, the simulations predict that roof type will increase acceptable temperatures by a range of 8% (701 hours, or 29 days) to 13% (1139 hours, or 47 days) according to EN 15251 limits. When hourly temperatures are compared between buildings with single vs. double-layer roofs, the comparisons show that the modifications tend to increase operative temperatures below 21.26 °C by averages of .75 °C to 1.3 °C with a maximum increase of 2.6 °C. The modifications decrease operative temperatures above 33.72 °C by an average of 1.75 °C to 2.2 °C with a maximum decrease of 4.5 °C.

Discussion
Though roof modifications or ventilation schedules alone are not sufficient enough to lower operative temperatures to reach full thermal autonomy for current common slum building typologies, field tests and calibrated simulations show that they have the potential to lower operative temperatures below the upper acceptable limits by up to the equivalent of 22 to 47 days of the year according to the EN 15251 standard. Regardless of the standard used, roof modifications show the potential to decrease daily high indoor temperatures from .75 °C to 6 °C, depending on wall type and ventilation schedule. The impact of the roof assembly will increase as the roof area gets larger relative to wall area. This may be useful to consider for some of the RAY house typologies over others or for larger community building design. This will be discussed further in section 6.5.

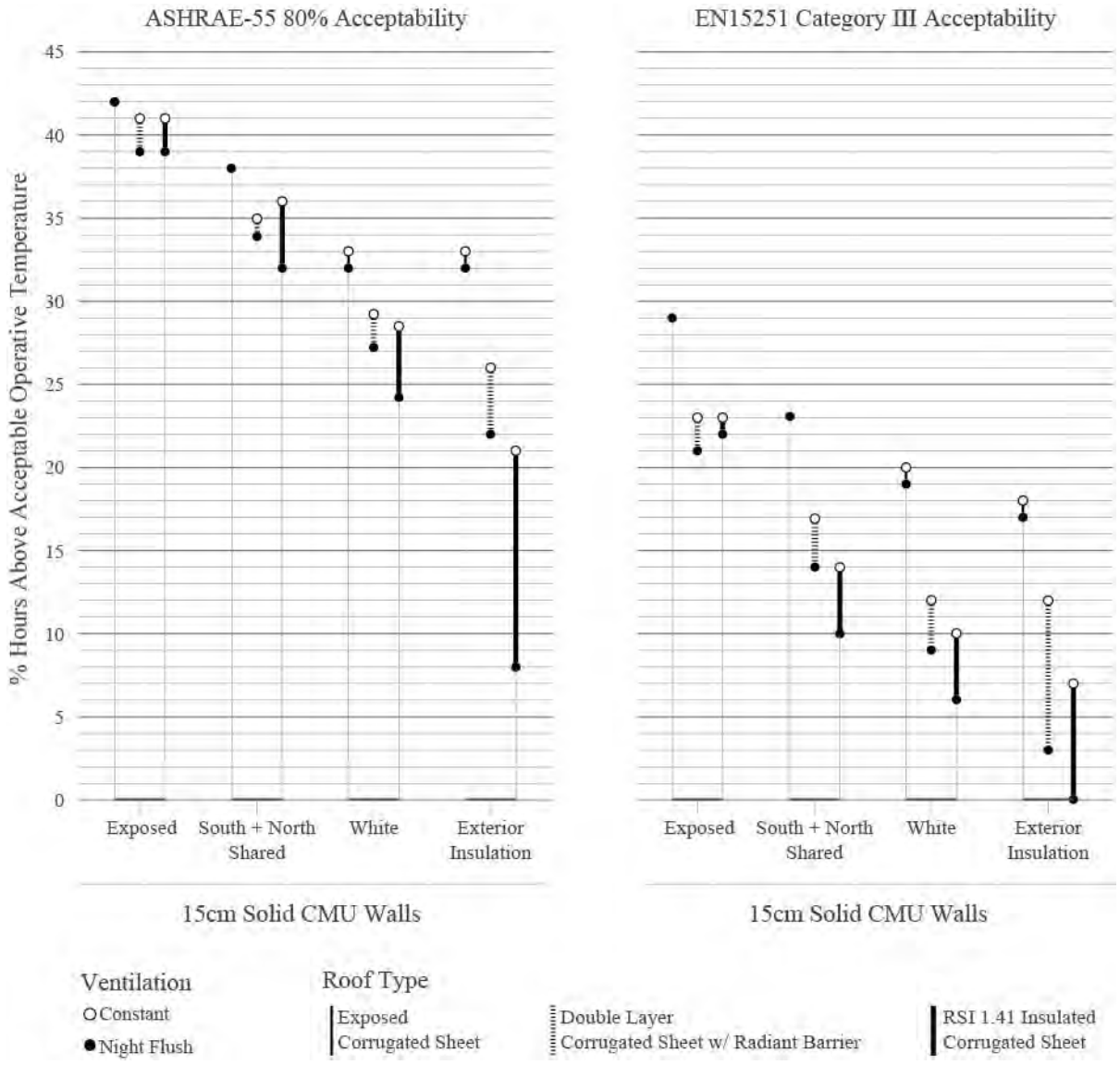

Figure 6.3 – Percent annual hours simulated indoor operative temperatures exceed ASHRAE-55 80% Acceptability Limits (left) and EN 15251 Category III Acceptability Limits (right).

6.3 Roof Panel Design Recommendations

Based on the results from test chamber research, refinements on two double-layer roof prototypes are proposed. The refinements shown are restricted to the use of corrugated tin sheet as the outer material for three practical reasons: cost, wider constructability, and wider availability of materials. This is not to say that double layer clay tile roofs should disregarded as viable option, especially for the RAY house typologies. This is briefly discussed next.

Traditional Clay Tile Roof Options for Wall Dominated Buildings
According to the existing building and test chamber analysis, it is reasonable to assume that clay tile roofs with false ceilings, like those found in the traditional Mistri house in our study, could be sufficient if the building is wall dominated and the walls are well protected or insulated on the exterior. The traditional Mistri house was the second best performing existing building out of the seven tested during the hottest days. To verify the initial findings, this relative performance needs to continue to be monitored through a full summer season. And though the comparison of existing buildings to test chamber performance is not equivalent, it is interesting to note that during the hottest day of the testing period, March 22nd, when daily high outside temperatures above 41 °C, the Mistri house ceiling reached a high temperature of 37 °C. That same day the insulated clay tile roof test chamber ceiling reached 34 °C. The difference of 3 °C in ceiling temperatures will likely have a minor effect on operative temperatures in well protected, wall dominated buildings. In addition to the seemingly comparable performance of the Mistri roof to the prototype roofs, Hunnarshala has already developed the more thermally massive mud-roll system that acts as both structure and heat protection to the interior. Thus the recommendation regarding double-layer clay tile prototypes is not to refine the first set of prototypes, but to more thoroughly test existing assembly typologies in the thermal field lab. This will be discussed further in section 6.5.

Double Layer Radiant Barrier Roof Panel – Design Refinement Proposal
Figure 6.4 shows a sectional perspective view of a 60 cm by 60 cm section of the double-layer radiant barrier prototype. Air gap dimensions remain the same, ranging from 7.5 cm to 10 cm. There is one refinement to this version over the initial prototype that benefits the design in three ways. Because the 60cm O.C. spacers fit the upper and lower layers along their entire length, made from stacked strips of corrugated tin sheet instead of a rectangular wooden spacer they can be mechanically fastened in multiple places to the upper and lower sheets to a) make the panel rigid, which greatly reduces or alleviates the need for roof framing, b) make the panel stronger by increasing the overall depth of the rigid panel from less than 1 mm to 10 cm, and c) provide continuous connection points every 60cm, so the radiant barrier can be sandwiched between the spacers and upper layers mechanically, which greatly reduces or entirely alleviates the need for an expensive adhesive connection between the barrier and tin sheet. The spacers for this panel can be constructed locally, as they only require widely available materials and have no welded connections. Production could also be scaled to a mass manufacture level and the spacers sold as a product along with the tin sheet.

Double Layer Insulated Roof Panel – Design Refinement Proposal
Figure 6.5 shows an sectional perspective view of a 60 cm by 60 cm section of the double-layer insulated panel prototype. Air gap dimensions remain the same, ranging from 7.5 cm to 10 cm. Instead of the insulation panels being rigid, separate and hung from the roof framing structure, they can be made with flexible outer material such as plastic sheet that is then stuffed with a recycled or organic insulative material such as shredded waste plastic or rice hulls. The flexible panels, or tubes, can then be stacked

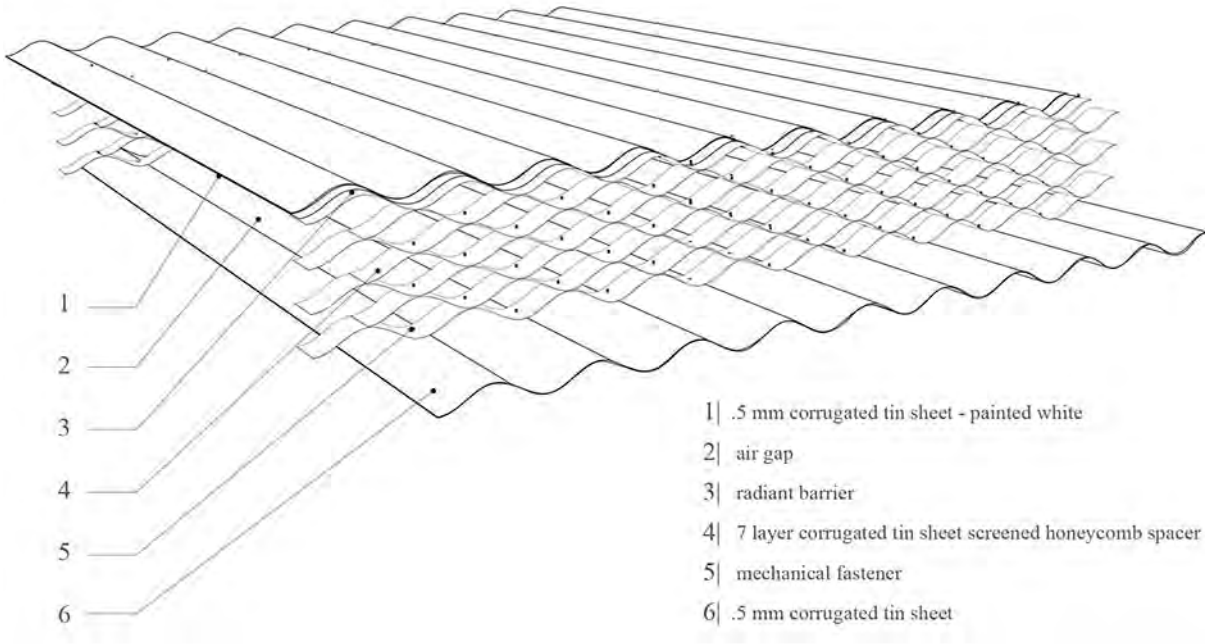

Figure 6.4 – Double-Layer Roof Panel with Radiant Barrier – Prototype 2 Design Proposal.

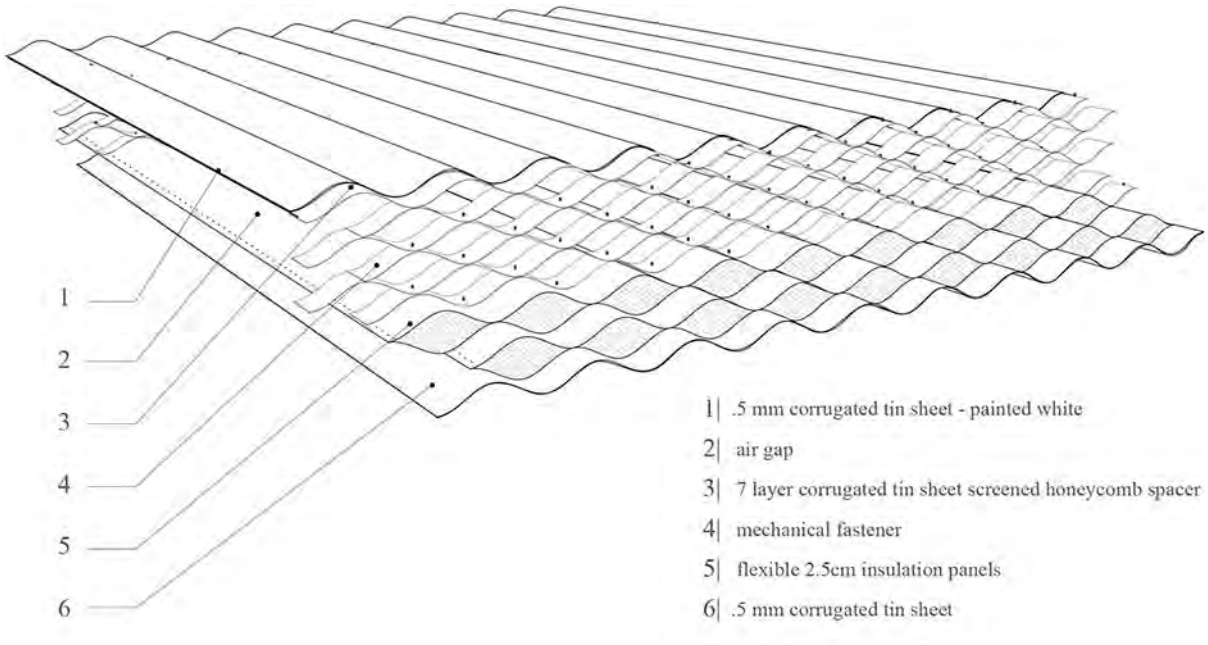

Figure 6.5 – Double-Layer Roof Panel Flexible Insulation – Prototype 2 Design Proposal.

on top of the lower tin sheet layer and mechanically held in place by the honeycomb spacers. This panel would similarly have the potential to be much more rigid, and strong, than the previous version. Another potential benefit to this assembly is that the insulation material, a potential fire risk, will be removed from the interior of the building. The spacers and insulation panels for this assembly can be constructed locally, as they only require widely available materials and have no welded connections. Production could also be scaled to a mass manufacture level and the spacers sold as a product along with the tin sheet.

6.4 Initial Cost Comparisons

In August 2014, during a co-design meeting at Hunnarshala, an initial cost benchmark range for new roof assemblies was set at 150 Rs/ft^2 (about \$2.50/ft^2) to a maximum of 225 Rs/ft^2 (about \$3.75/ft^2). This cost range includes provision for both materials and labor of local craftsman and builders. This range is based off the current cost of reinforced concrete slab roofs, which are generally regarded as a superior roof by building owners. The thought was that if a better performing roof could be offered for less than the price of a basic concrete slab roof, owners and builders would see its value.

Hunnarshala provided cost estimates of common Bhuj roof assemblies that include general material and labor costs, divided into separate costs for under structure and outer materials (6.1). These estimates come from Hunnarshala's experienced construction team and are perhaps specific to the Bhuj area only. Total costs for roofs commonly seen in Bhuj slums range from 115 Rs/ft^2 (about \$1.92/ft^2) for a single-layer asbestos cement sheet roof to 300 Rs/ft^2 (about \$5.00/ft^2) for a 15 mm thick reinforced concrete slab. Concrete slab roofs are often seen in the newer permanent slum re-development communities, but to a lesser degree than the single-layer framed roofs. Single-layer clay tile roofs at are also very commonly seen in and outside slum communities and range from 183 Rs/ft^2 (about \$3.05/ft^2) to 230 Rs/ft^2 (about \$3.83/ft^2).

At this stage we assume that the spacers can be manufactured off site but locally. The proposed modification cost estimates are based off the market price for outer materials, insulation/radiant barrier materials, and mechanical fasteners, and the cost of labor was estimated to be equivalent to the single-layer sheet and Mangalore tile estimates, as the actual installation process of the double-layer roofs will be similar to the single-layer installation process.

With these initial estimates, a case can be made that there is a potential for the tin sheet panels to be a higher-performing, lower cost choice than an un-finished concrete slab. At 185 Rs/ft^2 (about \$3.08/ft^2) to 205 Rs/ft^2 (about \$3.42/ft^2), these double-layer tin sheet variations fall in a similar price range to single-layer clay tile roofs. Currently, initial estimates for double-layer insulated clay tile roofs price them above estimates for Mangalore tile with mud roll insulation. Further discussion is needed, but these initial estimates indicate that the mud roll roofs should be considered a viable option, especially for the Bhuj RAY house typology.

Though these cost comparisons are promising, showing us we can make available better performing roof panels in an affordable price range, a major challenge will be to articulate the value of thermal performance to the end user. It is generally assumed that clay tile and concrete slab roofs are preferred for aesthetic reasons, and if an owner can afford these types, he will likely not choose a roof that isn't

Roof Type	Under Structure - Cost Rs/ft²		Outer Material - Cost Rs/ft²		Total Cost	
Double Sloping Roof	Material	Labor	Material	Labor	Rs/ft²	$/ft²
Single Layer .5mm Tin Sheet Painted White	70	40	35	10	155	2.58
Single Layer 6mm Asbestos Cement Sheet	35	40	30	10	115	1.92
Mangalore Pattern Tiles	100	60	15	8	183	3.05
Country Tiles with 25mm thick wood plank sub-structure	100	80	25	25	230	3.83
Manglalore Tiles with Mud-Roll Insulation	150	60	15	8	233	3.88
40cm Thatch Panel - Alang	100	60	140		300	5.00
Flat Roof						
Reinforced Concrete Slab 12 - 15cm thick	N/A	N/A	225 - 300		225 - 300	3.75 - 5.00
Ferrocement Channels with Mud Roll Insulation	80	50	90		220	3.67
Proposed Modifications For Review						
Double Layer .5mm Tin Sheet Painted White with Radiant Barrier	100	40	35	10	185	3.08
Double Layer .5mm Tin Sheet Painted White with Flexible Insulation Panels	120	40	35	10	205	3.42
Double Layer Clay Tile Rigid Insulation Panels as Bottom Layer	180	60	15	8	263	4.38

Table 6.1 – Existing and Proposed Roof Assemblies - Initial Cost Comparison.

to his tastes or looks less expensive, even if it performs better. For this reason, it would be beneficial at this stage to look into subsidy programs or grants from organizations where thermal performance *is* valued, such as international health organizations or from the RAY program itself, to incentivize owners to choose the better performing low-cost roofs, or mitigate the cost of the better performing but more expensive double-layer clay tile roofs.

6.5 Recommendations for Future Work

There are many ways to take this research forward. The work presented here resulted from the establishment of a committed international co-design team and construction of a thermal field lab in Bhuj that is intended to be used for years to come. Practically, this research reached a proof of concept stage for new roof assembly design. Along with the questions the research answers regarding comparative thermal performance of twelve common roof types, come many new questions about how to achieve full thermal autonomy in slum redevelopment housing. The research shows that this goal is technically within reach, but that the roof and ventilation schedules alone are only a few steps of many. The following topics layout possible next directions for further research.

Wall Protection and Exterior Insulation Solutions
In order to attempt to reach full thermal autonomy by low-cost, passive means, wall treatments must be closely examined in future work. As demonstrated in the test chambers, the presence of exterior wall insulation with thermally massive walls greatly decreases indoor temperatures during the day.

Wall Dominated vs. Roof Dominated Buildings
The impact of roof modifications will increase in buildings with roof areas that are larger in relation to wall area. Thus, roof modifications will have a more singular impact on roof dominated buildings, such as those we find in public and community buildings. It would be useful to investigate the relative impact of roof modifications on program types other than single family residential.

Though not evaluated in this thesis, the research brought about many co-design discussions about the impact of ceiling height on thermal comfort. The thought is that a higher ceiling will help cool the space due to stratification, allowing the hottest air in the space to remain far above occupants, while the occupants are cooled by the thermal mass heat sinks of surrounding walls and the ground. This is, of course, a valid hypothesis. However, this research shows that if the walls have insufficient thermal mass and are unprotected from direct solar radiation, increasing their area will cause them to be a major heat source during the day, instead of heat sink. Another parametric study should be done to better understand the benefits and drawbacks of wall dominated vs. roof dominated buildings.

Radiative Cooling and Roof Panel Operation
Nocturnal radiative cooling plays a significant role in the passive cooling of a building, especially in hot and arid climates that experience a large diurnal temperature shift. Results from this research suggest that radiative cooling may have as much, or more, of an impact on cooling the building at night than night flush ventilation. That said, roofs that radiate heat well on summer nights will also do so on winter nights, running the risk of severely over-cooling a space during a smaller but significant portion of the year. As detailed in chapter 2, passive cooling research from the past 35+ years has shown that it is possible to design roofs that maintain comfortable indoor temperatures year-round because they are

operable. Movable insulation panels can be installed to protect the interior from solar radiation during hot days, and removed at night to allow for radiative cooling, and operation can be reversed seasonally (Cook, 1989; La Roche and Givoni, 2002). However, the drawback of these operable systems is that the occupant must be willing and able to ardently manually operate their roof every night of the year. This is not to say that some amount of operation is out of the question, simply that it is recommended that design solutions be studied that minimize the need to change user behavior. There is also the potential to block the roof air gap seasonally instead of daily, to prevent excess over-cooling in the winter while allowing for the gap to be ventilated during the summer.

The double-layer tin sheet roof prototype proved to be the best balance between nighttime cooling and daytime protection of the five test cases, and requires no change in behavior from the occupant. Measured results for the hottest summer months have not been evaluated yet, and will be completed directly subsequent to this thesis. According to the research thus far, this roof type performs almost as well as the double-layer insulated type if the walls are properly designed. It is recommended that research into double-layer assemblies continue with a focus on radiative cooling potential with the need for minimal user operation.

Double-Layered Thermally Massive Roof Assemblies
Hunnarshala has already developed a double-layer, more thermally massive clay tile and mud roll roof assembly that integrates structure and heat protection with architectural design. This assembly type is aesthetically desirable, engages local artisans and is already in use in the Bhuj area. It is necessary to honor this already established type and evaluate the thermal performance of these roofs in the second round of test chamber testing. A similar case for testing of reinforced concrete (RCC) slab roofs can be made. It is recommended that if RCC roofs are built on the test chambers for a second round of testing, they are so built as controls. All members of the research team are interested in pursuing tests using ferrocement channels, clay tile, mud rolls, and RCC to better understand the performance of thermally massive roofs. Previous research undertaken by Hunnarshala has shown that thermally massive roofs run the risk of cooling down too slowly at night. This risk needs to be assessed, so that widely used thermally massive roof assemblies can significantly contribute to interior thermal comfort.

Implementation and Scalability to the End User
Because the measured results show that roof modifications to these types is significant, but small, a major challenge arises in value creation for the demand side of the value chain. This needs rigorous study that was not in the scope of this research. Also, with more research on the supply side of the value chain, more accurate cost estimates can be made to see if the proposed panels can be produced at low cost on a mass scale.

If large scale production is possible, the potential for the technology to be available in multiple climates arises. Though not in the scope of this thesis, it now becomes necessary to predict roof modifications' effectiveness in climates other than hot and arid. This study is planned to be completed directly subsequent to this thesis research.

Bibliography

ANSI/ASHRAE (2013). *Standard 55-2013, Thermal Environmental Conditions for Human Occupancy*. Atlanta, GA: American National Standards Institute American Society of Heating Refrigerating and Air Conditioning Engineers. 34

Azhar, G. S., D. Mavalankar, A. Nori-Sarma, A. Rajiva, P. Dutta, A. Jaiswal, P. Sheffield, K. Knowlton, and J. J. Hess (2014, January). Heat-related Mortality in India: Excess All-cause Mortality Associated with the 2010 Ahmedabad Heat Wave. *PloS one 9*(3). 30

Balaram, S. (2009). Design in India: The Importance of the Ahmedabad Declaration. *Design Issues 25*(4), 54–79. 25

Basu, R. (2009, January). High Ambient Temperature and Mortality: A Review of Epidemiologic Studies from 2001 to 2008. *Environmental Health : A Global Access Science Source 8*, 40. 30

Brake, D. J. and G. P. Bates (2002). Deep Body Core Temperatures in Industrial Workers Under Thermal Stress. *Journal of Occupational and Environmental Medicine / American College of Occupational and Environmental Medicine 44*(2), 125–135. 29

Bravo, G. and E. González (2013). Thermal Comfort in Naturally Ventilated Spaces and Under Indirect Evaporative Passive Cooling Conditions in Hot-Humid Climate. *Energy and Buildings 63*, 79–86. 21

Brown, T. and J. Wyatt (2008). Design Thinking for Social Innovation IDEO. *Stanford Social Innovation Review 8*(1), 30–35. 26

Chang, P.-C., C.-M. Chiang, and C.-M. Lai (2008, January). Development and Preliminary Evaluation of Double Roof Prototypes Incorporating RBS (Radiant Barrier System). *Energy and Buildings 40*(2), 140–147. 21

Climate CHIP (2015). Excel Heat Stress Calculator | Climate CHIP. http://climatechip.org/node/78. 30

Cook, J. (1989). *Passive Cooling*. Solar Heat Technologies: 8. Cambridge, MA: MIT Press. 18, 19, 21, 153

Dube, R. K. and G. S. P. Rao (2005). Extreme Weather Events over India in the last 100 years. *Journal of Indian Geophysical Union 9*(3), 173–187. 30

Epstein, Y. and D. S. Moran (2006). Thermal Comfort and the Heat Stress Indices. *Industrial Health 44*(3), 388–398. 29

Finucane, E. W. . (2006). Thermal Stress. In *Definitions, Conversions, and Calculations for Occupational Safety and Health Professionals* (Third ed.)., Chapter 5, pp. 1–15. Boca Raton: CRC/Taylor & Francis. 30

Givoni, B. (1976). *Man, Climate and Architecture*. Architectural science series. London : Applied Science Publishers, 1976. 8, 13, 17, 18, 19, 20, 21

Givoni, B. (2011). Indoor Temperature Reduction by Passive Cooling Systems. *Solar Energy 85*(8), 1692–1726. 21

Givoni, B. and P. La Roche. Modelling Radiant Cooling System for Developing Countries. In *ISES 2001 Solar World Congress*, Adelaide, Australia, pp. 175–182. 8

Hunnarshala Foundation (2013). Slum Free City Bhuj Presentation. Technical report, The Hunnarshala Foundation, Bhuj, India. 15

Koenigsberger, O. H. (1974). *Manual of Tropical Housing and Building*. London: Longman. 16, 18

Krüger, E., E. González Cruz, and B. Givoni (2010). Effectiveness of Indirect Evaporative Cooling and Thermal Mass in a Hot Arid Climate. *Building and Environment 45*(6), 1422–1433. 21

La Roche, P. and B. Givoni (2002). The Effect of Heat Gain on the Performance of a Radiant Cooling System. In *PLEA 2002 Conference*, Toulouse, France, pp. 1–6. 21, 23, 153

Levitt, B., M. S. Ubbelohde, G. Loisos, and N. Brown (2013). Thermal Autonomy as Metric and Design Process. http://www.coolshadow.com/research/Levitt_Thermal Autonomy as Metric and Design Process.pdf. 15

Liljegren, J. C., R. A. Carhart, P. Lawday, S. Tschopp, and R. Sharp (2008). Modeling the Wet Bulb Globe Temperature Using Standard Meteorological Measurements. *Journal of Occupational and Environmental Hygiene 5*(10), 645–655. 30

Manu, S., Y. Shukla, R. Rawal, R. de Dear, and L. Thomas (2014). An Introduction to the India Model for Adaptive (Thermal) Comfort, IMAC 2014. Technical report, Centre for Advanced Research in Building Science and Energy, CEPT University, Ahmedabad, India. 35

Medina-Ramón, M. and J. Schwartz (2007, December). Temperature, Temperature Extremes, and Mortality: A Study of Acclimatisation and Effect Modification in 50 US cities. *Occupational and Environmental Medicine 64*(12), 827–33. 30

Melles, G., I. de Vere, and V. Misic (2011). Socially Responsible Design: Thinking Beyond the Triple Bottom Line to Socially Responsive and Sustainable Product Design. *CoDesign 7*(3-4), 143–154. 39

Meng, Q. and W. Hu (2005, January). Roof cooling effect with humid porous medium. *Energy and Buildings 37*(1), 1–9. 21

Mevada, S. (2008). *Continuity and Transformation of Kutch House-Form*. Undergraduate, CEPT University, Ahmedabad, India. 8, 35, 36

MHUPA (2013). Rajiv Awas Yojana (RAY) Scheme Guidelines 2013-2022. Technical report, Government of India Ministry of Housing and Urban Poverty Alleviation. 15

Mink, A. and P. V. Singh Parmar, Vikram Kandachar (2014). Responsible Design and Product Innovation from a Capability Perspective. In J. et al van den Hoven (Ed.), *Responsible Innovation 1: Innovative Solutions for Global Issues*, Chapter 8, pp. 113–148. Dordrecht: Springer ScienceCBusiness Media. 39

Morelli, N. (2007). Social Innovation and New Industrial Contexts: Can Designers Industrialize Socially Responsible Solutions? *Design Issues 23*(4), 3–21. 25, 26

National Institute of Design (1979). Ahmedabad Declaration on Industrial Design for Development: Major Recommendations for the Promotion of Industrial Design for Development. In *UNIDO-ICSID 79*. National Institure of Design. 26

Nicol, J. F. and M. Wilson (2010). An overview of the European Standard EN 15251. 34

O'Neill, M. S., A. Zanobetti, and J. Schwartz (2005, June). Disparities by Race in Heat-related Mortality in Four US Cities: the Role of Air Conditioning Prevalence. *Journal of Urban Health : Bulletin of the New York Academy of Medicine 82*(2), 191–7. 30

OSHA (1999). OSHA's Campaign to Prevent Heat Illness in Outdoor Workers | Using the Heat Index - Estimating Work Rates or Loads. 29

Papanek, V. J. (1972). *Design for the Real World; Human Ecology and Social Change*. New York, Pantheon Books [1972, c1971]. 8, 25

Pearlmutter, D. and I. a. Meir (1995). Assessing the Climatic Implications of Lightweight Housing in a Peripheral Arid Region. *Building and Environment 30*(3), 441–451. 8, 21, 22, 23

Prasad, C., G. Dutt, S. Sathyanarayan, and V. Kappu Rao (1979). Studies on Sky-Therm Cooling. In *Indian Academy of Sciences*, Volume 2, pp. 339–356. Springer India. 19

Rapoport, A. (1969). *House Form and Culture*. Englewood Cliffs, N.J: Prentice-Hall. 16

Rudofsky, B. (1964). *Architecture Without Architects, a Short Introduction to Non-Pedigreed Architecture*. New York: Museum of Modern Art. 16, 17

Sanders, E. B.-N. and P. J. Stappers (2008). Co-Creation and the New Landscapes of Design. *CoDesign 4*(1), 5–18. 26

Satrasala, V. (2014). *Innovation & Evaluation of Roofing Component in Hot & Dry Climate- A Case of Bhuj-Kutch- CEPT*. Master of architecture in sustainable architecure, Center for Environmental Planning and Technology. 8, 24, 100

Schumacher, E. F. (1989). *Small is Beautiful : Economics as if People Mattered*. New York : Perennial Library, 1989, c1973. 39

UTCI (2003). UTCI Assessment Scale : UTCI Categorized in Terms of Thermal Stress, Glossary of Terms for Thermal Physiology. *Journal of Thermal Biology 28*, 75–106. 13, 31

UTCI (2015). Universal Thermal CLimate Index. http://www.utci.org/. 31

Wanphen, S. and K. Nagano (2009, February). Experimental Study of the Performance of Porous Materials to Moderate the Roof Surface Temperature by its Evaporative Cooling Effect. *Building and Environment 44*(2), 338–351. 21

WHO (2010). International Workshop on Housing , Health and Climate Change : Developing guidance for health protection in the built environment mitigation and adaptation responses Meeting Report. Technical report, World Health Organization. 15